Synthesis and Applications of Green Catalysts in Organic Synthesis: Heterogeneous Catalysis by Solid Supported Compounds and Nanoparticles

THESIS

SUBMITTED FOR THE AWARD OF THE DEGREE OF

Doctor of Philosophy
In
Chemistry

BY

NAYEEM AHMED

UNDER THE SUPERVISION OF
PROF. ZEBA N. SIDDIQUI

DEPARTMENT OF CHEMISTRY
ALIGARH MUSLIM UNIVERSITY
ALIGARH (INDIA)
2016

ABSTRACT

Catalysis lies at the heart of green chemistry, providing essential tools for the synthesis of valuable products in a sustainable manner. Today a major challenge lies in the identification and development of efficient heterogeneous catalytic processes that can achieve cost-effective and eco-friendly production of fine, commodity, and pharmaceutical chemicals. Therefore, the search for highly selective and active catalysts, espe cially those that can be readily recycled, is vital for the development of sustainable chemical processes. Hence, continuous efforts have been devoted toward the development of heterogeneous catalysts which are recyclable, cost effective and contain highly accessible active sites.

For more than a century, heterocycles have constituted one of the largest areas of research in organic chemistry. Their immense contribution towards the development of society from a biological and industrial point of view has vastly improved the quality of life. Among the approximately 20 million chemical compounds identified by the end of the second millennium, more than two-thirds are fully or partially aromatic and approximately half are heterocyclic. As a majority of drug-like compounds and natural products contain a heterocyclic nucleus at their core, ever increasing attention has been paid towards the development of novel clean processes employing nontoxic reagents, catalysts and solvents for the synthesis of important heterocycles.

In this context, the thesis entitled **"Synthesis and Applications of Green Catalysts in Organic Synthesis: Heterogeneous Catalysis by Solid Supported Compounds and Nanoparticles"** clearly reflects the objective, which is to develop the green heterogeneous catalysts and evaluation of their catalytic activity by synthesizing biologically relevant heterocyclic compounds such as pyridine, pyrimidine, piperidine and tetrazole derivatives. The research work described in the thesis is divided into five chapters. The chapter wise organization of the thesis is as follows:

CHAPTER 1

General Introduction

Green chemistry is a philosophy that puts forward sustainable concepts which are designed to reduce or eliminate chemicals and chemical processes that have negative environmental impacts. Over the last decade the environmental setup for synthetic

organic chemists has changed to a considerable degree and the main focus has now shifted towards more environment friendly and sustainable synthesis. Therefore, the development of environmentally benign organic reactions has become a crucial and demanding research area in modern organic chemical research. Developing green chemistry methodologies is a challenge that may be viewed through the framework of the “Twelve Principles of Green Chemistry. These principles identify catalysis as one of the most important tools for implementing green chemistry. In recent years, heterogeneous catalysts have gained much attention, as a result of economic and environmental benefits. They make synthetic processes clean, safe and high-yielding. The use of heterogeneous solid catalysts being in a different phase than the reagents and products has an obvious advantage in terms of easy separation from the reaction mixture, allowing the recovery of the solid and eventually its reuse.

Nano-catalysis has emerged as a sustainable and competitive alternative to conventional catalysis since the nanoparticles possess a high surface-to-volume ratio, which enhances their activity and selectivity, while at the same time maintaining the intrinsic features of a heterogeneous catalyst. These high reactivities are due to high surface areas combined with unusually reactive morphologies when compared to their bulk counterparts. Therefore, with the developments in nanotechnology, a wide variety of nanostructured catalysts or supported nanostructured catalysts have been applied to various organic transformations. Thus, this chapter describes scope of the present work giving insights about heterogeneous catalysis and green pathways for organic transformations.

CHAPTER 2

Sustainable nano-catalytic transformation of β-enaminones to pyridine derivatives

β-Enaminones are versatile intermediates used for the synthesis of heterocyclic compounds and drug intermediates. Because of the presence of nucleophilic character of enamine moiety and the elctrophilic character of enone moiety, they have been used as synthons for the synthesis of pyrroles, oxazoles, pyridinones, tricyclic benzo[a]quinolizines, benzodiazepines, pyrimidines, pyrazoles, isoxazoles and quinolines. In view of the mentioned properties and importance of enaminones in heterocyclic synthesis, this chapter is divided into two sections involving synthesis of novel 1,4-dihydropyridines and pyridine derivatives from β-enaminones under green reaction conditions using heterogeneous nano-catalysts.

Section A: Synthesis of 1,4-dihydropyridines from β-enaminones using meso alumina– sulphuric acid (Al-OSO_3H) as catalyst in water

1,4-Dihydropyridine (1,4 DHPs) derivatives represent an important class of compounds with remarkable pharmacological efficiency. Most importantly they have been used as effective calcium channel modulators for the treatment of cardio-vascular disorders. The other biological profiles of 1,4 DHPs are selective adenosine-A3 receptor antagonism, sirtuin activation and inhibition, anticonvulsant, and radioprotective activities.

Immobilization of catalysts on solid support provides an ideal method for combining the advantages of homogeneous catalysts with the advantages of heterogeneous catalysts. Therefore, the development of solid acid catalysts has received great deal of attention in organic chemistry and chemical industries. In this context, this section deals with the synthesis of mesoporous alumina sulphuric acid as a heterogeneous and recyclable solid acid catalyst and evaluation of its activity for the synthesis of novel 1,4-dihydropyridine derivatives **(3a-n)** *via* pseudo four component addition and cyclisation involving β-enaminone **(1a-b)**, aldehydes **(2a-g)** and ammonium acetate in aqueous media (**Scheme 2)**. The catalyst showed excellent catalytic activity giving products in high yields **(81-90%)** and could be reused for seven successive catalytic cycles. The catalyst was characterized by FT-IR, XRD, FE-SEM, EDX and TG analyses. The mesoporosity of alumina was determined by BET and TEM analyses. The amount of acid groups present on alumina was calculated by using neutralization titration method and was found to be 3.6 meq/g.

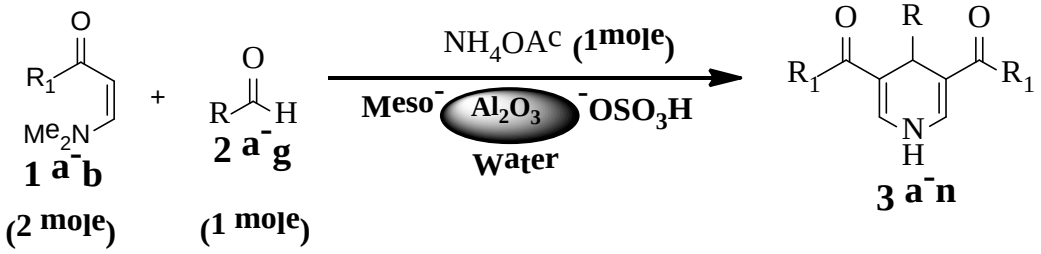

Scheme 2

Section B: ZnO nanoparticles catalysed solvent-free synthesis of novel pyridines *via* β-enaminones

Pyridine derivatives constitute one of the most important classes of heterocyclic compounds which widely occur as key structural subunits in numerous natural products that exhibit many interesting biological activities. The prevalence of pyridines in nature (e.g., in the coenzyme vitamin B6 family and in numerous

alkaloids) and their central role as versatile building blocks in the synthesis of natural products as well as biologically active compounds has led to a continued interest in the development of practical synthesis for these derivatives. These derivatives possess large spectrum of biological activities like anti-prion, anti-hepatitis B virus, anti-bacterial and anti-cancer. Recently, some of these compounds have been recognized as potential targets for the development of new drugs for the treatment of Parkinson's disease, hypoxia, asthma, kidney disease, epilepsy, cancer, and Creutzfeldt–Jacob disease.

The use of nano-sized inorganic solid oxides as heterogeneous catalysts has received much attention because of their high level of chemoselectivity, environmental compatibility, simplicity of operation, and availability at low cost. Catalytic efficiency depends on the surface area of the catalyst. As nanoparticles provide a very large surface area because of their high surface to volume ratio and low-coordinated sites, their use as catalysts is quite encouraging. ZnO NPs have been explored as powerful catalysts for several organic transformations due to their eco-friendly nature. Therefore, this section deals with ZnO nanoparticles catalyzed synthesis of pyranyl pyridine derivatives **(5a-p)** involving β-enaminone **(1a, 1c)**, active methylene compounds **(4a-i)** and ammonium acetate under solvent-free conditions **(Scheme 4)**. ZnO nanoparticles were characterized by XRD, SEM and TEM analyses. The catalyst was found to retain good catalytic activity up to six cycles.

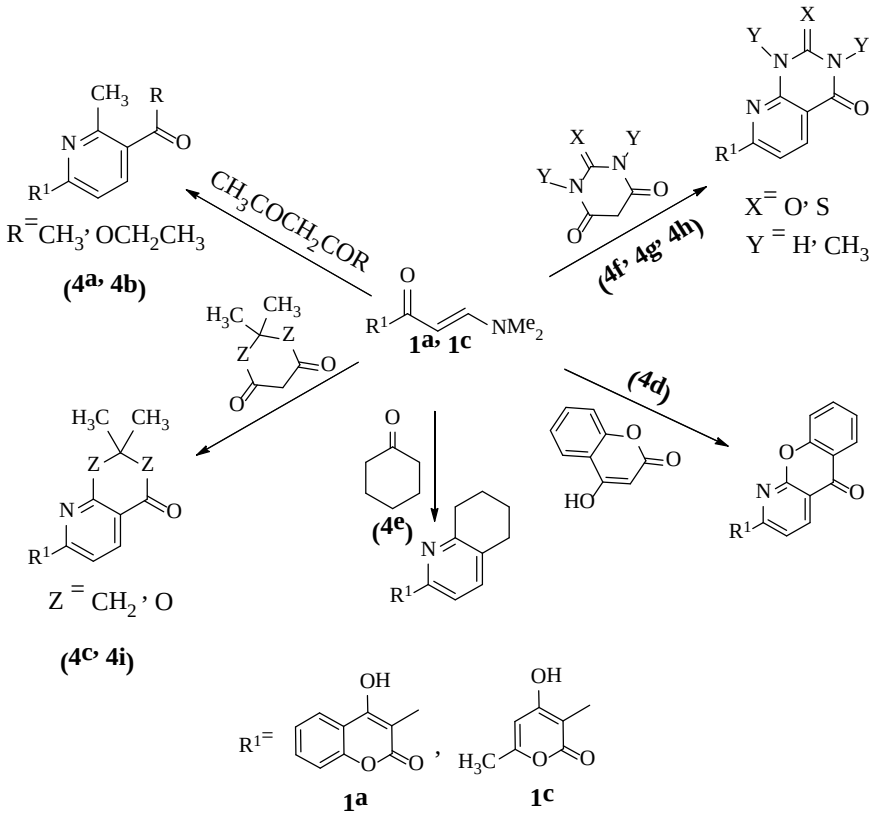

Scheme 4

CHAPTER 3:

Sulphated silica tungstic acid: an efficient and recyclable heterogeneous catalyst for the synthesis of tetrahydropyrimidines and dihydropyrimidines

Tetrahydropyrimidines (THPMs)/ Dihydropyrimidines (DHPMs) represent an important group of highly valuable heterocyclic motifs in the field of medicinal chemistry. THPMs are found in both natural as well as synthetic organic compounds. Many THPMs containing an amino acid show interesting and diverse pharmacological profiles like HIV protease inhibiting, antineoplastic, antiproleferative, herbicidal, muscarinic agonist, anti-inflammatory and antiviral activities. DHPMs usually display various biological activities such as calcium channel modulators, adrenergic receptor antagonist, mitotic kinesin inhibitor, antiviral, antibacterial, etc. and compounds such as enastron, monastrol and piperastrol are well known biologically active DHPMs which have already been developed into drugs.

Immobilization of catalysts on solid support is an ideal method for combining the advantages of homogeneous catalysts with the advantages of heterogeneous catalysts which leads to clean chemical synthesis from both environmental and commercial

point of view. In modern material science, silica is the ubiquitous inorganic platform used in systems designed for catalysis, separation, filtration, sensing, optoelectronics and environmental technology. Due to the favourable chemical and physical properties of silica surfaces, it is possible to impart nearly any reactive functional group that one requires on a silica surface (e.g., sulfonic, amine, carboxyl, thiol, epoxy, and so forth) through well-known silane chemistry. Taking advantages of the mentioned properties of silica, in this chapter, we have described the synthesis of sulphated silica immobilized tungstic acid (SSTA) and used it for three-component synthesis of THPMs/DHPMs **(8a-w)** by using aldehydes **(2a-b, 2d-g, 6a-f)**, active methylene compounds **(4a-b, 7a-b)** and urea under solvent-free conditions **(Scheme 7)**. The catalyst was characterized by FT-IR, XRD and SEM-EDX analyses. The stability of the catalyst was evaluated by TG analysis. The optimum concentration of H^+ of SSTA was found to be 0.40 meq/gram of the support. The catalyst can be reused for six cycles without any significant loss of activity.

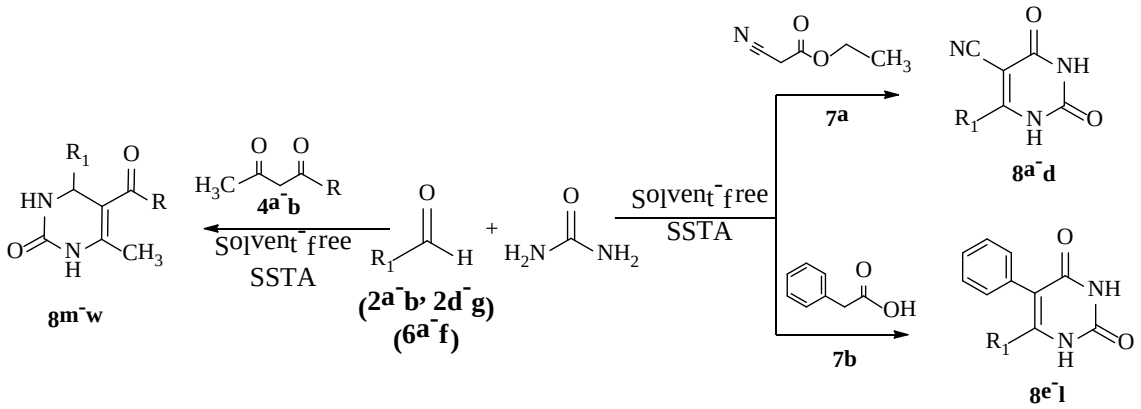

Scheme 7

CHAPTER 4:

Chitosan as a support for dispersion of catalytically active lanthanides

In recent years, biopolymers have gained a lot of attention for their use as supporting materials. Chitosan, a biodegradable polymer derived from marine waste in very large quantities, is optimally suited for this purpose. The interesting chemo-physical and biological properties of chitosan like, hydrophilic character, biodegradability, non-toxicity and biocompatibility provide a wide spectrum of opportunities for the development of functional materials. Inertness toward air and moisture, and easy chemical modifications due to the presence of both amino and hydroxyl groups, make it a versatile supporting material. This chapter is divided into two sections involving immobilization of Ce(III) and Dy(III) nanoparticles on chitosan and their application

as catalysts for the synthesis of spiropiperidine and hexahydropyrimidine derivatives under green reaction conditions.

Section A: Sustainable synthesis of spiropiperidine derivatives using cerium(III) immobilised chitosan as an efficient and recyclable heterogeneous catalyst

The piperidine ring unit forms the core of a large family of alkaloids and natural products with strong medicinal and interesting structural properties. Recently spiro-substituted piperidines have received considerable attention due to their important pharmacological profiles like selective and potent σ receptor ligands which can be used in the treatment of cocaine abuse, depressions, and epileptic disorders and 5-HT_{2B} receptor antagonists. In addition various plant alkaloids (sibirine, nitramine, isonitramine and nitrabirine) and animal toxins also contain spiropiperidine ring systems.

Cerium(III) halides have been found to be effective Lewis acid catalysts for organic transformations. Their water tolerant nature, low toxicity, easy to handle, easy availability and property of reusability without further purification have made them ideal choice for sustainable organic synthesis. Irrespective of these properties, their use in stoichiometric amounts is the main limitation from economic and environmental view point. Therefore, it is very important to develop a heterogenised version of Ce(III) salts to make them more environment friendly. In this context, this section describes the use of chitosan as a support for Ce(III) chloride and its application for the synthesis of spiropiperidine derivatives **(10a-o)** via multicomponent reaction of anilines **(9a-e)**, formaldehyde and active methylene compounds **(4c-d, 4j)** at room temperature in PEG-200 **(Scheme 10)**. The catalyst was characterized by FT-IR, XRD, SEM, EDX, TEM and ICP-AES analyses. The catalyst was found to retain its activity for a minimum of five catalytic cycles.

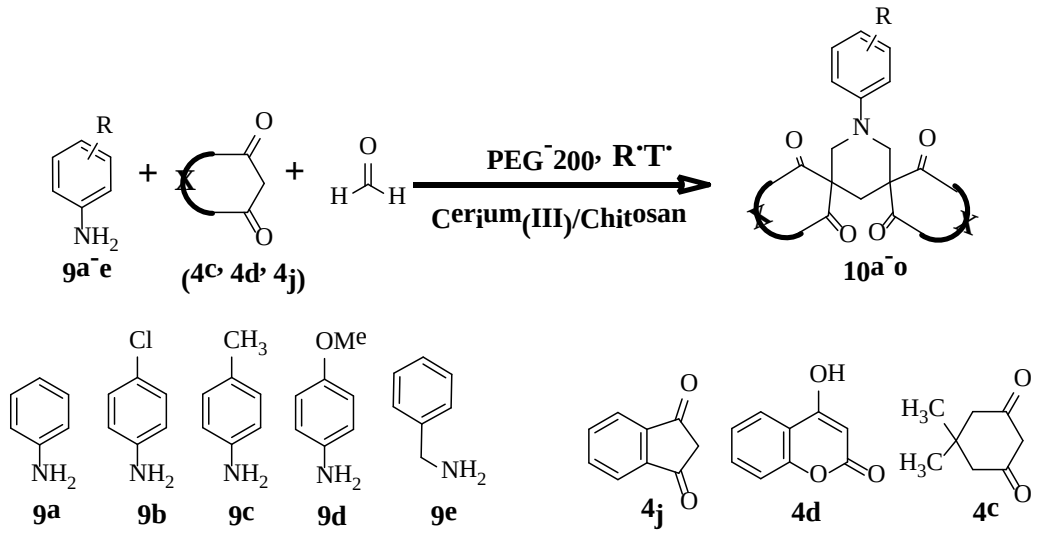

Scheme 10

Section B: Dysprosium(III) on chitosan: A recyclable heterogeneous catalyst for the synthesis of hexahydropyrimidines in water

Hexahydropyrimidines are one of the most commonly encountered heterocycles in medicinal chemistry with various biological profiles such as antibacterial, antiviral, antitumor and anti-inflammatory activities. These derivatives are also found in a number of alkaloids such as verbamethine and verbametrine. *N*-Substituted hexahydropyrimidines serve as key synthetic intermediates for spermidine-nitroimidazole drugs used for the treatment of A549 lung carcinoma. New trypanothione reductase inhibiting ligands used for the regulation of oxidative stress in parasite cells also contain this structural unit. Recently, appropriately substituted hexahydropyrimidines were found to be potent hepatitis C virus inhibitors.

Dysprosium (III) is an extremely mild and efficient Lewis acid catalyst having the ability to promote various types of carbon-carbon bond forming reactions, electrocyclizations and cycloadditions. It also exhibits similar stability towards air and water, ease of handling, Lewis acidity and oxophilicity as compared to other lanthanides. In this context, this section describes chitosan supported Dy(III) catalyzed eco-friendly synthesis of hexahydropyrimidine derivatives **(11a-l)** using aromatic amines **(9a-d ,9f)**, formaldehyde and active methylene compounds **(4b,4c,7a)** at room temperature in water (**Scheme 13)**. The catalyst was characterized by FT-IR, XRD, SEM, EDX, elemental mapping, TEM, ICP-AES and TG analyses. The catalyst was found to be recyclable up to six catalytic cycles.

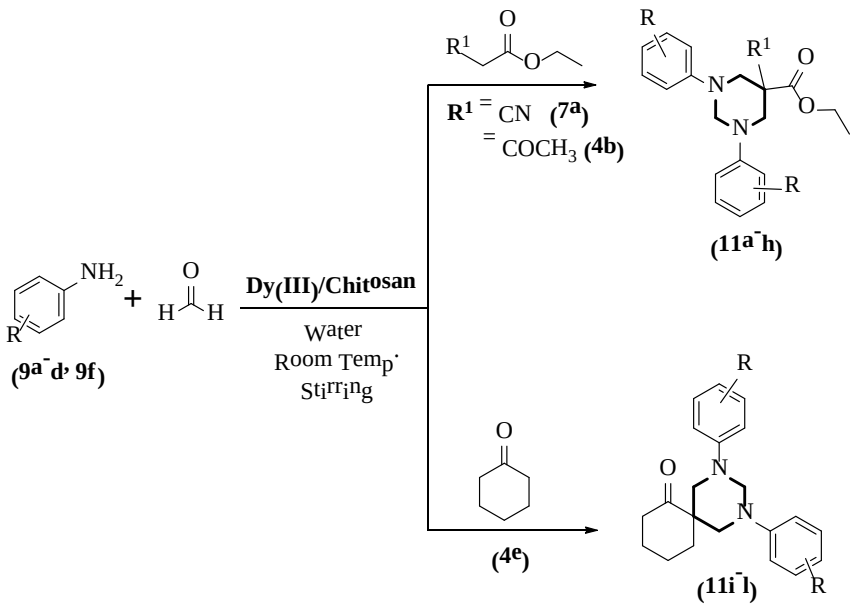

Scheme 13

CHAPTER 5: Silica molybdic acid (SMA) catalysed multicomponent synthesis of tetrazole derivatives under microwave irradiation in aqueous media

Among various heterocycles tetrazoles and their derivatives represent an important class of *N*-containing heterocycles. 5-substituted tetrazoles are reported to possess biological profiles like potential drugs against schizophrenia and cerebral ischemia, antidiabetic, antiviral, antibacterial and antihypertensive activities. These compounds are regarded as important synthetic intermediates in synthetic organic chemistry and also show very good coordination properties. Being resistant to biological degradation, these derivatives have been used as isosteric substitutes for various functional groups in order to develop them as potential medicinal agents.

Heterogeneous catalysis is clearly on the rise in chemical industries due to increasing concerns about the development of new processes that minimize pollution. Among various heterogeneous catalysts developed over the past decades, silica supported catalysts have been the favourites, due to many advantageous properties of silica like excellent chemical and thermal stability, high surface area, good accessibility, and active components can be robustly anchored to the surface to provide well dispersed catalytic centres. Therefore, this chapter describes the synthesis of silica supported molybdic acid **(SMA)** and evaluation of its catalytic activity for the synthesis of functionalized tetrazole derivatives **(12a-l)** *via* three component reaction of aldehydes **(6a-c, 6e-i, 2b-c, 2e, 2i)**, malononitrile **(7c)** and sodium azide in water under microwave irradiation **(Scheme 16)**. The use of microwave (MW) irradiations as a

heat source represents a good alternative to conventional heating in the context of reducing the environmental impact of a synthetic process. The presented protocol tolerated aldehydes with diverse structural motifs giving corresponding tetrazoles in excellent yields (89-95%) and the catalyst was found to maintain good activity for a minimum of seven reaction cycles. The catalyst was characterized by FT-IR, XRD, XRF, SEM, EDX, elemental mapping and TG analyses. The amount of H^+ of the catalyst, calculated by back titration analysis, was found to be equal to 0.23 meq/gm of the catalyst.

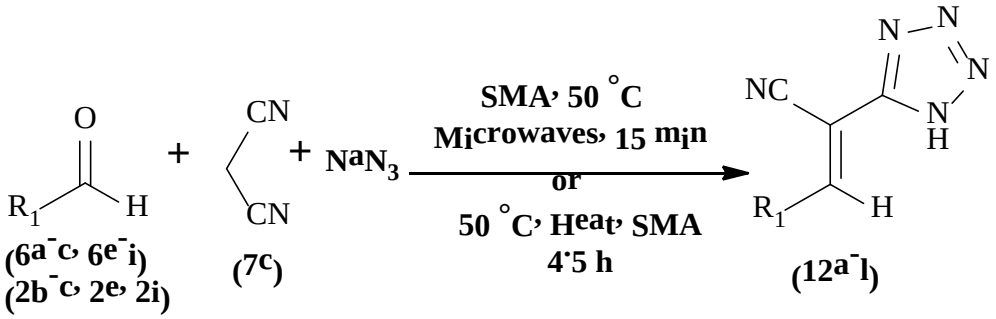

(6a-c, 6e-i)
(2b-c, 2e, 2i)
(7c)
(12a-l)

Scheme 16

CANDIDATE'S DECLARATION

I, **Nayeem Ahmed,** Department of **Chemistry** certify that the work embodied in this Ph.D thesis is my own bonafide work carried out by me under the supervision of **Prof. Zeba N. Siddiqui** at Aligarh Muslim University, Aligarh. The matter embodied in this Ph.D. thesis has not been submitted for the award of any other degree.

I declare that I have faithfully acknowledged, given credit to and referred to the research workers wherever their works have been cited in the text and the body of the thesis. I further certify that I have not willfully lifted up some other's work, para, text, data, result, etc. reported in the journals, books, magazines, reports, dissertations, thesis, etc., or available at web-sites and included them in this Ph.D. thesis and cited as my own work.

Date: ..... **(Signature of the candidate)**

NAYEEM AHMED
(Name of the candidate)

Certificate from the Supervisor

This is to certify that the above statement made by the candidate is correct to the best of our knowledge.

Signature of the Supervisor
Name & Designation: Dr. Zeba N. Siddiqui, Professor
Department: CHEMISTRY

(Signature of the Chairman of the Department with seal)

COURSE/ COMPREHENSIVE EXAMINATION/ PRE-SUBMISSION SEMINAR COMPLETION CERTIFICATE

This is to certify that Mr. **Nayeem Ahmed,** Department of **Chemistry** has satisfactorily completed the course work/comprehensive examination and pre-submission seminar requirement which is part of his Ph.D. programme.

Date: ……. **(Signature of the Chairman of the Department)**

COPYRIGHT TRANSFER CERTIFICATE

Title of the Thesis: **SYNTHESIS AND APPLICATIONS OF GREEN CATALYSTS IN ORGANIC SYNTHESIS: HETEROGENEOUS CATALYSIS BY SOLID SUPPORTED COMPOUNDS AND NANOPARTICLES**

Candidate's Name: **NAYEEM AHMED**

Copyright Transfer

The undersigned hereby assigns to the Aligarh Muslim University, Aligarh, copyright that may exist in and for the above thesis submitted for the award of Ph.D. degree.

(Signature of the Candidate)

Note: However, the author may reproduce or authorize others to reproduce material extracted verbatim from the thesis or derivative of the thesis for author's personal use provided that the source and the university's copyright notice are indicated

Dedicated to
my
Family

ACKNOWLEDGEMENTS

This is probably the most difficult part of this work to write, because printed words fail to express the depth of feelings hidden behind them and convey the actual extent of influence others cast on one's work or life. Before I proceed to mention at least a few special persons without whose support, co-operation and contribution, this work would have never come to fruition, let me express my deepest faith in Almighty Allah, the Omnipotent, the Omnipresent for it is indeed His blessings which provided me enough zeal to complete this work.

A debt of gratitude to my supervisor, **Prof. Zeba N. Siddiqui**, Department of Chemistry, Aligarh Muslim University, Aligarh, for her generosity, faith, encouragement and excellent guidance, that has been instrumental in completion of this thesis. The discussions with her were always a lifeline for new thoughts. Her valuable suggestions added to the output of the research, inspired me to have a better grip over my research field.

I am thankful to **Prof. M. Shakir**, Chairman, Department of Chemistry, Aligarh Muslim University, Aligarh, for providing the necessary research facilities.

I gratefully acknowledge the financial help from **UGC** in the form of Basic Scientific Research (**BSR)** Fellowship, and **CSIR** in the form of Senior Research Fellowship **(SRF)**. Financial assistance from UGC **DRS-II** is duly acknowledged.

Thanks are due to University Sophisticated Instrument Facility (USIF), Department of Physics and Department of Applied Physics, Aligarh Muslim University, Aligarh, for providing the SEM, TEM and XRD facilities. Thanks

also to SAIF Punjab University, Chandigarh, SAIF CDRI Lucknow and SAIF IIT Mumbai for providing NMR, Mass and ICP-AES spectral facilities.

I render my special thanks to my lab colleagues Dr. Farheen, Dr. Tabassum, Dr. Kulsum, Saima, Shaheen and Ryhaan for their help, and coordination extended by them.

Thanks to all my dear friends, Adil, Owais Mehraj, Dr. Irfan ul Haq, Dr. Niyaz A. Mir, Fayaz A. Bhat, Dr. Javid Ganie, Nazir Ahmad, Imtiyaz Rasool, Sheraz A. Bhat, Rayees A. Bhat, Tariq Mushtaq, Dr. Ashraf Mashrai, Tawseef, Himanshu, M. Sharique, M. Arsalan, Waseem, Asif, Abad, Khairoo, Faheem, Sharique, Tabassum Wajid, Ishfaq, Shakeel, Farooq, Bilal Masood, Shah Tariq, Imtiyaz Yousuf, Imtiyaz Bhat, and all those who have always stood by me.

Thanks also to Dr. M. Musthafa, Dr. M. Asad and Dr. Shawkat for their support and guidance.

I would like to express my gratitude to my parents and all the family members who have always been a source of inspiration and encouragement. Special thanks to my brothers, sisters and little children at home, who have been a bundle of joy in my life.

Nayeem Ahmed

CONTENTS

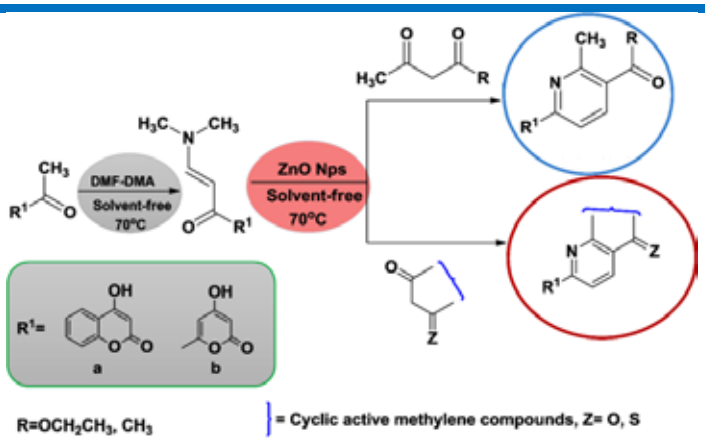

CHAPTER-3

SULPHATED SILICA TUNGSTIC ACID: AN EFFICIENT AND RECYCLABLE HETEROGENEOUS CATALYST FOR THE SYNTHESIS OF TETRAHYDROPYRIMIDINES AND DIHYDROPYRIMIDINES

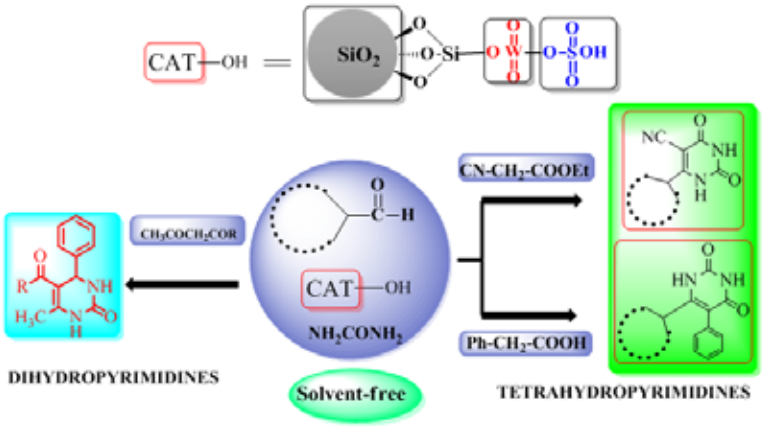

CHAPTER-4

CHITOSAN AS A SUPPORT FOR DISPERSION OF CATALYTICALLY ACTIVE LANTHANIDES

SECTION A

SUSTAINABLE SYNTHESIS OF SPIROPIPERIDINE DERIVATIVES USING CERIUM(III) IMMOBILISED CHITOSAN AS AN EFFICIENT AND RECYCLABLE HETEROGENEOUS CATALYST

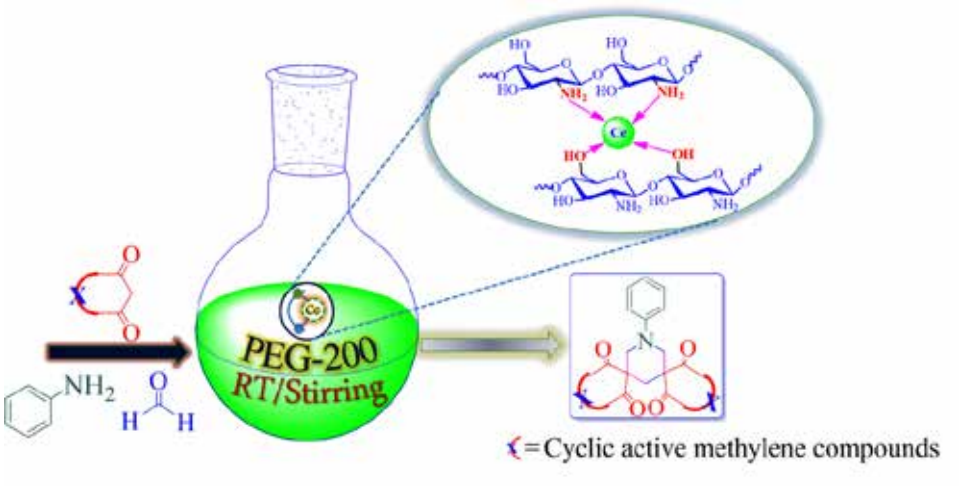

SECTION B:

DYSPROSIUM(III) ON CHITOSAN: A RECYCLABLE HETEROGENEOUS CATALYST FOR THE SYNTHESIS OF HEXAHYDROPYRIMIDINES IN WATER

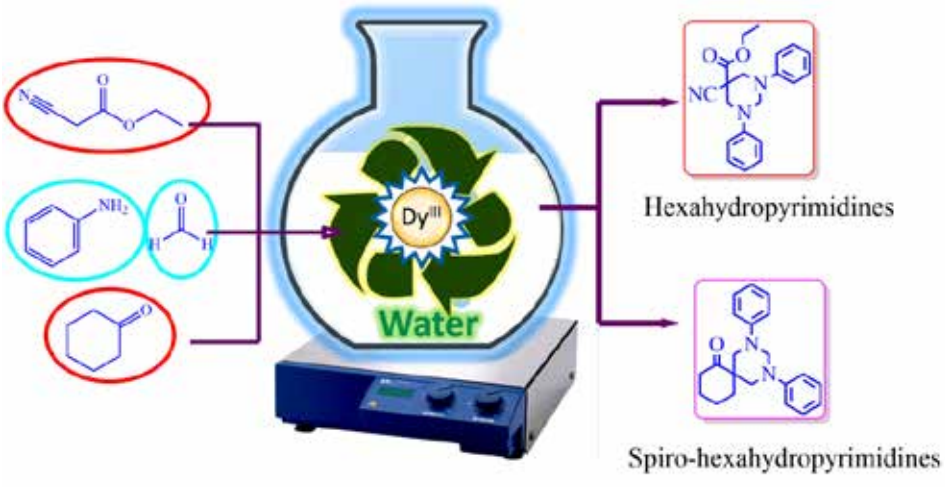

CHAPTER-5

SILICA MOLYBDIC ACID (SMA) CATALYSED MULTICOMPONENT SYNTHESIS OF TETRAZOLE DERIVATIVES UNDER MICROWAVE IRRADIATION IN AQUEOUS MEDIA

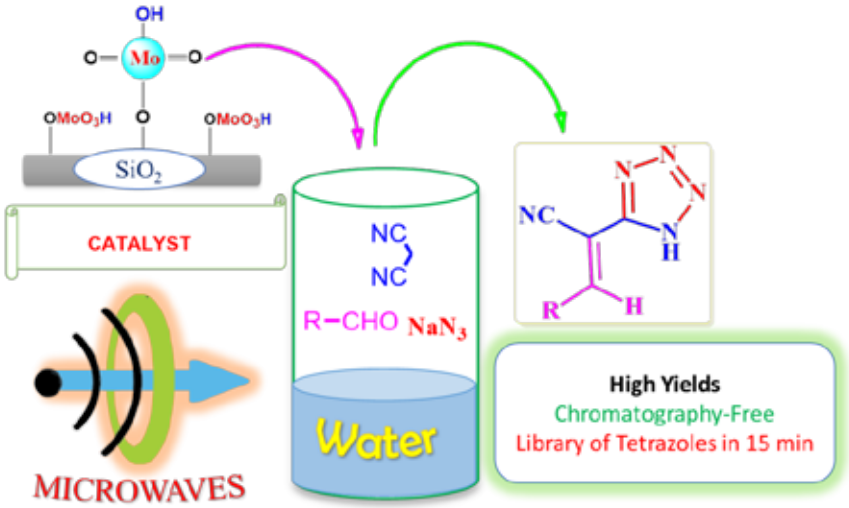

PUBLISHED PAPERS

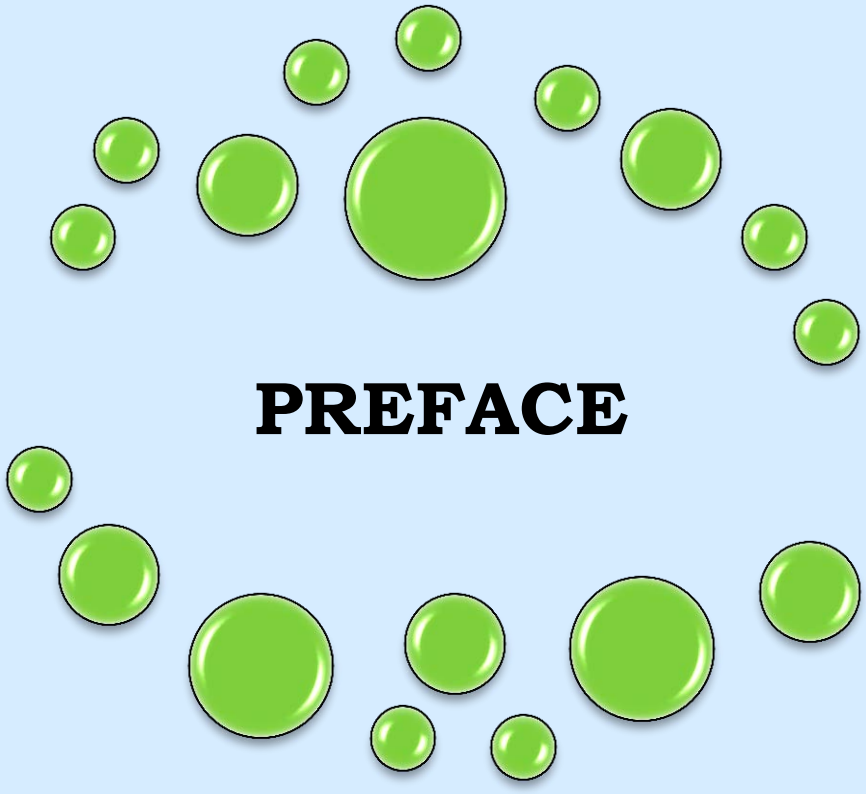

PREFACE

PREFACE

Green chemistry, also known as sustainable chemistry, is the design of chemical products and processes that reduce or eliminate the use or generation of hazardous substances. Green chemistry can be defined as the practice of chemical science and manufacturing in a manner that is sustainable, safe, non-polluting and consumes minimum amount of materials and energy. Developing green chemistry methodologies is a challenge that may be viewed through the framework of the 'Twelve Principles of Green Chemistry'. These principles identify catalysis as one of the most important tools for implementing green chemistry. In recent years, heterogeneous catalysts have gained much attention as a result of economic and environmental benefits. They make synthetic processes clean, safe and high-yielding. Therefore, the development of selective and reusable solid catalysts for organic reactions has been a very active area of research.

Heterocycles constitute one of the largest areas of research in organic chemistry. The majority of pharmaceuticals and agrochemicals are heterocycles while countless additives and modifiers used in industries ranging from cosmetics, information storage and plastics are also heterocyclic in nature. As a majority of drug-like compounds and natural products contain a heterocyclic nucleus at their core, ever increasing attention has been paid towards the development of novel clean processes employing nontoxic reagents, catalysts and solvents for the synthesis of important heterocycles.

The work embodied in the thesis entitled **"Synthesis and Applications of Green Catalysts in Organic Synthesis: Heterogeneous Catalysis by Solid Supported Compounds and Nanoparticles"** deals with the design and synthesis of heterogeneous catalysts and their applications for the synthesis of biologically relevant heterocyclic compounds. To discuss systematically, the thesis is divided into five chapters, which are as follows:

CHAPTER 1

Application of clean technologies in chemical synthesis has currently been the major area of focus in green chemistry. The eco-friendly and reusable heterogeneous catalysts have till now been the leaders in providing such clean technologies. Therefore, the catalysts which make the organic reactions environmentally benign and economically feasible are extremely demanded by the chemical industries. This

chapter describes the scope of the present work and gives insights about green chemistry and its importance in organic synthesis, heterogeneous catalysis by supported compounds and nanoparticles, nitrogen containing heterocycles and their biological importance, and green chemical pathways *viz* multicomponent reactions, solvent-free reactions and reactions in sustainable media.

CHAPTER 2

β-Enaminones are readily obtainable, versatile reagents used for the synthesis of novel heterocyclic compounds and drug intermediates. These compounds show both the nucleophilic and electrophilic characters and have therefore, been used as synthetic intermediates for the synthesis of many biologically important compounds. This chapter is dedicated to the synthesis of different kinds of heterocycles under different conditions and contains two sections-A and B.

Section A

Among the many nitrogen containing heterocycles, 1,4-dihydropyridine substructures are among the most prevalent having versatile biological profiles such as selective adenosine-A3 receptor antagonism, sirtuin activation and inhibition, antitumor, antidiabetic, anticonvulsant photosensitizing and radioprotective activities. The immobilization of a homogeneous catalyst on a solid surface is one of the major challenges in catalysis as it facilitates the separation of the catalyst and the reaction products, and also gives rise to reusability of the catalyst. In this section, we have synthesised mesoporous alumina sulphuric acid as a heterogeneous and recyclable solid acid catalyst and evaluated its catalytic efficiency for the synthesis of 1,4-dihydropyridine derivatives **(3a-n)** via pseudo four component addition and cyclisation involving β-enaminone **(1a-b)**, different aldehydes **(2a-g)** and ammonium acetate in aqueous media. The catalyst showed excellent catalytic activity giving products in high yields **(81-90%)** and could be reused for seven successive catalytic cycles. The substrate scope of the reaction was demonstrated by successful tolerance of aromatic aldehydes with electron donating/electron withdrawing groups as well as aliphatic/alicyclic aldehydes. The catalyst was characterized by FT-IR, XRD, FE-SEM, EDX and TG analyses. The mesoporosity of alumina was determined by BET and TEM analyses.

Section B

Pyridine derivatives widely occur as key structural subunits in various natural products that exhibit many interesting biological profiles like anti-prion, anti-hepatitis

B virus, anti-bacterial and anti-cancer activities. These derivatives are also present in drugs used for the treatment of Parkinson's disease, hypoxia, asthma, kidney disease, epilepsy, cancer, and Creutzfeldt–Jacob disease. ZnO NPs, due to their cheapness, easy to synthesise, requirement of mild conditions and non-toxic nature have proven to be successful catalysts for several organic transformations. Therefore, in this section, the synthesis of pyranyl pyridine derivatives **(5a-p)** involving the reaction of β-enaminone **(1a, 1c)**, active methylene compounds **(4a-i)** and ammonium acetate under solvent-free conditions, using ZnO NPs as catalyst has been described. The catalyst showed excellent catalytic activity giving pyridine derivatives in excellent yields **(91-96%)** and was recyclable up to six cycles. ZnO nanoparticles were characterized by XRD, SEM and TEM analyses, and the final products were characterized by using IR, ^{1}H, ^{13}C NMR, ESI-MS and elemental analyses techniques.

CHAPTER 3

Tetrahydropyrimidines (THPMs)/ Dihydropyrimidines (DHPMs) represent an important group of highly valuable heterocyclic motifs in the field of medicinal chemistry showing diverse pharmacological profiles like calcium channel modulators, HIV protease inhibiting, antineoplastic, anti-inflammatory, antiviral, antiproleferative, herbicidal, and antibacterial activities. Silica supported catalysts are innovative heterogeneous catalysts which have found a special place in green chemistry. Because of many advantageous properties of silica like excellent chemical and thermal stability, high surface area and good accessibility, its use as supporting material has grown manifold. In this chapter we have discussed the synthesis and catalytic application of sulphated silica immobilized tungstic acid **(SSTA)**. The catalyst was evaluated for its catalytic activity by synthesizing THPMs/DHPMs **(8a-w)** from aldehydes **(2a-b, 2d-g, 6a-f)** active methylene compounds **(4a-b, 7a-b)** and urea under solvent-free conditions. The catalyst was found to be highly efficient affording the products in excellent yield **(82-96%)** in short time period (8-31 min). The catalyst was characterized by FT-IR, XRD SEM-EDX and TG analyses. The structures of the final products were elucidated by using IR, ^{1}H, ^{13}C NMR, ESI-MS and elemental analyses techniques.

CHAPTER 4

In the last decades, lanthanides as Lewis acids have found widespread use in the development of green chemistry as mild and efficient catalysts. A prominent feature of lanthanides is their stability and activity in protic media, making them ideal for use

as stable Lewis acids in water. Chitosan, a biodegradable polymer has gained a lot of attention for its use as supporting material in catalysis. It's interesting chemo-physical properties like, hydrophilic character, biodegradability, non-toxicity, inertness toward air and moisture, and easy chemical modifications due to the presence of both amino and hydroxyl groups make it a versatile supporting material. This chapter describes synthesis of spiropiperidines and hexahydropyrimidines under different reaction conditions and is divided into sections-A and B.

Section A

Ce(III) salts as Lewis acids have been extensively used in reduction, C−C, C−N and C−O bond formation reactions. This extensive use of Ce(III) salts is attributed to their properties like moderate to low toxicity, water tolerance, easy to handle, availability at moderate cost and suitability for use without purification. Spiro-substituted piperidines have received considerable attention because of their important pharmacological profiles like selective and potent σ receptor ligands that can be used in the treatment of cocaine abuse, depression and epileptic disorders, and 5-HT_{2B} receptor antagonists. These motifs are also found in large family of alkaloids and natural products with strong biological profiles and interesting structural properties. In this section chitosan has been used as a support for the dispersion of catalytically active Ce(III) species and used for the synthesis of spiropiperidine derivatives **(10a-o)** via multicomponent reaction of substituted anilines **(9a-e)**, formaldehyde and different active methylene compounds **(4c-d, 4j)** at room temperature in PEG-200. The catalyst was characterized by FT-IR, XRD, SEM, EDX, TEM and ICP-AES analyses. The structures of spiropiperidines were characterized by IR, ^{1}H & ^{13}C NMR, ESI-MS and elemental analyses techniques. The catalyst was found to retain its activity for a minimum of five catalytic cycles.

Section B

In the field of medicinal chemistry hexahydropyrimidine derivatives are one of the most commonly encountered structures with various biological profiles such as antibacterial, antiviral, antitumor and anti-inflammatory activities. These derivatives are found in a number of alkaloids and also serve as key synthetic intermediates for spermidine-nitroimidazole drugs. Dysprosium(III) is an extremely mild and efficient Lewis acid catalyst having the ability to promote various types of carbon–carbon bond forming reactions, electrocyclizations and cycloadditions. In this context, this section deals with the catalytic evaluation of chitosan supported Dy(III) species for the

synthesis of hexahydropyrimidine derivatives **(11a-l)** employing amines **(9a-d, 9f)**, formaldehyde and active methylene compounds **(4b,4c,7a)** at room temperature in water. The structures of the final products were elucidated by using spectral (IR, ^{1}H, ^{13}C NMR and ESI-MS) and elemental analysis data. The catalyst was characterized by FT-IR, XRD, SEM, EDX, Elemental mapping, TEM, ICP-AES and TG analyses. The catalyst was found to be recyclable up to six catalytic cycles.

CHAPTER 5

Tetrazole derivatives represent an important class of *N*-containing heterocycles reported to possess biological profiles like potential drugs against schizophrenia and cerebral ischemia, antidiabetic, antiviral, antibacterial and antihypertensive activities. The close similarity between the acidity of tetrazole group and carboxylic group has led to their development as potential bioisosteric replacements for carboxylic acid groups. They also serve as important synthons in synthetic organic chemistry and as ligands in coordination chemistry. In modern material science, silica is the most commonly used inorganic supporting material in systems designed for catalysis. Due to the favourable chemical and physical properties of silica surfaces, it is possible to impart nearly any reactive functional group through well-known silane chemistry. In this context, this chapter deals with the synthesis of silica supported molybdic acid **(SMA)** and evaluation of its catalytic activity for the synthesis of functionalized tetrazole derivatives **(12a-l)** via three component reaction of aldehydes **(6a-c, 6e-i, 2b-c, 2e, 2i)**, malononitrile **(7c)** and sodium azide in water using microwave irradiation. The presented protocol tolerated aldehydes with diverse structural motifs giving corresponding tetrazoles in excellent yield (89-95%). The catalyst was characterized by FT-IR, XRD, XRF, SEM, EDX, elemental mapping and TG analyses, and was found to maintain good activity for a minimum of seven reaction cycles.

Abbreviations and Symbols

AcOH	Acetic acid
Aq.	Aqueous
BET	Brunauer–Emmett–Teller
Bz	Benzyl
$CDCl_3$	Deuterated chloroform
$CHCl_3$	Chloroform
CSA	Camphor sulfonic acid
DCM	Dichloromethane
DMF	N, N-Dimethylformamide
DMSO	Dimethyl sulfoxide
EtOH	Ethanol
FT-IR	Fourier transform infrared
g	Gram
h or hrs	Hours
Hz	Hertz
Me	Methyl
MeOH	Methanol
mg	Milligram
mL	Millilitre
mmol	Millimole
M.p.	Melting point
meq.	milliequivalent
M.W.	Molecular weight
MW	Microwave
NMR	Nuclear magnetic resonance
PEG	Poly ethylene glycol
p-TSA/TsOH	*para*-Toluenesulfonic acid
RT	Room temperature
SMA	Silica molybdic acid
STA	Silica tungstic acid
SSTA	Sulphated silica tungstic acid

GENERAL REMARKS

- Melting points were determined on a Reichert Thermovar instrument and are uncorrected.
- The ^{1}H NMR and ^{13}C NMR spectra were recorded on Bruker DRX-300 and Bruker Avance II-400 Spectrometer using tetramethyl silane (TMS) as an internal standard, DMSO-d_6/$CDCl_3$ as solvent. Chemical shifts are reported in ppm downfield from TMS as internal standard and coupling constants *J* are given in Hz.
- The micro-analytical data were collected on an Elementar vario EL III elemental analyser and their results were found to be in agreement with the calculated values.
- FT-IR spectra were obtained using a Perkin–Elmer RXI spectrometer in KBr. The spectra were recorded in the 400–4000 cm^{-1} wave-number range.
- Mass spectra were obtained on Micromass Quattro II (ESI) and THERMO Finnigan LCQ Advantage max ion trap mass (ESI-MS) spectrometer.
- All starting materials of commercial grade were purchased from Sigma-Aldrich (Switzerland), Merck (Mumbai, India) and used without further purification.
- The purity of all compounds was checked by TLC on glass plates coated with silica gel (E-Merck G_{254}). The plates were run in chloroform-methanol (3:1) mixture as mobile phase and were visualized by iodine vapours.
- X-ray diffractograms (XRD) of the catalyst were recorded in the 2θ range of 10–80° (scan rate of 4° min^{-1}) on a Rigaku Miniflex X-ray diffractometer with Ni-filtered Cu Kα radiation at a wavelength of 1.54060°A.
- The SEM-EDX analyses was done using a JEOL JSM-6510 scanning electron microscope equipped with energy dispersive X-ray spectrometer (acc. voltage: 20 kV) at different magnification.
- Transmission electron microscope (TEM) images were obtained using JEM-2100 F model (acc. voltage: 200 kV) with magnification up to 100000x.
- Thermogravimetric (TG) analysis data was obtained with a DTG-60H, with a heating rate of 25 °C min^{-1} from 100 to 1000 °C under N_2 atmosphere.
- Nitrogen adsorption–desorption isotherms were obtained using a Quantachrome Autosorb 1C at 77 K.
- ICP-AES analysis was performed on ARCOS from M/s. Spectro, Germany.
- The FE-SEM characterization of the catalyst was performed on QUANTA 200 FEG from FEI Netherlands.
- Microwave synthesis was carried out using Microwave Synthesis Reactor, monowave 300 (Anton paar).

LIST OF PUBLICATIONS

Publications from the research work presented in the thesis

1. Zeba N. Siddiqui, **Nayeem Ahmed**, Farheen Farooq and Kulsum Khan, ***Tetrahedron Letters***, 54 (2013) 3599.

2. **Nayeem Ahmed** and Zeba N. Siddiqui, ***Journal of Molecular Catalysis A: Chemical***, 394 (2014) 232.

3. **Nayeem Ahmed** and Zeba N. Siddiqui, ***Journal of Molecular Catalysis A: Chemical,*** 387 (2014) 45.

4. **Nayeem Ahmed** and Zeba N. Siddiqui, ***ACS Sustainable Chemistry & Engineering***, 3 (2015) 1701.

5. **Nayeem Ahmed**, Saima Tarannum and Zeba N. Siddiqui, ***RSC Advances***, 5 (2015) 50691.

6. **Nayeem Ahmed** and Zeba N. Siddiqui, ***RSC Advances***, 5 (2015) 16707.

CHAPTER 1

GENERAL INTRODUCTION

GENERAL INTRODUCTION

It is widely acknowledged that there is a growing need for more environmentally acceptable processes in the chemical industry. This trend towards what has become known as 'Green Chemistry' puts forward sustainable concepts, which are designed to reduce or eliminate chemicals and chemical processes that have negative environmental impacts. *A reasonable definition of green chemistry is formulated as: Green chemistry efficiently utilizes (preferably renewable) raw materials, eliminates waste and avoids the use of toxic and/or hazardous reagents and solvents in the manufacture and application of chemical products.*[1] Green chemistry addresses the environmental impact of both chemical products and the processes by which they are produced. It primarily aims to eliminate waste at source rather than at the end. An alternative term, which is currently favoured by the chemical industry, is sustainable technologies. *Sustainable development has been defined as meeting the needs of the present generation without compromising the ability of future generations to meet their own needs.*[2]

1.1. *Heterogeneous catalysis:*

Catalysis is one of the main pillars of "green chemistry", and the development of environmentally benign catalysts is one of the vital challenges faced by the chemists.[3] A sustainable and "green" catalyst must, therefore, possess specific features including low preparation cost, high activity, great selectivity, high stability, efficient recovery, and recyclability. Heterogeneous catalysis involves a system in which a catalyst exists in a different phase to that of the reactants. Generally, the catalyst is usually a solid and the reactants are either gases or liquids. In recent years, heterogeneous catalysts have gained much attention, as a result of economic and environmental benefits. They make synthetic processes clean, safe and high-yielding.[4] The use of heterogeneous solid catalysts being in a different phase than the reagents and products have an obvious advantage in terms of easy separation from the reaction mixture, allowing the recovery of the solid and eventually its reuse, provided that the solid (catalyst) has not become deactivated during the course of the reaction.[5]

The development of selective and reusable solid catalysts for organic reactions has been a very active area of research. Acid catalysed processes play a key role in pharmaceutical, agrochemical and oil refining industries.[6-7] They are also used in the manufacture of a wide variety of specialty chemicals such as, flavours and fragrances.[8] Many of these processes involve the use of traditional Brønsted acids

(H_2SO_4, HF, HCl, *p*-toluenesulfonic acid etc.) or Lewis acids ($AlCl_3$, $ZnCl_2$, BF_3 etc.) as catalysts under homogeneous conditions and their subsequent neutralization leads to the generation of inorganic salts which eventually end up in aqueous waste streams. Therefore, the promising solution to this problem of salt generation is the replacement of traditional Brønsted and Lewis acids with recyclable solid acids and bases.[9-13] The benefits of using the recyclable acid catalysts are outlined below:

- *Facilitation of separation and recycling which results in simpler processes and less production costs.*
- *Solid acids are safer and easier to handle than their highly corrosive and expensive liquid counterparts, e.g. H_2SO_4, HF.*
- *Use of solid acid evades the contamination of products by avoiding neutralization.*

With the advancement in nanoscience and nanotechnology, a wide variety of nano-catalysts or solid-supported nano-catalysts have been applied to various transformations.[14] These catalysts have proven to be highly successful because of their high activity and selectivity due to their small size (1–100 nm) and exposed active sites. However, the decrease in the size to nanometer scale causes rise in the surface free energy which leads to aggregation of the particles into small clusters and degrades the catalytic efficiency. Further, as the size of particles decreases to nano scale, separation through conventional means becomes difficult. Thus, in order to harness full potential of these nanoparticles it is very important to employ suitable support materials which will lead to the development of efficient and recyclable catalytic systems.

1.2. *Nitrogen-containing heterocycles:*

Heterocycles by far form the largest of classical divisions of organic chemistry and have immense biological and industrial applications. The majority of pharmaceuticals and agrochemicals are heterocycles[15] while countless additives and modifiers used in industries ranging from cosmetics, information storage and plastics are also heterocyclic in nature. Nitrogen-containing heterocycles are widely distributed in nature and play a vital role in the metabolism of all living cells. Among nitrogen containing heterocycles, pyridine derivatives are important as they are present in many pharmacologically active compounds.[16-18] These derivatives possess large spectrum of biological activities such as anti-bacterial, anti-prion, anti-hepatitis B virus, and anti-cancer.[19] Some derivatives have become lead compounds in the search

of new drugs for Parkinson's disease, hypoxia, asthma, kidney disease, epilepsy, cancer, and Creutzfeldt–Jacob disease.[20-22] Naturally occurring compounds such as vitamins, niacin and pyridoxine, and a number of alkaloids including nicotine contain the pyridine nucleus. Due to their applications as herbicides, fungicides or bactericides these derivatives are also very important for the agrochemical industry.[23,24] The presence of pyridine ring in about 7000 drugs demonstrates the significance of these derivatives in pharmaceutical industries.[25,26]

The pyrimidine nucleus has wide occurrence in nature and is found in nucleotides, thiamine (vitamin B1) and alloxan (diabetes inducing compound).[27] Many synthetic compounds such as barbiturates and the HIV drug, zidovudine contain this nucleus. The presence of pyrimidine nucleus as base in thymine, cytosine and uracil, which are the essential binding blocks of DNA and RNA, is one possible reason for their activity. Many of the promising biological profiles shown by pyrimidine derivatives are anti-microbial, analgesic, anti-viral, anti-inflammatory, anti-HIV, anti-tubercular, anti-tumour, anti-neoplastic, anti-malarial and cardiovascular activities.[28]

1.3. *Green pathways:*

(i) *Multicomponent reactions (MCRs):*

Multicomponent reactions (MCRs) have recently gained much importance in synthetic organic chemistry. MCRs are defined as one-pot reactions in which at least three different substrates join through covalent bonds to give the product. They allow the creation of several bonds in a single operation and offer remarkable advantages like good synthetic efficiency, high intrinsic atom economy, good selectivity, and procedural simplicity. They are very important from green chemistry view point as they reduce the number of steps in a reaction, decrease energy consumption and minimize waste generation. The MCRs have been successfully used for the creation of diverse range of chemical libraries of drug-like compounds and therefore are widely used in pharmaceutical industries. Therefore, the design of new MCRs with improved efficiencies has been an area of great interest.[29]

(ii) *Solvent-free reactions:*

Due to growing concerns about the environment and human health, solvent-free organic synthesis has become a major area of focus in organic chemistry. Toxic, flammable and expensive nature of organic solvents have put the spot light on solvent-free reactions.[30] As solvents constitute the major part of waste generation in organic synthesis, solvent-free approach contributes to sustainability by eliminating or

minimising the waste generation. Overall, the advantages of solvent-free organic synthesis are shorter reaction times, cleaner reaction products and environmentally more benign conditions as compared with the classical reactions.[31]

(iii) *Green solvents:*

(a) *Polyethylene glycols (PEGs):*

Polyethylene glycols (PEGs) are inexpensive, non-toxic, non-volatile, thermally stable compounds which serve as suitable media for environmentally sustainable organic transformations. They are available in a wide range of molecular weights, and their complete toxicity profiles are also available. They are components in many consumer products such as shampoos and other personal care items, and have been approved by the U.S. Food and Drug Agency for internal consumption. Their solubility in water leads to easy separation and recovery of products from the reaction medium.[32-34]

(b) *Water:*

Water is the most abundant and environmentally benign solvent in nature and possesses the remarkable ability to catalyse chemical transformations between some insoluble organic reactants. This phenomenon is termed as “on-water” catalysis by Sharpless and co-workers and was first observed in the late 1930s and is only now being widely adopted.[35-38] Subsequent mechanistic studies have established that this behaviour results from enforced hydrophobic interactions[39] and stabilization of the activated complex by hydrogen-bond formation.[40] Therefore, performing the reactions in water constitutes a very important challenge for green chemistry, as the combination of the synthetic efficiency of multicomponent protocols and the environmental benefits of using water as the reaction medium, lead the processes close to the ideal synthetic reaction.

Keeping in view the importance of heterogeneous catalysts in the field of green chemistry and pharmaceutical industries, the research work undertaken involves the design and synthesis of heterogeneous catalysts and evaluation of their catalytic activity by synthesizing biologically relevant heterocyclic compounds. All the processes developed are highly efficient, green and environment friendly.

REFERENCES

1. R. A. Sheldon, C. R. Acad. Sci. Paris, IIc, Chimie/Chemistry, 3 (2000) 541.
2. C. G. Brundtland, Our Common Future, The World Commission on Environmental Development, Oxford University Press, Oxford, (1987).
3. R. A. Sheldon, I. Arends, U. Hanefeld, Green Chemistry and Catalysis, Wiley-vch, (2007).
4. A. Abad, P. Concepcion, A. Corma, H. Garcia, Angew. Chem. Int. Ed. 44 (2005) 4066.
5. J. A. Gladysz, Chem. Rev. 102 (2002) 3215.
6. B. W. Cue, J. Zhang, Green Chem. Lett. Rev. 2 (2009) 193.
7. (a) H. Hattori, Top. Catal. 53 (2010) 432; (b)Y. M. Sani, W. M. A. W. Daud, A.R. Abdul Aziz, Appl. Catal. A: Gen. 470 (2014) 140.
8. D. Rowe, Chemistry and Technology of Flavours and Fragrances, John Wiley & Sons, (2009).
9. R. A. Sheldon, H. van Bekkum (Eds.), Fine Chemicals through Heterogeneous Catalysis, Wiley-VCH, Weinheim, (2001).
10. W. Holderich, Catal. Today 62 (2000) 115.
11. A. Corma, H. Garcia, Chem. Rev. 103 (2003) 4307.
12. R. A. Sheldon, R. S. Downing, Appl. Catal. A: Gen. 189 (1999) 163.
13. A. Mitsutani, Catal. Today 73 (2002) 57.
14. S. B. Kalidindi, B. R. Jagirdar, ChemSusChem 5 (2012) 65.
15. R. Dua, S. Shrivastava, S. K. Sonwane, S. K. Srivastava, Advan. Biol. Res. 5 (2011) 120.
16. M. T. Cocco, C. Congiu, V. Lilliu, V. Onnis, Eur. J. Med. Chem. 40 (2005) 1365.
17. D. L. Boger. S. Nakahara, J. Org. Chem. 56 (1991) 880.
18. D. L. Boger, A. M. Kasper, J. Am. Chem. Soc. 111 (1989) 1517.
19. A. Chaubey, S. N. Pandeya, Asian J. Pharm. Clin. Res. 4 (2011) 5.
20. T. R. K. Reddy, R. Mutter, W. Heal, K. Guo, V. J. Gillet, S. Pratt, B. Chen, J. Med. Chem. 49 (2006) 607.
21. B. B. Fredholm, A. P. Ijzerman, K. A. Jacobson, K. N. Klotz, J. Linden, Pharmacol. Rev. 53 (2001) 527.
22. K. Guo, R. Mutter, W. Heal, T. R. K. Reddy, H. Cope, S. Pratt, M. J. Thompson, B. Chen, Eur. J. Med. Chem. 43 (2008) 93.

23. G. Matolcsy, Pesticide Chemistry, Elsevier Scientific, Amsterdam, Oxford, (1988) p.427.
24. R. T. Meister, Farm Chemicals Handbook, Vol. 86, Meister Publishing Co, Willoughby, Ohio. (2000).
25. H. J. Roth, A. Kleemann, (eds) Pharmaceutical Chemistry, Drug synthesis, Vol 1, Prentice Hall Europe, London, (1988) p.407.
26. A. Kleemann, J. Engel, B. Kutscher, D. Reichert, Pharmaceutical Substances: Syntheses, Patents Applications, 4th edn, Georg Thieme Verlag, Stuttgart. (2001).
27. I. M. Lagoja, Chem. Biodiv. 2 (2005) 1.
28. V. Yerragunta, P. Patil, V. Anusha, T. K. Swamy, D. Suman, T. Samhitha, PharmaTutor 1 (2013) 39.
29. R. C. Cioc, E. Ruijter, R. V. A. Orru, Green Chem. 16 (2014) 2958.
30. S. Aparicio, R. Alcalde, Green Chem. 11 (2009) 65.
31. M. S. Singh, S. Chowdhury, RSC Adv. 2 (2012) 4547.
32. D. Sun, H. Zhai, Catal. Commun. 8 (2007) 1027.
33. J. Chen, S. K. Spear, J. G. Huddleston, R. D. Rogers, Green Chem. 7 (2005) 64.
34. V. V. Namboodiri, R. S. Varma, Green Chem. 3 (2001) 146.
35. S. Narayan, J. Muldoon, M. G. Finn, V. V. Fokin, H. C. Kolb, K. B. Sharpless, Angew. Chem. Int. Ed. 44 (2005) 3275.
36. A. Chanda, V. V. Fokin, Chem. Rev. 109 (2009) 725.
37. R. N. Butler, A. G. Coyne, Chem. Rev. 110 (2010) 6302.
38. C. J. Li, Chem. Rev. 105 (2005) 3095.
39. R. Breslow, Acc. Chem. Res. 24 (1991) 159.
40. J. Chandrasekhar, S. Shariffskul, W. L. Jorgensen, J. Phys. Chem. B. 106 (2002) 8078.

CHAPTER 2

SUSTAINABLE NANO-CATALYTIC TRANSFORMATION OF β-ENAMINONES TO PYRIDINE DERIVATIVES

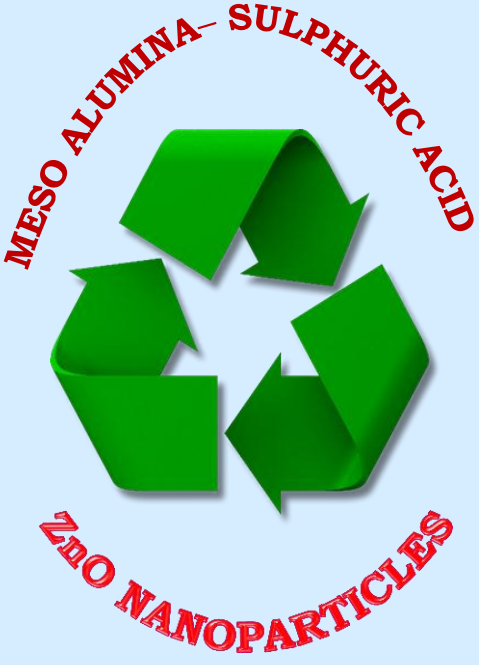

2.1. INTRODUCTION

β-Enaminones are versatile synthetic intermediates that have been extensively utilized as building blocks in organic synthesis.[1] These compounds possess a nitrogen functionality and an electron-withdrawing carbonyl group on adjacent alkene carbons **(Figure 1)**, and thus show both the nucleophilic and electrophilic characters. In these compounds the amine group pushes and the carbonyl group pulls electron density, which make them a typical push-pull ethylenes. Moreover, the carbonyl group, conjugated to the enamine moiety, gives this system enough stability to be easily prepared and can be isolated and stored under normal conditions. Thus, these compounds have served as synthons for the synthesis of many therapeutic agents such as antitumor, antibacterial, antimalarial, and anti-inflammatory as well as anticonvulsant agents.[2-3]

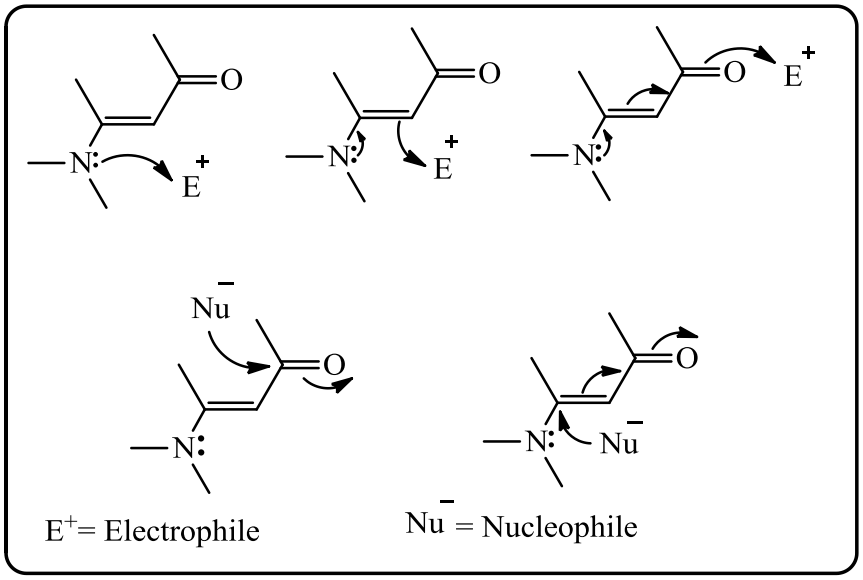

Fig. 1. Complementary electronic interaction of enaminones with electrophile/nucleophile.

Synthesis of some of the important six membered *N*-heterocyclic compounds from β-enaminones is outlined below **(Figure 2)**.[4]

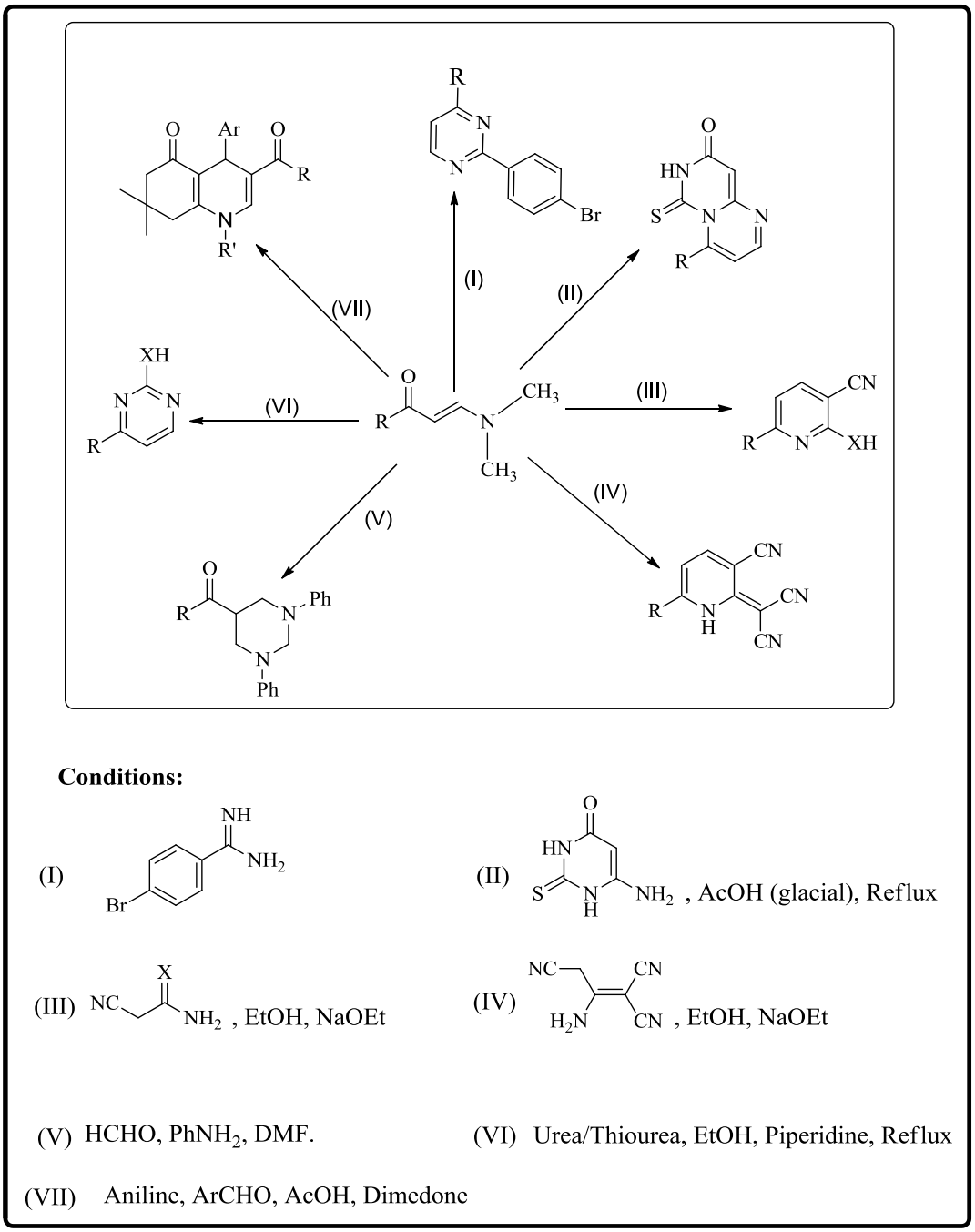

Fig. 2. Synthesis of some important six membered *N*-heterocycles from β-enaminones.

In this chapter we have described the synthesis of various novel 1,4-dihydropyridines and pyridine derivatives employing β-enaminones as synthons under green reaction conditions using heterogeneous nano-catalysts.

SECTION A

SYNTHESIS OF 1,4-DIHYDROPYRIDINES FROM β-ENAMINONES USING MESO ALUMINA–SULPHURIC ACID (Al-OSO_3H) AS CATALYST IN WATER *

Among nitrogen containing heterocycles, 1,4-dihydropyridines (1,4-DHPs) are among the most predominant and are found in many biologically active pharmaceuticals and natural products. Well known calcium agonists Felodipine, Nicardipine, Nimodipine, Nifedipine **(Figure 3)** and NADPH contain this structural motif. DHPs also exhibit interesting biological profiles such as selective adenosine-A3 receptor antagonism, sirtuin activation and inhibition, antitumor, antidiabetic, anticonvulsant photosensitizing and radioprotective activities.[5-7] Conventionally, Hantzsch reaction, reduction of pyridines, addition to pyridines or cycloadditions are the main routes for the synthesis of 1,4-DHPs, but Hantzsch reaction still remains the commonly used approach for the synthesis of these compounds.[8]

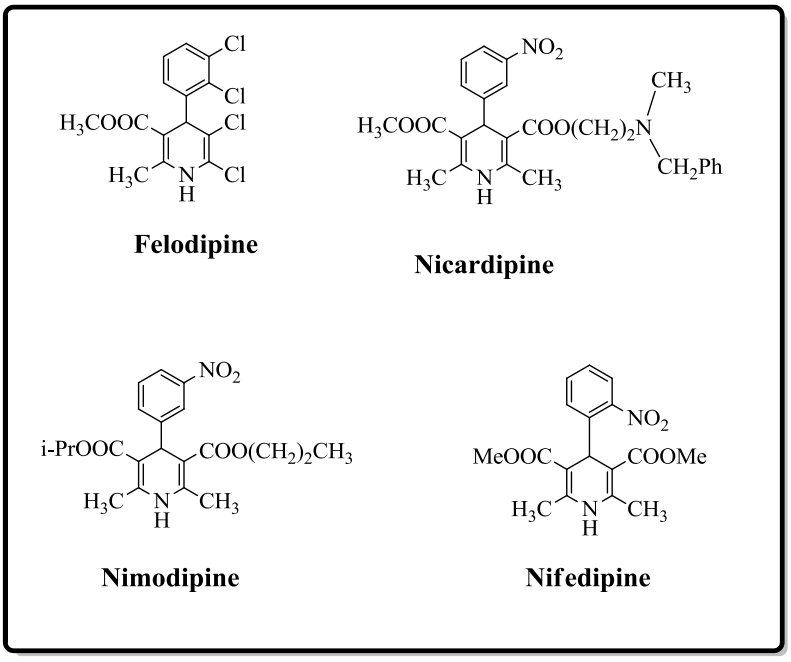

Fig. 3. Some important biologically active 1,4-dihydropyridines.

2.2. REVIEW OF LITERATURE

Recently, 1,4-DHPs have been synthesised *via* enaminones and few reports available in literature employ L-Proline/MeOH, TMSCl, TsOH/DCE, $NaAuCl_4$ and AcOH[9-12] as catalytic systems. However, these methods exhibit limited substrate tolerance and

* Nayeem Ahmed, Zeba N. Siddiqui, ***Journal of Molecular Catalysis A: Chemical***, 394 (2014) 232.

reactivity, suffer from low yields, and use of toxic solvents. Hence it is highly desirable to develop a new protocol for the synthesis of 1,4-DHPs using enaminones, which is highly efficient, environmentally benign and tolerates wide range of substrates.

Some recent and important methods of synthesizing 1,4-dihydropyridine derivatives via enaminones are discussed below:

2.2.1. Synthesis of pyrazolyl dihydropyridine derivatives.[13]

R. Sridhar and P. T. Perumal developed a 3,4,5-trifluorobenzeneboronic acid catalysed, ionic liquid mediated mild, simple and environmentally benign protocol for the synthesis of dihydropyridines. The reaction involves cyclocondensation of ethyl 3-aminocrotonate, pyrazole carbaldehyde and a β-keto ester to afford dihydropyridine derivatives in very good yields.

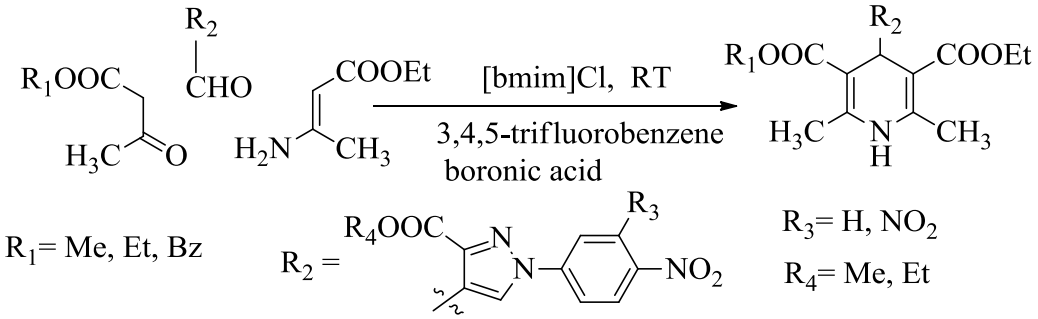

2.2.2. Synthesis of dihydropyridine *C*-glycoconjugates by organocatalytic Hantzsch cyclocondensation.[9]

D. R. B. Ducatti *et al.* reported the synthesis of dihydropyridine *C*-glycoconjugates via the reaction of *C*-glycosyl aldehyde, enamino ester and β-ketoester using L-proline as a catalyst in methanol. The protocol successfully applied for the synthesis of symmetrically and unsymmetrically substituted DHP *C*-glycoconjugates of biological relevance. The noteworthy feature of this protocol is very high stereoselectivity (de >95%) of the reaction.

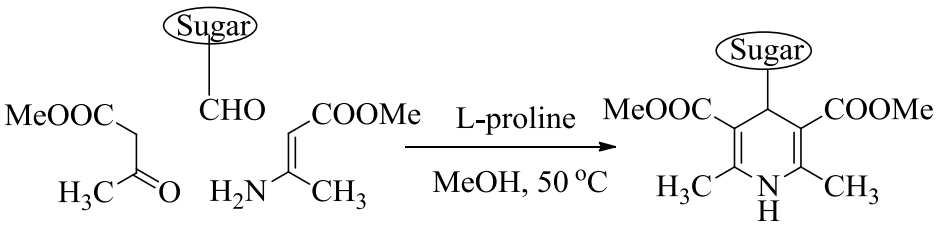

2.2.3. One-pot synthesis of 1,4-dihydropyridine derivatives using Me_3SiCl and Et_3SiI as catalysts.[10]

M. Mirza-Aghayana *et al.* reported the synthesis of 1,4-dihydropyridine derivatives by one-pot cyclocondensation of methyl 3-aminocrotonate and a range of aldehydes in the presence of chlorotrimethylsilane as a catalyst under solvent-free conditions. Short reaction time and high yield of products are the highlights of this protocol.

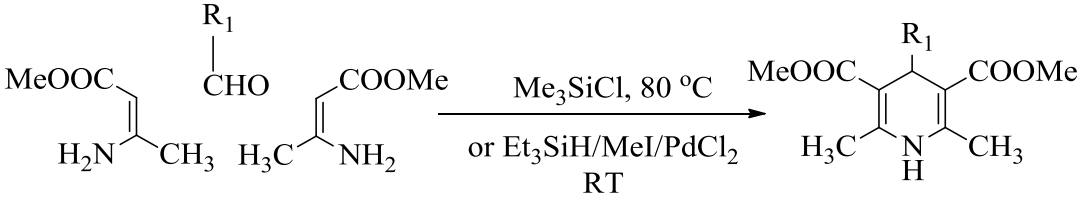

R_1= C_6H_5, 4-$NO_2C_6H_4$, 3-$NO_2C_6H_4$, 3-$OMeC_6H_4$, 4-OHC_6H_4, 4-ClC_6H_4, 2-C_4H_3S

2.2.4. An efficient acid-catalysed synthesis of 1,4-dihydropyridines *via* the reaction of enaminones with aldehydes.[11]

J. Yang *et al*. developed an efficient method for the synthesis of 1,4-DHPs without substituents at the C-2 and C-6 positions through an acid-catalysed reaction of enaminones with aldehydes. The reaction involves formation of divinylmethanes and their subsequent intramolecular cyclization to afford 1,4-dihydropyridines.

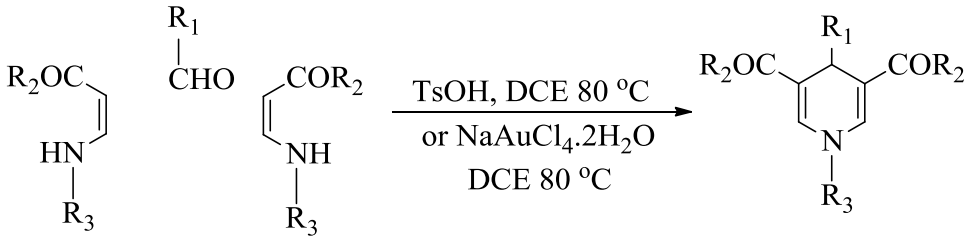

R_1= C_6H_5,4-ClC_6H_4, 4-$NO_2C_6H_4$, 4-MeC_6H_4, 4-$OMeC_6H_4$, 2-thienyl

R_2= C_6H_5, *n*-Hex, OEt R_3= 4-$OMeC_6H_4$, 4-ClC_6H_4, $PhCH_2$, *n*-Bu, 

2.2.5. Regioselective synthesis of unsymmetrical 1,4-dihydropyridines and 1,2-dihydropyridines.[14]

J. P. Wan *et al.* described the reaction of α,β-unsaturated aldehydes, amines, and enaminones leading to the synthesis of various (1,3,4-trisubstituted)-1,4-dihydropyridines in aqueous DMF along with 1,2-dihydropyridines. The steric and electronic effects originating from the amino group were the reasons for the regioselectivity shown by the reaction.

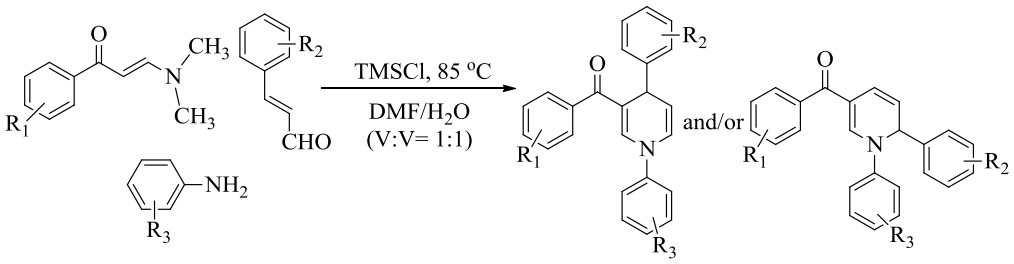

R_1= H, 4-Cl, 4-OMe, 4-NO_2 R_2= H, 2-Cl. R_3= H, 4-Cl, 4-Me, 4-Br, 4-F

2.2.6. An efficient multicomponent synthesis of 4-aryl dihydropyridines using enaminones.[12]

An efficient three component synthesis of 4-aryl 1,4-dihydropyridines *via* the reaction of enaminones, primary amines and aldehydes has been reported by N. A. Al-Awadi *et al.* Appropriately substituted derivatives exhibited an interesting photoluminescence behaviour suggesting their potential application as suitable photoinduced intramolecular electron-transfer systems.

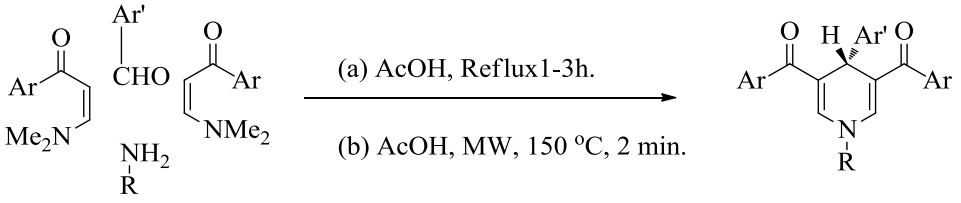

R= H, C_6H_5, 4-OHC_6H_4, 4-$CH_3C_6H_4$, *t*-butyl. Ar = C_6H_5, 2-thienyl, 2-furyl. Ar'= C_6H_5, 4-ClC_6H_4

2.3. PRESENT WORK

Many industrial processes are catalysed by strong Brønsted acid catalysts including sulfuric acid, *p*-toluenesulfonic acid etc. However, such homogeneous acids result in considerable energy wastage and the generation of large amounts of chemical waste. Moreover, they require neutralization, cannot be regenerated from homogeneous reaction mixtures and are also harmful to the environment. Therefore, a very promising solution to this problem is by replacing such conventional ‘‘homogeneous Brønsted acids” with recyclable solid acids and the simplest strategy to perform this task is by immobilization on the surface of an insoluble solid.[15] Among various catalytic nanomaterials, γ-Al_2O_3 is an important supporting material in heterogeneous catalysis due to its porous morphology, ultrafine crystallite size, large surface area and, high thermal and chemical stabilities. Fine dispersion of active species because of large surface area and open porosity enable efficient contact of the catalyst with the reactant molecules.[16] In the present work, taking advantages of the above mentioned properties of mesoporous alumina, we have designed the synthesis of mesoporous

alumina sulphuric acid (Meso-Al-OSO_3H) as a heterogeneous and recyclable catalyst and used it for the synthesis of novel 1,4-dihydropyridine derivatives *via* pseudo four component addition and cyclisation involving β-enaminone, aldehydes and ammonium acetate in aqueous media.

2.4. RESULTS AND DISCUSSION

The sulfonic acid functionalised alumina catalyst was prepared by reaction of mesoporous alumina with chlorosulfonic acid **(Scheme 1)**. The amount of acid groups present on alumina was calculated by using neutralization titration method and was found to be 3.6 meq/g.

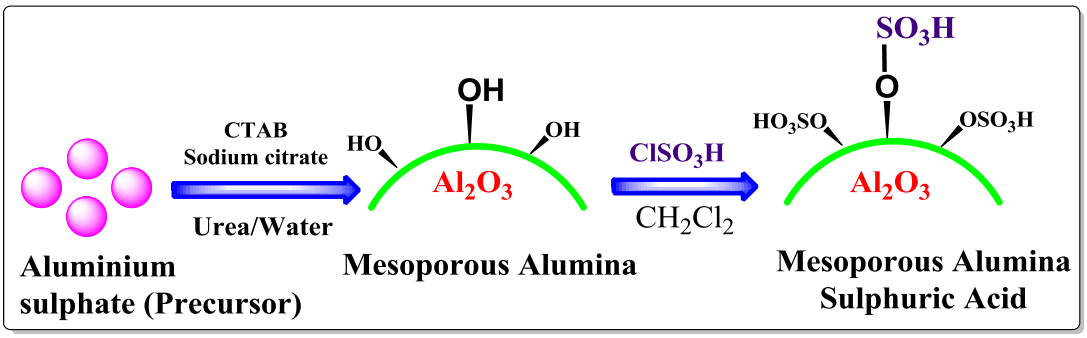

Scheme 1: Schematic representation of the synthesis of the Meso-Al-OSO_3H.

2.4.1. Characterization of the catalyst

2.4.1a. FT-IR spectral analysis

The FT-IR spectra of the alumina nanoparticles **(Figure 4a)** and meso-Al-OSO_3H **(Figure 4b)** are shown in Figure 4. In the spectrum of alumina, the characteristic stretching frequency of surface OH group was obtained at 3400 cm^{-1}. The bending and stretching vibrations of Al–O group were present in the range 500–1000 cm^{-1}.[17] In the spectrum of functionalized alumina, the asymmetric and symmetric stretching modes of O=S=O group were obtained as a broad band at 1120 cm^{-1}. Whereas the S–O stretching band at 600–700 cm^{-1} merged with the bending and stretching bands of Al–O group.[18] The functionalization of alumina by sulfonic acid groups also lead to decrease in the intensity of bands centred around 500–1000 cm^{-1}. The IR spectra thus, confirmed the successful functionalization of alumina nanoparticles by sulfonic acid groups.

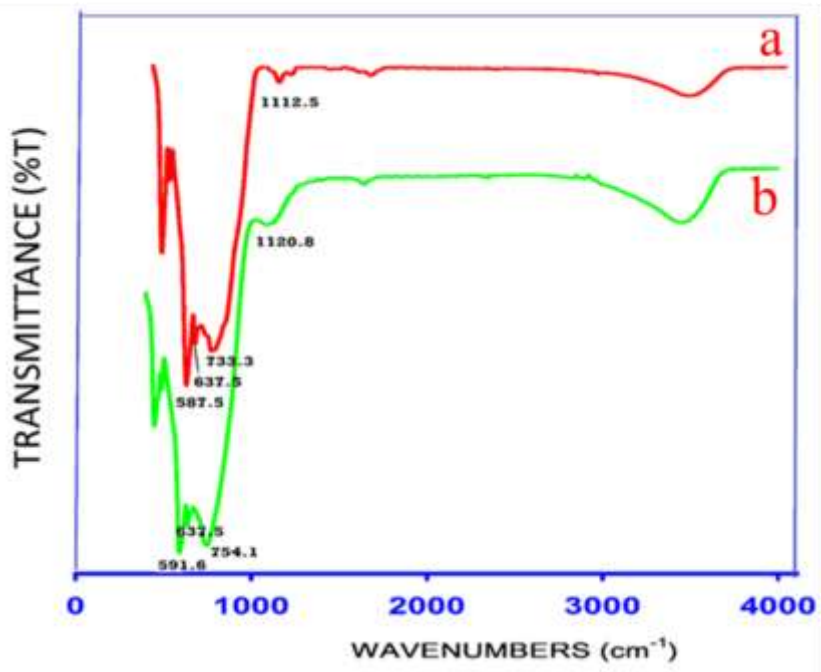

Fig. 4. FT-IR spectra of **(a)** Mesoporous alumina and **(b)** Meso-Al-OSO_3H

2.4.1b. XRD analysis

The XRD analysis was performed in order to observe the formation of γ-Al_2O_3 and meso-Al-OSO_3H **(Figure 5)**. The XRD pattern of alumina **(Figure 5a)** shows diffraction peaks corresponding to γ-Al_2O_3 (broad peaks around 30, 45, 60 and 65°) and α-Al_2O_3 (sharp peaks around 25, 35, 40, 50, 55°) phases.[19] Meso-Al-OSO_3H **(Figure 5b)** showed similar XRD pattern to that of γ-Al_2O_3. However, some extra peaks and slight changes in the nature of peaks were observed, which may be due the presence of sulfonic acid groups on the surface of alumina.

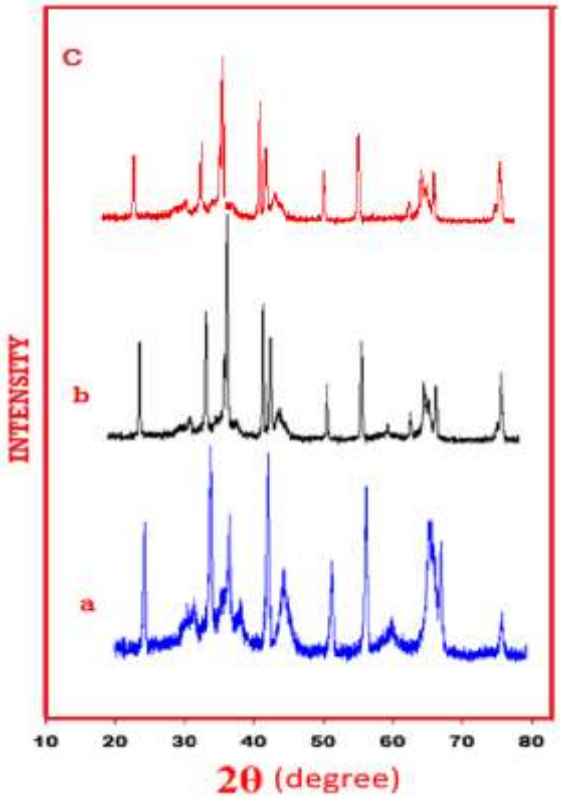

Fig. 5. Powder XRD spectra of **(a)** γ-Al_2O_3 **(b)** meso-Al-OSO_3H and **(c)** meso-Al-OSO_3H after seven catalytic cycles.

2.4.1c. FE-SEM and EDX analysis

The spherical shape of the synthesised mesoporous alumina nanoparticles was observed by FE-SEM analysis **(Figure 6a & b)** which showed the particle size in the range of 400 nm. The surface of alumina after functionalization with sulfonic acid groups is shown in **Figure 6c**. It was observed that shape and surface morphology of alumina particles is retained after being functionalized with sulfonic acid groups. The successful functionalization was further confirmed by EDX analysis **(Figure 6d)** which showed the presence of S in addition to Al and O elements.

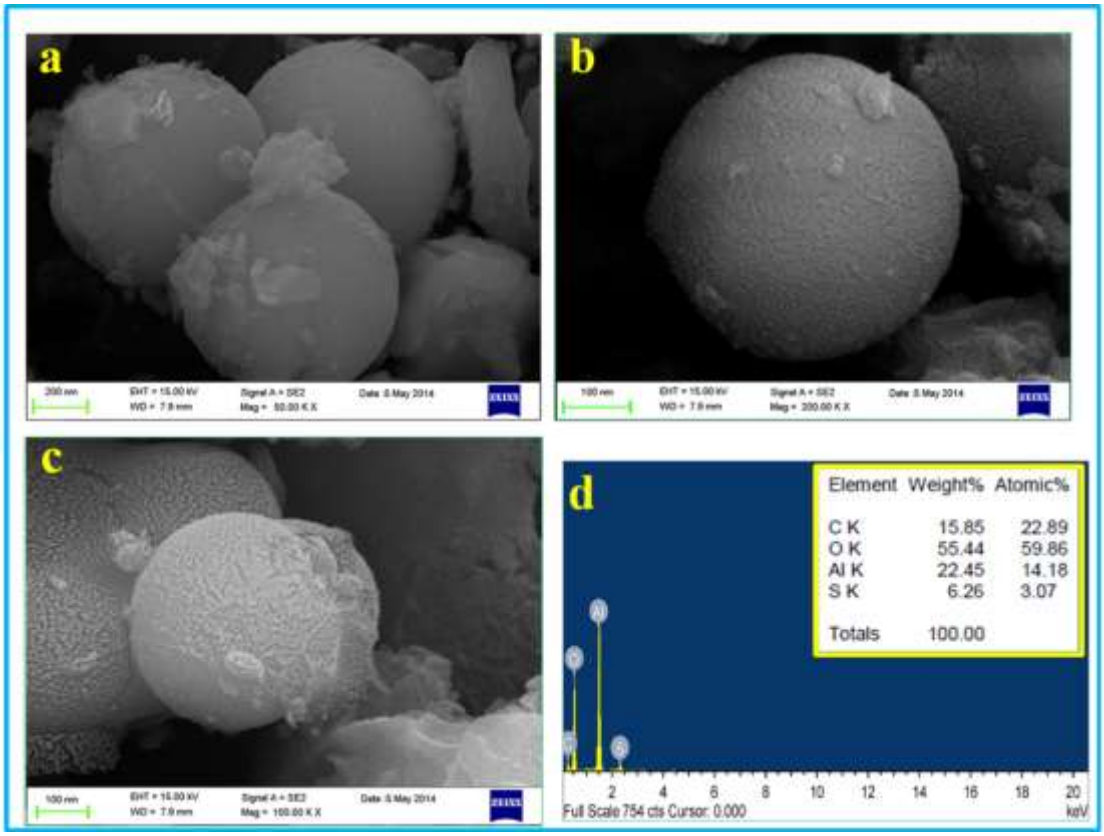

Fig. 6. FE-SEM images **(a & b)** of freshly synthesised γ-Al_2O_3 at different magnifications **(c)** of meso-Al-OSO_3H and **(d)** EDX analysis of meso-Al-OSO_3H.

2.4.1d. BET and TEM analysis

The mesoporous structure of γ-alumina was confirmed by N_2 adsorption/desorption isotherms **(Figure 7a)**. The sample showed the presence of type IV isotherm (definition by IUPAC)[20] which is a characteristic of mesoporous material. The surface area of the sample was found to be 529.54 m^2/g. The pore size distributions were also obtained from these adsorption isotherms and the pore volume and average pore size were 0.5 cc/g and 5.5 nm respectively **(Figure 7b)**. The less broadening in the pore width peak denotes the presence of uniform size pores. In order to further confirm the mesoporous structure of the synthesized alumina particles, TEM analysis **(Figure 8)** was performed. The images showed wormhole-like porous structure of the molecules with uniform pore size distribution. All these analyses proved the mesoporous nature of synthesized alumina nanoparticles.

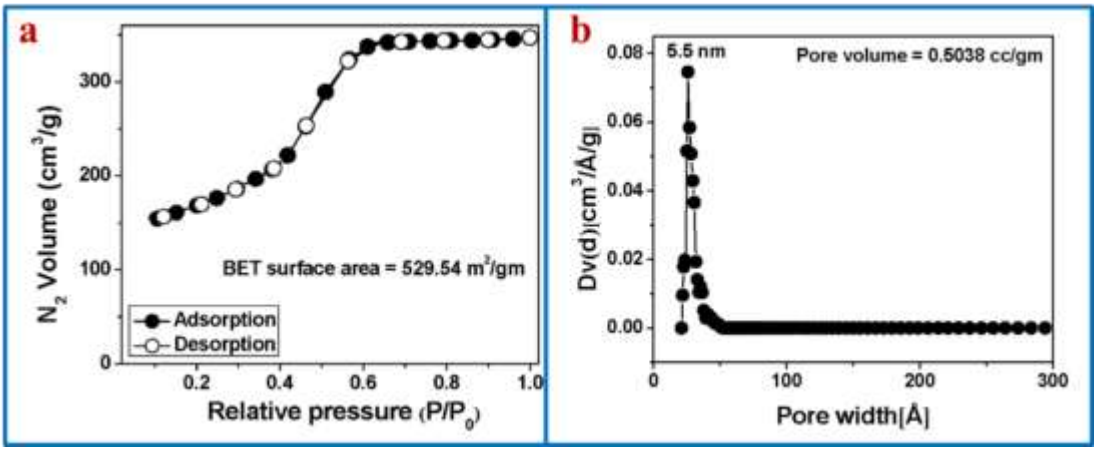

Fig. 7. (a) Nitrogen adsorption isotherm and **(b)** pore size distribution of mesoporous alumina.

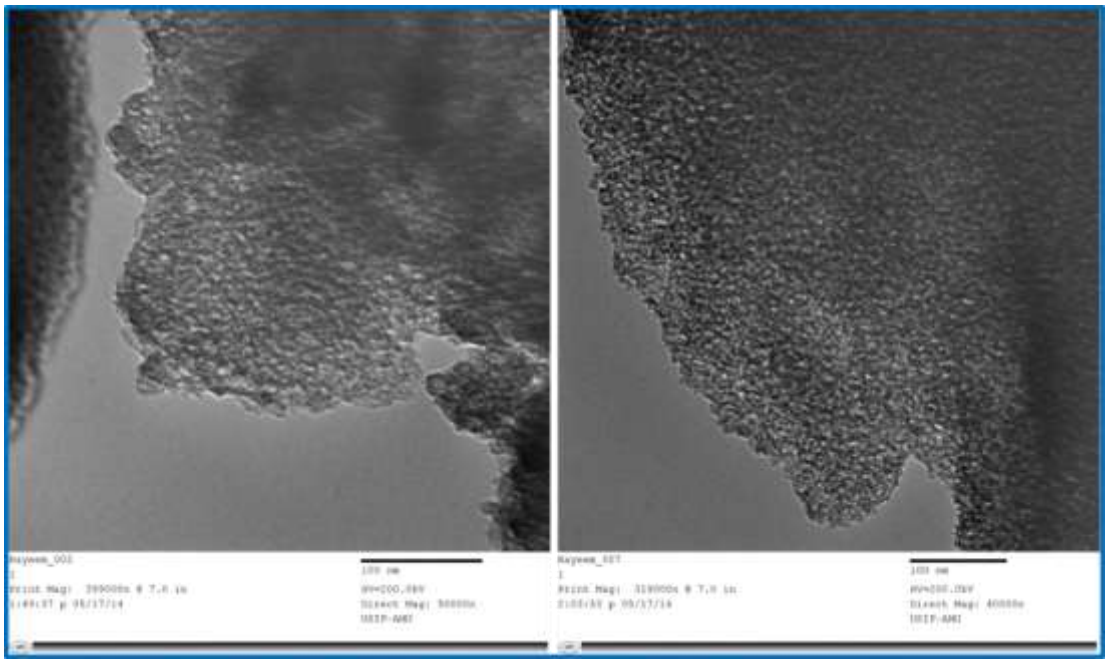

Fig. 8. TEM images of mesoporous alumina showing uniform pore distribution.

2.4.1e. TG Analysis

TG analysis was performed in order to evaluate the thermal stability and successful incorporation of sulfonic acid groups on mesoporous alumina surface. The TGA curve of mesoporous alumina **(Figure 9b)** showed a weight loss of 8.97 % up to 180 ° C due to the evaporation of moisture trapped in alumina framework. The TG curve then did not show any further weight loss up to 600 °C. In the TG curve of meso-Al-OSO_3H **(Figure 9a)**, the first weight loss below 100 °C (13.7 % up to 200 °C) was due to the removal of solvent and water molecules trapped in alumina matrix. Another weight loss of 8.9 % beginning from 300 °C up to 600 °C was attributed to the decomposition of sulfonic acid groups from the mesoporous alumina surface. The TG

curve, thus, showed successful incorporation of sulfonic acid groups on the alumina surface.

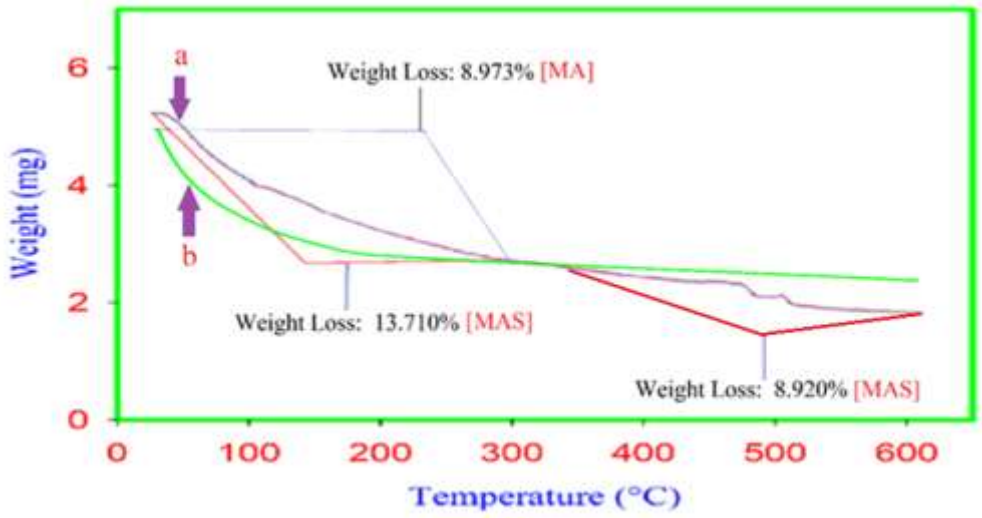

Fig. 9. TG analysis **(a)** of meso-Al-OSO_3H acid [MAS] and **(b)** of mesoporous alumina [MA].

2.4.2. Optimization of reaction conditions

2.4.2a. Optimization of catalysts

Keeping in view the environmental concerns as well as the vast utility and scope of reactions carried out in water, we chose water as the preferred solvent for our reaction. Catalyst optimization experiments were done in order to find right catalyst for our reaction. The reaction between enaminone **1b**, benzaldehyde (**2a)** and ammonium acetate was chosen as the model reaction. When the reaction was tried in the absence of any catalyst no product formation was observed, indicating the need of a catalyst. When ZnO, MgO, meso-Al_2O_3, AcOH and H_2SO_4 were used as catalysts, unsatisfactory results were obtained **(Table 1, entries 1-5)**. An improvement in the yields of the product was observed when heterogenized sulphuric acid catalysts were tried. Among silica, zirconia and alumina supported sulphuric acid, alumina sulphuric acid catalysed reaction showed better results **(Table 1, entries 6-8)**. Sulphuric acid supported on organic polymers also showed poor results in comparison to alumina sulphuric acid **(Table 1, entries 11 & 12)**. We then tried the reaction using sulphuric acid supported on silica and alumina nanoparticles **(Table 1, entries 13 & 14)** the yields of the product increased substantially with decrease in time taken for completion of the reaction. The results obtained showed that the nano-alumina sulphuric acid **(Table 1, entry 14)** was the most efficient catalyst for this reaction.

The higher activity shown by alumina supported sulphuric acid may be due to fine dispersion of sulfonic acid groups on the surface of alumina as compared to other supports. In order to further improve our catalytic system, we used mesoporous alumina as a support for functionalizing sulphuric acid, the results obtained were very promising and lesser amount of the catalyst was needed to efficiently catalyse this reaction **(Table 1, entry 16)**. This higher activity shown by mesoporous alumina sulphuric acid is due to the porous structure generating a very high surface area which in turn leads to higher number of sites being available for functionalization with sulfonic acid group.

Table 1: Effect of various catalysts on the model reaction.

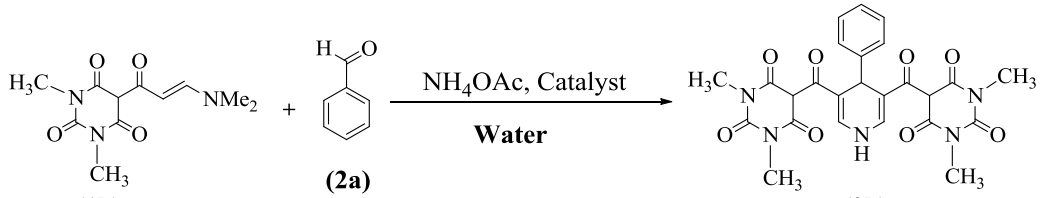

(1b) **(2a)** **(3h)**

Entry	Catalyst	Condition	Time	Yield (%)
1	ZnO (10 mol%)	H_2O /reflux	8.4 h	54
2	MgO (10 mol%)	H_2O /reflux	9.5 h	48
3	Meso-Al_2O_3 (10 mol%)	H_2O /reflux	12.5 h	29
4	AcOH (10 mol%)	H_2O /reflux	7.0 h	61
5	H_2SO_4 (10 mol%)	H_2O /reflux	6.2 h	58
6	H_2SO_4-SiO_2 (200mg)	H_2O /reflux	3.5 h	72
7	H_2SO_4-ZrO_2 (200mg)	H_2O /reflux	4.2 h	62
8	H_2SO_4-Al_2O_3 (200mg)	H_2O /reflux	3.0 h	75
9	NH_2SO_3H-SiO_2 (200mg)	H_2O /reflux	3.4 h	66
10	TsOH-SiO_2 (200mg)	H_2O /reflux	4.1 h	64
11	H_2SO_4-Cellulose (200mg)	H_2O /reflux	5.8 h	59
12	H_2SO_4-Xanthan (200mg)	H_2O /reflux	5.2 h	61
13	H_2SO_4-nanoSiO_2 (100mg)	H_2O /reflux	2.2 h	78
14	H_2SO_4-nanoAl_2O_3 (100mg)	H_2O /reflux	1.8 h	81
15	H_2SO_4-Meso-Al_2O_3 (100mg)	H_2O /reflux	45 min	90
16	H_2SO_4-Meso-Al_2O_3 (50mg)	H_2O /reflux	45 min	90

2.4.2b. Effect of solvents/Hydrophobic effect

In order to establish water as a preferred solvent, the model reaction was studied using different solvents **(Table 2)**. Using AcOH, MeOH and EtOH as solvents, unsatisfactory yield of product was obtained **(Table 2, entries 2-4)**. $CHCl_3$ and DMF

as solvents again showed unsatisfactory results **(Table 2, entries 5&6)**. Excellent results in short span of time were obtained by using water as a solvent for the reaction **(Table 2, entry 7)**. This enhanced reactivity can be attributed to the strong hydrogen bond interaction at the organic/water interface, which stabilizes the reaction intermediates and enhances the rate of reaction.[21] To further understand this impressive rate enhancement for on-water reactions, controlled experiments were undertaken. Firstly, under neat conditions the reaction completed in 1.5 h with 77% product yield **(Table 2, entry 1)**. We then performed the reaction by using different concentrations of various solvents with water. Mixing of 0.5 mL of EtOH to the water containing the reaction mixture produced no effect. Addition of further 1-2 mL of EtOH again did not display any remarkable effect **(Table 2, entries 8 & 9)**. Addition of 3-4 mL of EtOH turned the reaction mixture homogeneous, and then the rate of reaction decreased considerably **(Table 2, entry 10)**. We then tried this experiment with MeOH and found similar results. Upon examining the results we found that the large rate enhancements occurred if the reaction was conducted in heterogeneous conditions than in homogeneous aqueous solution and hydrophobic effects act prominently as neat reaction was not as faster as reaction using water. These studies established the supremacy of water as a solvent for this reaction.

Table 2: Effect of different solvents on the model reaction.

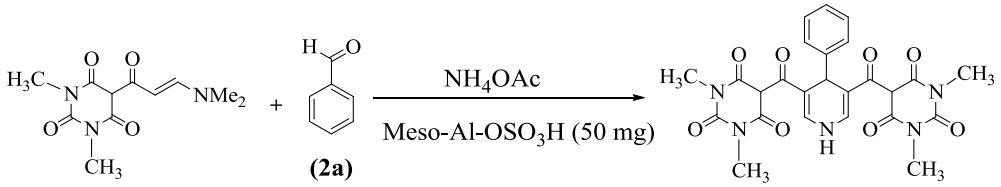

(1b) **(2a)** **(3h)**

Entry	Solvent	Time	Yield (%)
1	Neat	1.5 h	77
2	AcOH (5mL)	4 h	56
3	MeOH (5mL)	5 h	53
4	EtOH (5mL)	5 h	61
5	$CHCl_3$ (5mL)	5 h	Incomplete
6	DMF (5mL)	3 h	48
7	H_2O (5mL)	45 min	90
8	H_2O (5mL)/ EtOH (1mL)	45 min	88
9	H_2O (5mL)/ EtOH (2mL)	50 min	86
10	H_2O (5mL)/ EtOH (3mL)	3.5 h	73

2.4.2c. Catalyst loading

In order to obtain maximum yield in lesser amount of time, effect of the catalyst loading on the model reaction was studied. It was found that the yield of the product increased from 76% to 90% when the catalyst amount was increased from 0.03 g to 0.05 g. Further increase of catalyst amount to 0.1 g did not improve product yield **(Table 3)**.

Table 3: Effect of catalyst loading on the model reaction.

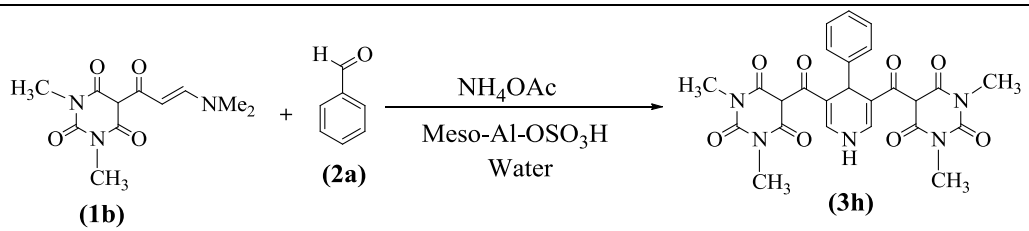

(1b) **(2a)** **(3h)**

Entry	Catalyst loading (g)	Time (min)	Yield (%)
1	0.03	63	76
2	0.05	45	90
3	0.10	45	90
4	0.15	45	88
5	0.20	45	86

2.4.2d. Catalytic reaction

With these encouraging results in hand, we then explored the scope of the reaction by using different aromatic aldehydes **(2a-g)**, enaminones **(1a, 1b)** and ammonium acetate as substrates under the optimized reaction conditions **(Table 4)**. Aromatic aldehydes with electron donating/electron withdrawing groups as well as aliphatic/alicyclic aldehydes reacted successfully to furnish the final products **(3a-n)** in good yields **(Scheme 2)**. The structure of the final product was well characterized by using spectral (IR, ^{1}H, ^{13}C NMR and ESI-MS) and elemental analysis data. I.R. spectrum of **3h (Figure 10)** showed broad peak due to NH stretching at 3431 cm^{-1}. Absorption band at 1731 cm^{-1} was assigned to stretching of two C=O groups (C1") connected to dihydropyridine ring, whereas, absorption band for six C=O groups (C2', C4', C6') of two pyrimidinetrione moieties appeared at 1672 cm^{-1}. The C=C stretching band was observed at 1604 cm^{-1}. The ^{1}H NMR spectrum **(Figure 11)** showed a broad singlet for NH proton of dihydropyridine ring at δ 10.28. Five aromatic protons in the form of multiplet at δ 7.4-7.8 were clearly discernible. H2, H6 protons of dihydropyridine ring appeared as a singlet at δ 7.25, whereas H4 proton was present as a singlet at δ 5.29. ^{13}C NMR **(Figure 12)** showed signals at δ 184.63,

172.11 and 165.21 for C1", C4'/ C6' and C2' carbons respectively. Other peaks were present at their normal values and are provided in experimental section. Further structural confirmation was made by ESI-Mass spectrum **(Figure 13)** which showed the molecular ion peak as the base peak at m/z 522.1 (M^++1).

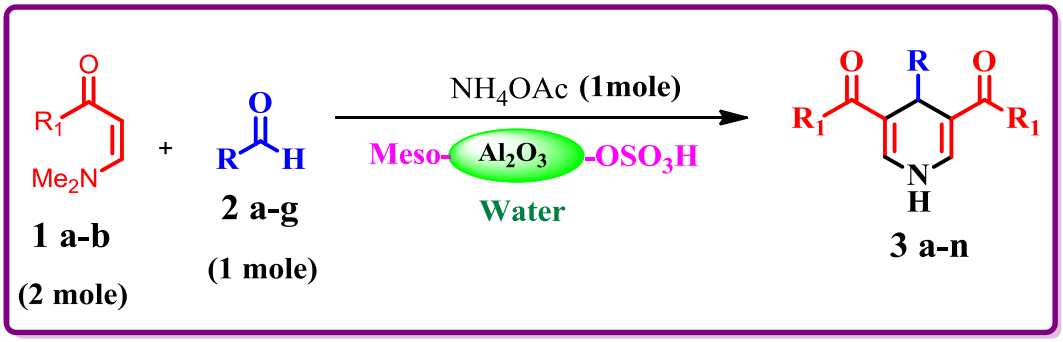

Scheme 2: General scheme for the synthesis of dihydropyridines **(3a-n)**

Table 4: Synthesis of dihydropyridines

Entry	Enaminone	Aldehyde	Product	Time (min)	Yield (%)
1	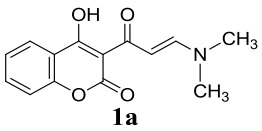 **1a**	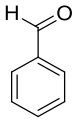 **2a**	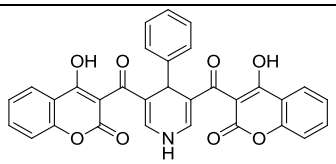 **3a**	53	89
2	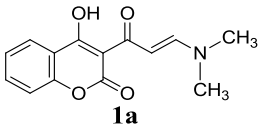 **1a**	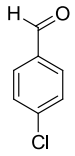 **2b**	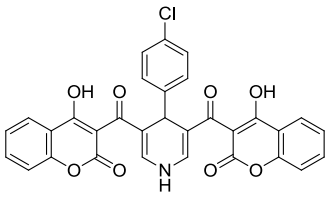 **3b**	51	86
3	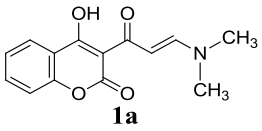 **1a**	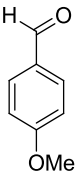 **2c**	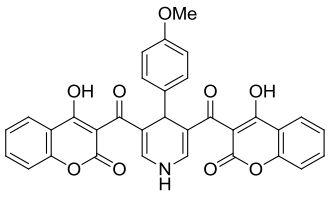 **3c**	57	85
4	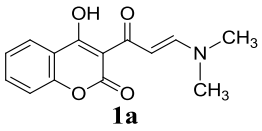 **1a**	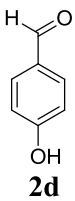 **2d**	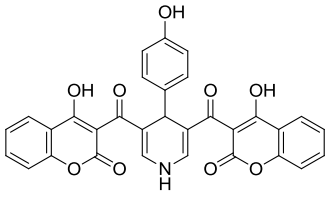 **3d**	51	87

5	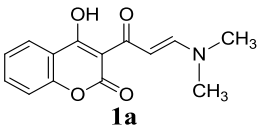 **1a**	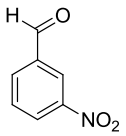 **2e**	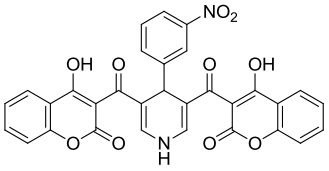 **3e**	50	83
6	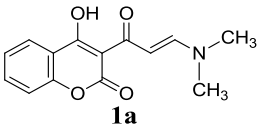 **1a**	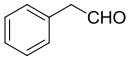 **2f**	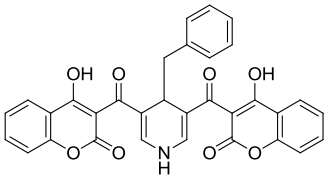 **3f**	65	84
7	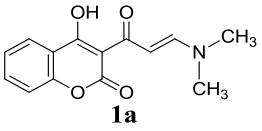 **1a**	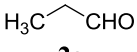 **2g**	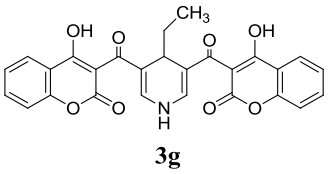 **3g**	68	81
8	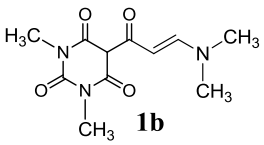 **1b**	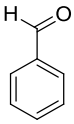 **2a**	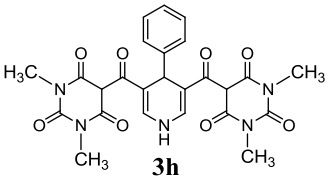 **3h**	45	90
9	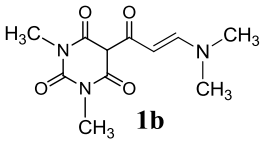 **1b**	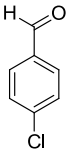 **2b**	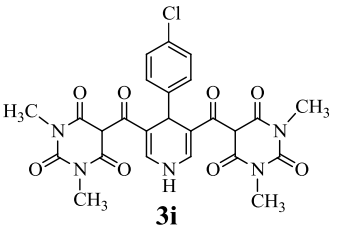 **3i**	43	89
10	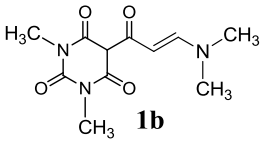 **1b**	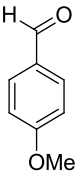 **2c**	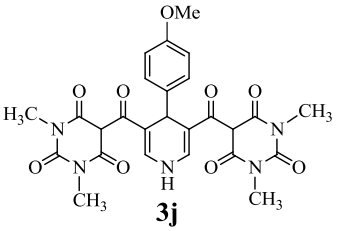 **3j**	48	87
11	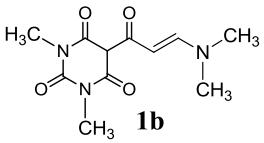 **1b**	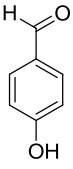 **2d**	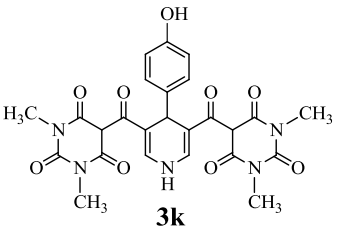 **3k**	41	90

12	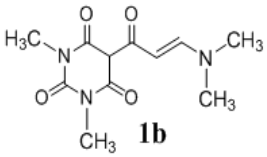 **1b**	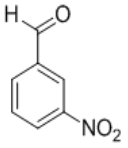 **2e**	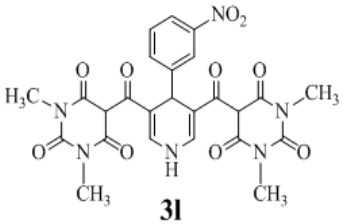 **3l**	40	86
13	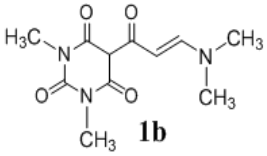 **1b**	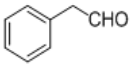 **2f**	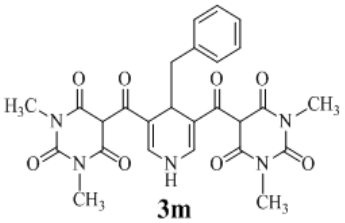 **3m**	45	85
14	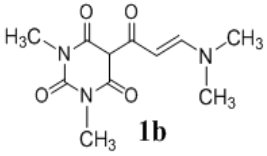 **1b**	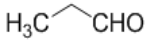 **2g**	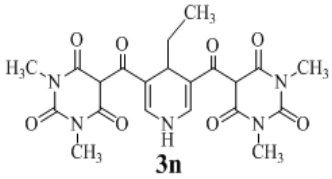 **3n**	52	82

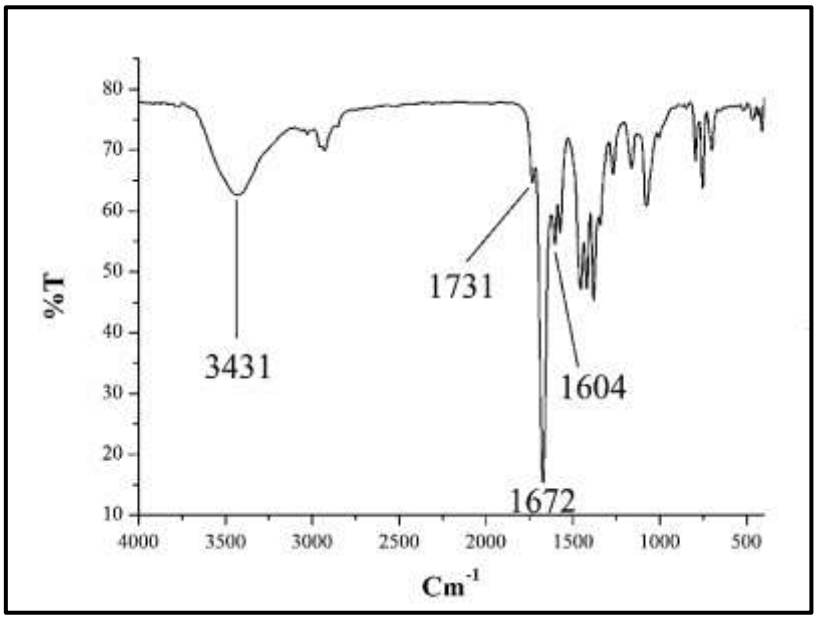

Fig. 10. FT-IR spectrum of **3h**

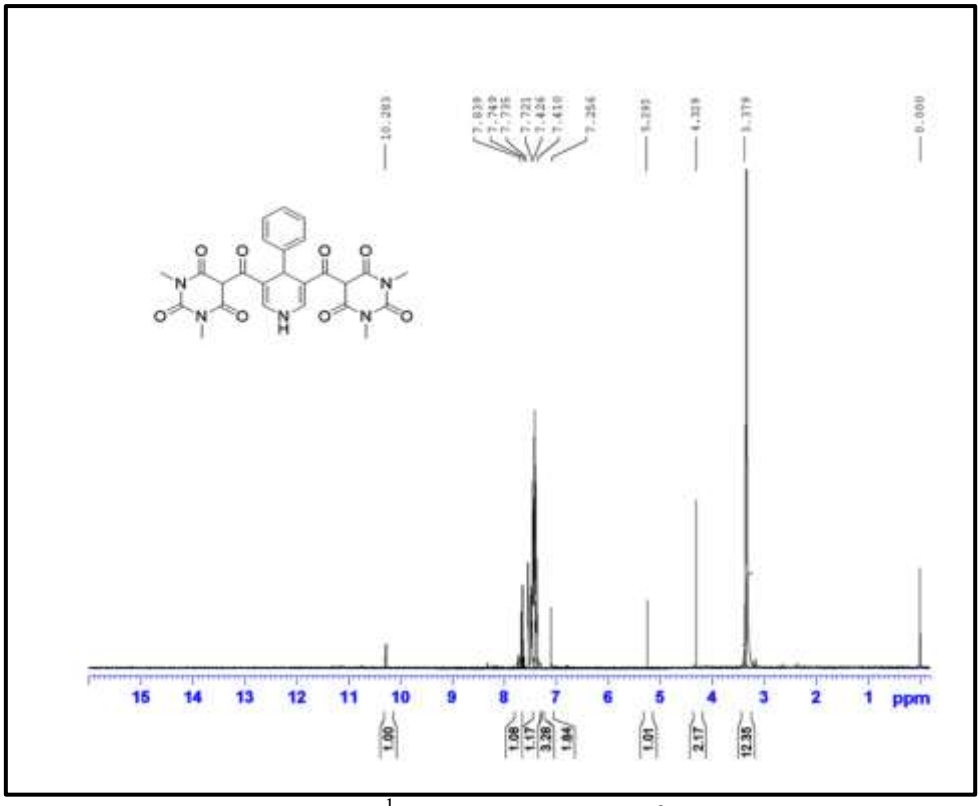

Fig. 11. ^{1}H-NMR spectrum of **3h**

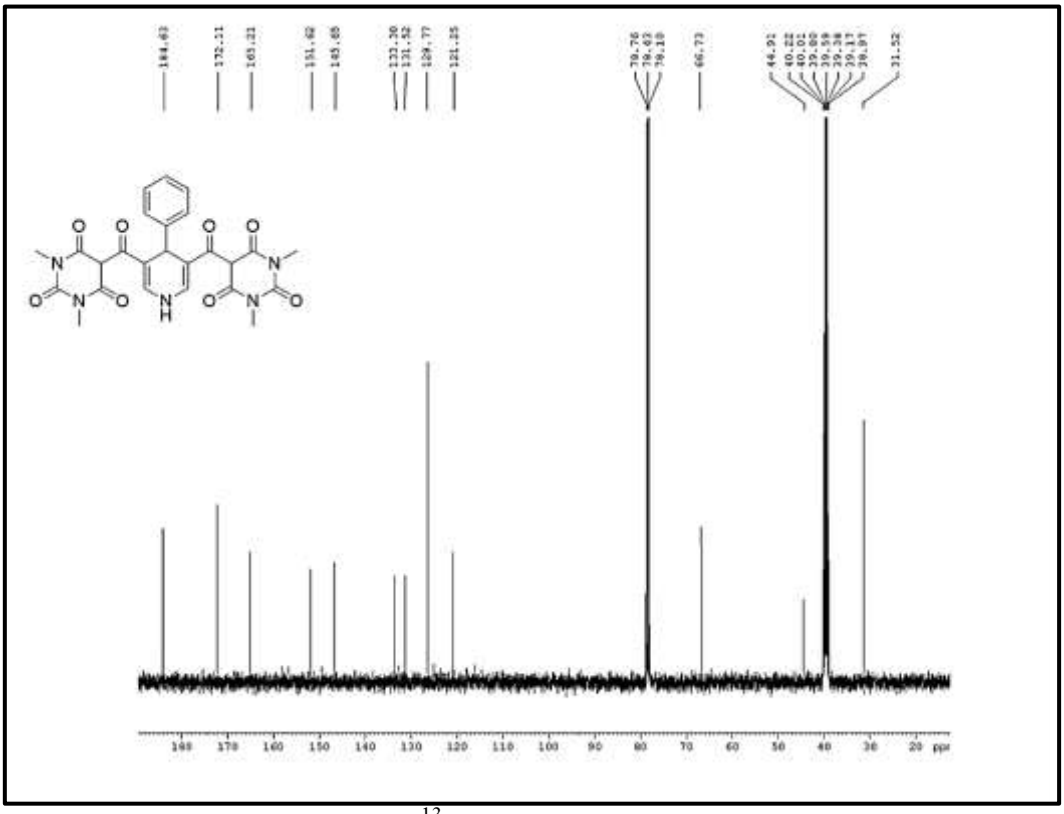

Fig. 12. ^{13}C-NMR spectrum of **3h**

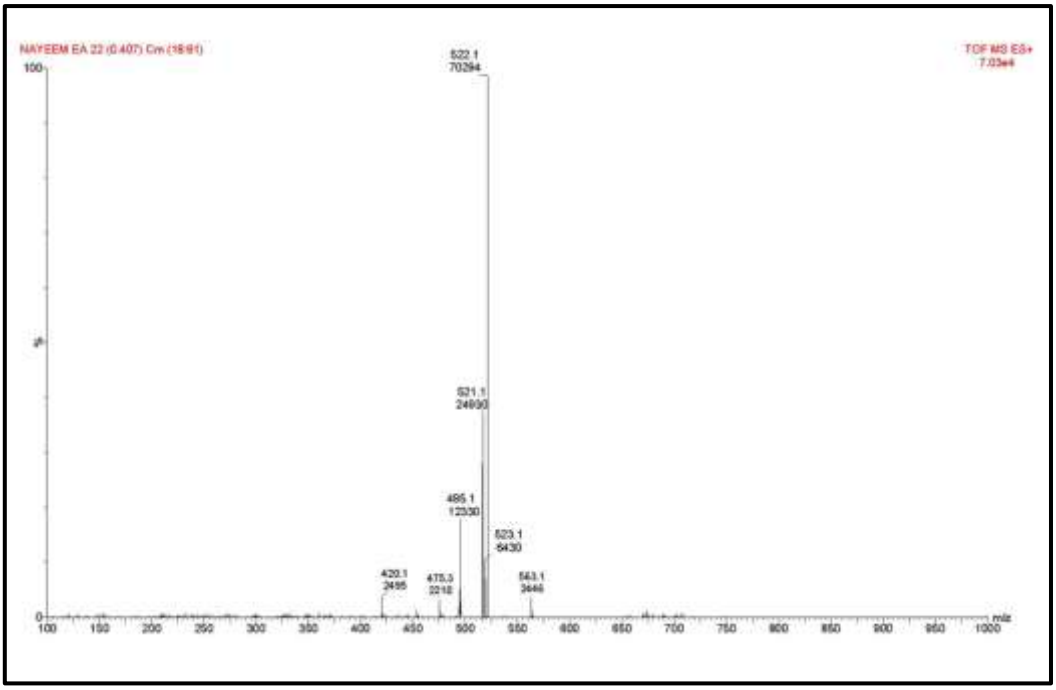

Fig. 13. ESI-Mass spectrum of **3h**

2.4.3. Reaction mechanism

The plausible mechanism is proposed in **scheme 3**. First the catalyst activates the aldehyde group of **2a** after which it undergoes nucleophilic addition of double bond of enaminone **1b** to form **B**. Intermediate **C** then undergoes benzylic substitution by another molecule of enaminone **1b** followed by loss of water molecule to generate divinylic compound **D**. This divinylic compound then undergoes Michael addition with ammonia followed by elimination of dimethyl amine to give **F**. Cyclisation of **F** by intramolecular Michael addition with amine followed by elimination of another molecule of dimethyl amine generates the product **3h**. The catalyst could be regenerated in the last step and reused for further catalytic cycles.[8c]

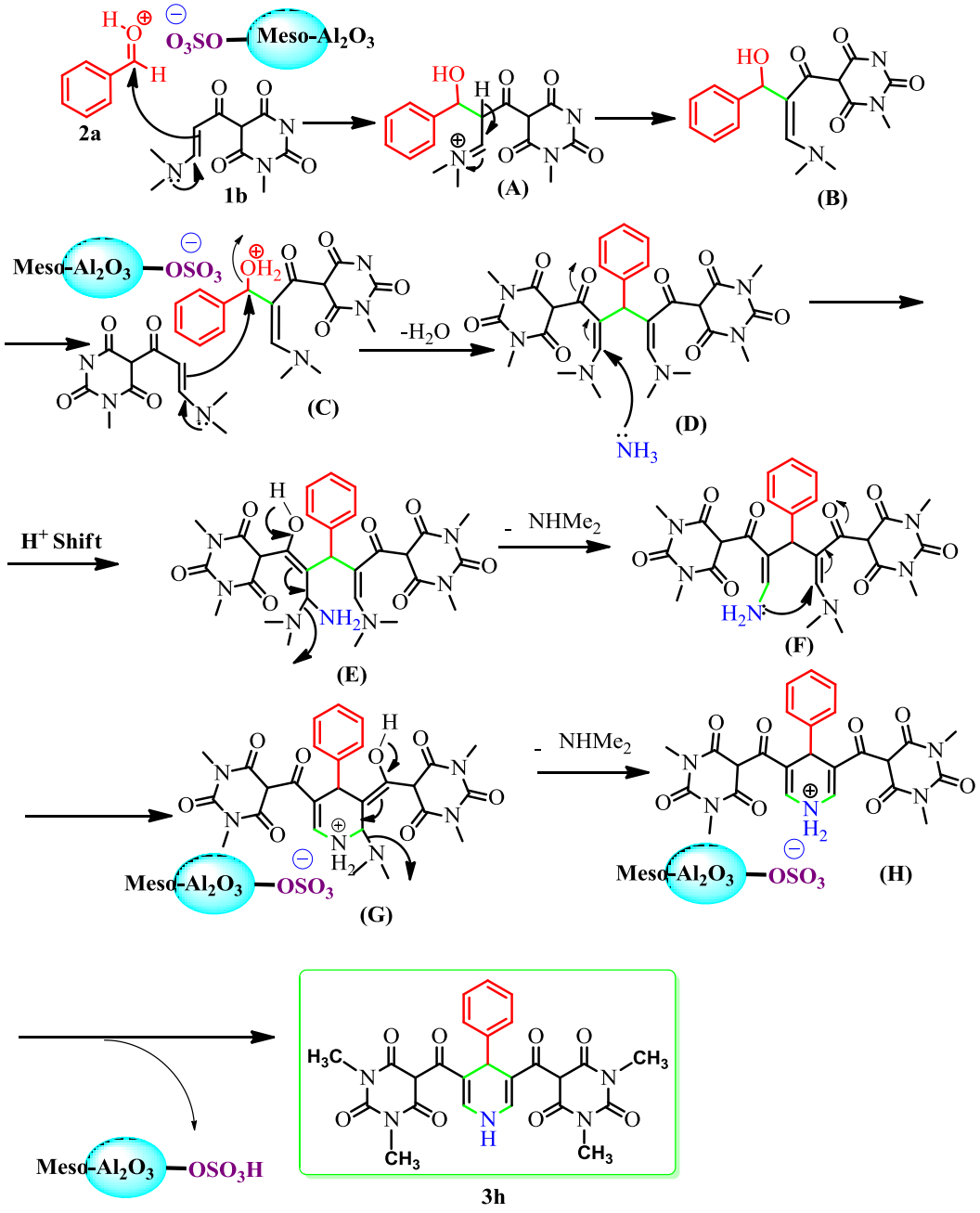

Scheme 3: Plausible reaction mechanism for the formation of **3h**.

2.4.4. Hot filtration test

A hot-filtration test was performed using mesoporous alumina sulphuric acid as a catalyst in order to check any leaching of catalyst into the solution during the reaction. A mixture of β-enaminone **1b** (1 mmol), aldehyde **2a** (0.5 mmol), ammonium acetate (0.7 mmol) and catalyst (50 mg) in 5 mL ethanol was refluxed for 30 min and immediately filtered under hot reaction conditions. The obtained reaction mixture without any catalyst was then further refluxed for 6 h under the same reaction conditions and it was observed that there was no further product formation and the

reaction could not proceed to completion. This result clearly demonstrates the heterogeneous nature of the prepared catalyst.

2.4.5. Catalyst recyclability

In order to explore the extent of recyclability of our catalytic system, the catalyst was recovered by filtration from the reaction mixture of enaminone **1b**, benzaldehyde **(2a)** and ammonium acetate in water, washed with ethanol (3×15 mL), ethyl acetate (2×10 mL), dried at 100 °C for 1.5 h, and reused in subsequent runs. The catalyst was found to retain its activity for a minimum of seven reaction cycles and displayed almost high catalytic performance with over 85% product yield **(Table 5)**. The XRD **(Figure 3c)** of the catalyst after seven runs showed that the structure of the catalyst is not altered during its reuse.

Table 5: Recycling data of mesoporous alumina sulphuric acid for the model reaction.

No. of runs	Run 1	Run 2	Run 3	Run 4	Run 5	Run 6	Run 7
Time (min)	45	45	45	45	45	45	45
Yield (%)	90	90	90	87	85	83	83

2.5. CONCLUSION

In summary, mesoporous alumina sulphuric acid has been synthesised and evaluated as a catalyst for the preparation of new 1,4-dihydropyridines *via* β-enaminones in water. This new efficient, green and convenient method provides an opportunity to use water and avoid environmentally harmful conventional organic solvents. The substrate scope of the reaction is also demonstrated by the tolerance of alicyclic and aliphatic aldehydes in addition to aromatic aldehydes. Thus, this simple procedure is a better and more practical alternative to existing methods in view of green chemistry.

2.6. EXPERIMENTAL

2.6.1. Preparation of mesoporous alumina

In a typical synthesis, *N*-Cetyl-*N,N,N*-trimethylammonium bromide (CTAB) (0.2 mmol), $Al_2(SO_4)_3.18H_2O$ (1mmol), $CO(NH_2)_2$ (4 mmol), and sodium tartrate (0.7 mmol) were dissolved in distilled water to form a clear solution (36 mL) under vigorous stirring for 0.5 h. The solution was placed in an autoclave with a Teflon liner and was maintained at 165 °C for 8 h. The autoclave was then allowed to cool and the white precipitate obtained was collected, washed thoroughly with distilled water and then dried at 80 °C for 12 h. The sample was then calcined at 550 °C for 3 h to remove the template.[22]

2.6.2. Preparation of mesoporous alumina supported sulphuric acid

A 0.5 L suction flask was equipped with a constant pressure dropping funnel. The gas outlet was connected to a vacuum system through an adsorbing solution of alkali trap. Mesoporous alumina (1g) was added into the flask and stirred for 10 min in dry CH_2Cl_2 (20 mL). Chlorosulfonic acid (1mL) was added drop wise over a period of 30 min at room temperature. After complete addition of chlorosulfonic acid, the reaction mixture was stirred for 90 min, while the residual HCl was eliminated by suction. The mesoporous alumina sulphuric acid obtained as solid, was separated from the reaction mixture by filtration and washed several times with dried CH_2Cl_2, ethanol. Finally the catalyst was dried at 120 °C for three hours.

2.6.3. Determination of H^+ ion concentration of mesoporous alumina sulphuric acid

H^+ ion concentration of the catalyst was determined by neutralization titration analysis. 100 mg of catalyst was stirred in 20 mL of 0.1N NaOH solution for 30 min in an Erlenmeyer flask. The excess amount of base was then neutralised by the addition of 0.1N HCl solution to the equivalence point of titration. The amount of acid groups was found to be 3.6 meq/g.

2.6.4. General procedure for "On water" synthesis of dihydropyridines

A mixture of β-enaminone (10 mmol), aldehyde (5 mmol), ammonium acetate (7 mmol) and catalyst (250 mg) in 10 mL water was refluxed in an oil bath for appropriate period of time **(Table 4)**. After completion of reaction (monitored by TLC), the reaction mixture was allowed to cool and added ethyl acetate to extract the product. The catalyst as insoluble solid was separated by filtration, washed with ethyl acetate (3 x 10 mL) and reused for further catalytic cycles. The filtrate was washed with water (3 × 10 mL), dried over anhydrous Na_2SO_4 and evaporated under reduced pressure. The crude product was recrystallized from suitable solvent (Ethanol or DMSO) to afford pure product.

2.6.5. Spectral data of synthesised compounds

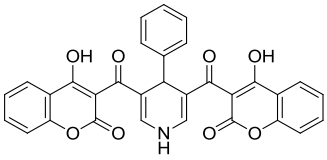 **3a**	*3,5-Bis(4-hydroxy-1-benzopyran-2-one-3-carbonyl)-4-phenyl-1,4-dihydropyridine*. Yellow solid, **M.P.** 240-245 °C. **Anal. Calcd** ($C_{31}H_{19}NO_8$): C, 69.79; H, 3.59; N, 2.63. **Anal. Found** ($C_{31}H_{19}NO_8$) C, 69.75; H, 3.63; N, 2.58. **IR (**KBr, cm^{-1}): 3594 (OH), 3479 (NH), 1709 (COO), 1676 (CO), 1610 (C=C). **^{1}H NMR** (400 MHz, DMSO-d_6): δ 10.22 (s, 1H, NH), 7.31-8.37 (m, Ar-H, 13H), 7.11 (s, 2H), 5.48 (s, 1H). **^{13}C NMR** (100 MHz, DMSO-d_6): δ 186.28, 175.36, 162.76, 154.47, 148.56, 143.17, 135.22, 132.76, 127.13, 126.75, 125.21, 123.07, 122.51, 120.15, 118.12, 101.33, 55.21. **ESI-MS** m/z 534.1 (M^++1).
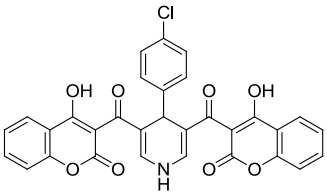 **3b**	*3,5-Bis(4-hydroxy-1-benzopyran-2-one-3-carbonyl)-4-(4-chloro)phenyl-1,4-dihydropyridine.* Yellow solid, **M.P.** 230-235 °C. **Anal. Calcd** ($C_{31}H_{18}ClNO_8$) C, 65.56; H, 3.19; N, 2.47. **Anal. Found** ($C_{31}H_{18}ClNO_8$) C, 65.62; H, 3.14; N, 2.42. **IR** (KBr, cm^{-1}): 3623 (OH), 3430 (NH), 1710 (COO), 1677 (CO), 1610 (C=C). **^{1}H NMR** (400 MHz, DMSO-d_6): δ 10.39 (s, 1H, NH), 7.29-8.35 (m, Ar-H, 12H), 7.08 (s, 2H), 5.34 (s, 1H). **^{13}C NMR** (100 MHz, DMSO-d_6): δ 184.55, 173.71, 160.63, 154.21, 149.07, 143.13, 136.26, 132.09, 131.32, 127.41, 126.92, 125.27, 123.53, 122.11, 120.72, 100.94, 55.61. **ESI-MS** m/z 568.1 (M^++1).
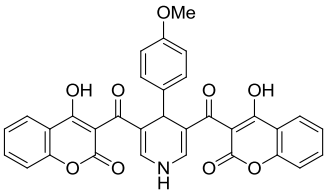 **3c**	*3,5-Bis(4-hydroxy-1-benzopyran-2-one-3-carbonyl)-4-(4-methoxy)phenyl-1,4-dihydropyridine*. Yellow solid, **M.P.** 225-230 °C. **Anal. Calcd** ($C_{32}H_{21}NO_9$) C, 68.21; H, 3.76; N, 2.49. **Anal. Found** ($C_{32}H_{21}NO_9$) C, 68.25; H, 3.71; N, 2.52. **IR** (KBr, cm^{-1}): 3638 (OH), 3448 (NH), 1726 (COO), 1662 (CO), 1600 (C=C). **^{1}H NMR** (400 MHz, DMSO-d_6): δ 10.54 (s, 1H, NH), 7.28-8.33 (m, Ar-H, 12H), 6.99 (s, 2H), 5.42 (s, 1H), 4.12 (s, 3H). **^{13}C NMR** (100 MHz, DMSO-d_6): δ 185.25, 172.11, 161.28, 159.54, 155.21, 148.47, 144.14, 136.89, 132.21, 128.51, 125.18, 124.21, 123.75, 122.09, 120.76, 101.02, 68.23, 56.18. **ESI-**

	MS m/z 564.2 (M^++1).
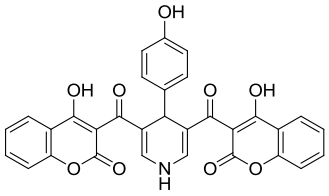 **3d**	*3,5-Bis(4-hydroxy-1-benzopyran-2-one-3-carbonyl)-4-(4-hydroxy)phenyl-1,4-dihydropyridine*. Yellow solid, **M.P.** 228-233 °C. **Anal. Calcd**. ($C_{31}H_{19}NO_9$) C, 67.76; H, 3.49; N, 2.55. **Anal. Found** ($C_{31}H_{19}NO_9$) C, 67.80; H, 3.44; N, 2.51. **IR** (KBr, cm^{-1}): 3641 (OH), 3437 (NH), 1721 (COO), 1661 (CO), 1607 (C=C). **^{1}H NMR** (400 MHz, DMSO-d_6): δ 10.42 (s, 1H, NH), 7.26-8.32 (m, Ar-H, 12H), 7.02 (s, 2H), 5.44 (s, 1H). **^{13}C NMR** (100 MHz, DMSO-d_6): δ 184.55, 173.14, 162.04, 159.22, 154.72, 148.71, 141.25, 134.14, 131.22, 128.03, 124.88, 124.03, 123.25, 121.91, 120.17, 101.33, 55.64. **ESI-MS** m/z 550.1 (M^++1).
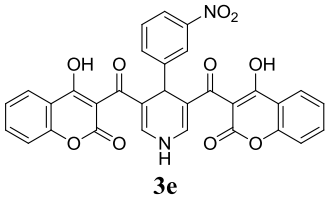 **3e**	*3,5-Bis(4-hydroxy-1-benzopyran-2-one-3-carbonyl)-4-(3-nitro)phenyl-1,4-dihydropyridine.* Orange solid, **M.P.** 240-245 °C. **Anal. Calcd** ($C_{31}H_{18}N_2O_{10}$) C, 64.36; H, 3.14; N, 4.84. **Anal. Found** ($C_{31}H_{18}N_2O_{10}$) C, 64.31; H, 3.18; N, 4.79. **IR** (KBr, cm^{-1}): 3638 (OH), 3425 (NH), 1712 (COO), 1673 (CO), 1610 (C=C). **^{1}H NMR** (400 MHz, DMSO-d_6): δ 10.38 (s, 1H, NH), 7.31-8.35 (m, Ar-H, 12H), 7.14 (s, 2H), 5.51 (s, 1H). **^{13}C NMR** (100 MHz, DMSO-d_6): δ 181.23, 172.41, 161.73, 159.22, 149.17, 146.54, 145.25, 133.11, 131.03, 129.23, 128.22, 127.52, 124.76, 123.53, 122.78, 121.49, 119.2, 100.41, 56.61. **ESI-MS** m/z 579.1 (M^++1).
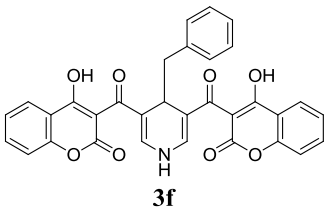 **3f**	*3,5-Bis(4-hydroxy-1-benzopyran-2-one-3-carbonyl)-4-(Phenylmethyl)-1,4-dihydropyridine*. Yellow solid, **M.P.** 250-255 °C. **Anal. Calcd** ($C_{32}H_{21}NO_8$) C, 70.20; H, 3.87; N, 2.56. **Anal. Found** ($C_{32}H_{21}NO_8$) C, 70.24; H, 3.82; N, 2.60. **IR** (KBr, cm^{-1}): 3645 (OH), 3437 (NH), 1714 (COO), 1676 (CO), 1616 (C=C). **^{1}H NMR** (400 MHz, DMSO-d_6): δ 10.19 (s, 1H, NH), 7.29-8.36 (m, Ar-H, 13H), 7.13 (s, 2H), 4.41 (t, 1H), 3.11 (d, 2H). **^{13}C NMR** (100 MHz, DMSO): δ 182.28, 171.54, 161.36, 157.76, 150.47, 141.56, 131.76, 127.23, 126.27, 125.41, 123.13,

	122.16, 120.11, 118.65, 101.01, 42.11, 35.21, 33.11. **ESI-MS** m/z 548.2 (M^++1).
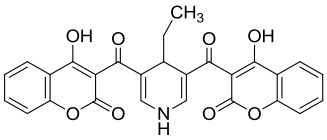 **3g**	*3,5-Bis(4-hydroxy-1-benzopyran-2-one-3-carbonyl)-4-ethyl-1,4-dihydropyridine*. Light yellow solid, **M.P.** 280-285 °C. **Anal. Calcd** ($C_{27}H_{19}NO_8$) C, 66.80; H, 3.95; N, 2.89. **Anal. Found** ($C_{27}H_{19}NO_8$) C, 66.76; H, 3.99; N, 2.84. **IR** (KBr, cm^{-1}): 3639 (OH), 3431 (NH), 1713 (COO), 1672 (CO), 1611 (C=C). **^{1}H NMR** (400 MHz, DMSO-d_6): δ 10.22 (s, 1H, NH), 7.28-7.98 (m, Ar-H, 8H), 7.01 (s, 2H), 4.53 (t, 1H), 2.07 (m, 2H), 1.12 (t, 3H). **^{13}C NMR** (100 MHz, DMSO): δ 183.13, 171.96, 161.76, 156.48, 148.92, 129.23, 127.44, 126.42, 125.17, 120.10, 118.68, 102.13, 45.12, 29.24, 18.76. **ESI-MS** m/z 486.1 (M^++1).
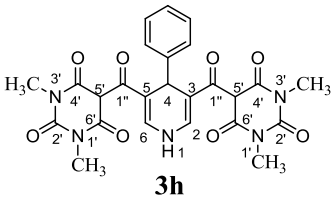 **3h**	*3,5-Bis(1,3-dimethyl-2,4,6-pyrimidinetrione-5-carbonyl)-4-phenyl-1,4-dihydropyridine.* Yellow solid, **M.P.** 250-255 °C. **Anal. Calcd** ($C_{25}H_{23}N_5O_8$) C, 57.58; H, 4.45; N, 13.43. **Anal. Found** ($C_{25}H_{23}N_5O_8$) C, 57.53; H, 4.50; N, 13.39. **IR** (KBr, cm^{-1}): 3431 (NH), 1731 (CO), 1672 (CO), 1604 (C=C). **^{1}H NMR** (400 MHz, DMSO-d_6): δ 10.28 (s, 1H, NH), 7.41-7.83 (m, 5H, Ar-H), 7.25 (s, 2H), 5.29 (s, 1H), 4.32 (s, 2H), 3.37 (s, 12H, 4 x CH_3). **^{13}C NMR** (100 MHz, DMSO-d_6): δ 184.63, 172.11, 165.21, 151.62, 145.65, 133.30, 131.52, 128.77, 121.25, 66.73, 44.91, 31.52. **ESI-MS** m/z 522.1 (M^++1).
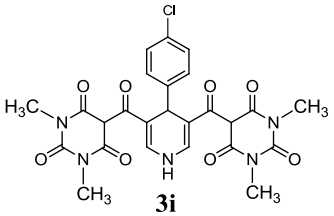 **3i**	*3,5-Bis(1,3-dimethyl-2,4,6-pyrimidinetrione-5-carbonyl)-4-(4-chlorophenyl)-1,4-dihydropyridine.* Yellow solid, **M.P.** 245-250 °C. **Anal. Calcd** ($C_{25}H_{22}ClN_5O_8$) C, 54.01; H, 3.99; N, 12.60. **Anal. Found** ($C_{25}H_{22}ClN_5O_8$) C, 54.05; H, 4.02; N, 12.56. **IR** (KBr, cm^{-1}): 3435 (NH), 1742 (CO), 1666 (CO), 1615 (C=C). **^{1}H NMR** (400 MHz, DMSO-d_6): δ 10.48 (s, 1H, NH), 7.48-7.82 (m, 4H, Ar-H), 7.15 (s, 2H), 5.41 (s, 1H), 4.71 (s, 2H), 3.22 (s, 12H, 4 x CH_3). **^{13}C NMR** (100 MHz, DMSO-d_6): δ 186.12, 174.42, 166.52, 150.91, 145.54, 134.29, 132.15,

	128.63, 121.82, 65.97, 44.07, 32.14. **ESI-MS** m/z 556.2 (M^++1).
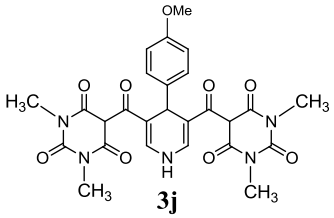 **3j**	*3,5-Bis(1,3-dimethyl-2,4,6-pyrimidinetrione-5-carbonyl)-4-(4-methoxyphenyl)-1,4-dihydropyridine***.** Yellow solid, **M.P.** 230-235 °C. **Anal. Calcd** ($C_{26}H_{25}N_5O_9$) C, 56.62; H, 4.57; N, 12.70. **Anal. Found** ($C_{26}H_{25}N_5O_9$) C, 56.65; H, 4.52; N, 12.66. **IR** (KBr, cm^{-1}): 3442 (NH), 1728 (CO), 1665 (CO), 1611 (C=C). **^{1}H NMR** (400 MHz, DMSO-d_6): δ 10.31 (s, 1H, NH), 7.41-7.83 (m, 4H, Ar-H), 7.11 (s, 2H), 5.37 (s, 1H), 4.65 (s, 2H), 3.88 (s, 3H), 3.27 (s, 12H, 4 x CH_3). **^{13}C NMR** (100 MHz, DMSO-d_6): δ 188.43, 172.06, 167.19, 159.22, 152.16, 144.26, 134.07, 131.36, 120.18, 64.66, 59.73, 45.11, 32.87. **ESI-MS** m/z 552.1 (M^++1).
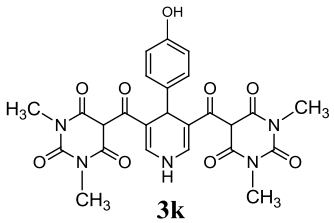 **3k**	*3,5-Bis(1,3-dimethyl-2,4,6-pyrimidinetrione-5-carbonyl)-4-(4-hydroxyphenyl)-1,4-dihydropyridine***.** Yellow solid, **M.P.** 245-250 °C. **Anal. Calcd** ($C_{25}H_{23}N_5O_9$) C, 55.87; H, 4.31; N, 13.03. **Anal. Found** ($C_{25}H_{23}N_5O_9$) C, 55.91; H, 4.27; N, 12.99. **IR** (KBr, cm^{-1}): 3450 (NH), 3068 (OH), 1730 (CO), 1641 (CO), 1613 (C=C). **^{1}H NMR** (400 MHz, DMSO-d_6): δ 10.52 (s, 1H, NH), 7.27-7.81 (m, 5H, Ar-H), 7.03 (s, 2H), 5.44 (s, 1H), 4.69 (s, 2H), 3.37 (s, 12H, 4 x CH_3). **^{13}C NMR** (100 MHz, DMSO-*d_6*): δ 184.04. 172.12, 159.38, 153.17, 141.23, 138.44, 133.57, 120.22, 119.54, 71.33, 43.29, 34.78. **ESI-MS** m/z 538.1 (M^++1).
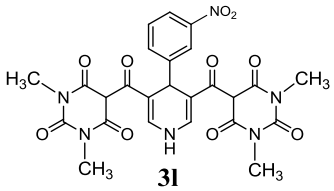 **3l**	*3,5-Bis(1,3-dimethyl-2,4,6-pyrimidinetrione-5-carbonyl)-4-(3-nitrophenyl)-1,4-dihydropyridine.* Orange solid, **M.P.** 240-245 °C. **Anal. Calcd**. ($C_{25}H_{22}N_6O_{10}$) C, 53.01; H, 3.91; N, 14.84. **Anal. Found** ($C_{25}H_{22}N_6O_{10}$) C, 53.06; H, 3.88; N, 14.79. **IR** (KBr, cm^{-1}): 3426 (NH), 1722 (CO), 1661 (CO), 1593 (C=C). **^{1}H NMR** (400 MHz, DMSO-d_6): δ 10.44 (s, 1H, NH), 7.51-7.84 (m, 4H, Ar-H), 7.18 (s, 2H), 5.47 (s, 1H), 4.78 (s, 2H), 3.21 (s, 12H, 4 x CH_3). **^{13}C NMR** (100 MHz, DMSO-d_6): δ 187.11, 173.72, 165.44, 152.04, 146.87, 142.64, 134.14, 131.88,

	129.79, 120.53, 65.37, 43.84, 32.02. **ESI-MS** m/z 567.1 (M^++1).
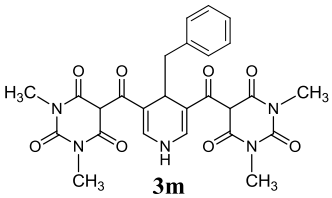 **3m**	*3,5-Bis(1,3-dimethyl-2,4,6-pyrimidinetrione-5-carbonyl)-4-(Phenylmethyl)-1,4-dihydropyridine.* Yellow solid, **M.P.** 285-290 °C. **Anal. Calcd** ($C_{26}H_{25}N_5O_8$) C, 58.31; H, 4.71; N, 13.08. **Anal. Found** ($C_{26}H_{25}N_5O_8$) C, 58.36; H, 4.68; N, 13.04. **IR** (KBr, cm^{-1}): 3473 (NH), 1735 (CO), 1651 (CO), 1607 (C=C). **^{1}H NMR** (400 MHz, DMSO-d_6): δ 10.14 (s, 1H, NH), 7.29-7.61 (m, 5H, Ar-H), 6.95 (s, 2H), 5.17 (t, 1H), 4.24 (s, 2H), 3.24 (d, 2H), 3.01 (s, 12H, 4 x CH_3). **^{13}C NMR** (100 MHz, DMSO-d_6): δ 182.87, 172.54, 161.79, 141.32, 139.72, 131.11, 129.35, 127.07, 115.27, 78.57, 44.75, 37.11, 29.82. **ESI-MS** m/z 536.1 (M^++1).
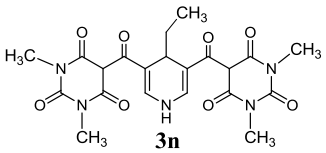 **3n**	*3,5-Bis(1,3-dimethyl-2,4,6-pyrimidinetrione-5-carbonyl)-4-ethyl-1,4-dihydropyridine*. Yellow solid, **M.P.** >300 °C. **Anal. Calcd** ($C_{21}H_{23}N_5O_8$) C, 53.28; H, 4.90; N, 14.79. **Anal. Found** ($C_{21}H_{23}N_5O_8$) C, 53.24; H, 4.86; N, 14.74. **IR** (KBr, cm^{-1}): 3431 (NH), 1725 (CO), 1667 (CO), 1610 (C=C). **^{1}H NMR** (400 MHz, DMSO-d_6): δ 10.22 (s, 1H, NH), 7.05 (s, 2H), 4.54 (s, 2H), 4.49 (t, 1H), 3.32 (s, 12H, 4 x CH_3), 2.12 (m, 2H), 1.17 (t, 3H). **^{13}C NMR** (100 MHz, DMSO-d_6): δ 185.13, 171.32, 161.04, 139.25, 115.77. 72.23, 41.42, 36.52, 29.57, 18.71. **ESI-MS** m/z 474.1 (M^++1).

REFERENCES:

1. (a) B. Stanovnik, J. Svete, Chem. Rev. 104 (2004) 2433; (b) A. Z. A. Elassara, A. A. El-Khairb, Tetrahedron 59 (2003) 8463; (c) S. Muthusaravanan, C. Sasikumar, B. D. Bala, S. Perumal, Green Chem. 16 (2014) 1297; (d) W. J. Hao, J. Q. Wang, X. P. Xu, S. L. Zhang, S. Y. Wang, S. J. Ji, J. Org. Chem. 78 (2013) 12362.
2. (a) J. E. Foster, J. M. Nicholson, R. Butcher, J. P. Stables, I. O. Edafiogho, A. M. Goodwin, M. C. Henson, C. A. Smith, K. R. Scott, Bioorg. Med. Chem. 7 (1999) 2415; (b) J. P. Michael, C. B. Koning, G. D. Hosken, T. V. Stanbury, Tetrahedron 57 (2001) 9635.
3. (a) D. L. Boger, T. Ishizaki, J. R. J. Wysocki, S. A. Munk, P. A. Kitos, O. Suntornwat, J. Am. Chem. Soc. 111 (1989) 6461; (c) I. O. Edafiogho, K. V. V. Ananthalakshmi, S. B. Kombian, Bioorg. Med. Chem. 14 (2006) 5266; (d) N. D. Eddington, D. S. Cox, R. R. Roberts, J. P. Stables, C. B. Powell, K. R. Scott, Curr. Med. Chem. 7 (2000) 417; (e) N. N. Salama, N. D. Eddington, D. Payne, T. L. Wilson, K. R. Scott, Curr. Med. Chem. 11 (2004) 2093.
4. (a) S. Muthusaravanan, S. Perumal, A. I. Almansour, Tetrahedron Lett. 53 (2012) 1144; (b) A. A. E. Hassan, Int. j. Org. Chem. 4 (2014) 68; (c) S. Muthusaravanan, B. D. Bala, S. Perumal, Tetrahedron Lett. 54 (2013) 5302.
5. (a) R. Lavilla, J. Chem. Soc. Perkin Trans. 1 (2002) 1141; (b) J. Moreau, J. P. Hurvois, M. D. Mbaye, J. L. Renaud, Targets Heterocycl. Syst. 13 (2009) 201.
6. (a) C. O. Kappe, Eur. J. Med. Chem. 35 (2000) 1043; (b) T. Godfraind, R. Miller, M. Wibo, Pharmacol. Rev. 38 (1986) 321.
7. (a) A. Sausins, G. Duburs, Heterocycles 27 (1988) 269; (b) M. F. Gordeev, D. V. Patel, B. P. England, S. Jonnalagadda, J. D. Combs, E. M. Gordon, Bioorg. Med. Chem. 6 (1998) 883; (c) M. F. Gordeev, D. V. Patel, E. M. Gordon, J. Org. Chem. 61 (1996) 924.
8. (a) D. M. Stout, A. I. Meyers, Chem. Rev. 82 (1982) 223; (b) A. Sausins, G. Duburs, Heterocycles 27 (1988) 269. (c) J. P. Wan, Y. Liu, RSC Adv. 2 (2012) 9763.
9. D. R. B. Ducatti, A. Massi, M. D. Noseda, M. E. R. Duarte, A. Dondoni, Org. Biomol. Chem. 7 (2009) 1980.
10. M. Mirza-Aghayana, M. K. Langrodi, M. Rahimifard, R. Boukherroub, Appl. Organometal. Chem. 23 (2009) 267.

11. J. Yang, C. Wang, X. Xie, H. Li, Y. Li, Eur. J. Org. Chem. (2010) 4189.
12. N. A. Al-Awadi, M. R. Ibrahim, M. H. Elnagdi, E. John, Y. A. Ibrahim, Beilstein J. Org. Chem. 8 (2012) 441.
13. R. Sridhar, P. T. Perumal, Tetrahedron 61 (2005) 2465.
14. J. -P. Wan, S. F. Gan, G. L. Sun, Y. J. Pan, J. Org. Chem. 74 (2009) 2862.
15. (a) M. J. Climent, A. Corma, S. Iborra, Chem. Rev. 111 (2011) 1072; (b) M. A. Zolfigol, Tetrahedron 57 (2001) 9509; (c) B. M. Reddy, P. M. Sreekanth, P. Lakshmanan, J. Mol. Cat. A: Chem. 237 (2005) 93; (d) A. Praminik, S. Bhar, Catal. Commun. 20 (2012) 17.
16. S. H. Cai, S. N. Rashkeev, S. T. Pantelides, K. Sohlberg, Phys. Rev. B 67 (2003) 224104.
17. (a) A. D. Cross, An Introduction to Practical IR Spectroscopy, 2nd ed., Butterworth, London, 1964. (b) A. Teimouri, A. N. Chermahini, H. Salavati, L. Ghorbanian, J. Mol. Cat. A: Chem. 373 (2013) 38.
18. (a) M. A Zolfigol, A. Khazaei, M. Mokhlesi, F. Derakhshan-Panah, J. Mol. Cat. A: Chem. 370 (2013) 111. (b) A. R. Kiasat, S. Noorizadeh, M. Ghahremani, S. J. Saghanejad, J. Mol. Str. 1036 (2013) 216.
19. X. Su, S. Chen, Z. Zhou, Appl. Surf. Sci. 258 (2012) 5712.
20. S. J. Gregg, K. S. W. Sing, Adsorption, Surface Area and Porosity, Academic Press, London, 1982.
21. (a) R. Breslow, Acc. Chem. Res. 24 (1991) 159. (b) J. Chandrasekhar, S. Shariffskul, W. L. Jorgensen, J. Phys. Chem. B. 106 (2002) 8078.
22. M. B. Yue, T. Xue, W. B. Jiao, Y. M. Wang, M. Y. He, Solid State Sci. 13 (2011) 409.

SECTION B

ZnO NANOPARTICLES CATALYSED SOLVENT-FREE SYNTHESIS OF NOVEL PYRIDINES *VIA* β-ENAMINONES*

Pyridine derivatives are among one of the most important nitrogen-containing heterocycles. These derivatives are found in numerous medicinally important natural products[1-3] and exhibit many interesting biological profiles like anti-HIV, anti-viral, anti-bacterial, anti-diabetic, antimalarial and anti-cancer activities.[4] These derivatives have been of specific interest to pharmaceutical industries and there are a number of drugs in market containing this nucleus.[5] *Isoniazide* is an antibiotic used for tuberculosis treatment, dermatitis herpetiformis is treated by *Sulphapyridine*, *Rabeprazole* is used as an antiulcer drug, *Niaprazine* is used as an antihistamine, bronchodilator and sedative, *Piroxicam* is used to relieve the pain, tenderness, inflammation and stiffness caused by arthritis, *Niflumic* acid shows antirheumatic and analgesic effects, *Doxylamine* is an antihistamine used for short-term treatment of insomnia and also to treat allergy, colds and respiratory infections. Some representative structures are given in **figure 14**. Pyridine derivatives (polyvinyl pyridine etc.) have also found use in polymer industries.[5b]

Traditionally, pyridine derivatives have been synthesised *via* condensation of amine and carbonyl compounds, [5+1] condensation of 1,5-dicarbonyls with ammonia, Bohlmann-Rahtz pyridine synthesis, Hantzsch pyridine synthesis and recently aza-Diels–Alder reaction between enamines and 1,2,4-triazine led to the formation of pyridines.[6]

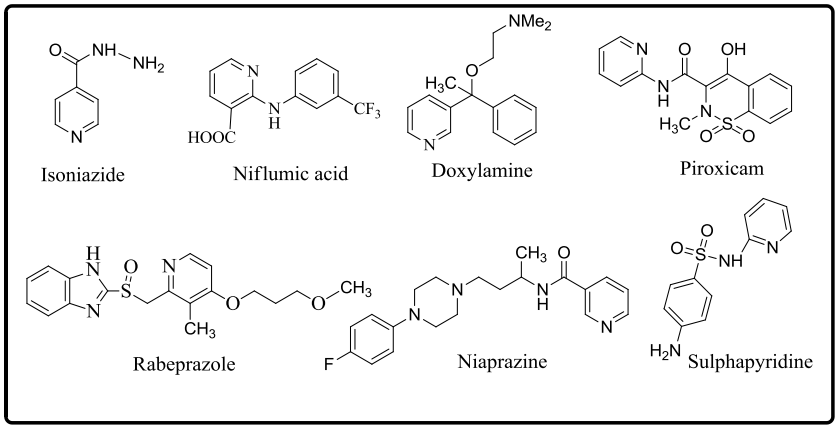

Fig. 14. Representative drugs based on pyridines

* Zeba N. Siddiqui, Nayeem Ahmed, Farheen Farooq, Kulsum Khan, ***Tetrahedron Letters***, 54 (2013) 3599.

2.7. Review of literature

Some recent examples of the synthesis of pyridine derivatives *via* β-enaminones

2.7.1. Regioselective synthesis of pyridine derivatives using enaminones.[7]

S. Kantevari *et al.* reported a regioselective one-pot, three-component condensation of enaminones, dicarbonyl compounds and ammonium acetate in the presence of a catalytic amount of $K_5CoW_{12}O_{40}.3H_2O$ in isopropyl alcohol (IPA). This protocol has merits like short reaction time, high yield, simple work-up procedure and the catalyst recyclability.

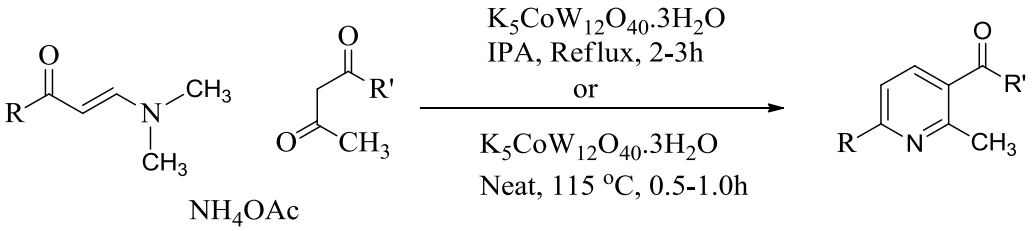

R= 1-Naphthyl, C_6H_5, 4-ClC_6H_4, 4-$CH_3C_6H_4$, 4-$CH_3OC_6H_4$, 4-BrC_6H_4 R'= OC_2H_5, CH_3

2.7.2. Synthesis of 2,3,6-trisubstituted pyridines *via* enaminones in AcOH.[8]

B. Al-Saleh *et al.* reported an efficient method for the synthesis of 2,3,6-trisubstituted pyridines by refluxing a mixture of enaminone, acetyl acetone or ethyl acetoacetate and ammonium acetate in acetic acid.

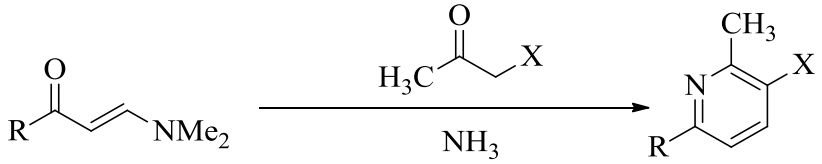

R= 2-Naphthyl, 4-ClC_6H_4, 4-$CH_3C_6H_4$, 4-$CH_3OC_6H_4$ X=$COCH_3$, CO_2Et

2.7.3. Synthesis of 2,3-disubstituted-6-arylpyridines from enaminones using Montmorillonite K10.[9]

G. J. Reddy *et al.* described an efficient method for the synthesis of 2,3-disubstituted-6-arylpyridines from enaminones in isopropyl alcohol (IPA) using montmorillonite K10 as a solid acid heterogeneous catalyst. Simple experimental and product isolation procedures coupled with high purity and yield of the products are the highlights of the presented protocol.

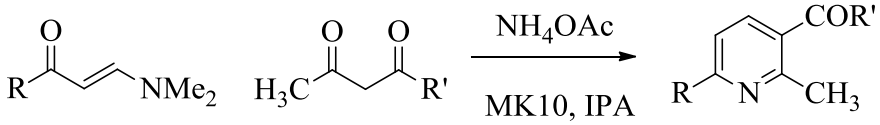

R= C_6H_5, 4-ClC_6H_4, 4-BrC_6H_4, 4-FC_6H_4, 4-$CH_3OC_6H_4$, 2-Thienyl

R'= CH_3, OC_2H_5

2.7.4. Diversity-oriented synthesis of novel aryl and heteroaryl tethered pyridines.[10]

S. Kantevari *et al.* presented diversity oriented synthesis of substituted pyridines and dihydro-6*H*-quinolin-5-ones tethered with aryls and heteroaryls in very good yields using $CeCl_3.7H_2O$-NaI as a catalyst in refluxing isopropyl alcohol. Appropriately substituted derivatives were found to be promising antitubercular agents.

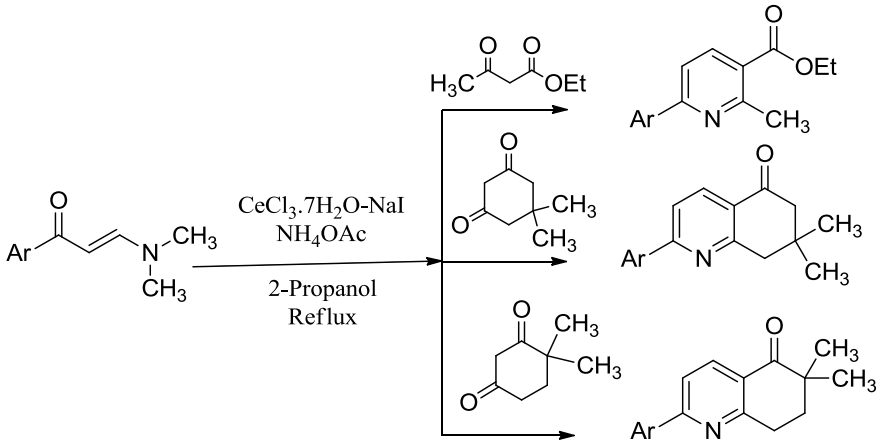

Ar = C_6H_5, 4-MeC_6H_4, 4-ClC_6H_4, 4-BrC_6H_4, 4-$NO_2C_6H_4$, 2-naphthyl, 2-indolyl, 2-thiophenyl

2.7.5. Silica supported sodium hydrogen sulphate ($NaHSO_4$–SiO_2) catalysed synthesis of pyridines.[11]

Z. N. Siddiqui and F. Farooq reported the use of $NaHSO_4$–SiO_2 as an efficient, mild and reusable catalyst for the synthesis of novel pyridine derivatives *via* heterocyclic β-enaminone. The remarkable features of this methodology are high yields, simple experimental and work-up procedures and solvent-free conditions.

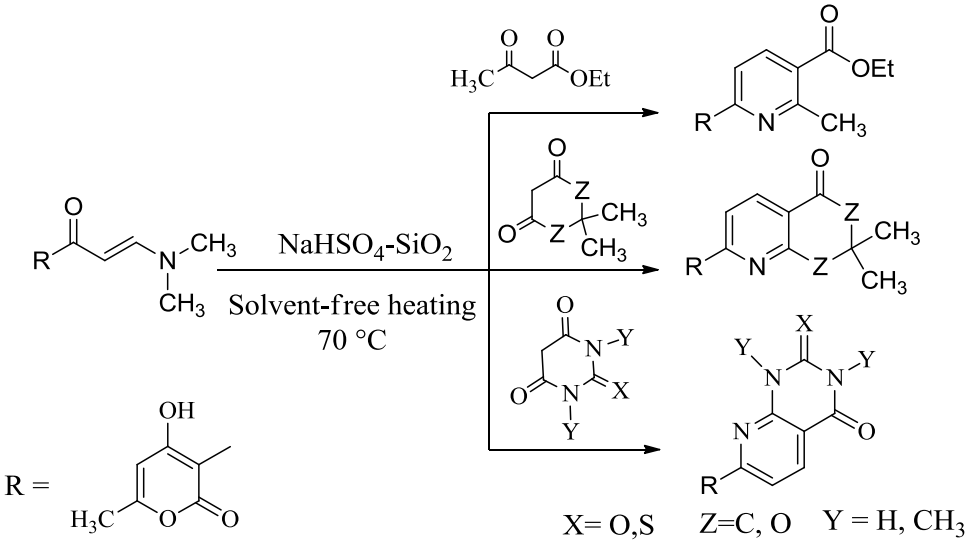

2.7.6. Chitosan catalysed synthesis of novel uracil based pyridine derivatives.[12]

Z. N. Siddiqui reported an efficient chitosan catalysed synthesis of novel uracil based pyridine derivatives using β-enaminone. The remarkable features of this protocol are chitosan as a biodegradable catalyst, solvent-free conditions and high yields.

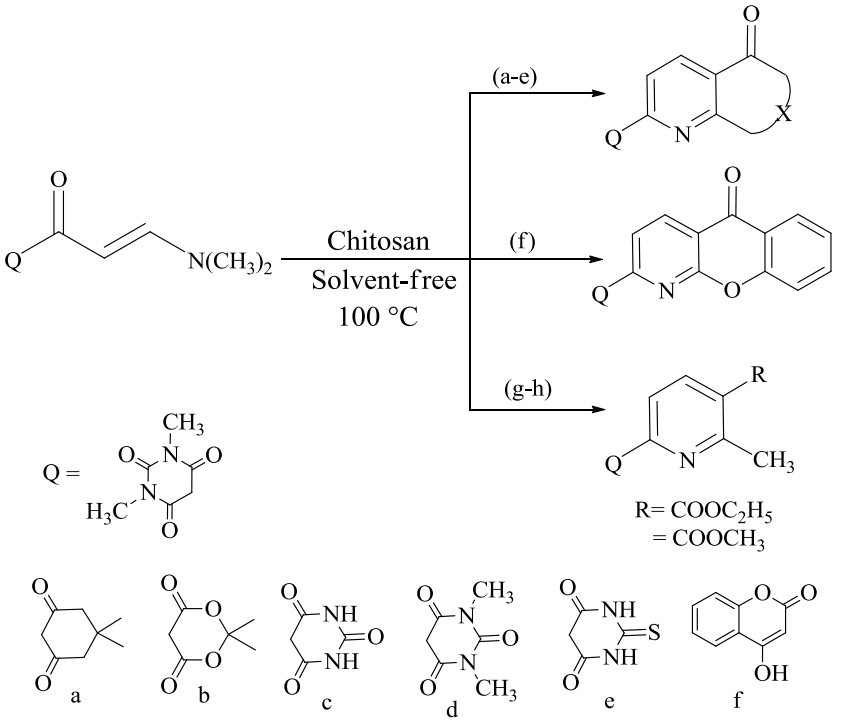

2.8. PRESENT WORK

The application of metal nanoparticles (NPs) in organic synthesis has attracted immense attention in recent years as one of the most promising solution towards efficient reactions under mild and environmentally benign conditions in the context of Green Chemistry.[13] Nano-sized inorganic solid oxides have shown a lot of promise as heterogeneous catalysts due to their properties like high level of chemoselectivity, environmental compatibility, simplicity of operation, presence of both Lewis acid and Lewis base character at their surface, and availability at low cost.[14] Nanoparticles have a characteristic high surface to volume ratio, and as a result large fraction of surface atoms are exposed to reactant molecules, therefore, their use as catalysts is quite promising.[15] ZnO NPs as heterogeneous catalyst has received considerable attention because of its cheapness, easy to synthesise, requirement of mild conditions, non-toxic nature and environmental advantages i.e., minimum execution time, low corrosion, waste minimization, recycling, easy transport and disposal of the catalyst.[16] Therefore, their use as powerful catalyst for several organic transformations has been quite encouraging.[17-20]

In this section, we have described ZnO nanoparticles catalyzed efficient, solvent-free, regioselective synthesis of novel pyridines through Michael addition, cyclodehydration and elimination sequence.

2.9. RESULTS AND DISCUSSION

2.9.1. Characterization of ZnO nanoparticles

2.9.1a. XRD analysis

Freshly synthesized ZnO nanoparticles showed XRD peaks which corresponded to hexagonal wurtzite structure **(Figure 15a)**. The crystallite size of the nanoparticles was calculated using Debye Scherrer formula

$D = K \lambda/\beta \cos \theta$

Where, K is constant, λ is the wavelength of employed x-rays (1.54056 Å), β is corrected full width at half maximum and θ is Bragg's angle.

The 2θ value from the equation comes out to be at 35.815 and therefore, the calculated crystallite size of the powder particles was found to be 25 nm. The strong and narrow diffraction peaks indicated that the product has good crystallinity.

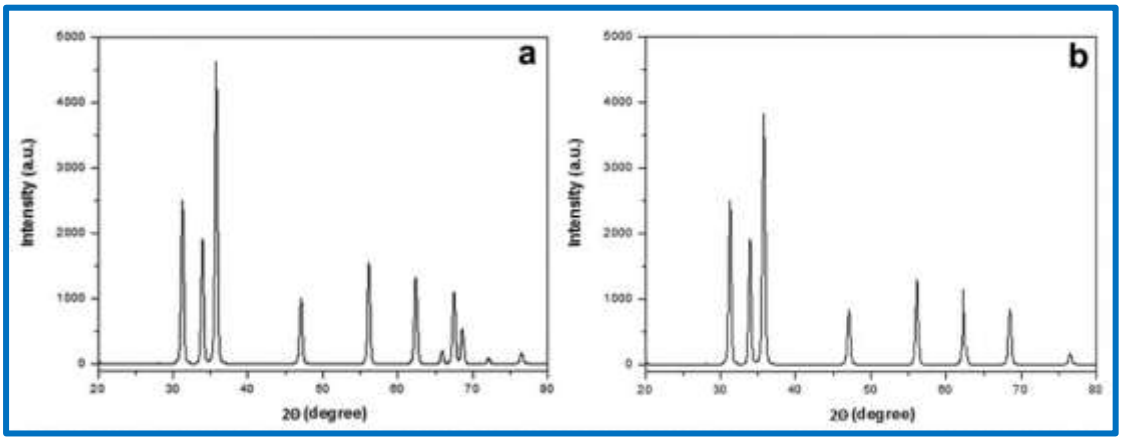

Fig. 15. (a) XRD pattern of synthesized nanoparticles and (**b**) XRD spectrum of ZnO NPs after six catalytic cycles.

2.9.1b. SEM and TEM analyses

The confirmation of the nanostructured morphology of ZnO particles was obtained from the analysis of SEM and TEM micrographs. SEM micrograph **(Figure 16a)** showed the size of nanoparticles in nanometers and TEM micrograph **(Figure 16b)** confirmed the average size between 15-25 nm.

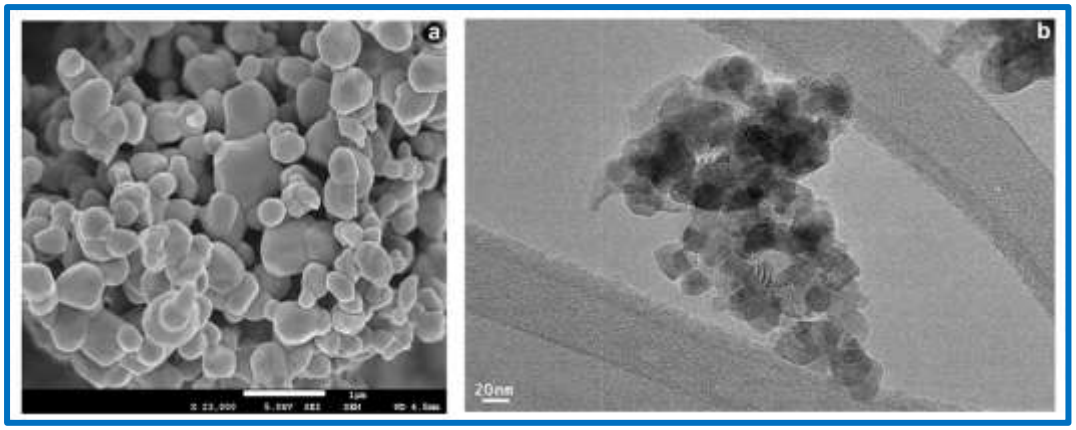

Fig. 16. (a) SEM image and (**b**) TEM image of synthesized nanoparticles.

2.9.2. Optimization of reaction conditions

2.9.2a. Effect of different catalysts and solvents

To recognize the optimization of the reaction conditions, the reaction was studied by employing a series of catalysts and solvents as well as solvent-free conditions with the expectation to maximize the product yield in short reaction times **(Table 6)**. Initially, β-enaminone **1a**, ethyl acetoacetate **(4b)** and ammonium acetate were refluxed in the presence of AcOH as the solvent without any catalyst. The reaction took longer time period of 24 h to complete and afforded product in less yield **(Table 6, entry 1)**. Taking AcOH as a solvent the reaction was carried out using different Brønsted acids like sulfamic and sulfuric acid **(Table 6, entries 2 & 5)** but the catalysts failed to promote these reactions. These catalysts were then used with different solvent like water and EtOH **(Table 6, entries 3, 4 & 6)** but again these catalysts failed to promote the reaction. We then tried the reaction with Zn-proline as a catalyst in water but the reaction failed to produce any yield **(Table 6, entry 14)**. However Zn-proline in AcOH gave product in moderate yield **(Table 6, entry 15)**. L-Proline in AcOH also failed to catalyse the reaction **(Table 6, entry 16)**. The reactions were then tried with different Lewis acid catalysts like P_2O_5, Al_2O_3, P_2O_5-silica, P_2O_5-alumina, ZnO and MgO using EtOH as a solvent or under solvent free conditions and the results are given in **Table 6 (entries 7-12 & 17-19)**. When the reaction was tried using $NaHSO_4$-SiO_2 as catalyst under solvent free condition **(Table 6, entry 13)**, the reaction completed in 2.5 h giving a moderate product yield of 75%. The reactions done under solvent-free condition gave better product yields in less reaction time. Encouraged by these results we then tried these reactions with ZnO nanoparticles using solvents like AcOH, EtOH and surprisingly the results were satisfactory **(Table 6, entries 20, 21)**.

In non-polar solvent like hexane **(entry 22)**, ZnO NPs could not catalyse the reaction. We then tried the reaction using ZnO NPs under solvent free conditions and the results obtained were excellent as the yield was 96% and time taken was only 40 min at 70 °C **(Table 6, entry 23)**. Analyzing the above results we found that the Lewis acids catalyzed the reaction very efficiently under solvent free conditions and among these Lewis acids ZnO nanoparticles proved to be most efficient catalyst for the mentioned reaction.

Table 6: Effect of different catalysts and solvents on model reaction.

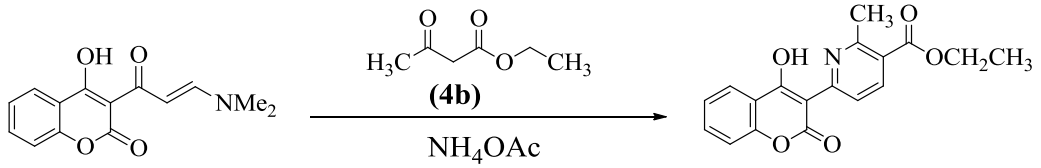

Entry	Catalyst	Solvent	Temp (°C)	Time	Yield (%)
1	nil	AcOH	reflux	24 hrs	65
2	Sulfamic acid (10 mol%)	AcOH	reflux	24 hrs	No reaction
3	Sulfamic acid (10 mol%)	H_2O	reflux	24 hrs	No reaction
4	Sulfamic acid (10 mol%)	EtOH	reflux	24 hrs	No reaction
5	Sulfuric acid (0.1 mL)	AcOH	reflux	24 hrs	No reaction
6	Sulfuric acid (0.1 mL)	EtOH	reflux	24 hrs	No reaction
7	P_2O_5 (10 mol%)	EtOH	reflux	13 hrs	68
8	P_2O_5 (10 mol%)	Solvent-free	100	6 hrs	73
9	Alumina (10 mol%)	Solvent-free	100	5.4 hrs	76
10	P_2O_5-Silica (200 mg)	EtOH	reflux	8 hrs	71
11	P_2O_5-Silica (200 mg)	Solvent-free	100	2 hrs	84
12	P_2O_5-Alumina (200 mg)	Solvent-free	100	1.5 hrs	87
13	$NaHSO_4$-Silica (200 mg)	Solvent-free	70	2.5 hrs	75
14	Zn-Proline (10 mol%)	H_2O	reflux	24 hrs	No reaction
15	Zn-Proline (10 mol%)	AcOH	reflux	10 hrs	78
16	L-Proline (10 mol%)	AcOH	reflux	24 hrs	No reaction
17	ZnO(Bulk) (10 mol%)	EtOH	reflux	5 hrs	78
18	ZnO(Bulk) (10 mol%)	Solvent-free	90	2.5 hrs	85
19	MgO(Bulk) (10 mol%)	Solvent-free	90	3.2 hrs	83

20	ZnO NPs (10 mol%)	EtOH	reflux	4 hrs	88
21	ZnO NPs (10 mol%)	AcOH	reflux	6 hrs	76
22	ZnO NPs (10 mol%)	Hexane	reflux	24 hrs	No reaction
23	ZnO NPs (10 mol%)	Solvent-free	70	40 min	96

2.9.2b. Effect of catalyst loading

Taking ZnO nanoparticles as the right catalyst, we then concentrated our attention towards optimization of the amount of the catalyst for the reaction **(Table 7)**. The results indicated that the use of 10 mol% ZnO NPs was optimum to produce the best results of 96% product yield. The use of 5 mol% ZnO NPs diminished the product yield, whereas increasing the amount of catalyst to 15-20 mol% did not had any profound effect on the reaction.

Table 7: Effect of catalyst loading on model reaction.

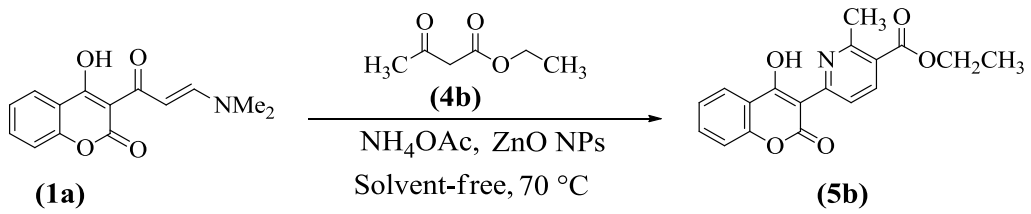

Entry	Amount of catalyst	Time (min)	Yield (%)
1	5 mol%	65	92
2	10 mol%	40	96
3	15 mol%	40	94
4	20 mol%	40	93

2.9.2c. Effect of temperature

The effect of temperature on the rate of reaction was studied by conducting the reaction at RT, 40 °C , 70 °C, 100 °C and 120 °C under the standard reaction conditions using ZnO NPs as catalyst **(Table 8)**. The results showed that the catalytic performance of the catalyst strongly increased with the reaction temperature. It was found that at 70 °C maximum product yield was obtained.

Table 8: Effect of temperature on the model reaction using ZnO nanoparticles.

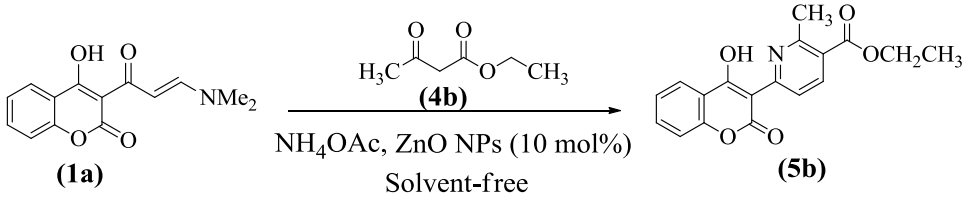

Entry	Temp (°C)	Time (min)	Yield (%)
1	Room Temp	2h	No reaction
2	40	2h	No reaction
3	70	40	96
4	100	40	92
5	120	40	89

2.9.2d. Catalytic reaction

Therefore, at a constant temperature of 70°C under solvent-free condition, 10 mol% ZnO NPs were used as catalyst for this reaction as the maximum yield (96%) was obtained under these conditions. Hence, these optimized conditions were applied for all experiments taking appropriate amounts of β-enaminone, active methylene compounds and ammonium acetate under solvent-free conditions in the presence of 10 mol% ZnO NPs **(Scheme 4)**.

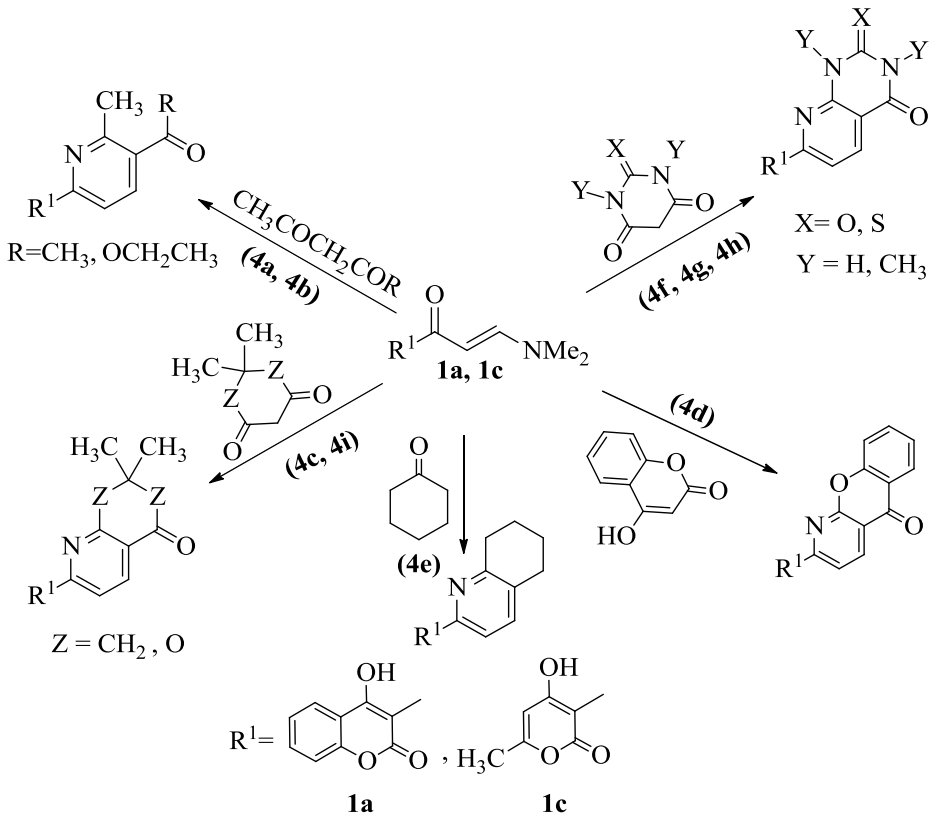

Scheme 4: Synthesis of pyridine derivatives.

All the reactions proceeded smoothly and afforded a library of pyridine derivatives **(5a-p)** in excellent yields (89-96%) **(Table 9)**. The reactions were consistently carried out at the 1 mmol scale. However, no change of product yield was observed when the reactions were carried out at more than 1 mmol scale (up to the 10 mmol scale). From the view point of green chemistry, it was positive to find that the final products could be isolated, almost in pure form, by filtration due to insolubility of catalyst in safe organic solvents. As the synthesis of pyridines involves nucleophilic attack of active methylene compound followed by attack of ammonia and then cyclization step , the hindrance produced by the fusion of benzene ring to the pyran moiety can be the reason for the increased time period (40-59 min) for benzopyran substituted pyridines **(5a-h)** compared to pyran substituted pyridines **(5i-p)** (4-15 min).

Table 9: Synthesis of heteroaryl pyridine derivatives.

Entry	4a-i	Product	Time (min)	Yield (%)
1	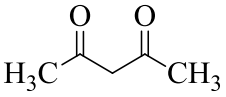 **4a**	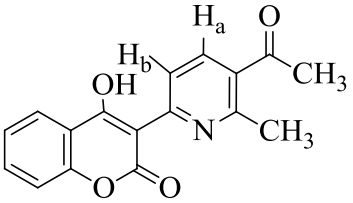 **5a**	48	95
2	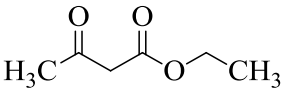 **4b**	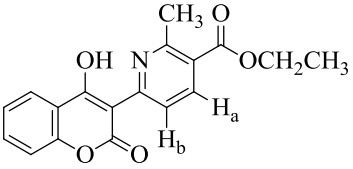 **5b**	40	96
3	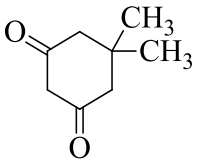 **4c**	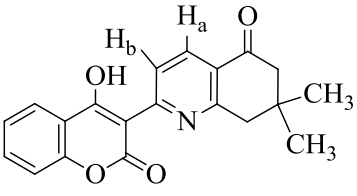 **5c**	45	96
4	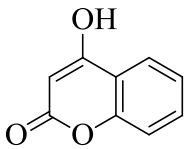 **4d**	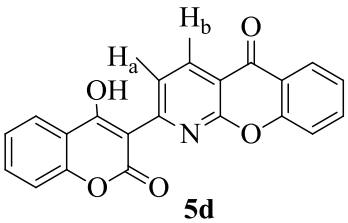 **5d**	53	91

5	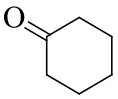 **4e**	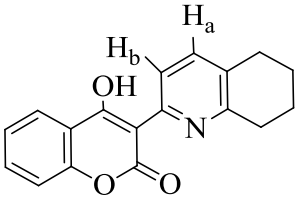 **5e**	59	92
6	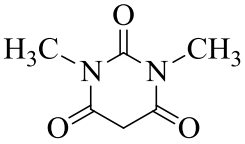 **4f**	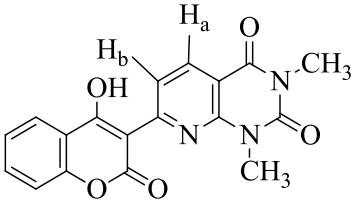 **5f**	43	93
7	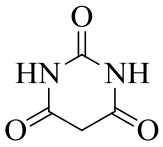 **4g**	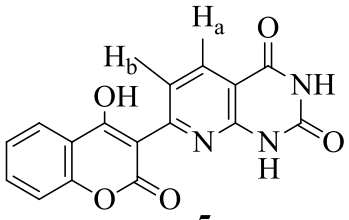 **5g**	56	91
8	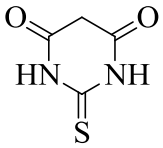 **4h**	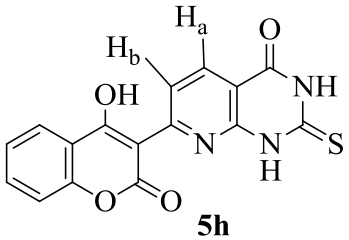 **5h**	54	91
9	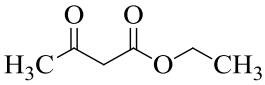 **4b**	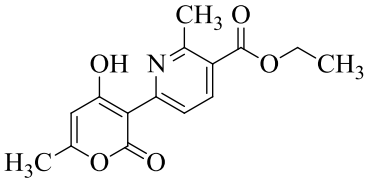 **5i**	5	94
10	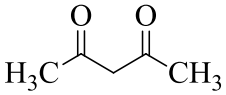 **4a**	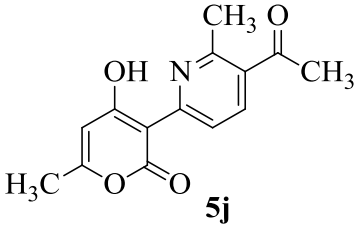 **5j**	4	91

11	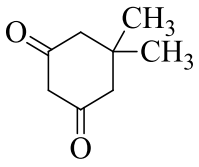 **4c**	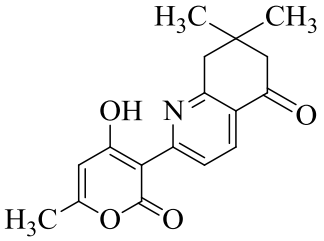 **5k**	8	92
12	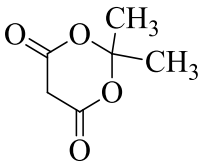 **4i**	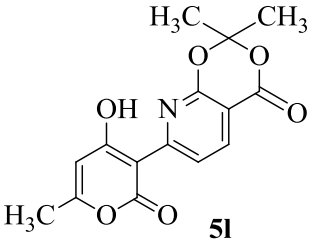 **5l**	9	90
13	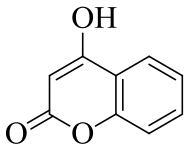 **4d**	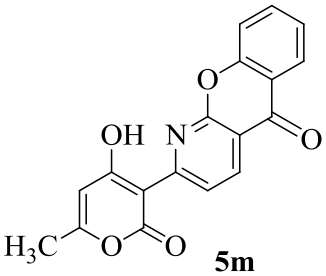 **5m**	12	89
14	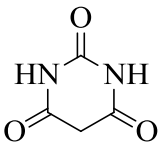 **4g**	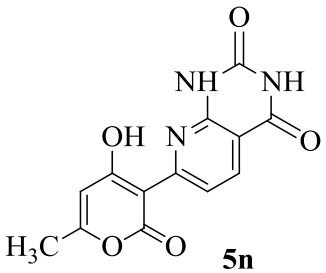 **5n**	15	92
15	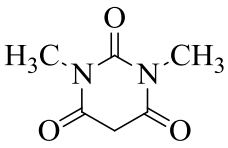 **4f**	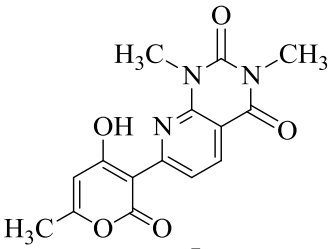 **5o**	10	93
16	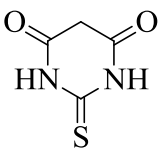 **4h**	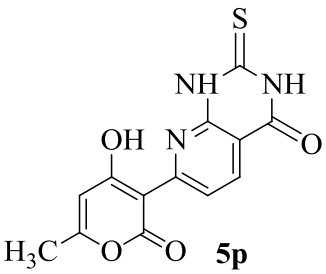 **5p**	15	92

The structures of the final products were well characterized by IR, ^{1}H, ^{13}C NMR, ESI-MS and elemental analysis techniques. I.R. spectrum of **5b (Figure 17)** showed stretching for OH group of benzopyran moiety at 3200cm^{-1}. Coumarin carbonyl and carbonyl group of ethyl ester showed absorption bands at 1714 cm^{-1} and 1690 cm^{-1}, respectively. In the ^{1}H-NMR spectrum **(Figure 18)**, OH proton appeared as singlet at δ 19.32. The presence of distinctive doublets at δ 9.02 and δ 8.47 for H_a and H_b protons confirmed the formation of pyridine ring. ^{13}C-NMR **(Figure 19)** showed distinctive peaks for CH_3 and CH_2 carbons of ester functionality at δ14.27 and 61.87, respectively. The peaks at δ 163.79 and 156.26 were assigned to carbonyl carbons of ethyl ester and coumarin moiety, respectively. All other peaks were obtained at their correct values and are given in experimental section. Further structural confirmation was provided by ESI-Mass spectrum **(Figure 20)** which showed the molecular ion peak as a base peak at m/z 326.1(M^{+}+1).

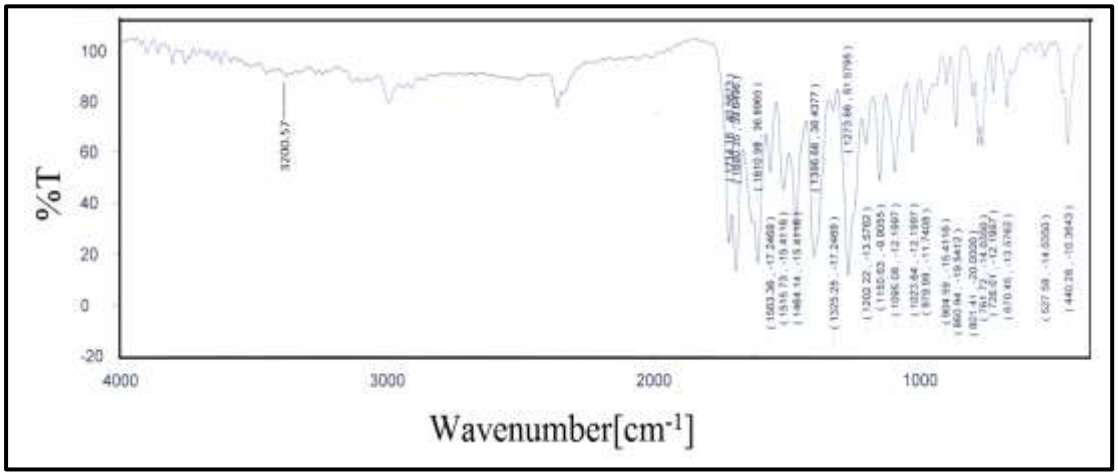

Fig. 17. FT-IR spectrum of **5b**

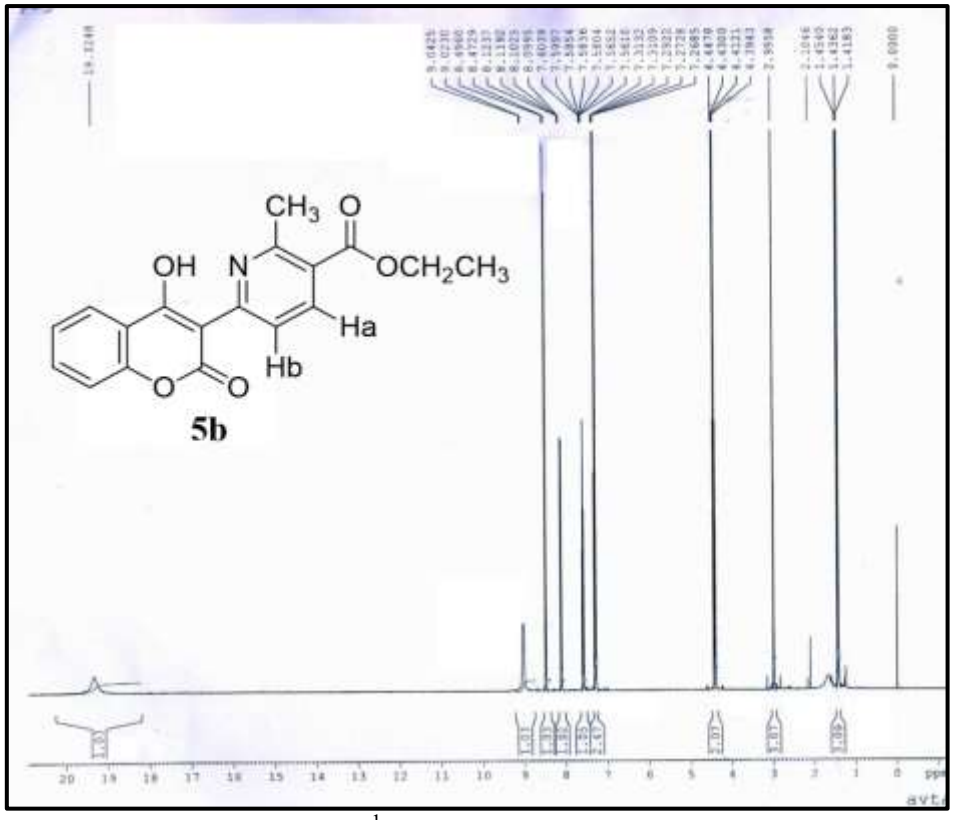

Fig. 18. ^{1}H-NMR spectrum of **5b**

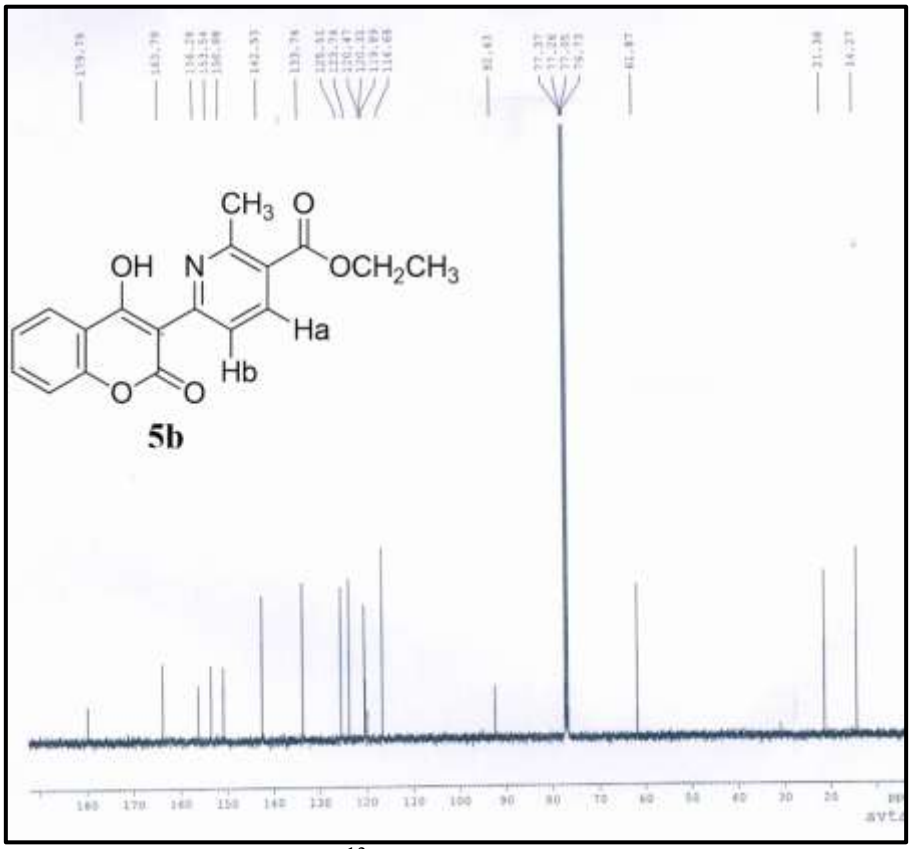

Fig. 19. ^{13}C-NMR spectrum of **5b**

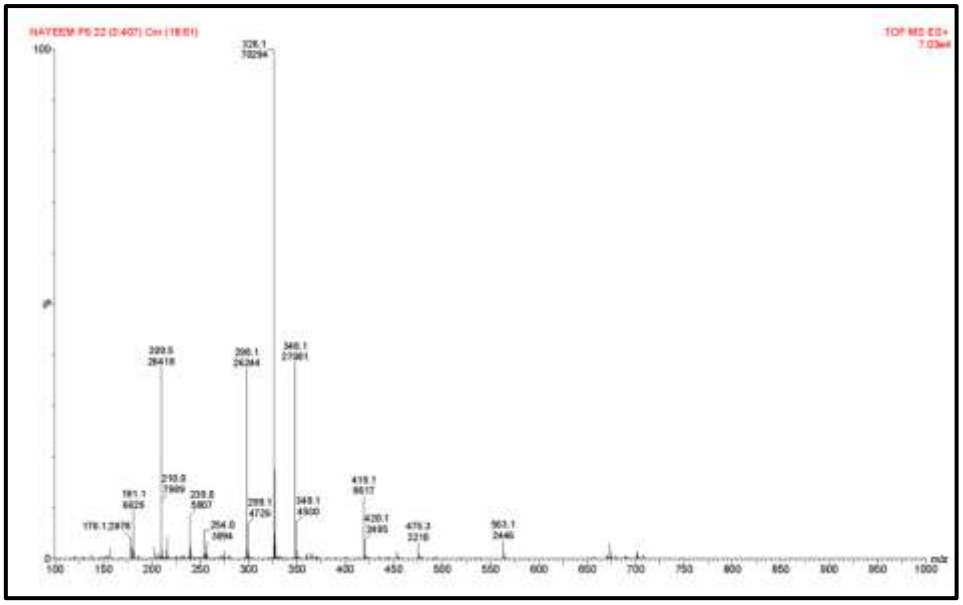

Fig. 20. ESI-Mass spectrum of **5b**

A plausible mechanism for the reaction in the presence ZnO NPs has been shown in **Scheme 5**. The mechanism involves Michael addition in which activated **4b** attacks on the activated double bond of β-enaminone **(1a)** to give adduct **(I)**. Attack of NH_3 on carbonyl group of adduct **(I)** gives intermediate **(J)**, which undergoes further intramolecular cyclization to generate intermediate **(K)**. Loss of dimethyl amine followed by aromatization of **K** gives the final product **5b**.

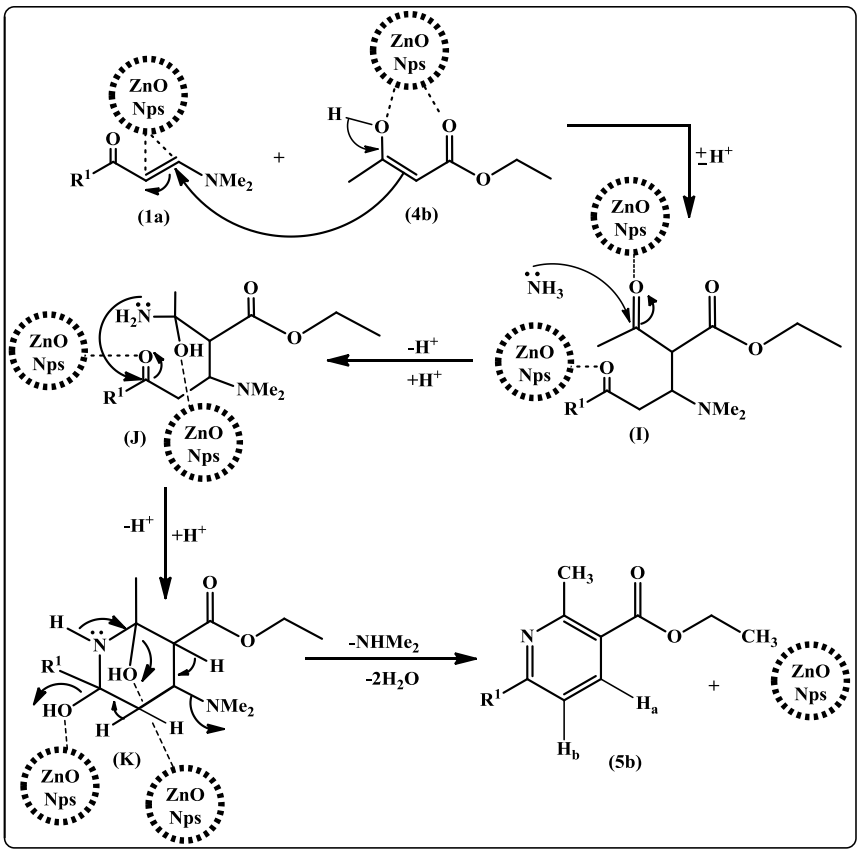

Scheme 5: Plausible mechanism for the formation of pyridine derivative **5b**.

2.9.3. Catalyst recyclability

Recyclability of the catalyst was evaluated by the model reaction comprising β-enaminone **1a**, ethyl acetoacetate **4b**, and ammonium acetate in the presence of 10 mol% ZnO NPs under solvent-free conditions. After completion of reaction, the catalyst was recovered, washed with ethanol and dried at 120 °C. The catalyst was then reused for subsequent cycles and was found to retain good catalytic activity up to six cycles **(Figure 21)**. The XRD pattern after six catalytic cycles indicated that the crystallinity of ZnO nanoparticles was preserved during the course of reaction **(Figure 15b)**.

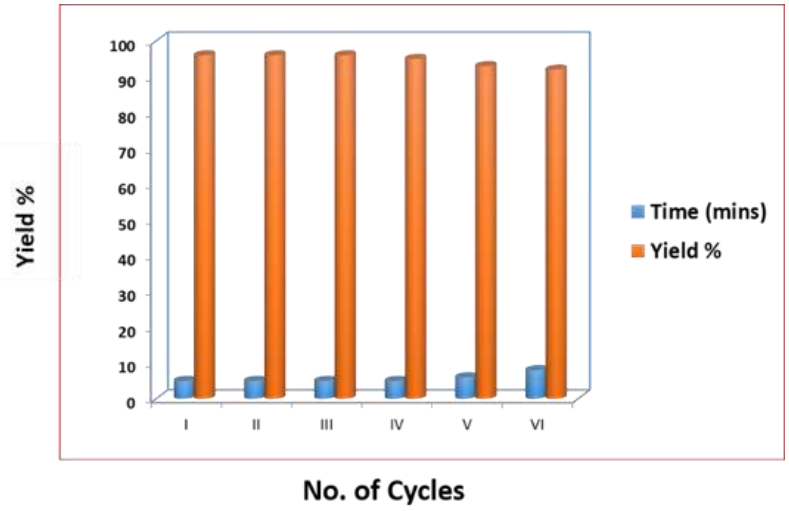

Fig. 21. Recycling data of ZnO nanoparticles for the model reaction.

2.10. CONCLUSION

In conclusion, ZnO nanoparticles were found to be an efficient catalyst for simple, cost effective and green synthesis of novel benzopyran substituted pyridines via β-enaminones under solvent-free conditions. Recyclable catalyst, high yield of products, ease of work-up, and the ecologically clean procedure, will make the present method a sustainable alternative to the existing methodologies for the synthesis of substituted pyridines.

2.11. EXPERIMENTAL

2.11.1. Preparation of ZnO nanoparticles

ZnO nanoparticles were synthesised by sol-gel method by the following procedure. To 100 mL double distilled water, citric acid was added in order to maintain the pH of the solution at 2. Then 20 g of zinc acetate was added to this solution with constant stirring. After adding zinc acetate, 10 mL of PEG-600 was added and the solution was continuously stirred for 45 min at a constant temperature of 40 °C. Ammonia solution was then added drop wise till white precipitate is obtained. The precipitate, as obtained was centrifuged, dried at 120 °C and calcined at 600 °C for two hours. The nanoparticles were then grinded, characterized and used as catalyst.

2.11.2. General procedure for the synthesis of substituted pyridine derivatives

A mixture of β-enaminones **1a, 1c** (1mmol), active methylene compounds **4a-i** (1mmol), ammonium acetate (6 mmol) and10 mol% ZnO nanoparticles was taken in a round bottom flask and heated at a constant temperature of 70 °C with continuous stirring, under solvent free condition, for a specified period of time **(Table 9)**. After completion of the reaction (monitored by TLC), the reaction mixture was allowed to

cool and added ethanol or DMSO depending on the solubility of the compound. The mixture was filtered in order to recover the catalyst, which was then washed with ethanol, dried in oven at 120 °C and reused for subsequent cycles. The compounds were recrystallized from ethanol or DMSO.

2.11.3. Spectral data of synthesized compounds

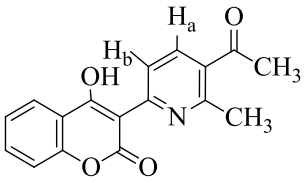 **5a**	*3-Acetyl-6-(4-hydroxy-1-benzopyran-2-one-3-yl)-2-methyl-pyridine* Light yellow crystals, **M.P.** 290-295 °C. **Anal. Calcd** ($C_{17}H_{13}NO_4$): C, 69.21; H, 4.41; N, 4.74 **Anal. Found** ($C_{17}H_{13}NO_4$): C, 69.23; H, 4.42; N, 4.72. **IR** (KBr, cm^{-1}): 3354 (OH), 1694, 1615 (C=O). **^{1}H NMR** (400 MHz, DMSO-d_6): δ 2.12 (3H,s), 2.65 (3H,s), 7.25-8.05 (4H,m,Ar-H), 8.59 (1H,d,H_b, *J*=9.1), 8.95 (1H,d,H_a, *J*=9.1), 19.02 (1H,s,OH). **^{13}C NMR** (100 MHz, DMSO-d_6): δ 171.95, 162.94, 157.83, 153.76, 150.13, 147.43, 133.91, 131.89, 127.73, 120.96, 119.48, 116.21, 112.11, 105.68, 103.23, 32.76, 27.95. **ESI-MS:** (*m/z*) 296 (M^++1).
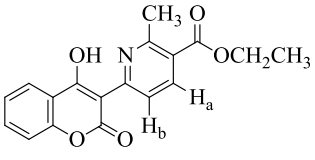 **5b**	*3-Ethoxycarbonyl-6-(4-hydroxy-1-benzopyran-2-one-3-yl)-2-methyl-pyridine* Light yellow crystals, **M.P.** 255-258 °C. **Anal. Calcd** ($C_{18}H_{15}NO5$): C, 66.52; H, 4.62; N, 4.30 **Anal. Found** ($C_{18}H_{15}NO5$): C, 66.51; H, 4.63; N, 4.28. **IR** (KBr, cm^{-1}): 3200 (OH), 1714, 1691 (C=O). **^{1}H NMR** (400MHz, DMSO-d_6): δ 1.43 (3H,t,), 2.99 (3H,s), 4.4 (2H,q), 7.2-8.1(4H,m,Ar-H), 8.47 (1H,d,H_b, *J*=9.2), 9.02 (1H,d,H_a, *J*=8.8), 19.32 (1H,S,OH). **^{13}C NMR** (100 MHz, DMSO-d_6): δ 179.79, 163.79, 156.26, 153.54, 150.88, 142.53, 133.74, 125.51, 123.74, 120.47, 120.31, 119.89, 116.68, 92.43, 61.87, 21.36, 14.27. **ESI-MS:** (*m/z*) 326.1 (M^++1).
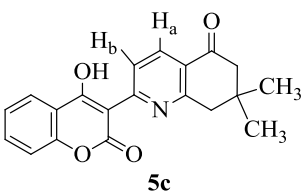 **5c**	*7,7-Dimethyl-5-oxo-2-(4-hydroxy-1-benzopyran-2-one-3-yl)-5,6,7,8 tetrahydroquinoline* Yellow crystals, **M.P.** >300 °C. **Anal. Calcd** ($C_{20}H_{17}NO_4$): C, 71.70; H, 5.07; N, 4.17 **Anal. Found** ($C_{20}H_{17}NO_4$): C, 71.72; H, 5.08; N, 4.15. **IR** (KBr, cm^{-1}): 3368 (OH), 1652, 1615

	(C=O). **^{1}H NMR** (400MHz, DMSO-d_6): δ 1.13 (6H,s), 2.58 (2H,s), 3.18 (2H,s), 7.2-8.04 (4H,m,Ar-H), 8.42 (1H,d,H_b, *J*=9.5), 8.92 (1H,d,H_a, *J*=9.1), 18.86 (1H,s,OH). **^{13}C NMR** (100 MHz, DMSO-d_6): δ 193.40, 178.83, 176.05, 170.67, 156.55, 153.30, 138.08, 133.82, 130.32, 125.25, 123.59, 122.62, 120.29, 116.16, 102.28, 62.89, 50.54, 32.81, 27.57. **ESI-MS:** (*m/z*) 336 (M^++1).
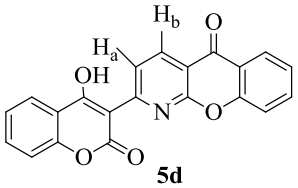 **5d**	*2-(4-hydroxy-1-benzopyran-2-one-3-yl)-pyrido[2,3-b]-chroman-5-one* Yellow solid, **M.P.** 290-295 °C. **Anal. Calcd** ($C_{21}H_{11}NO_5$): C, 70.65; H, 3.08; N, 3.92 **Anal. Found** ($C_{21}H_{11}NO_5$): C, 70.66; H, 3.11; N, 3.90. **IR** (KBr, cm^{-1}): 3364 (OH), 1723, 1671 (C=O). **^{1}H NMR** (400MHz, DMSO-d_6): δ 7.16-8.23 (8H,m,Ar-H), 8.35 (1H,d,H_b, *J*=9.2), 8.75 (1H,d,H_a, *J*=9.1), 18.72 (1H,d,OH). **^{13}C NMR** (100 MHz, DMSO-d_6): δ 175.25, 170.11, 164.28, 160.21, 156.47, 154.14, 148.89, 136.21, 130.51, 125.18, 124.21, 123.75, 122.09, 120.76, 119.22, 118.08, 117.55, 116.16, 110.38, 108.72, 101.02. **ESI-MS:** (*m/z*) 358 (M^++1).
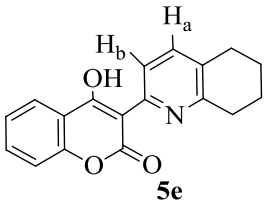 **5e**	*(4-hydroxy-1-benzopyran-2-one-3-yl)-5,6,7,8 tetrahydroquinoline* Yellow solid, **M.P.** 250-253 °C. **Anal. Calcd** ($C_{18}H_{15}NO_3$): C, 73.78; H, 5.12; N, 4.77. **Anal. Found** ($C_{18}H_{15}NO_3$): C, 73.76; H, 5.14; N, 4.78. **IR** (KBr, cm^{-1}): 3283 (OH), 1706 (C=O). **^{1}H NMR** (400MHz, DMSO-d_6): δ 1.2 (4H,q), 2.5 (2H,t), 3.29 (2H,d), 7.16-7.95 (4H,m,Ar-H), 8.16 (1H,d,H_b, *J*=9.2), 8.61 (1H,d,H_a *J*=9.1), 18.49 (1H,s,OH). **^{13}C NMR** (100 MHz, DMSO-d_6): δ 176.28, 168.36, 156.76, 152.47, 148.56, 138.22, 135.76, 127.23, 125.44, 123.17, 122.06, 120.10, 118.68, 101.21, 35.21, 32.11, 28.11, 26.89. **ESI-MS:** (*m/z*) 294 (M^++1).
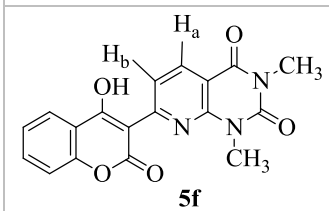 **5f**	*1,3-Dimethyl-7-(4-hydroxy-1-benzopyran-2-one-3-yl)-1H,3H-pyrido[2,3-d] pyrimidine-2,4-dione* Orange solid, **M.P.** 280-285 °C. **Anal. Calcd** ($C_{18}H_{13}N_3O_5$): C, 61.59; H, 3.70; N, 11.91 **Anal. Found** ($C_{18}H_{13}N_3O_5$): C,

	61.57; H, 3.72; N, 11.93. **IR** (KBr, cm^{-1}): 3150 (OH), 1690, 1626 (C=O). **^{1}H NMR** (400MHz, DMSO-d_6): δ 3.15 (3H,S), 3.26 (3H,S), 7.2-7.9 (4H,m,Ar-H), 8.3 (1H,d,H_b, *J*=9.3), 8.6 (1H,d,H_a, *J*=9.4), 18.1 (1H,S,OH). **^{13}C NMR** (100 MHz, DMSO-d_6): δ 176.96, 162.14, 158.13, 153.51, 149.33, 138.78, 137.21, 133.36, 124.98, 123.34, 115.81, 107.31, 105.19, 27.10, 26.14. **ESI-MS:** (*m/z*) 352 (M^++1).
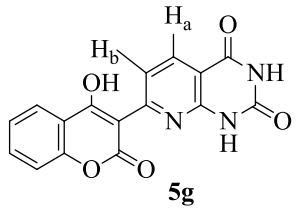 **5g**	*7-(4-hydroxy-1-benzopyran-2-one-3-yl)-1H,3H-pyrido[2,3-d]pyrimidine-2,4-dione* Orange solid, **M.P.** >300 °C. **Anal. Calcd** ($C_{16}H_9N_3O_5$): C, 59.51; H, 2.78; N, 13.00 **Anal. Found** ($C_{16}H_9N_3O_5$): C, 59.51; H, 2.75; N, 13.02. **IR** (KBr, cm^{-1}): 3172 (OH), 1701, 1618 (C=O). **^{1}H NMR** (400MHz, DMSO-d_6): δ 6.9 (1H,s,NH), 7.07 (1H,s,NH), 7.25-8.13 (4H,m,Ar-H), 8.24 (1H,d,H_b, *J*=9.2), 8.58 (1H,d,H_a, *J*=9.4), 18.06 (1H,s,OH). **^{13}C NMR** (100 MHz, DMSO-d_6): δ 183.29, 180.93, 168.32, 160.16, 153.36, 151.12, 148.48, 133.53, 125.00, 123.06, 118.85, 115.86, 109.75, 104.40, 97.34, 96.56. **ESI-MS:** (*m/z*) 324 (M^++1).
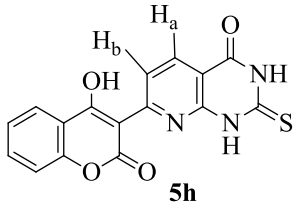 **5h**	*2-Thioxo-7-(4-hydroxy-1-benzopyran-2-one-3-yl)-1H,3H-pyrido[2,3-d]pyrimidine-4-one* Orange solid, **M.P.** >300 °C. **Anal. Calcd** ($C_{16}H_9N_3O_5$): C, 56.68; H, 2.65; N, 12.39 **Anal. Found** ($C_{16}H_9N_3O_5$): C, 56.65; H, 2.67; N, 12.38. **IR** (KBr, cm^{-1}): 3170 (OH), 1723, 1619 (C=O). **^{1}H NMR** (400MHz, DMSO-d_6): δ 6.96 (1H,s,NH), 7.15-7.99 (4H,m,Ar-H), 8.09 (1H,s,NH), 8.36 (1H,d,H_b, *J*=9.3), 8.53 (1H,d,H_a, *J*=9.4), 18.37 (1H,s,OH). **^{13}C NMR** (100 MHz, DMSO-d_6): δ 185.13, 175.96, 167.76, 158.62, 153.51, 147.65, 144.62, 140.12, 133.93, 125.08, 123.21, 118.49, 115.98, 106.81, 98.21, 97.11. **ESI-MS:** (*m/z*) 340 (M^++1).
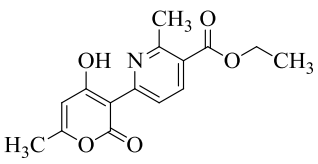 **5i**	*3-Ethoxycarbonyl-6-(4-hydroxy-6-methyl-2-oxo-2H-1-pyran-3-yl)-2-methyl-pyridine*[11] Light yellow solid, **M.P.** 201°C. **Anal. Calcd** ($C_{15}H_{15}NO_5$): C, 62.34; H, 5.23; N, 4.84; **Anal. Found** ($C_{15}H_{15}NO_5$)**:** C,

	62.22; H, 5.14; N, 4.71. **IR** (KBr, cm^{-1}): 3065 (OH), 1717 (C=O), 1697 (C=O). **^{1}H NMR** (400 MHz, $CDCl_3$): δ 1.42 (3H, t), 2.22 (3H, s), 2.92 (3H, s), 4.44 (2H, q, J = 7.2 Hz), 5.86 (1H, s), 8.44 (1H, d, J = 9.3 Hz, H_b), 8.85 (1H, d, J = 9.3 Hz, H_a). **^{13}C NMR** (100 MHz, DMSO-d_6): δ 182.5. 164.4, 163.4, 163.2, 156.19, 151.2, 142.2, 120.2, 119.7, 106.2, 91.9, 61.7, 21.5, 20.0, 14.2. **ESI-MS:** (*m/z*) 290.1 (M^++1).
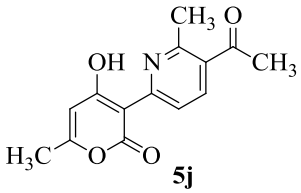 **5j**	*3-Acetyl-6-(4-hydroxy-6-methyl-2-oxo-2H-1-pyran-3-yl)-2-methyl-pyridine*[11] Light yellow solid, **M.P.** 130 °C. **Anal. Calcd** ($C_{14}H_{13}NO_4$): C, 64.92; H, 5.05; N, 5.40; **Anal. Found** ($C_{14}H_{13}NO_4$): C, 64.81; H, 4.92; N, 5.28. **IR** (KBr, cm^{-1}): 3336 (OH), 1695 (C=O), 1672 (C=O). **^{1}H NMR** (400 MHz, $CDCl_3$): δ 2.17 (3H, s), 2.69 (3H, s), 2.75 (3H, s), 5.96 (1H, s), 8.62 (1H, d, J = 9.0 Hz, H_b), 8.68 (1H, d, J = 9.3 Hz, H_a). **^{13}C NMR** (100 MHz, DMSO-d_6): δ 196.76. 180.29, 163.4, 163.2, 156.2, 151.2, 142.3, 121.5, 120.0, 105.27, 92.4, 21.7, 20.2, 14.3. **ESI-MS:** (*m/z*) 260.1 (M^++1).
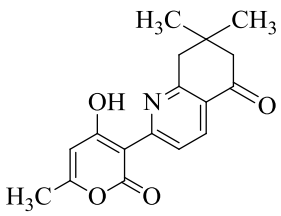 **5k**	*7,7-Dimethyl-5-oxo-2-(4-hydroxy-6-methyl-2-oxo-2H-1-pyran-3-yl)-5,6,7,8 tetrahydroquinoline*[11] Light yellow solid, **M.P.** >300 °C. **Anal. Calcd** ($C_{17}H_{17}NO_4$): C, 68.28; H, 5.73; N, 4.54; **Anal. Found** ($C_{17}H_{17}NO_4$): C, 68.15, H, 5.61; N, 4.54. **IR** (KBr, cm^{-1}): 3088 (OH), 1722, 1686 (C=O). **^{1}H NMR** (400 MHz, $CDCl_3$): δ 1.17 (6H, s), 2.22 (3H, s), 2.57 (2H, s), 3.02 (2H, s), 5.93 (1H, s), 8.42 (1H, d, J = 9.0 Hz, H_b), 8.93 (1H, d, J = 9.9 Hz, H_a). **^{13}C NMR** (100 MHz, DMSO-d_6): δ 194.0. 182.2, 163.7, 163.0, 157.9, 153.2, 137.8, 122.9, 120.7, 105.7, 92.9, 51.3, 42.6, 33.2, 30.9, 28.2, 20.10. **ESI-MS:** (*m/z*) 300.1 (M^++1).
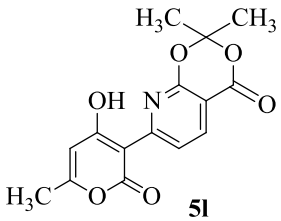 **5l**	*7-(4-Hydroxy-6-methyl-2-oxo-2H-pyran-3-yl)-2,2-dimethyl-1,3-dioxa-8-aza-quinoline-4-one*[11] Brown solid, **M.P.** >300 °C. **Anal. Calcd** ($C_{15}H_{13}NO_6$): C, 59.40; H, 4.29; N, 4.60; **Anal. Found** ($C_{15}H_{13}NO_6$): C, 59.53; H, 4.13; N, 4.72. **IR** (KBr, cm^{-1}): 3283 (OH), 1735 (C=O), 1688 (C=O). **^{1}H NMR** (400 MHz, $CDCl_3$): δ 1.61 (6H s),

	2.22 (3H, s), 5.89 (1H, s), 8.45 (1H, d, J = 9.0 Hz, H_b), 9.06 (1H, d, J = 9.0 Hz, H_a). **^{13}C NMR** (100 MHz, DMSO-d_6): δ 183.2, 164.0, 163.5, 163.1, 153.4, 151.2, 138.4, 119.4, 115.5, 106.0, 105.7, 92.9, 27.8, 27.1, 20.1. **ESI-MS:** (*m/z*) 304.1(M^++1).
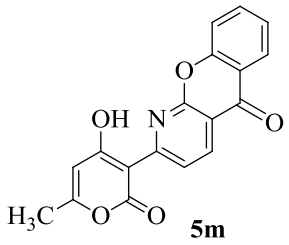 **5m**	*2-(4-hydroxy-6-methyl-2-oxo-2H-1-pyran-3-yl)-pyrido[2,3-b]-chroman-5-one*[11] White solid, **M.P.** >300 °C. **Anal. Calcd** ($C_{18}H_{11}NO_5$): C, 67.35; H, 3.45; N; 4.35; **Anal. Found** ($C_{18}H_{11}NO_5$): C, 67.20; H, 3.56; N, 4.48. **IR** (KBr, cm^{-1}): 3445 (OH), 3085 (OH), 1707 (C=O), 1670 (C=O). **^{1}H NMR** (400 MHz, $CDCl_3$): δ 2.22 (3H, s), 5.94 (1H, s), 7.41-8.10 (4H, m, Ar-H), 8.57 (1H, d, J = 9.6 Hz, H_b), 8.92 (1H, d, J = 9.0 Hz, H_a). **^{13}C NMR** (100 MHz, DMSO-d_6): δ 180.2, 172.7, 164.5, 162.7, 162.1, 154.4, 152.5, 139.9, 138.7, 137.7, 129.8, 127.5, 120.1, 118.4, 117.8, 105.9, 94.9, 19.4. **ESI-MS:** (*m/z*) 322.3 (M^++1).
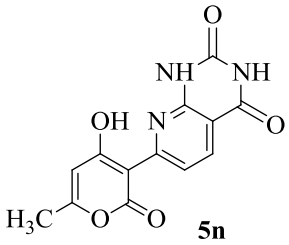 **5n**	*7-(4-Hydroxy-6-methyl-2-oxo-2H-1-pyran-3-yl)-1H,3H-pyrido[2,3-d]pyrimidine-2,4-dione*[11] Orange solid, **M.P.** >300 °C. **Anal. Calcd** ($C_{13}H_9N_3O_5$): C, 54.40; H, 3.16; N, 14.64; **Anal. Found** ($C_{13}H_9N_3O_5$): C, 54.26.; H, 3.08, N, 14.51. **IR** (KBr, cm^{-1}): 3396 (OH), 3225 (NH), 3038 (NH), 1684 (C=O). **^{1}H NMR** (400 MHz, $CDCl_3$): δ 2.12 (3H, s), 5.83 (1H, s), 8.07 (1H, d, J = 10.9 Hz, H_b), 8.48 (1H, d, J = 10.9 Hz, H_a), 9.97 (1H, s, NH), 10.10 (1H, s, NH). **^{13}C NMR** (100 MHz, DMSO-d_6): δ 184.4, 164.6, 163.6, 161.7, 155.5, 153.8, 151.1, 147.6, 125.6, 119.6, 104.6, 96.1, 19.5. **ESI-MS:** (*m/z*) 288.1 (M^++1).
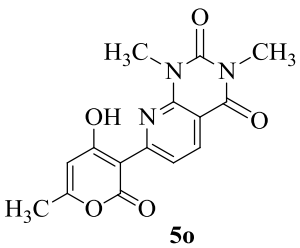 **5o**	*1,3-Dimethyl-7-(4-hydroxy-6-methyl-2-oxo-2H-1-pyran-3-yl)-1H,3H-pyrido[2,3-d] pyrimidine-2,4-dione*[11] Orange solid, **M.P.** 241 °C. **Anal. Calcd** ($C_{15}H_{13}N_3O_5$): C, 57.19; H, 4.16; N, 3.31; **Anal. Found** ($C_{15}H_{13}N_3O_5$): C, 57.08; H, 4.04; N, 3.18. **IR** (KBr, cm^{-1}): 3169 (OH), 1700 (C=O), 1672 (C=O). **^{1}H NMR** (400 MHz, $CDCl_3$): δ 2.13 (3H, s, CH_3), 3.14 (6H, s), 5.86 (1H, s), 8.20 (1H, d, J = 9.6 Hz, H_b), 8.57 (1H, d, J = 9.6 Hz, H_a). **^{13}C NMR** (100 MHz,

	DMSO-d_6): δ 182.4, 164.9, 164.8, 163.9, 160.9, 154.6, 151.9, 148.3, 125.2, 124.4, 105.0, 95.9, 27.0, 19.6. **ESI-MS:** (*m/z*) 316.1 (M^++1).
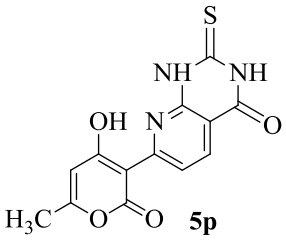 **5p**	*2-Thioxo-7-(4-hydroxy-6-methyl-2-oxo-2H-1-pyran-3-yl)-1H,3H-pyrido[2,3 d]pyrimidine-4-one*[11] Orange solid, **M.P.** >300 °C. **Anal. Calcd** ($C_{13}H_9N_3O_4S$): C, 51.53; H, 2.99; N, 14.82; **Anal. Found** ($C_{13}H_9N_3O_4S$): C, 51.39; H, 3.14; N, 14.65. **IR** (KBr, cm^{-1}): 3392 (OH), 3201 (NH), 3026 (NH), 1707 (C=O), 1651 (C=O). **^{1}H NMR** (400 MHz, $CDCl_3$): δ 2.15 (3H, s), 5.90 (1H, s), 8.20 (1H, d, J = 9.9 Hz, H_b), 8.46 (1H, d, J = 9.4 Hz, H_a), 10.20 (1H, s), 10.92 (1H, s). **^{13}C NMR** (100 MHz, DMSO-d_6): δ 184.4, 175.6, 164.6, 162.0, 161.3, 154.2, 151.6, 146.4, 123.2, 121.1, 104.1, 97.0, 19.6. **ESI-MS:** (*m/z*) 304.1 (M^++1).

REFERENCES:

1. M. T. Cocco, C. Congiu, V. Lilliu, V. Onnis, Eur. J. Med. Chem. 40 (2005) 1365.
2. D. L. Boger, S. Nakahara, J. Org. Chem. 56 (1991) 880.
3. D. L. Boger, A. M. Kasper, J. Am. Chem. Soc. 111 (1989) 1517.
4. A. Chaubey, S. N. pandeya, Asian J. Pharm. Clin. Res. 4 (2011) 5.
5. (a) C. Gonzalez-Bello, L. Castedo, Six-Membered Heterocycles: Pyridines, Modern Heterocyclic Chemistry, First Edition., Edited by J. Alvarez-Builla, J. J. Vaquero, J. Barluenga, Wiley-VCH Verlag GmbH & Co. KGaA. (2011); (b) V. P. Raje, R. P. Bhat, S. D. Samant, Synlett (2006) 2676.
6. (a) D. M. Stout, A. I. Meyers, Chem. Rev. 82 (1982) 223; (b) A. Sausins, G. Duburs, Heterocycles 27 (1988) 269. (c) J. P. Wan, Y. Liu, RSC Adv. 2 (2012) 9763.
7. S. Kantevari, M. V. Chary, S. V. N. Vuppalapati, Tetrahedron 63 (2007) 13024.
8. B. Al-Saleh, M. M. Abdelkhalik, A. M. Eltoukhy, M. H. Elnagdi, J. Heterocycl. Chem. 39 (2002) 1035.
9. G. J. Reddy, D. Latha, C. Thirupathaiah, K. S. Rao, Tetrahedron Lett. 46 (2005) 301.
10. S. Kantevari, S. R. Patpi, D. Addla, S. R. Putapatri, B. Sridhar, P. Yogeeswari, D. Sriram, ACS Comb. Sci. 13 (2011) 427.
11. Z. N. Siddiqui, F. Farooq, J. Mol. Cat. A: Chem. 363-364 (2012) 451.
12. Z. N. Siddiqui, Tetrahedron Lett. 56 (2015) 1919.
13. J. A. Gladysz, Pure Appl. Chem. 73 (2001) 1319.
14. F. Lu, J. Ruiz Aranzaes, D. Astruc, Angew. Chem. Int. Ed. 44 (2005) 7399.
15. D. Astruc, F. Lu, J. R. Aranzaes, Angew. Chem. Int. Ed. 44 (2005) 7852.
16. F. M. Moghaddam, H. Saeidian, Z. Mirjafary, A. Sadeghi, J. Iran Chem. Soc. 6 (2009) 317.
17. M. Hosseini-Sarvari, H. Sharghi, S. Etemad, Helv Chim Acta 91 (2008) 715.
18. Z. Mirjafary, H. Saeidian, A. Sadeghi, F. M. Moghaddam, Catal. Commun. 9 (2008) 299.
19. B. V. Kumar, H. S. Bhojya naik, D. Girija, B. Kumar, J. Chem. Sci. 123 (2011) 615.
20. J. Safaei-Ghomi, M. A. Ghasemzadeh, Chinese Chem. Lett. 22 (2012) 1225.

CHAPTER 3

SULPHATED SILICA TUNGSTIC ACID: AN EFFICIENT AND RECYCLABLE HETEROGENEOUS CATALYST FOR THE SYNTHESIS OF TETRAHYDROPYRIMIDINES AND DIHYDROPYRIMIDINES

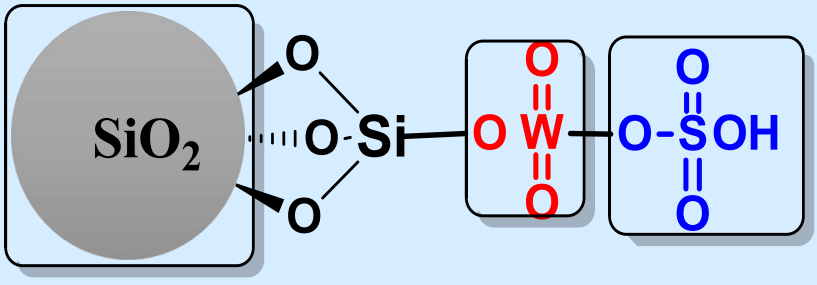

SULPHATED SILICA TUNGSTIC ACID: AN EFFICIENT AND RECYCLABLE HETEROGENEOUS CATALYST FOR THE SYNTHESIS OF TETRAHYDROPYRIMIDINES AND DIHYDROPYRIMIDINES*

3.1. INTRODUCTION

Tetrahydropyrimidines (THPMs)/ Dihydropyrimidines (DHPMs) represent an important group of highly valuable heterocyclic motifs in the field of medicinal chemistry. Dihydropyrimidines display a wide range of biological activities such as calcium channel modulators, adrenergic receptor antagonist, mitotic kinesin inhibitor, antiviral, antibacterial, etc.[1] Enastron, monastrol and piperastrol[2] are well known dihydropyrimidine derivatives which have already been marketed as drugs. THPMs have been reported to possess pharmacological profiles like HIV protease inhibiting activity,[3] antineoplastic activity[4] antiproleferative,[5] herbicidal activity,[6] muscarinic agonist activity,[7] anti-inflammatory[8] and antiviral properties.[9] The examples of approved therapeutic agents incorporating tetra- and di-hydropyrimidine molecular frameworks are given in **Figure 22**. DHPMs are commonly synthesised *via* Biginelli reaction and THPMs are usually synthesised via Biginelli-like transformation[10] or alternatively, using the two-step reaction involving Knoevenagel condensation followed by urea annulation.[11] The protocols for the synthesis of DHPMs are well documented in the literature but, multicomponent protocols for the synthesis of THPMs tolerating heteroaldehydes under heterogeneous conditions are unfortunately very rare. It is therefore highly desirable to develop new methods for the efficient synthesis of THPMs.

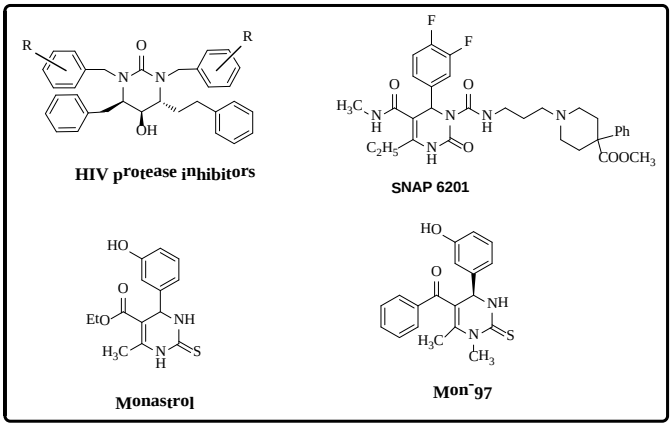

Fig. 22. Representative therapeutic agents based on tetra- and di-hydropyrimidines

* Nayeem Ahmed, Zeba N. Siddiqui, ***Journal of Molecular Catalysis A: Chemical,*** 387 (2014) 45.

3.2. REVIEW OF LITERATURE

Some recent examples of the synthesis of tetrahydropyrimidine derivatives.

3.2.1. Microwave-assisted synthesis of 1,2,3,4-tetrahydropyrimidine-5-carbonitrile derivatives[12]

A multicomponent reaction involving one-pot reaction of ethyl cyanoacetate, urea/thiourea and arylaldehydes in presence of ethanolic K_2CO_3 has been reported by S. B. Mohan *et al.* The synthesised compounds showed promising antitubercular activity.

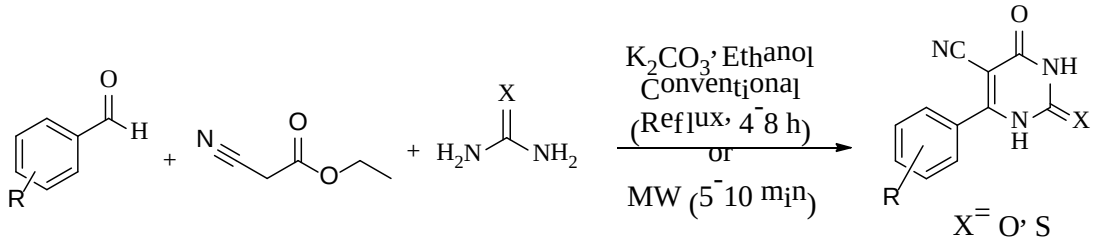

R= H, 4-F, 2-Cl, 3-Cl, 4-Cl, 4-Br, 3-Br, 3-OH,4-OCH_3

3.2.2. One pot synthesis of thioxopyrimidine derivatives in ethanol[13]

S. Kambe *et al.* synthesised thioxopyrimidine derivatives via reaction of aldehydes, thiourea and ethyl cyanoacetate in refluxing ethanol using K_2CO_3 as a catalyst.

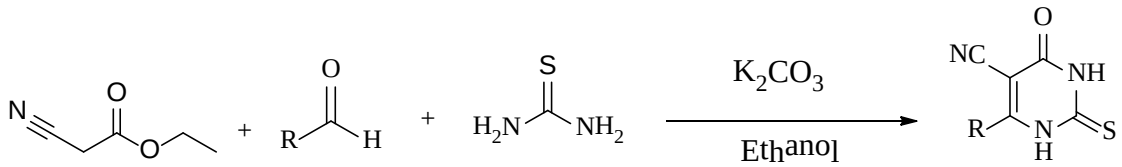

R= C_6H_5, 4-$CH_3C_6H_4$, 4-$OCH_3C_6H_4$, 4-ClC_6H_4

3.2.3. Synthesis of pyrimidine derivatives as anti-cancer agents[14]

M. M. M. Ramiz *et al.* synthesised 1,2,3,4-tetrahydropyrimidine-5-carbonitrile derivatives using ethanolic K_2CO_3 and AcOH as a reaction medium. These derivatives were then successively functionalised by glycosides and were found to display good anti-cancer potential.

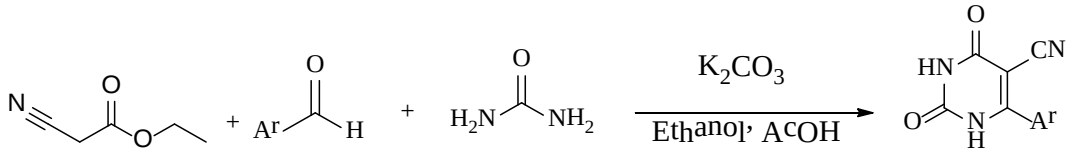

Ar = C_6H_5, 4-$CH_3C_6H_4$, 4-$OCH_3C_6H_4$

3.2.4. Synthesis of tetrahydropyrimidine analogs as anti-inflammatory agents[15]

D. K. Lokwani *et al.* synthesised a series of 1,2,3,4-tetrahydropyrimidine derivatives and evaluated them for their anti-inflammatory potential. The synthesised compounds showed promising anti-inflammatory activity.

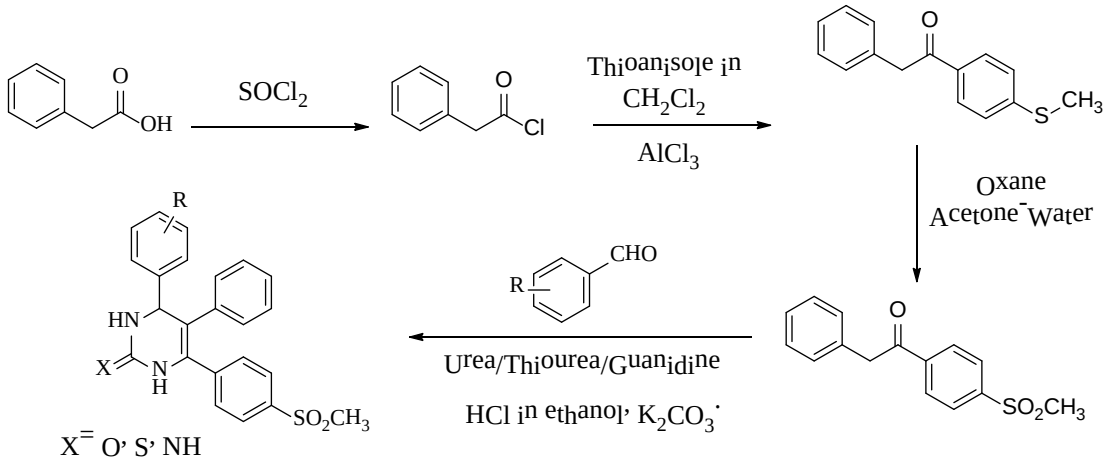

Some recent examples of the synthesis of dihydropyrimidine derivatives.

3.2.5. Titanium dioxide supported on multi-walled carbon nanotubes (TiO_2–MWCNTs) catalysed Biginelli reaction[16]

J. Safari and S. G. Ravande reported an efficient synthesis of 3,4-dihydropyrimidin-2-(1*H*)-ones using TiO_2–MWCNTs as catalyst under microwave irradiation. Reusable catalyst, solvent-free conditions, high yield and short reaction time are highlights of this protocol.

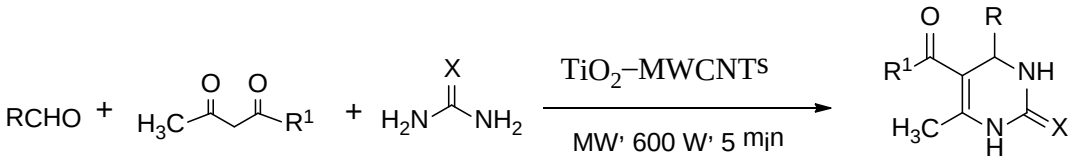

R = C_6H_5, 4-OCH_3-C_6H_4, 4-F-C_6H_4, 4-NO_2-C_6H_4, 4-Cl-C_6H_4, 4-OH-C_6H_4 X = O, S

R^1 = OEt, OMe

3.2.6. Fe_3O_4@mesoporous SBA-15: A magnetically recoverable catalyst for Biginelli reaction[17]

A magnetically separable Fe_3O_4@mesoporous SBA-15 was used for highly efficient synthesis of 3,4-dihydropyrimidin-2(1*H*)-ones *via* Biginelli reaction under mild reaction conditions. The simple separation and reuse of the Fe_3O_4@mesoporous SBA-15 along with high turnover frequencies and good yield of the products are merits of this protocol.

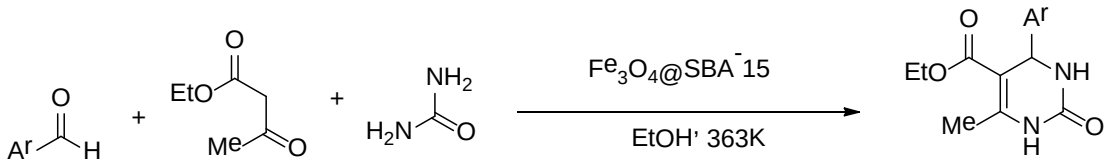

Ar = C_6H_5, 4-NO_2-C_6H_4, 4-Cl-C_6H_4, 4-OCH_3-C_6H_4, 3-Br-C_6H_4, 2-OCH_3-C_6H_4, 4-CH_3-C_6H_4, 2-Furyl

3.2.7. Catalytic performance of bismuth vanadate ($Bi_2V_2O_7$) nanocatalyst for Biginelli reaction[18]

S. Khademinia *et al.* synthesised bismuth vanadate nanocatalyst and evaluated its catalytic activity for the synthesis of 3,4-dihydropyrimidin-2(1*H*)-ones. The catalyst was synthesised by solid state method and showed excellent catalytic efficiency by giving high yields in 60 min under solvent-free conditions.

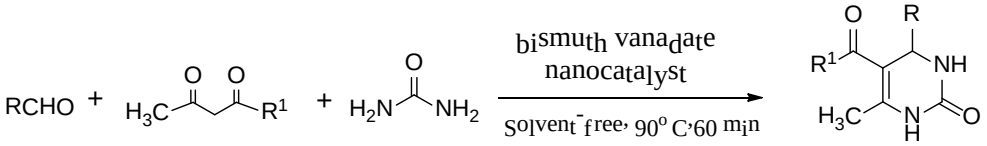

R = C_6H_5, 4-OCH_3-C_6H_4, 4-Cl-C_6H_4, 4-Br-C_6H_4, 2-Cl-C_6H_4, 2-Br-C_6H_4 R^1 = OEt, OMe

3.2.8. Biginelli reaction catalysed by zeolite supported on heteropolyacid[19]

An eco-friendly protocol for the synthesis of 3,4-dihydropyrimidin-2(1*H*)-ones using molybdophosphoric acid (HPA) supported on Y zeolite was reported by M. Moghaddas *et al.* The catalyst was recyclable and the products were obtained in excellent yields.

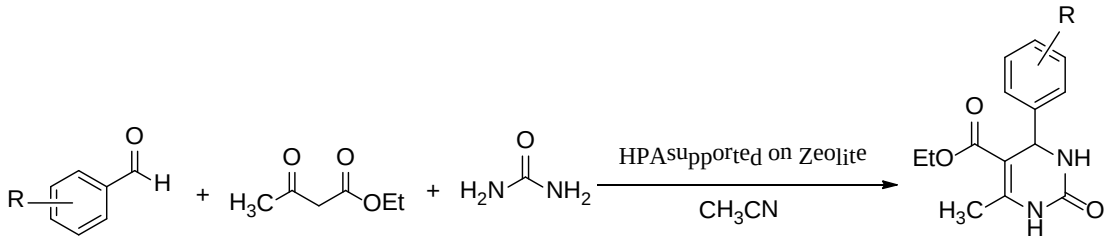

R = 2-NO_2, 3-NO_2, 4-NO_2, 4-Me, 3-MeO, 2-Cl, 4-MeO, 4-$C(CH_3)_3$, 2-OH

3.2.9. Nano–γ–Fe_2O_3–SO_3H catalysed synthesis of 3,4-dihydropyrimidin-2(1*H*)-ones[20]

A simple, efficient, magnetically separable and recyclable nano–γ–Fe_2O_3–SO_3H catalysed process for the synthesis of 3,4-dihydropyrimidin-2-(1*H*)-ones under solvent-free thermal or microwave conditions has been reported by E. Kolvari *et al.*

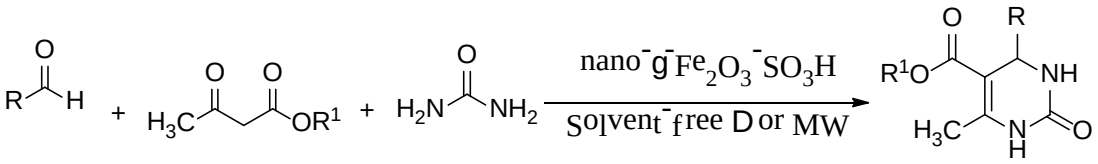

R^1 = Et, Me

R = Ph, *p*-MeC$_6$H$_4$, *p*-ClC$_6$H$_4$, *p*-OHC$_6$H$_4$, *p*-NO$_2$C$_6$H$_4$, *p*-FC$_6$H$_4$, *o*-OHC$_6$H$_4$, 3,4-diMeOC$_6$H$_3$, *o*-ClC$_6$H$_4$, 4-OH-3-EtOC$_6$H$_3$, *m*-OHC$_6$H$_4$

3.2.10 Bis[(L)prolinato-N,O]Zn catalysed synthesis of 3,4-dihydropyrimidin-2(1*H*)-ones in water[21]

Z. N. Siddiqui described an efficient synthesis of 3,4-dihydropyrimidin-2(1*H*)-one derivatives using bis[(L)prolinato-N,O]Zn as an inexpensive and mild Lewis acid catalyst in water. Short reaction time, high yields, clean process and low loading of catalyst are merits of this protocol.

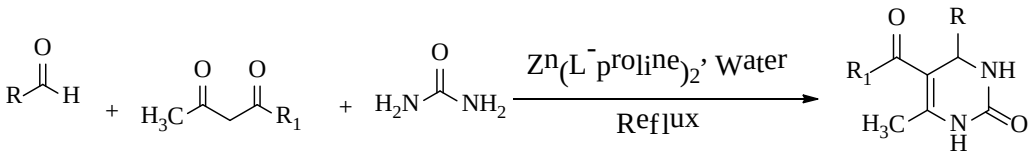

R = C$_6$H$_5$, 4-ClC$_6$H$_4$, 2-ClC$_6$H$_4$, 4-OHC$_6$H$_4$, 3-NO$_2$C$_6$H$_4$

R_1 = OCH$_2$CH$_3$, CH$_3$

3.2.11 MCM-41 supported perchloric acid catalysed synthesis of 3,4-dihydropyrimidin-2(1*H*)-ones/thiones[22]

K. Khan and Z. N. Siddiqui reported mesoporous silica (MCM-41) supported perchloric acid catalysed synthesis of dihydropyrimidinones under solvent-free conditions.

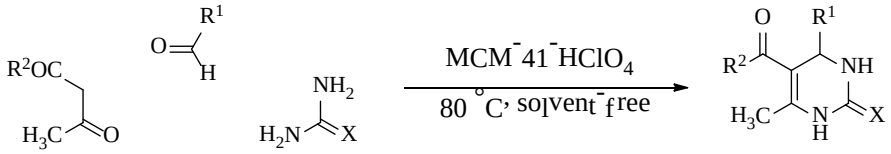

R^1 = C$_6$H$_5$, 4-ClC$_6$H$_4$, 2-ClC$_6$H$_4$, 4-OHC$_6$H$_4$, 3-NO$_2$C$_6$H$_4$,4-NO$_2$C$_6$H$_4$, 4-CH$_3$OC$_6$H$_4$, 4-CH$_3$C$_6$H$_4$

R^2 = OEt, OMe X = O, S

3.2.12 Synthesis of dihydropyrimidine derivatives using sulfonic acid functionalized polypropylene fiber (PPF-SO_3H) as a catalyst[23]

X. Shi *et al.* reported one-pot three-component synthesis of 3,4-dihydropyrimidin-2-(1*H*)-ones/thiones using sulfonic acid-functionalized polypropylene fiber as a

heterogeneous catalyst. Advantages of this protocol are good yield, low catalyst loading, simple work-up procedure and catalyst recyclability.

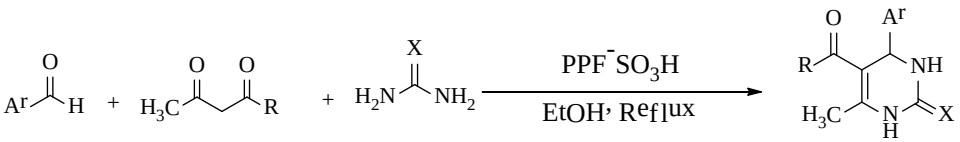

Ar = C_6H_5, 2-$CH_3OC_6H_4$, 3-$CH_3OC_6H_4$, 4-$CH_3OC_6H_4$, 4-FC_6H_4, 4-ClC_6H_4, 4-BrC_6H_4, 4-OHC_6H_4, 4-$NO_2C_6H_4$, 4-$CF_3C_6H_4$, 1-naphthyl, 2-furenyl, 2-thienyl.

R = OEt, Me X = O, S

3.2.13 ZnO catalysed synthesis of dihydropyrimidinones under solvent-free conditions[24]

F. Tamaddon and S. Moradi reported controllable synthesis of dihydropyrimidinones using ZnO or nano ZnO as a catalyst under solvent-free synthesis.

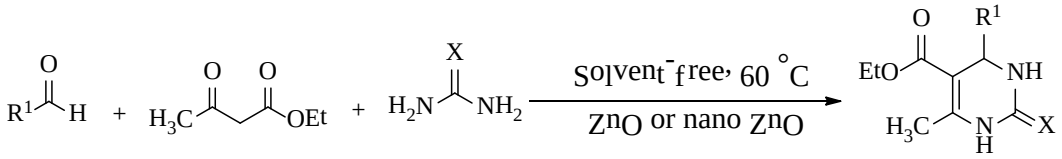

R^1 = C_6H_5, 4-$CH_3OC_6H_4$, 4-$CH_3C_6H_4$, 4-$N(Me)_2C_6H_4$, 4-ClC_6H_4, 2-OHC_6H_4, 4-$NO_2C_6H_4$

X = O, S

3.2.14 Synthesis of dihydropyrimidinones using silica-bonded *N*–propyl sulfamic acid as a recyclable catalyst[25]

S. R. Jetti *et al.* reported a simple and efficient silica-bonded *N*–propyl sulfamic acid (SBNPSA) catalysed synthesis of dihydropyrimidinones/thiones by condensation of different aromatic aldehydes with ethyl acetoacetate and urea/thiourea.

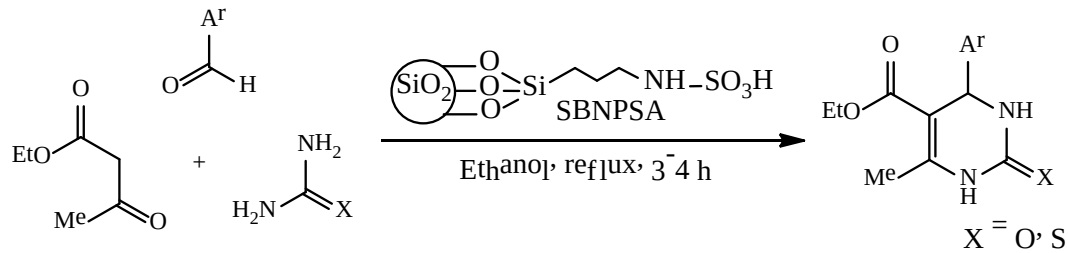

X = O, S

Ar = C_6H_5, 4-$NO_2C_6H_4$, 3-ClC_6H_4, 4-ClC_6H_4, 3-BrC_6H_4, 4-$CH_3OC_6H_4$, 3-$NO_2C_6H_4$, 4-FC_6H_4

3.3. PRESENT WORK

The development of environmentally benign organic reactions has become a crucial and demanding area of research in modern organic chemistry. Therefore, preparation of new heterogeneous catalysts with improved efficiency has been the subject of immense interest and the best trend is to transform a successful homogeneous catalyst into a heterogeneous catalyst. Immobilization of catalysts on solid support is an ideal

method for combining the advantages of homogeneous catalysts like high activity and selectivity with the advantages of heterogeneous catalysts like availability of active sites, easy catalyst separation, long catalytic life, thermal stability, low hygroscopic properties, easy handling and reusability.[26-29] Among various solid supports, silica is usually a preferred support due to its many advantageous properties like excellent chemical and thermal stability, high surface area and good accessibility. Due to encouraging chemical and physical properties of silica surfaces it is possible to functionalize the surface by any functional group (e.g., sulfonic, amine, carboxyl, thiol, epoxy, and so forth) that one requires on a silica.[30-33] As a result, numerous modifications can be made for specific applications with the use of a combination of inorganic materials and functional groups. In the present work, taking advantage of the above mentioned properties of silica, we have synthesized sulphated silica immobilized tungstic acid **(SSTA)** and used it for the preparation of THPMs and DHPMs under solvent-free conditions.

3.4. RESULTS AND DISCUSSION

Scheme 6 demonstrates the concise route for the preparation of SSTA catalyst. Sodium tungstate (Na_2WO_4) reacted with silica chloride to produce silica tungstic acid (STA) which on reaction with chlorosulfonic acid gave sulphated silica tungstic acid (SSTA). The optimum concentration of H^+ was determined by titration of the aqueous suspension of the weighed amount of thoroughly washed catalyst with standard NaOH solution. The strength of NaOH solution was kept very low (0.01 N) in order to minimise errors caused by reaction of NaOH with Lewis acid groups and to avoid the consumption of the base in the hydrolysis of the silica frameworks. The optimum concentration of H^+ of SSTA was found to be 0.40 meq/gram of the support. The concentrations of the residual H^+ on the recovered catalyst were measured (provided in recycling study) after successive experiments. The studies showed very small or marginal loss of H^+, which signified that SO_3H moiety was tightly anchored with STA, probably through a covalent linkage. The reaction of aldehyde **(6b)** (6-methyl-3-formyl chromone) with urea and ethyl cyanoacetate **(7a)** in the presence of SSTA (preheated at 120 °C for 3h) occurred with high efficiency giving 94% product (THPM) yield. The same reaction in the presence of SSTA after keeping it at an ambient atmosphere for 5 days produced similar observation which confirmed that there was no deteriorating effect of atmospheric oxygen or moisture towards the activity of the catalyst. The catalyst thus, exhibited significant stability towards heat

and moisture which provided further evidence for covalent linkage and the potential of efficient recycling.

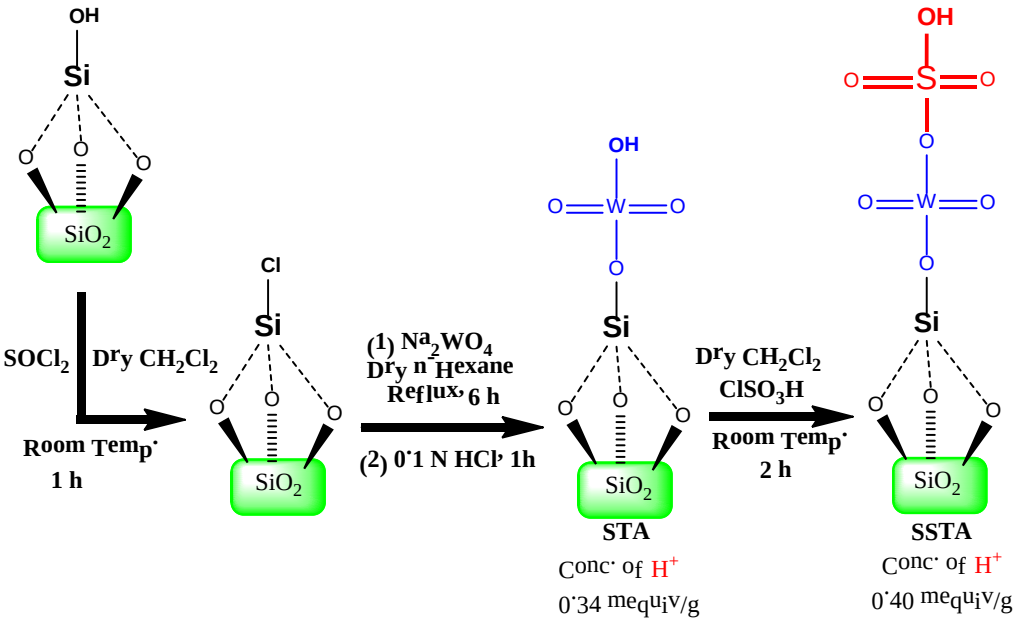

Scheme 6: Schematic representation of the synthesis of the catalyst.

3.4.1. Characterization of the catalyst

3.4.1a. FT-IR spectral analysis of the catalyst

The incorporation of sulfonic groups and tungsten moieties on silica surface was analysed by FT-IR spectra of sodium tungstate, STA and SSTA respectively **(Figure 23)**. In the FT-IR spectrum of sodium tungstate **(Figure 23a)**, the WO_4^{2-} stretching frequency was observed at 1683 cm^{-1}. In the spectra of STA **(Figure 23b)**, WO_4^{2-} stretching frequency appeared at 1650 cm^{-1} along with peaks corresponding to SiO_2 stretching band. Due to bonding with silica, a decrease in the intensity of WO_4^{2-} stretching band of STA was observed. The introduction of SO_3^{2-} groups in STA led to further decrease in the intensity of the WO_4^{2-} stretching band which appeared at 1642 cm^{-1}. In the spectrum of SSTA **(Figure 23c)**, OH stretching frequency was obtained at 3448 cm^{-1}. The asymmetric and symmetric stretching vibrations of SO_3^{2-} group obtained around 1300 and 1200 cm^{-1} merged with the broad absorption peak between 1000 and 1500 cm^{-1}, which showed some increase in intensity and little increase in broadening as compared to broad peak of STA. The peaks corresponding to SiO_2-Cl and SiO_2 stretching were also observed in SSTA. The IR spectrum thus, confirms the successful sulfonation of STA.

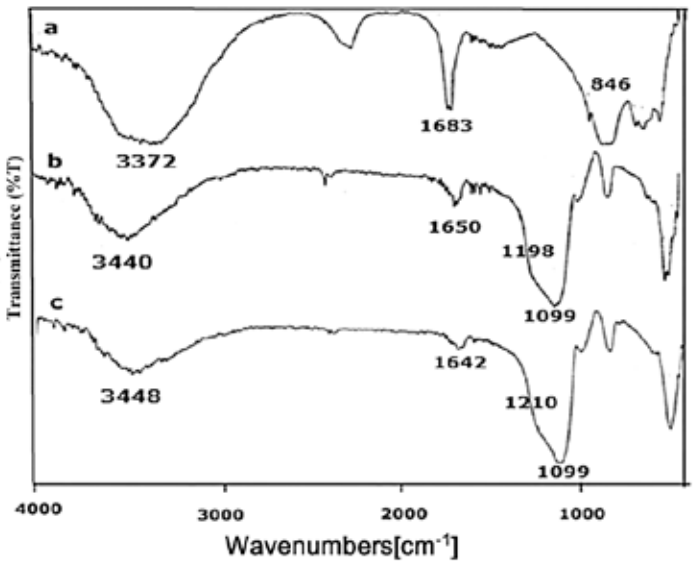

Fig. 23. FT-IR spectra of **(a)** sodium tungstate **(b)** silica tungstic acid and **(c)** SSTA.

3.4.1b. XRD spectral analysis

The XRD patterns of the catalyst **(Figure 24b)** were similar to that of the support **(Figure 24a)**. The WO_3 group exhibits a broad peak around $2\theta = 22°$ which merges with the broad peak shown by SiO_2 at around $2\theta = 20\text{-}25°$.[34,35]

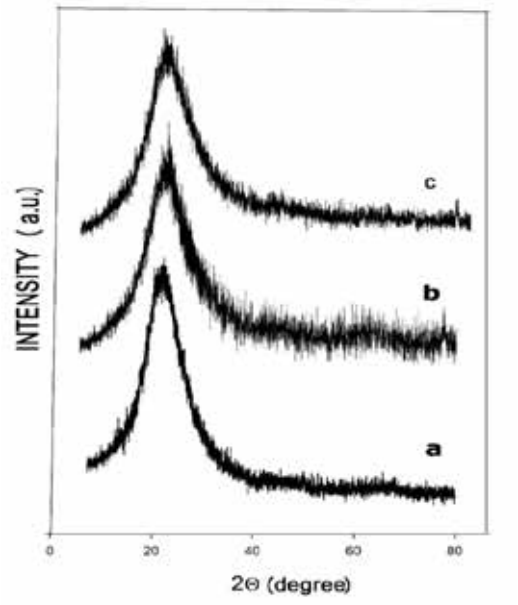

Fig. 24. (**a)** Powder XRD pattern of SiO_2 **(b)** XRD pattern of fresh SSTA **(c)** XRD pattern of the catalyst after six catalytic cycles.

3.4.1c. SEM/EDX Analysis of the catalyst

The surface morphologies of silica and functionalised silica analysed by SEM analysis **(Figure 25a,b&c)**, revealed the change in surface morphology of silica gel upon functionalization. Furthermore, the formation of expected sulphated catalytic

system was also confirmed by EDX analysis **(Figure 25d)** which showed the presence of sulphur in addition to silicon and tungsten elements.

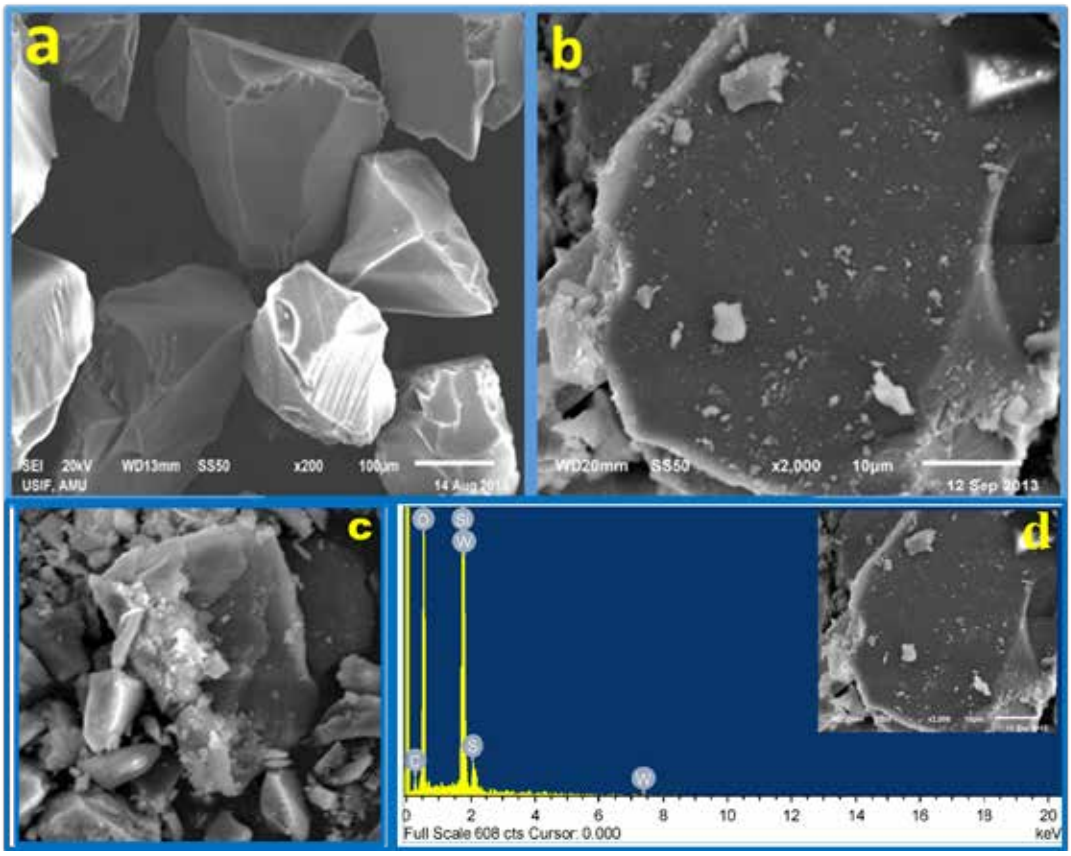

Fig. 25. SEM images **(a)** of SiO_2 support **(b)** of freshly synthesised SSTA **(c)** of recycled SSTA and **(d)** EDX analysis of SSTA.

3.4.1d. TG analysis of the catalyst

TG analysis **(Figure 26)** was done in order to evaluate the thermal stability of the catalyst. The first weight loss of 19% at ~100 °C was due to the loss of solvent molecules present in silica gel framework. The second weight loss of ~7% at 550 °C can be attributed to the decomposition of sulphate and tungstate groups from the surface of silica. The TG analysis thus, confirmed that the catalyst is stable up to 550 °C.

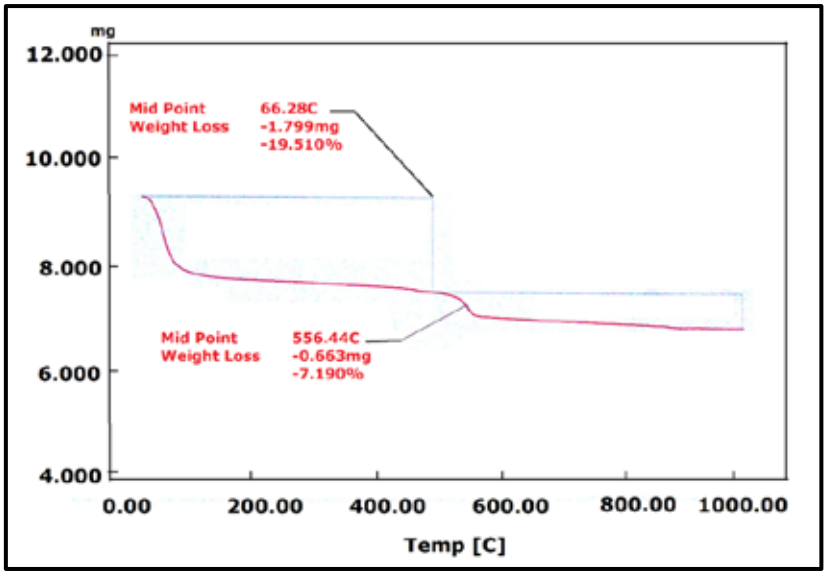

Fig. 26. TG analysis of SSTA catalyst.

3.4.2. Optimization of reaction conditions

3.4.2a. Effect of different reaction media

Our initial study was focused on the development of the optimal reaction conditions for this transformation and included screening of different catalysts and solvents **(Table 10)**. The reaction of 6-methyl-3-formyl chromone **(6b)**, urea and ethyl cyanoacetate **(7a)** was chosen as a model reaction. When the reaction was carried out in the presence of sulphuric acid in ethanol at reflux temperature, product **8b** was obtained in 56% yield after 8 hours **(entry 1)**. When sulphuric acid was used under solvent-free condition at 70 °C, 67% product yield was obtained in 4.2 h **(entry 3)**. As the solvent-free approach produced same yield in less time, this approach was further explored for optimization of reaction conditions. As sulphuric acid failed to give satisfactory results, we then examined the effect of the differently supported sulphuric acids under solvent-free condition. Cellulose, xanthan, PEG and camphor (organic polymers) supported sulphuric acid gave unsatisfactory yields **(entries 6-9)**. Among silica and zirconia supported sulphuric acids, the use of H_2SO_4-SiO_2 showed better results **(entry 4)**. In order to further improve our protocol we then turned our attention towards recently synthesised catalyst Silica Tungstic acid (STA) and the results obtained were better than different organic polymers supported acid, but were unsatisfactory than H_2SO_4-SiO_2. As a simplistic means to improve it, we then introduced SO_3H groups in STA. This strategy was found to be very effective as excellent product yield (94%) was obtained in only 15 min **(entry 13)**. The catalyst was then further compared with different Lewis acids i.e., $FeCl_3$, $ZnCl_2$, ZnO and

MgO under solvent-free condition and the results were unsatisfactory **(entries 20-23)**. Different solvents were used in order to further optimize the reaction conditions. The results obtained by the use of solvents like ethanol, methanol and isopropanol, hexane and toluene **(entries 14-19)** revealed that the solvent-free approach is the best approach for obtaining maximum yield in less time.

Table 10: Effect of catalysts/solvents in different reaction conditions on the model reaction.

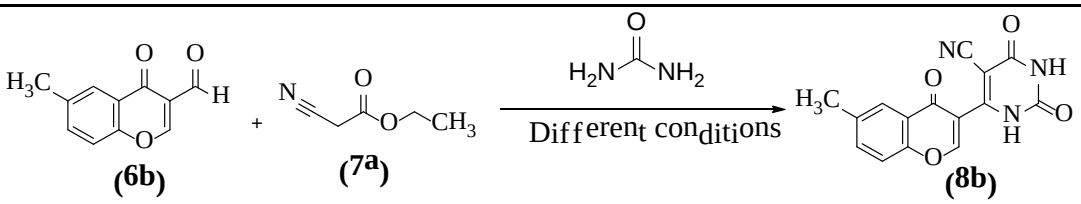

(6b) **(7a)** **(8b)**

Entry	Catalyst	Condition	Time	Yield%
1	H_2SO_4 (10 mol%)	Ethanol/reflux	8 h	56
2	H_2SO_4 (10 mol%)	Iso-propanol/reflux	8.5 h	53
3	H_2SO_4 (10 mol%)	Solvent-free/70 °C	4.2 h	67
4	H_2SO_4-SiO_2 (200mg)	Solvent-free/70 °C	40 min	82
5	H_2SO_4-ZrO_2 (200mg)	Solvent-free/70 °C	2 h	62
6	H_2SO_4-Cellulose (200mg)	Solvent-free/70 °C	65 min	65
7	H_2SO_4-Xanthan (200mg)	Solvent-free/70 °C	60 min	68
8	H_2SO_4-PEG (200mg)	Solvent-free/70 °C	90 min	58
9	CSA (200mg)	Solvent-free/70 °C	2.5 h	45
10	NH_2SO_3H-SiO_2 (200mg)	Solvent-free/70 °C	55 min	71
11	Na_2WO_3 (10 mol%)	Solvent-free/70 °C	3.2 h	67
12	STA (200mg)	Solvent-free/70 °C	90 min	78
13	STA-OSO_3H (200mg)	Solvent-free/70 °C	15 min	94
14	STA-OSO_3H (200mg)	Ethanol/reflux	2 h	73
15	STA-OSO_3H (200mg)	Iso-propanol/reflux	2.5 h	65
16	STA-OSO_3H (200mg)	Methanol/reflux	3.1 h	59
17	STA-OSO_3H (200mg)	CH_2Cl_2/reflux	3.5 h	46
18	STA-OSO_3H (200mg)	Hexane/reflux	4.2 h	23
19	STA-OSO_3H (200mg)	Toluene/reflux	4.5 h	25
20	$FeCl_3$ (10 mol%)	Solvent-free/70 °C	6 h	36
21	$ZnCl_2$ (10 mol%)	Solvent-free/70 °C	5.4 h	41
22	ZnO (10 mol%)	Solvent-free/70 °C	6h	No reaction
23	MgO (10 mol%)	Solvent-free/70 °C	6h	No reaction

3.4.2b. Effect of catalyst loading

After optimizing the catalyst and solvent, we next investigated the optimum amount of catalyst for the reaction. Carrying out the reaction with more than 200 mg of catalyst produced no significant effect on yield. Decreasing the amount of the catalyst to 100 mg reduced the yield to 43% **(Table 11)**. Therefore, 200 mg of SSTA was chosen as the optimum amount of the catalyst.

Table 11: Effect of catalyst loading on the model reaction.

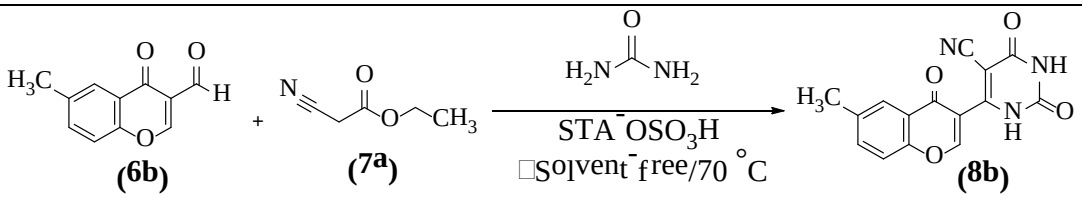

(6b) **(7^a)** **(8b)**

Entry	Amount of catalyst	Time(min)	Yield (%)
1	250 mg	15	92
2	200 mg	15	94
3	150 mg	30	68
4	100 mg	45	43

3.4.2c. Effect of temperature

The effect of temperature was examined in the range from RT to 100 °C using SSTA as catalyst under solvent-free condition. The reaction was not successful at RT and with further increase in temperature the results also improved **(Table 12)**. At 70 °C and 80 °C the reaction completed in 15 min with almost same yield. Further increase in the temperature could not show any profound effect on the reaction. So, 70 °C was chosen as the optimum temperature for performing the reaction.

Table 12: Effect of different temperatures on the model reaction.

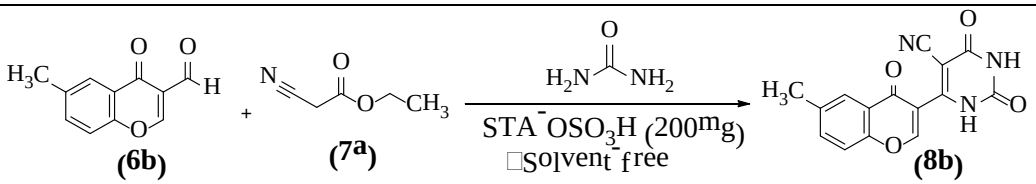

(6b) **(7^a)** **(8b)**

Entry	Temp. (°C)	Time	Yield (%)
1	RT	8h	No reaction
2	40	7h	45
3	70	15min	94
4	80	15 min	92
5	100	15 min	87

3.4.3. Catalytic reaction

3.4.3a. Synthesis of tetrahydropyrimidines

After optimizing the conditions, we then explored the scope of the reaction by using different heterocyclic aldehydes, ethyl cyanoacetate or phenylacetic acid and urea as substrates under these conditions **(Scheme 7)**. It was observed that the reaction successfully tolerated aldehydes with different heterocyclic substituents to furnish the final products in good yields. When ethylcyano acetate was replaced by phenylacetic acid, the desired compounds were again obtained in good yields albeit with little longer reaction time **(Table 13)**.

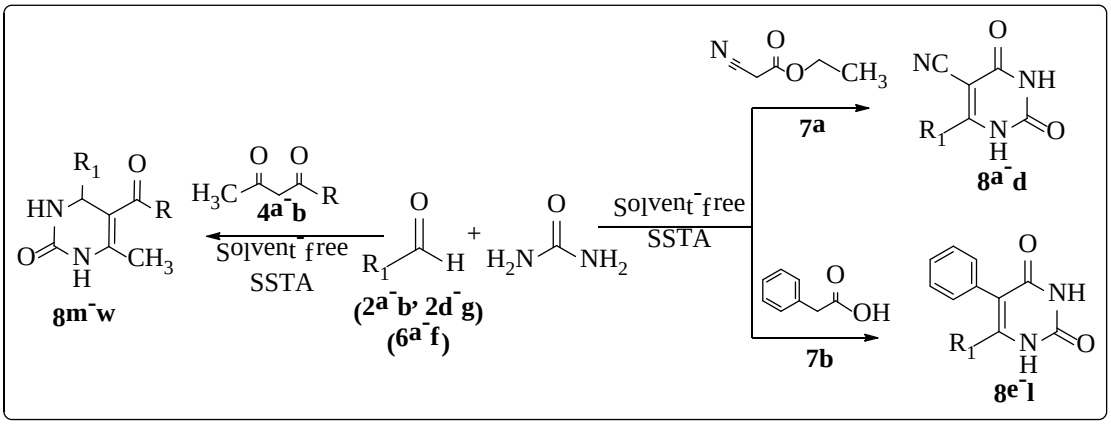

Scheme 7: Synthesis of different tetrahydropyrimidines **(8a-l)** and dihydropyrimidinone derivatives **(8m-w)**.

The structures of the final products were characterized by using IR, ^{1}H, ^{13}C NMR, ESI-MS and elemental analyses techniques. The I.R. spectrum of **8b (Figure 27)** showed two NH stretching frequencies at 3444 and 3281 cm^{-1}, respectively. The CN stretching band was present at 2224 cm^{-1}. The peak at 1730 cm^{-1} was assigned to two C=O groups of tetrahydropyrimidine moiety. The chromone C=O group showed absorption band at 1654 cm^{-1}. The ^{1}H-NMR spectrum **(Figure 28)** showed two distinctive singlets of NH protons at δ 11.21 and 8.77. A singlet at δ 7.37 was assigned to H-2' proton of chromone moiety. Three aromatic protons of chromone moiety appeared as multiplet in the range of δ 7.4-7.8. The methyl singlet was present at δ 3.36. In the ^{13}C-NMR spectra **(Figure 29)**, peaks for C=O group of chromone moiety and C=O groups of tetrahydropyrimidine ring were obtained at 180.22, 168.21 and 162.44, respectively. Further structural confirmation was provided by ESI-Mass spectrum **(Figure 30)** which showed the molecular ion peak as the base peak at m/z 296.1 (M^{+}+1).

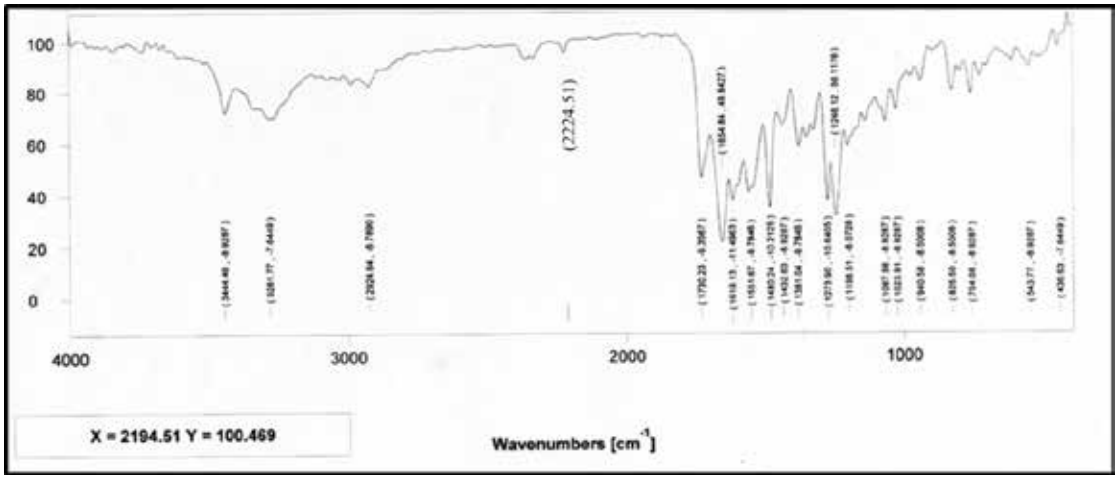

Fig. 27. FT-IR spectrum of **8b**

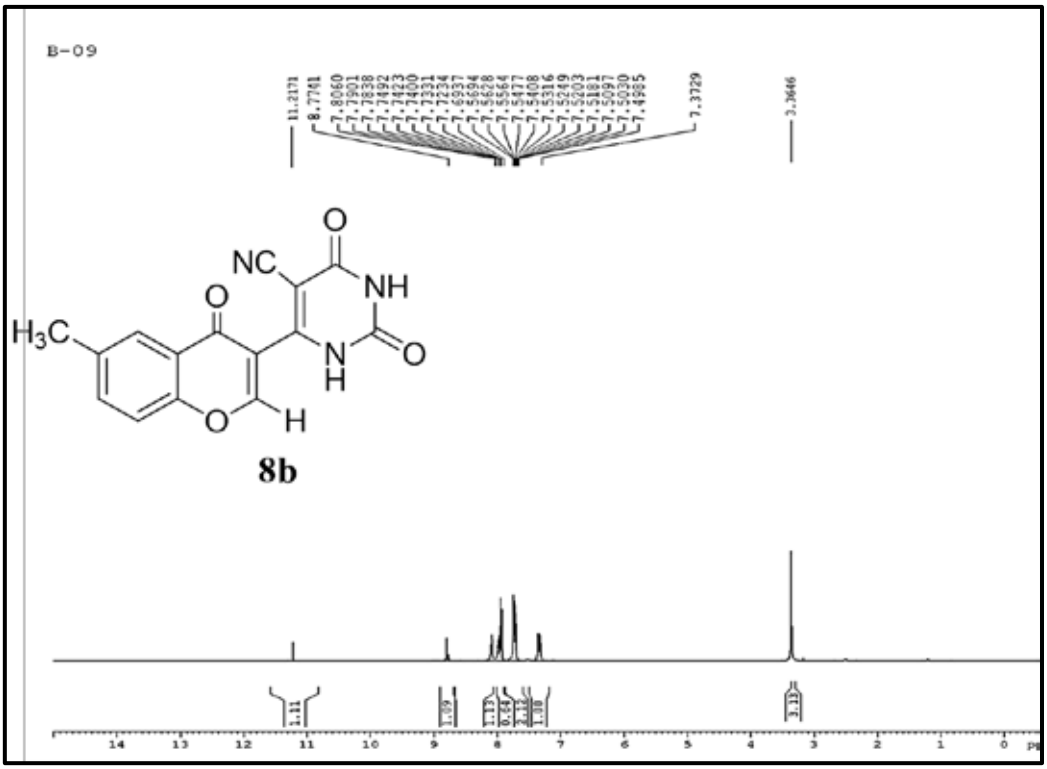

Fig. 28. ^{1}H-NMR spectrum of **8b**

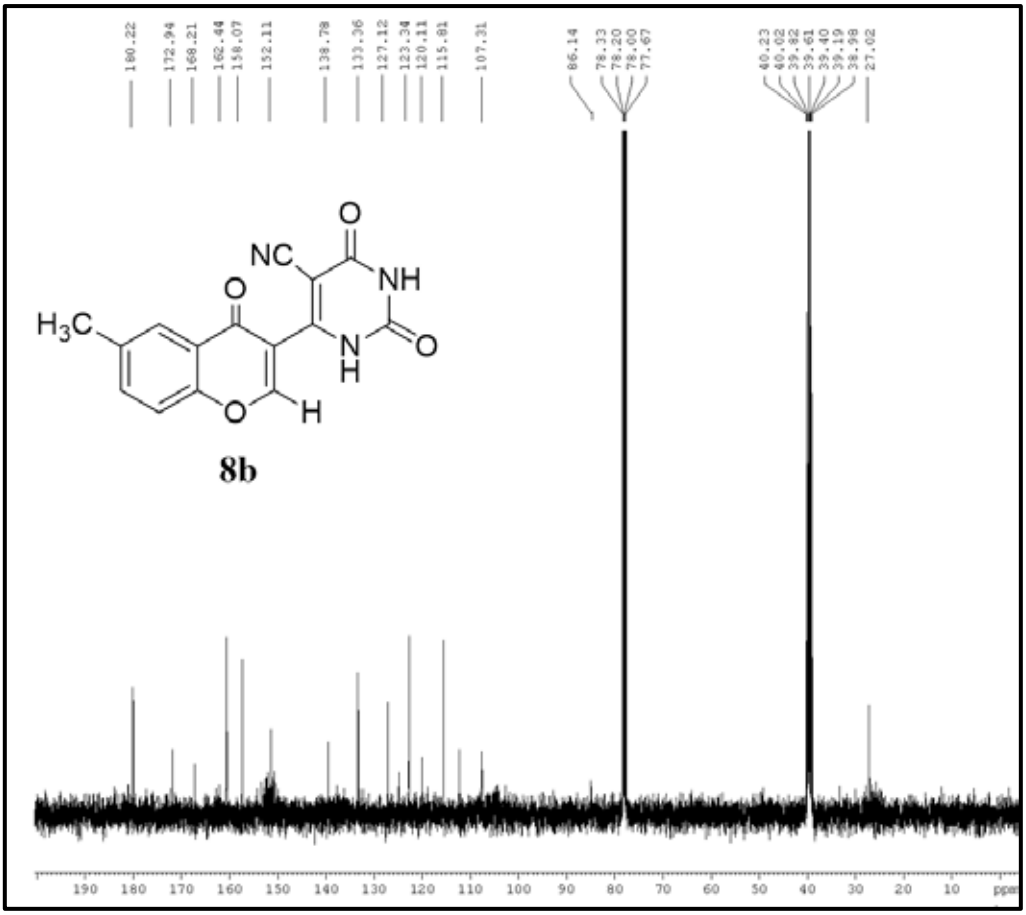

Fig. 29. ^{13}C-NMR spectrum of **8b**

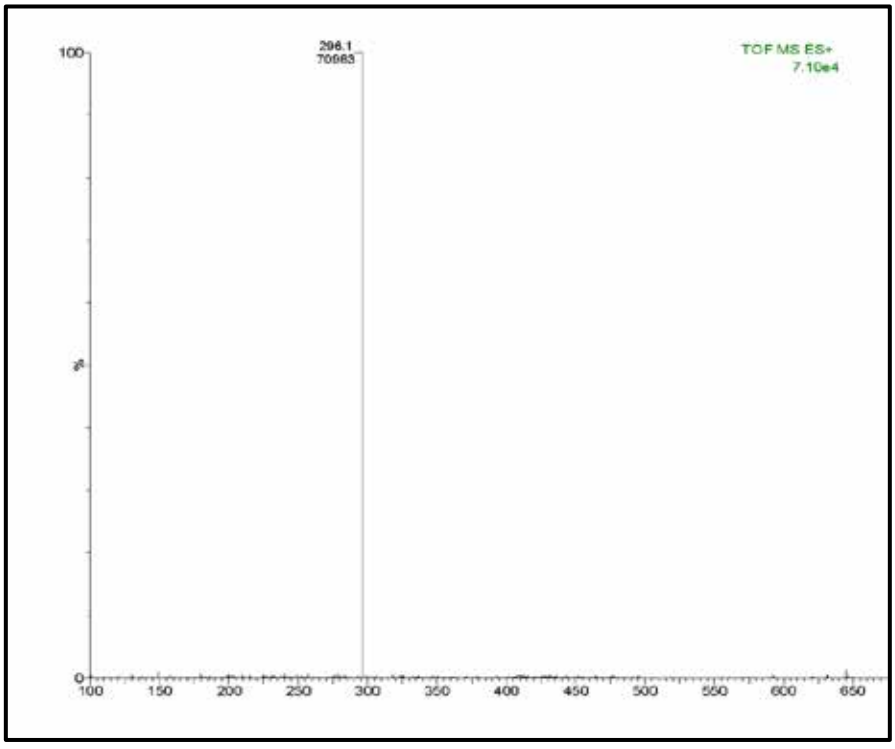

Fig. 30. ESI-Mass spectrum of **8b**

3.4.3b. Synthesis of dihydropyrimidines

The catalytic system was also evaluated for the synthesis of dihydropyrimidinones via biginelli condensation. Several aromatic and heterocyclic aldehydes reacted with 1,3-dicarbonyl compounds and urea under similar reaction conditions and gave excellent results. Both β-ketoesters and β-diketones gave excellent results within short reaction time **(Table 13, entries 13-23)**. Aldehydes containing both electron releasing and withdrawing groups reacted efficiently to furnish the products in excellent yield. In order to show the superiority of our catalytic system, a comparison with other reported catalysts in the literature was made, and the study showed the superiority of our catalytic system in terms of reaction conditions, time and product yield **(Table 14)**.

Table 13: Synthesis of tetrahydropyrimidines and dihydropyrimidinones using SSTA catalyst under solvent free conditions at 70 °C.

Entry	Aldehydes	4a,b & 7a,b	Product (8a-w)	Time (min)	Yield (%)
1	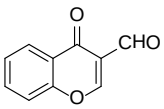 **6a**	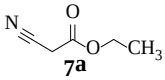 **7a**	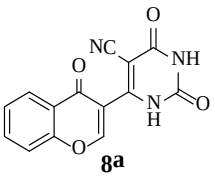 **8a**	16	91
2	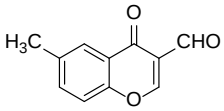 **6b**	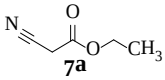 **7a**	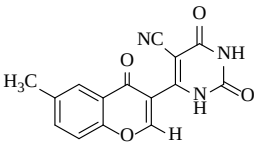 **8b**	15	94
3	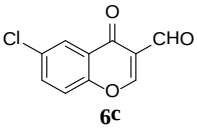 **6c**	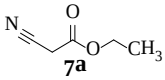 **7a**	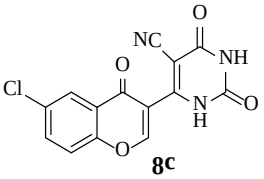 **8c**	15	90
4	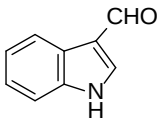 **6d**	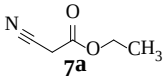 **7a**	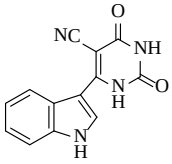 **8d**	20	88

5	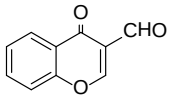 **6a**	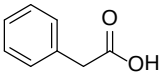 **7b**	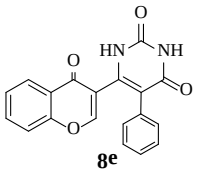 **8e**	21	87
6	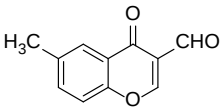 **6b**	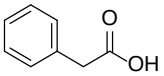 **7b**	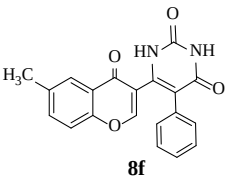 **8f**	20	90
7	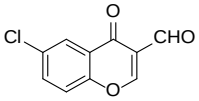 **6c**	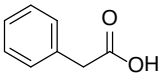 **7b**	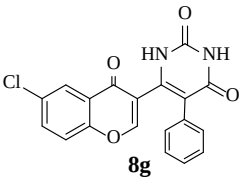 **8g**	20	86
8	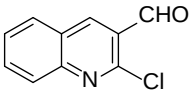 **6e**	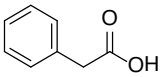 **7b**	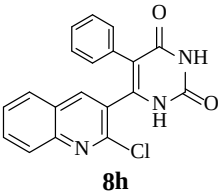 **8h**	25	85
9	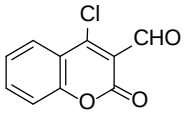 **6f**	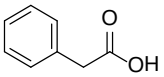 **7b**	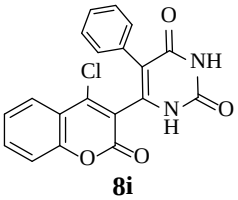 **8i**	31	82
10	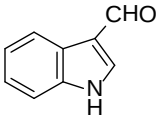 **6d**	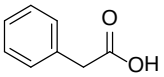 **7b**	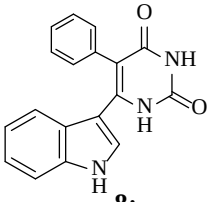 **8j**	22	84
11	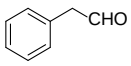 **2f**	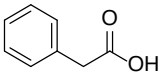 **7b**	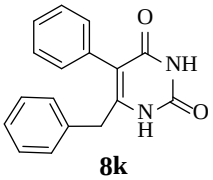 **8k**	23	83
12	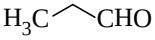 **2g**	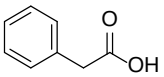 **7b**	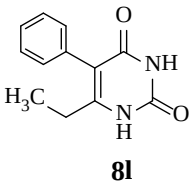 **8l**	27	82

13	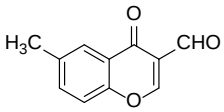 **6b**	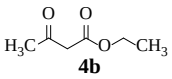 **4b**	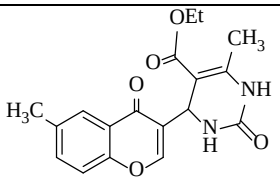 **8m**	10	94
14	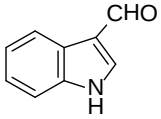 **6d**	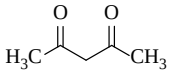 **4a**	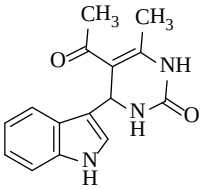 **8n**	12	92
15	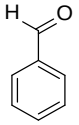 **2a**	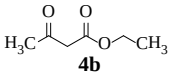 **4b**	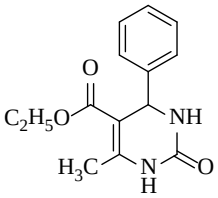 **8o**	10	96
16	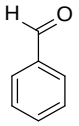 **2a**	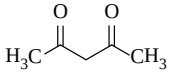 **4a**	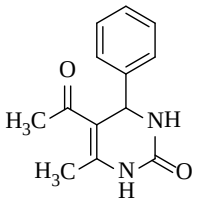 **8p**	12	95
17	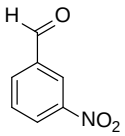 **2e**	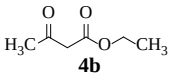 **4b**	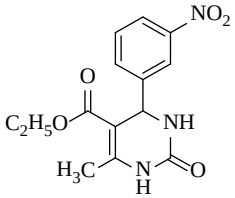 **8q**	08	95
18	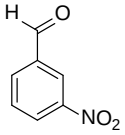 **2e**	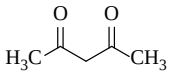 **4a**	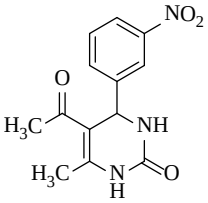 **8r**	10	94
19	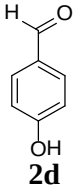 **2d**	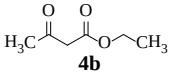 **4b**	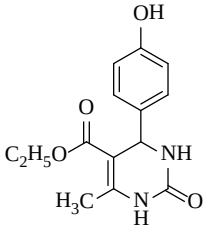 **8s**	09	94

20	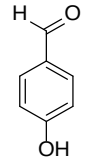 **2d**	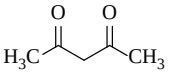 **4a**	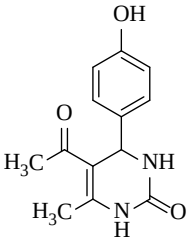 **8t**	12	95
21	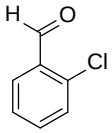 **2h**	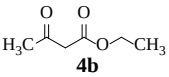 **4b**	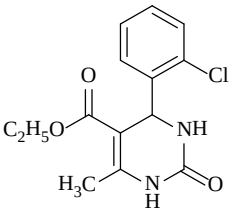 **8u**	08	93
22	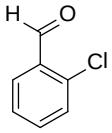 **2h**	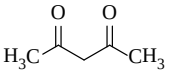 **4a**	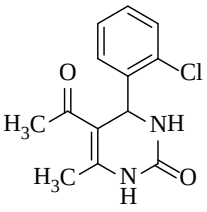 **8v**	10	93
23	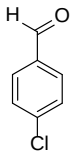 **2b**	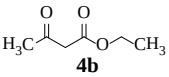 **4b**	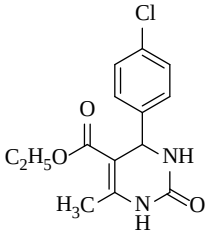 **8w**	10	94

Table 14: Effect of different reported catalysts for formation of dihydropyrimidines.

Entry	Catalyst	Reaction conditions	Yield (%)	Time	No. of recycles.	Ref.
1	SSTA	70 °C /Solvent-free	96	10 min	06	Present work.
2	Sulfated tungstate	80 °C/solvent free	92	60 min	04	36
3	PS–PEG–SO_3H	80 °C /Dioxane: 2-propanol (4:3)	80	10 h	06	37
4	Silica sulfuric acid	Reflux/Ethanol	91	6h	05	38
5	β-cyclodextrin	100°C /Solvent-free	85	3h	05	39
6	$[Al(H_2O)_6](BF_4)_3$	Reflux/CH_3CN	85	20h	04	40

7	Fe_3O_4/PAA-SO_3H	RT/Solvent-free	90	2h	06	41
8	Cellulose –SO_3H	100°C/Water	85	4.5h	04	42
9	$Cu(OTf)_2$	100°C/Ethanol	65	60 min	Nil	43
10	Tetra-butyl ammonium bromide	100°C/KOH	96	40 min	Nil	44

3.4.4. Reaction mechanism

A plausible mechanism for the formation of tetrahydropyrimidines **(8a-l)** is depicted in **Scheme 8**. Protonation of aldehyde **(6a-f, 2f-g)** by SSTA activates the substrate, which then undergoes Knoevenagel condensation with ethyl cyanoacetate **(7a)** to form alkene derivative **(L)**. Addition of urea to **L**, followed by elimination of ethoxy group leads to another intermediate **(M)**. Intramolecular Michael addition followed by dehydrogenation then affords the product **(8a-l)**. The catalyst is regenerated and can be subsequently reused for six catalytic cycles.[13,14]

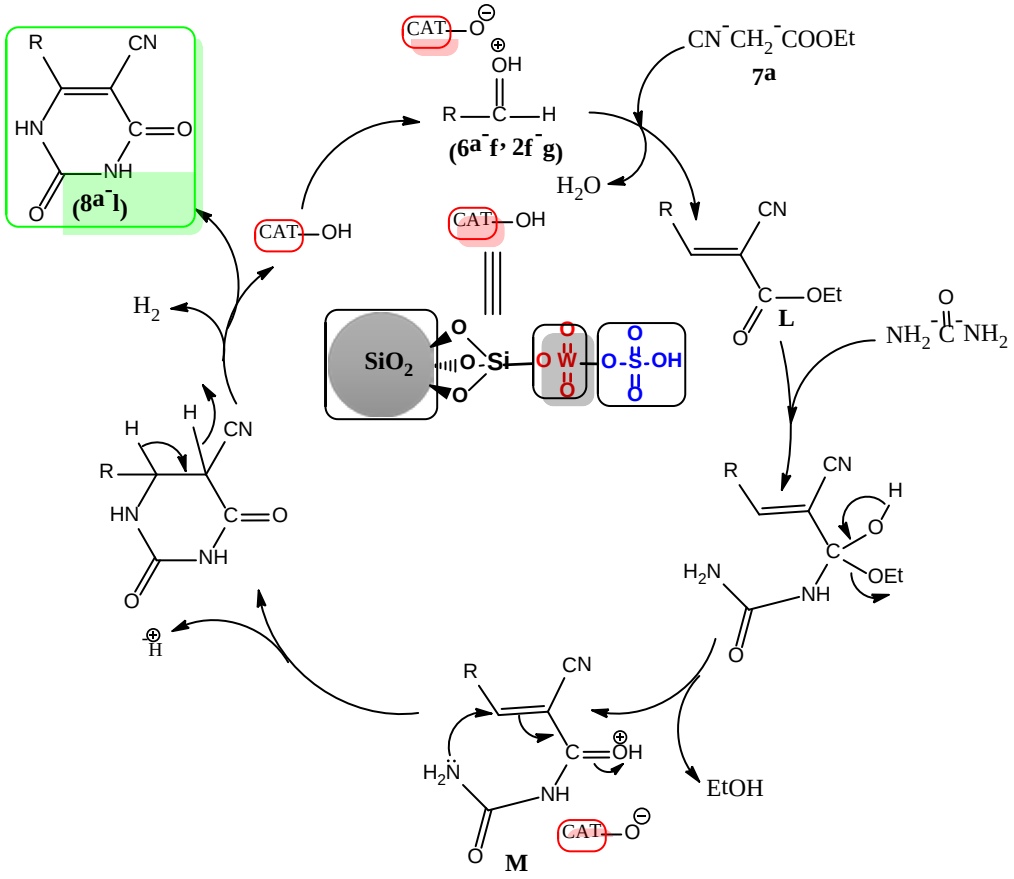

Scheme 8: plausible mechanism for the formation of tetrahydropyrimidines.

3.4.5. Recyclability of the catalyst

Recyclability of the catalyst was evaluated by the reaction of 6-methyl-3-formylchromone, ethyl cyanoacetate and urea in the presence of SSTA under solvent-free conditions. After completion of the reaction the product was recovered by extracting the mixture with ethanol and the remaining catalyst was then filtered, washed with ethanol (3x15 mL), ethyl acetate (2x10 mL), dried at 100 °C for 1 hour and reused for subsequent cycles. It was found that the catalyst exhibited good catalytic activity for six cycles **(Table 15)**. The XRD **(Figure 24c)** and SEM images **(figure 25c)** of the catalyst after six catalytic cycles showed that the morphology of the catalyst does not alter during recycling.

Table 15: Recycling data of SSTA for the model reaction showing concentrations of residual H^+ on the used support after successive experiments.

Catalyst recycles	Time (min)	Yield (%)	Conc. of residual H^+
1	15	94	0.40 meq/gram
2	15	94	0.40 meq/gram
3	15	94	0.35 meq/gram
4	15	92	0.35 meq/gram
5	15	91	0.30 meq/gram
6	15	89	0.25 meq/gram

3.5. CONCLUSION

In conclusion, sulphated silica tungstic acid (SSTA) proved to be an efficient catalyst for eco-friendly synthesis of various tetrahydropyrimidines and dihydropyrimidines by one pot reaction of aldehydes, urea and active methylene compounds. The catalyst is easy to prepare, highly efficient, and easily recoverable by simple filtration. The catalyst could be reused for six cycles without any significant loss of activity.

3.6. EXPERIMENTAL

3.6.1. Preparation of silica chloride

$SOCl_2$ (20 g) was added drop wise to the silica gel (20 g) in dry CH_2Cl_2 (50 mL) at room temperature under stirring. Evolution of copious amounts of HCl and SO_2 occurred instantaneously. After stirring for another 1h, the solvent was removed under reduced pressure. The silica chloride thus obtained was used in the following experiments.[45]

3.6.2. Preparation of silica tungstic acid

A mixture of silica chloride (6.00 g) and sodium tungstate (7.03 g) in dry n-hexane (10 mL) was stirred under refluxing conditions for 6 h. After completion of the reaction, the reaction mixture was filtered, washed with distilled water, dried and then stirred in the presence of 0.1 N HCl (40 mL) for an hour. Finally, the mixture was filtered, washed thoroughly with distilled water, and dried to afford STA.[46]

3.6.3. Preparation of sulphated silica tungstic acid (SSTA)

A 0.5 L suction flask was equipped with a constant pressure dropping funnel. The gas outlet was connected to a vacuum system through an adsorbing solution of alkali trap. STA (2.5 g) was added into the flask and stirred for 10 min in dry CH_2Cl_2 (0.075 L). Chlorosulfonic acid (1.75 g) was added drop wise over a period of 30 min at room temperature. After completion of the addition, the mixture was stirred for 90 min, while the residual HCl was eliminated by suction. Then the SSTA was separated from the reaction mixture and washed several times with dried CH_2Cl_2. Finally SSTA was dried at 120 °C for three hours.

3.6.4. General procedure for synthesis of tetrahydropyrimidines

Aldehyde (3 mmol), ethyl cyanoacetate or phenyl acetic acid (3 mmol), urea (4.5 mmol) and SSTA (200 mg) were mixed by stirring in a 25 mL round bottom flask for specified time **(Table 13)** at a temperature of 70 °C. The reaction mixture was cooled and ethanol was added to solubilize the product. The remaining solid catalyst was filtered, washed with ethanol (3x15 mL) and ethyl acetate (2x10 mL) and reused for further catalytic cycles. The filtrate was evaporated under reduced pressure to obtain the product. The crude product was further purified by recrystallization from suitable solvent (Ethanol or DMSO).

3.6.5. General procedure for synthesis of dihydropyrimidines

Aldehyde (3 mmol), ethyl acetoacetate or acetyl acetone (3.5 mmol), urea (4.5 mmol) and SSTA (200 mg) were mixed in a 25 mL round bottom flask for specified time **(Table 13)** at a temperature of 70 °C. The reaction mixture was cooled and added ethanol to solubilize the product. Catalyst was recovered by above mentioned procedure. The filtrate was evaporated under reduced pressure to obtain the product. The compounds were recrystallized from ethanol.

3.6.6. Spectral data of Synthesized compounds

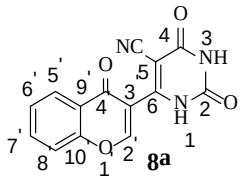 **8a**	*6-(4-oxo-4H-[1]benzopyran-3-yl)-2,4-dioxo-1,2,3,4-tetrahydropyrimidine-5-carbonitrile.* White solid, **M.p.** 210-215 °C. **Anal**. **Calcd** ($C_{14}H_7N_3O_4$): C, 59.79; H, 2.51; N, 14.94. **Anal. Found** ($C_{14}H_7N_3O_4$): C, 59.75; H, 2.54; N, 14.95. **IR** (KBr, cm^{-1}):1647 (C=O), 1732 (2xC=O), 2218 (CN), 3262 (NH), 3442 (NH). **^{1}H NMR** (400 MHz, DMSO-d_6): δ 10.86 (s, 1H, NH), 8.18 (s, 1H, NH), 6.67 (s, 1H, H-2'), 7.1-7.9 (m, 4H, Ar-H). **^{13}C NMR** (100 MHz, DMSO-d_6): δ 179.14, 169.24, 167.52, 161.32, 156.86, 150.29, 135.27, 133.21, 127.44, 124.18, 121.51, 113.94, 109.11, 91.21. **ESI-MS** m/z 282.1 (M^+ +1).
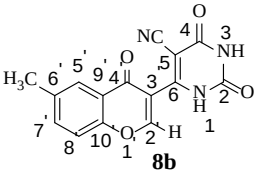 **8b**	*6-(6-methyl-4-oxo-4H-[1]benzopyran-3-yl)-2,4-dioxo-1,2,3,4-tetrahydropyrimidine-5-carbonitrile*. White solid, **M.p.** 225-230 °C. **Anal. Calcd** ($C_{15}H_9N_3O_4$): C, 61.02; H, 3.07; N, 14.23. **Anal. Found** ($C_{15}H_9N_3O_4$): C, 61.05; H, 3.03; N, 14.26. **IR** (KBr, cm^{-1}):1654 (C=O), 1730 (2xC=O), 2224(CN), 3281 (NH), 3444 (NH).**^{1}H NMR** (400 MHz, DMSO-d_6): δ 11.21 (s, 1H, NH), 8.74 (s, 1H, NH), 7.37 (s, 1H, H-2'), 7.4-7.8 (m, 3H, Ar-H), 3.36 (s, 3H, CH_3). **^{13}C NMR** (100 MHz, DMSO-d_6): δ 180.22, 172.94, 168.21, 162.44, 158.07, 152.11, 138.78, 133.36, 127.12, 123.34, 120.11, 115.81, 107.31, 86.14, 27.02. **ESI-MS** m/z 296.1 (M^+ +1).
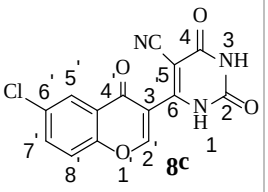 **8c**	*6-(6-chloro-4-oxo-4H-[1]benzopyran-3-yl)-2,4-dioxo-tetrahydropyrimidine-5-carbonitrile.* White solid, **M.p.** 220-225 °C. **Anal. Calcd** ($C_{14}H_6ClN_3O_4$): C, 53.27; H, 1.92; N, 13.31. **Anal. Found** ($C_{14}H_6ClN_3O_4$): C, 53.25; H, 1.95; N, 13.27. **IR** (KBr, cm^{-1}):1694 (C=O), 1738 (2xC=O), 2233 (CN), 3297(NH), 3396 (NH). **^{1}H NMR** (400 MHz, DMSO-d_6): δ 10.86 (s, 1H, NH), 8.25 (s, 1H, NH), 7.01(s, 1H, H-2'), 7.2-7.8 (m, 3H, Ar-H). **^{13}C NMR** (100 MHz, DMSO-d_6): δ 181.02, 171.23, 168.47, 163.72, 154.24,

	149.89, 136.76, 135.21, 132.70, 130.49, 124.09, 119.76, 113.28, 88.76. **ESI-MS** m/z 316.2 (M^+ +1).
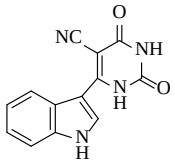 **8d**	*6-(indol-3-yl)-2,4-dioxo-1,2,3,4-tetrahydropyrimidine-5-carbonitrile*. Orange solid, **M.p.** 203-208 °C. **Anal. Calcd** ($C_{13}H_8N_4O_2$): C, 61.90; H, 3.20; N, 22.21. **Anal. Found** ($C_{13}H_8N_4O_2$): C, 61.86; H, 3.25; N, 22.23. **IR** (KBr, cm^{-1}): 1736 (2xC=O), 2218 (CN), 3166 (NH), 3241 (NH), 3389 (NH). **^{1}H NMR** (400 MHz, DMSO-d_6): δ 11.06 (s, 1H, NH), 9.82 (s, 1H, NH-Indole), 8.31 (s, 1H, NH), 8.23 (s, 1H), 7.2-8.0 (m, 4H, Ar-H). **^{13}C NMR** (100 MHz, DMSO-d_6): δ 174.56, 168.24, 154.51, 141.09, 131.24, 129.82, 127.29, 126.87, 124.17, 121.75, 119.05, 115.12, 92.43. **ESI-MS** m/z 253.2 (M^+ +1).
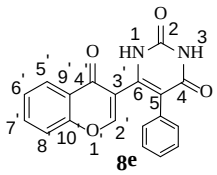 **8e**	*6-(4-oxo-4H-[1]benzopyran-3-yl)-5-phenyl-1,2,3,4-tetrahydropyrimidine-2,4-dione*. White solid, **M.p.** 240-245 °C. **Anal. Calcd** ($C_{19}H_{12}N_2O_4$): C, 68.67; H, 3.64; N, 8.43. **Anal. Found** ($C_{19}H_{12}N_2O_4$): C, 68.62; H, 3.67; N, 8.41. **IR** (KBr, cm^{-1}):1664 (C=O), 1743 (2xC=O), 3257(NH), 3389 (NH). **^{1}H NMR** (400 MHz, DMSO-d_6): δ 10.13 (s, 1H, NH), 8.94 (s, 1H, NH), 6.63 (s, 1H, H-2'), 7.4-7.8 (m, 9H, Ar-H). **^{13}C NMR** (100 MHz, DMSO-d_6): δ 182.72, 172.53, 165.24, 161.56, 157.54, 149.11, 134.62, 132.35, 129.21, 128.79, 127.54, 125.57, 122.72, 121.90, 119.81, 112.46, 102.63. **ESI-MS** m/z 333.1(M^+ +1).
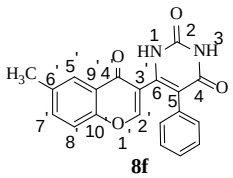 **8f**	*6-(6-methyl-4-oxo-4H-[1]benzopyran-3-yl)-5-phenyl-1,2,3,4-tetrahydropyrimidine-2,4-dione***.** White solid, **M.p.** 260-265 °C. **Anal. Calcd** ($C_{20}H_{14}N_2O_4$): C, 69.36; H, 4.07; N, 8.09. **Anal. Found** ($C_{20}H_{14}N_2O_4$): C, 69.32; H, 4.02; N, 8.11. **IR** (KBr, cm^{-1}):1652 (C=O), 1735 (2xC=O), 3270(NH), 3447 (NH). **^{1}H NMR** (400 MHz, DMSO-d_6): δ 10.73 (s, 1H, NH), 8.52 (s, 1H, NH), 6.44 (s, 1H, H-2'), 7.1-8.2 (m, 8H, Ar-H), 3.35 (s, 3H, CH_3). **^{13}C NMR** (100 MHz, DMSO-d_6): δ 181.54, 170.21, 166.18, 159.38, 157.72, 151.02,

	134.52, 133.11, 128.92, 127.09, 126.76, 124.61, 123.17, 121.34, 118.87, 111.76, 102.77, 28.55. **ESI-MS** m/z 347.1 (M^+ +1).
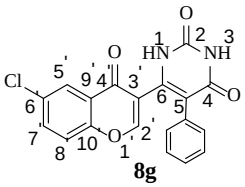 **8g**	*6-(6-chloro-4-oxo-4H-[1]benzopyran-3-yl)-5-phenyl-1,2,3,4-tetrahydropyrimidine-2,4-dione*. White solid, **M.p.** 265-270 °C. **Anal. Calcd** ($C_{19}H_{11}ClN_2O_4$): C, 62.22; H, 3.02; N, 7.64. **Anal. Found** ($C_{19}H_{11}ClN_2O_4$): C, 62.18; H, 3.05; N, 7.59. **IR** (KBr, cm^{-1}):1695 (C=O), 1739 (2xC=O), 3292(NH), 3400(NH). **^{1}H NMR** (400 MHz, DMSO-d_6): δ 10.63 (s, 1H, NH), 8.24 (s, 1H, NH), 6.69 (s, 1H, H-2'), 7.0-7.7 (m, 8H, Ar-H). **^{13}C NMR** (100 MHz, DMSO-d_6): δ 180.22, 169.83, 164.76, 156.92, 154.24, 149.82, 135.19, 132.79, 131.27, 130.97, 129.51, 127.16, 126.48, 124.06, 122.84, 120.41, 104.73. **ESI-MS** m/z 367.2 (M^+ +1).
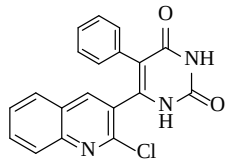 **8h**	*6-(2-chloro-4quinolinyl)-5-phenyl-1,2,3,4-tetrahydropyrimidine-2,4-dione*. Yellow solid, **M.p.** 262-267 °C. **Anal. Calcd.** ($C_{19}H_{12}ClN_3O_2$): C, 65.24; H, 3.46; N, 12.01. **Anal. Found** ($C_{19}H_{12}ClN_3O_2$): C, 65.19; H, 3.42; N, 12.04. **IR** (KBr, cm^{-1}): 1738 (2xC=O), 3281(NH), 3393 (NH). **^{1}H NMR** (400 MHz, DMSO-d_6): δ 11.24 (s, 1H, NH), 8.32 (s, 1H, NH), 8.01(s, 1H), 7.1-7.9 (m, 9H, Ar-H). **^{13}C NMR** (100 MHz, DMSO-d_6): δ 176.81, 162.25, 155.88, 151.17, 148.62, 142.51, 138.36, 134.44, 133.92, 131.02, 129.87, 128.19, 127.23, 126.38, 124.79, 124.05, 108.62. **ESI-MS** m/z 350.1 (M^+ +1).
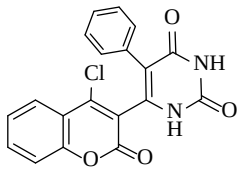 **8i**	*6-(4-chloro-2-oxo-2H-[1]benzopyran-3-yl)-5-phenyl-1,2,3,4-tetrahydropyrimidine-2,4-dione***.** Yellow solid, **M.p.** 220-225 °C. **Anal. Calcd.** ($C_{19}H_{11}ClN_2O_4$): C, 62.22; H, 3.02; N, 7.64. **Anal. Found** ($C_{19}H_{11}ClN_2O_4$): C, 62.26; H, 3.19; N, 7.67. **IR** (KBr, cm^{-1}):1635 (C=O), 1727 (2xC=O), 3219(NH), 3378 (NH). **^{1}H NMR** (400 MHz, DMSO-d_6): δ 11.21 (s, 1H, NH), 8.77 (s, 1H, NH), 7.31-8.09 (m, 9H, Ar-H). **^{13}C NMR** (100 MHz,

	DMSO-d_6): δ 174.67, 167.24, 158.34, 156.22, 149.07, 141.18, 139.63, 135.80, 132.23, 131.40, 129.57, 127.81, 126.09, 124.28, 123.77, 120.11, 109.29. **ESI-MS** m/z 367.1 (M^+ +1).
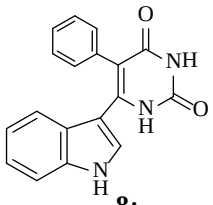 **8j**	*6-(indol-3-yl)-5-phenyl-1,2,3,4-tetrahydropyrimidine-2,4-dione.* Orange solid, **M.p.** 230-235 °C. **Anal. Calcd.** ($C_{18}H_{13}N_3O_2$): C, 71.28; H, 4.32; N, 13.85. **Anal. Found** ($C_{18}H_{13}N_3O_2$): C, 71.32; H, 4.28; N, 13.81. **IR** (KBr, cm^{-1}): 1733 (2xC=O), 3157(NH), 3284 (NH), 3421(NH). **^{1}H NMR** (400 MHz, DMSO-d_6): δ 10.54 (s, 1H, NH), 9.24 (s, 1H, NH-indole), 8.18 (s, 1H, NH), 7.82 (s, 1H), 6.84-7.23 (m, 9H, Ar-H). **^{13}C NMR** (100 MHz, DMSO-d_6): δ 175.24, 162.39, 151.08, 144.76, 141.87, 136.48, 132.77, 130.93, 129.16, 127.51, 126.92, 123.41, 122.83, 118.79, 112.27, 109.33. **ESI-MS** m/z 304.1(M^+ +1).
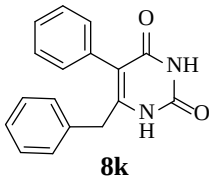 **8k**	*6-(Phenyl methyl)-5-phenyl-1,2,3,4-tetrahydropyrimidine-2,4-dione.* White solid, **M.p.** 210-215 °C. **Anal. Calcd.** ($C_{17}H_{14}N_2O_2$): C, 73.37; H, 5.07; N, 10.07. **Anal. Found** ($C_{17}H_{14}N_2O_2$): C, 73.39; H, 5.04; N, 10.11. **IR** (KBr, cm^{-1}): 1723 (2xC=O), 3285 (NH), 3401 (NH). **^{1}H NMR** (400 MHz, DMSO-d_6): δ 10.92 (s, 1H, NH), 8.87 (s, 1H, NH), 7.14-7.53 (m, 10H, Ar-H), 4.35 (s, 2H, CH_2). **^{13}C NMR** (100 MHz, DMSO-d_6): δ 171.24, 158.39, 148.08, 140.76, 137.48, 132.47, 129.96, 129.23, 128.11, 127.03, 124.88, 105.51, 38.82. **ESI-MS** m/z 279.1 (M^+ +1).
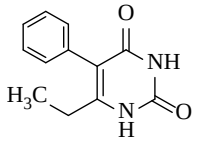 **8l**	*6-(Ethyl)-5-phenyl-1,2,3,4-tetrahydropyrimidine-2,4-dione.* White solid, **M.p.** 160-165 °C. **Anal. Calcd.** ($C_{12}H_{12}N_2O_2$): C, 66.65; H, 5.59; N, 12.96. **Anal. Found** ($C_{12}H_{12}N_2O_2$): C, 66.61; H, 5.63; N, 12.93. **IR** (KBr, cm^{-1}): 1731 (2xC=O), 3291 (NH), 3414 (NH). **^{1}H NMR** (400 MHz, DMSO-d_6): δ 10.32 (s, 1H, NH), 8.27 (s, 1H, NH), 7.01-7.33 (m, 5H, Ar-H), 2.95 (q, 2H, CH_2), 1.34 (t, 3H, CH_3). **^{13}C NMR** (100 MHz, DMSO-d_6): δ 168.41, 156.13, 149.87, 135.22, 129.07, 128.51, 127.92,

	101.25, 27.02, 18.71. **ESI-MS** m/z 217.1 (M^+ +1).
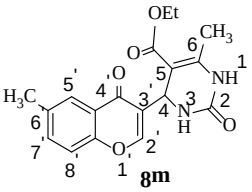 **8m**	*5-Ethoxycarbonyl-6-methyl-4-(6-methyl-4-oxo-4H-[1]benzopyran-3-yl)-3,4 dihydropyrimidin-2 (1H)-one***.** White solid, **M.p.** 297-300 °C. **Anal. calcd**. ($C_{18}H_{18}N_2O_5$): C, 63.15; H, 5.29; N, 8.18, **Anal. Found.** ($C_{18}H_{18}N_2O_5$): C, 63.21; H, 5.37; N, 8.14. **IR** (KBr, cm^{-1}):1646 (C=O), 1706 (C=O), 3122 (NH), 3242 (NH). **^{1}H NMR** (400 MHz, DMSO-d_6): δ 1.09 (t, *J* = 7.2 Hz, 3H, CH_3), 2.25 (s, 3H, CH_3), 2.42 (s, 3H, CH_3), 3.98 (q, *J* = 6.9 Hz, 2H, OCH_2), 5.24 (s, 1H, H-4), 7.62-7.22 (m, 3H, Ar-H), 7.85 (br s, 1H, NH), 8.11 (s, 1H, H-2'), 9.22 (s, 1H, NH). **^{13}C NMR** (100 MHz, DMSO-d_6): δ 176.22, 166.18, 152.83, 149.76, 147.61, 143.32, 134.89, 131.25, 128.72, 126.11, 125.66, 114.84, 101.28, 72.14, 51.48, 28.62, 21.22, 18.17. **ESI-MS** m/z 343.1 (M^+ +1).
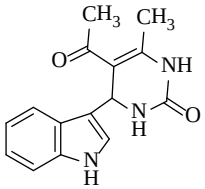 **8n**	*5-Acetyl-6-methyl-4-(indol-3-yl)-3,4-dihydropyrimidin-2(1H)-one***.** Orange solid, **M.p.** 208-210 °C. **Anal. calcd**. ($C_{15}H_{15}N_3O_2$): C, 66.87; H, 5.61; N, 15.61. **Anal. Found**. ($C_{15}H_{15}N_3O_2$): C, 66.83; H, 5.57; N, 15.57. **IR** (KBr, cm^{-1}):1668 (C=O), 3167 (NH). **^{1}H NMR** (400 MHz, DMSO-d_6): δ 2.38 (s, 3H, CH_3), 2.49 (s, 3H, $COCH_3$), 5.29 (s, 1H, H-4), 7.13 (s, 1H), 8.01-7.30 (m, 4H, Ar-H), 8.15 (br s, 1H, NH), 8.53 (s, 1H, NH), 12.5 (s, 1H, NH).**^{13}C NMR** (100 MHz, DMSO-d_6): δ 181.76, 156.28, 138.91, 134.25, 128.42, 125.36, 120.11, 118.46, 116.08, 110.19, 102.56, 101.21, 58.89, 32.57, 21.06. **ESI-MS** m/z 270.1 (M^+ +1).
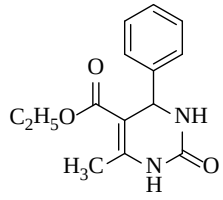 **8o**	*5-Ethoxycarbonyl-6-methyl-4-phenyl-3,4-dihydropyrimidin-2(1H)-one.*[22] White solid, **M.p.** 202-204 ^{o}C; **Anal. calcd**. ($C_{14}H_{16}N_2O_3$): C, 64.60; H, 6.19; N, 10.76. **Anal. Found**. ($C_{14}H_{16}N_2O_3$): C, 64.47; H, 6.24; N, 10.71. **IR** (KBr, cm^{-1}): 1650 (C=O), 1729 (C=O), 3122 (NH), 3245 (NH). **^{1}H NMR** (400 MHz, DMSO-d_6): δ 1.11 (t, *J* = 7.2 Hz, 3H, CH_3), 2.24 (s, 3H, CH_3), 4.01 (q,

	J = 7.2 Hz, 2H, OCH_2), 5.17 (s, 1H), 7.48-7.22 (m, 5H, Ar-H), 7.74 (br s, 1H, NH), 9.20 (br s, 1H, NH). **ESI-MS** m/z 261.1 (M^+ +1).
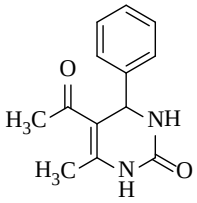 **8p**	*5-Acetyl-6-methyl-4-phenyl-3,4-dihydropyrimidin-2(1H)-one.* [21] White solid, **M.p.** 232-235 ^oC. **Anal**. **calcd**. ($C_{13}H_{14}N_2O_2$): C, 67.81; H, 6.12; N, 12.16. **Anal**. **Found**. ($C_{13}H_{14}N_2O_2$): C, 67.73; H, 6.22; N, 12.11. **IR** (KBr, cm^{-1}): 1650 (C=O), 1706 (C=O), 3267 (NH); **^{1}H NMR**: (400 MHz, DMSO-d_6) δ 2.10 (s, 3H, CH_3), 2.28 (s, 3H, $COCH_3$), 5.25(s, 1H), 7.35-7.23 (m, 5H, Ar-H), 7.83 (s, 1H, NH), 9.19 (s, 1H, NH). **ESI-MS** m/z 231.1 (M^+ +1)
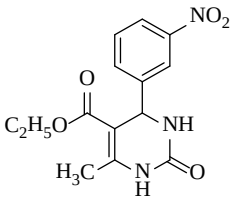 **8q**	*5-Ethoxycarbonyl-6-methyl-4-(3-nitrophenyl)-3,4-dihydropyrimidin-2(1H)-one.* [22] White solid, **M.p.** 227-229 °C. **Anal**. **calcd**. ($C_{14}H_{15}N_3O_5$: C, 55.08; H, 4.94; N, 13.76. **Anal**. **Found**. ($C_{14}H_{15}N_3O_5$): C, 55.16; H, 4.97; N, 13.70. **IR** (KBr, cm^{-1}): 1627 (C=O), 1706 (C=O), 3100 (NH), 3223 (NH); **^{1}H NMR** (400 MHz, DMSO-d_6) δ 1.11 (t, J = 7.2 Hz, 3H, CH_3), 2.26 (s, 3H, CH_3), 4.01 (q, J = 6.9 Hz, 2H, OCH_2), 5.30 (s, 1H), 8.14-7.62 (m, 4H, Ar-H), 7.90 (br s, 1H, NH), 9.37 (s, 1H, NH). **ESI-MS** m/z 306.1 (M^+ +1).
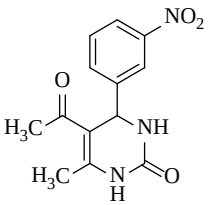 **8r**	*5-Acetyl-6-methyl-4-(3-nitrophenyl)-3,4-dihydropyrimidin-2(1H)-one.* [21] White solid, **M.p**. 220-225 °C. **Anal**. **calcd**. ($C_{13}H_{13}N_3O_4$): C, 56.72; H, 4.76; N, 15.26. **Anal**. **Found** ($C_{13}H_{13}N_3O_4$): C, 56.63; H, 4.85; N, 15.16.; **IR** (KBr, cm^{-1}): 1683 (C=O), 3275 (NH); **^{1}H NMR**: (400 MHz, DMSO-d_6) δ 2.05 (s, 3H, CH_3), 2.33 (s, 3H, $COCH_3$), 5.67 (s, 1H), 7.45-7.27 (m, 4H, Ar-H), 7.72 (s, 1H, NH), 9.26 (s, 1H, NH). **ESI-MS** m/z 276.1 (M^+ +1).

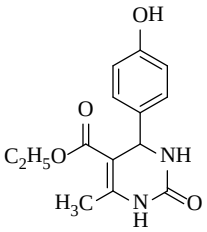 **8s**	*5-Ethoxycarbonyl-6-methyl-4-(4-hydroxyphenyl)-3,4-dihydropyrimidin-2(1H)-one*.[22] White solid, **M.p.** 227-229 °C. **Anal**. **calcd**. ($C_{14}H_{16}N_2O_4$): C, 60.86; H, 5.83; N, 10.13; **Anal**. **Found** ($C_{14}H_{16}N_2O_4$): C, 60.72; H, 5.89; N, 10.16. **IR** (KBr, cm^{-1}): 1646 (C=O), 1690 (C=O), 3122 (NH), 3246 (NH), 3515 (OH); **^{1}H NMR** (400 MHz, DMSO-d_6): δ 1.12 (t, *J* = 7.2 Hz, 3H, CH_3), 2.23 (s, 3H, CH_3), 4.01 (q, *J* = 7.2 Hz, 2H, OCH_2), 5.04 (s, 1H), 6.69 (d, 2H, *J* = 8.4 Hz, Ar-H), 7.04 (d, 2H, *J* = 8.4 Hz, Ar-H), 7.60 (br s, 1H, NH), 9.09 (br s, 1H, NH), 9.31 (s, 1H, OH). **ESI-MS** m/z 277.1 (M^+ +1).
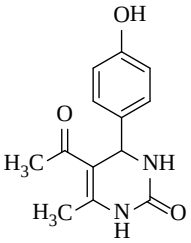 **8t**	*5-Acetyl-6-methyl-4-(4-hydroxyphenyl)-3,4-dihydropyrimidin-2(1H)-one*.[21] White solid, **M.p.** 231-234 °C. **Anal**. **calcd**. ($C_{13}H_{14}N_2O_3$): C, 63.40; H, 5.73; N, 11.37. **Anal**. **Found** ($C_{13}H_{14}N_2O_3$): C, 63.48; H, 5.82; N, 11.33. **IR** (KBr, cm^{-1}): 1647 (C=O), 1687 (C=O), 3120 (NH), 3283 (NH), 3516 (OH). ^{1}H NMR (400 MHz, DMSO-d_6): δ 2.10 (s, 3H, CH_3), 2.22 (s, 3H, CO-CH_3), 5.04 (s, 1H), 6.69 (d, 2H, *J* = 8.4 Hz, Ar-H), 7.04 (d, 2H, *J* = 8.4 Hz, Ar-H), 7.60 (s, 1H, NH), 9.09 (s, 1H, NH), 9.31 (s, 1H, OH). **ESI-MS** m/z 247.08 (M^+ +1).
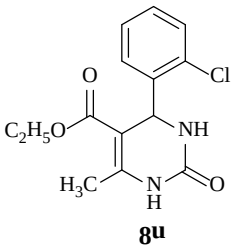 **8u**	*5-Ethoxycarbonyl-6-methyl-4-(2-chlorophenyl)-3,4-dihydropyrimidin-2(1H)-one*.[22] White solid, **M.p**. 214-216 ^{o}C.; **Anal**. **calcd**. ($C_{14}H_{15}N_2O_3Cl$): C, 57.05; H, 5.12; N, 9.50. **Anal**. **Found** ($C_{14}H_{15}N_2O_3Cl$): C, 57.12; H, 5.29; N 9.46. **IR** (KBr, cm^{-1}): 1650 (C=O), 1700 (C=O), 3115 (NH), 3230 (NH); **^{1}H NMR** (400 MHz, DMSO-d_6): δ 1.01 (t, *J* = 6.9 Hz, 3H, CH_3), 2.30 (s, *J* = 6.9 Hz, 3H, CH_3), 3.92 (q, 2H, OCH_2), 5.63 (s, 1H), 7.25-7.41 (m, 4H, Ar-H), 7.68 (br s, 1H, NH), 9.25 (br s, 1H, NH); **ESI-MS** m/z 295.11(M^+ +1).

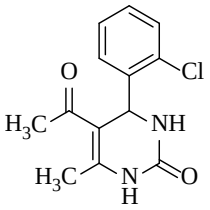 **8v**	*5-Acetyl-6-methyl-4-(2-chlorophenyl)-3,4-dihydropyrimidin-2(1H)-one*.[21] White solid, **M.p.** 303-305 °C. **Anal**. **calcd**. ($C_{13}H_{13}N_2O_2Cl$): C, 58.98; H, 4.95; N, 10.58. **Anal**. **Found** ($C_{13}H_{13}N_2O_2Cl$): C, 58.92; H, 4.97; N, 10.63. **IR** (KBr, cm^{-1}):1625 (C=O), 1708 (C=O), 3092 (NH), 3246 (NH). **^{1}H NMR**: (400 MHz, DMSO-d_6) δ 2.05 (s, 3H, CH_3), 2.33 (s, 3H, $COCH_3$), 5.67 (s, 1H), 7.45-7.27 (m, 4H, Ar-H), 7.72 (s, 1H, NH), 9.26 (s, 1H, NH). **ESI-MS** m/z 265.09 (M^++1).
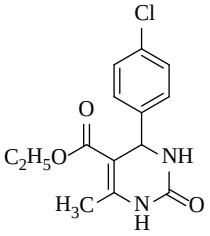 **8w**	*5-Ethoxycarbonyl-6-methyl-4-(4-chlorophenyl)-3,4-dihydropyrimidin-2(1H)-one*.[22] White solid, **M.p.** 213-215 °C. **Anal**. **calcd**. ($C_{14}H_{15}N_2O_3Cl$): C, 57.05; H, 5.13; N, 9.50, **Anal**. **Found** ($C_{14}H_{15}N_2O_3Cl$): C, 57.04; H, 5.02; N, 9.56. **IR** (KBr, cm^{-1}): 1651 (C=O), 1718 (C=O), 3120 (NH), 3243 (NH). **^{1}H NMR** (400 MHz, DMSO-d_6): δ 1.10 (t, *J* = 7.2 Hz, 3H, CH_3), 2.24 (s, 3H, CH_3), 4.01 (q, *J* = 6.9 Hz, 2H, OCH_2), 5.14 (s, 1H), 7.25-7.23 (d, 2H, *J* = 8.4 Hz), 7.40-7.37 (d, 2H, *J* = 8.1 Hz), 7.78 (br s, 1H, NH), 9.26 (s, 1H, NH). **ESI-MS** m/z 295.10 (M^+ +1).

REFERENCES

1. C. O. Kappe, Eur. J. Med. Chem. 35 (2000) 1043.
2. H. L. Luo, W. Yang, Y. Li, S. F. Yin, Chem. Nat. Compd. 46 (2010) 412.
3. (a) G. V. De Lucca, J. Liang, P. E. Aldrich, J. Calabrese, B. Cordova, R. M. Klabe, M. M. Rayner, C. H. Chang, J. Med. Chem. 40 (1997) 1707; (b) R. Garg, D. Patel, Bioorg. Med. Chem. Lett. 15 (2005) 3767.
4. J. L. Adams, T. D. Meek, S. M. Mong, R. K. Johnson, B. W. Metcalf, J. Med. Chem. 31 (1988) 1355.
5. S. Cesarini, A. Spallarossa, A. Ranise, S. Schenone, C. Rosano, P. L. Colla, G. Sanna, B. Busonera, R. Loddo, Eur. J. Med. Chem. 44 (2009) 1106.
6. (a) P. Babczinski, G. Sandmann, , R. R. Schmidt, K. Shiokawa, K. Yasui, Pestic. Biochem. Physiol. 52 (1995) 33; (b) P. Babczinski, M. Blunck, G. Sandmann, K. Shiokawa, K. Yasui, Pestic. Biochem. Physiol. 52 (1995) 45.
7. W. S. Messer Jr., Y. F. Abuh, Y. Liu, S. Periyasamy, D. O. Ngur, M. A. N. Edger, A. A. El-Assadi, S. Sheih, P. G. Dunbar, S. Roknich, T. Rho, Z. Fang, B. Ojo, H. Zhang, J. J. Huzl III, P. I. Nagy, J. Med. Chem. 40 (1997) 1230.
8. R. Pattarini, R. J. Smeyne, J. I. Morgan, Neuroscience 145 (2007) 654.
9. V. Nair, G. Chi, R. Ptak, N. Neamati, J. Med. Chem. 49 (2006) 445.
10. S. B. Mohan, B. V. V. R. Kumar, S. C. Dinda, D. Naik, S. P. Seenivasan, V. Kumar, D. N. Rana, P. S. Brahmkshatriya, Bioorg. Med. Chem. Lett. 22 (2012) 7539.
11. S. E. Mallakpour, A. R. Hajipour, K. Faghihi, N. Foroughifar, J. Bagheri, J. Appl. Polym. Sci. 80 (2001) 2416.
12. S. B. Mohan, B. V. V. R. Kumar, S. C. Dinda, D. Naik, S. P. Seenivasan, V. Kumar, D. N. Rana, P. S. Brahmkshatriya, Bioorg. Med. Chem. Lett. 22 (2012) 7539.
13. S. Kambe, K. Saito, H. Kishi, Synthesis (1979) 287.
14. M. M. M. Ramiz, W. A. El-Sayed, E. Hagag, A. A. H. Abdel-Rahman, J. Heterocycl. Chem. 48 (2011) 1028.
15. D. K. Lokwani, S. N. Mokale, D. B. Shinde, Eur. J. Med. Chem. 73 (2014) 233.
16. J. Safari, S. Gandomi-Ravandi, New J. Chem. 38 (2014) 3514.
17. J. Mondal, T. Sen, A. Bhaumik, Dalton Trans. 41 (2012) 6173.
18. S. Khademinia, M. Behzad, H. Samari Jahromi, RSC Adv. 5 (2015) 24313.
19. M. Moghaddas, A. Davoodnia, M. M. Heravi, N. Tavakoli-Hoseini, Chin. J. Catal. 33 (2012) 706.
20. E. Kolvari, N. Koukabi, O. Armandpour, Tetrahedron 70 (2014) 1383.
21. Z. N. Siddiqui, C. R. Chimie 16 (2013) 183.

22. K. Khan, Z. N. Siddiqui, Monatsh Chem. 146 (2015) 2097.
23. X. Shi, H. Yang, M. Tao, W. Zhang, RSC Adv. 3 (2013) 3939.
24. F. Tamaddon, S. Moradi, J. Mol. Cat. A: Chem. 370 (2013) 117.
25. S. R. Jetti, A. Bhatewara, T. Kadre, S. Jain, Chin. Chem. Lett. 25 (2014) 469.
26. T. Okuhara, Chem. Rev. 102 (2002) 3641.
27. J. H. Clark, Acc. Chem. Res. 35 (2002) 791.
28. A. Corma, H. Garcia, Chem. Rev. 103 (2003) 4307.
29. G. Sartori, R. Ballini, F. Bigi, G. Bosica, R. Maggi, P. Righi, Chem. Rev. 104 (2004) 199.
30. L. Wang, W. Zhao, W. Tan, Nano Res. 1 (2008) 99.
31. R. Bagwe, L. Hilliard, W. Tan, Langmuir 22 (2006) 4357.
32. Z. N. Siddiqui, N. Ahmed, Appl. Organometal. Chem. 27 (2013) 553.
33. M. Smaihi, T. Jermoumi, J. Marignan, R. D. Noble, J. Membr. Sci. 116 (1996) 211.
34. B. Karami, V. Ghashghaee, S. Khodabakhshi, Catal. Commun. 20 (2012) 71.
35. C. Santato, M. Odziemkowski, M. Ulmann, J. Augustynski, J. Am. Chem. Soc. 123 (2001) 10639.
36. S. D. Salim, K. G. Akamanchi, Catal. Commun. 12 (2011) 1153.
37. Z. J. Quan, Y. X. Da, Z. Zhang, X. C. Wang, Catal. Commun. 10 (2009) 1146.
38. P. S. M. Dabiri, M. A. Zolfigol, M. A. B. Fard, Tetrahedron Lett. 44 (2003) 2889.
39. N. A. Liberto, S. Silva, A. Fatima, S. A. Fernandes, Tetrahedron 69 (2013) 8245.
40. M. Litvic, I. Vecenaj, Z. M. Ladisic, M. Lovric, V. Vinkovic, M. Filipan-Litvic, Tetrahedron 66 (2010) 3463.
41. F. Zamani, E. Izadi, Catal. Commun. 42 (2013) 104.
42. A. Rajack, K. Yuvaraju, C. Praveen, Y.L.N. Murthy, J. Mol. Cat. A: Chem. 370 (2013) 197.
43. X. W. Liu, K. K. Pasunooti, H. Chai, C. N. Jensen, B. K. Gorityala, S. Wang, Tetrahedron Lett. 52 (2011) 80.
44. B. Ahmed, A. R. Khan, M. Keshari, Tetrahedron Lett. 50 (2009) 2889.
45. H. N. Karade, M. Sathe, M. P. Kaushik, Molecules 12 (2007) 1341.
46. B. Karami, V. Ghashghaee, S. Khodabakhshi, Catal. Commun. 20 (2012) 71.

CHAPTER 4

Chitosan as a support for dispersion of catalytically active lanthanides

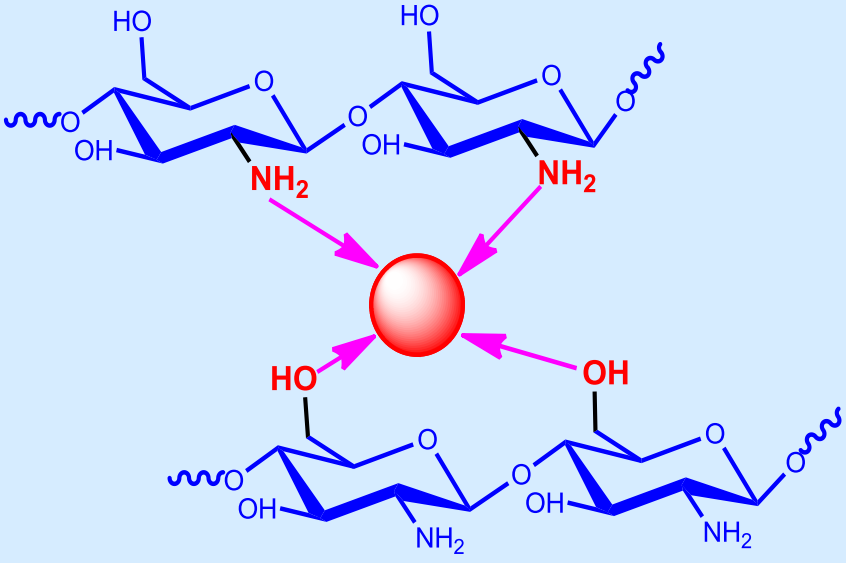

= Ce(III), Dy(III)

4.1. INTRODUCTION

During the last decades the use of lanthanides as efficient Lewis acids have found widespread use in the development of green chemistry.[1] According to Pearson's HSAB classification, trivalent lanthanides are considered to be hard acids and therefore have strong affinity toward hard bases such as oxygen donor ligands.[2] This strong oxophilicity is one of the most important characteristic features of lanthanide(III) compounds making them suitable as Lewis acid catalysts.[2] These elements display unique physical and chemical properties which differ from those of main group and transition elements. Low toxicity, availability at a moderate price, stability and activity in protic media make these elements attractive for use in organic synthesis.[3] The trivalent lanthanides (most common oxidation state) have found widespread use in carbon-carbon bond forming reactions and functional group transformation. Some lanthanides also display stable divalent states, and are therefore used for the reduction of organic functional groups and reductive coupling reactions.[4]

Chitosan, i.e. *N*-deacetylated chitin (poly(1–4)*N*-acetyl-*β*-D-glucosamine), is commercially the most important biocompatible polymer from an environmental or biomedical point of view. It is a biodegradable polysaccharide obtained by deacetylation of chitin **(Figure 31)**, which is the second most abundant natural polymer in the world after cellulose and the process of deacetylation is carried out to different degrees depending upon the targeted applications.[5] The physiological properties of chitosan, especially solubility, are determined by its molecular weight and degree of deacetylation. Chitosan is readily soluble in acidic solutions and insoluble in the majority of common solvents, and the acid solutions can be casted into films and fibres, or they can be precipitated into well-defined spherical particles by spraying into alkaline solution.[6] The property of non-solubility in common organic solvents has generated a lot of interest for its use as support in heterogeneous catalysis. The interesting chemo-physical and biological properties of chitosan like, hydrophilic character, biodegradability, non-toxicity and biocompatibility provide a wide spectrum of opportunities for the development of functional nano-, bio-, and hybrid materials.[7] The primary functional groups present in the chitosan polymer are hydroxyl, amino, and acetamido groups. It also has a property of strongly adsorbing and chelating a range of metal ions due to the presence of these functional groups and is prone to chemical modification. The high density of amino and hydroxyl groups of chitosan enables an effective functionalization and avoids the aggregation of metallic

nanoparticles.[8] As a result, many resulting applications of chitosan include waste water treatment, pharmaceutical and cosmetic preparations, heavy metal complexation, and heterogeneous catalysis.[9]

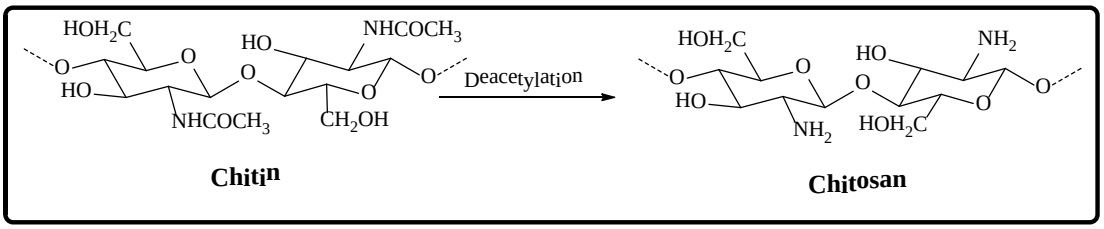

Fig. 31. Structures of chitin and chitosan

SECTION A

SUSTAINABLE SYNTHESIS OF SPIROPIPERIDINE DERIVATIVES USING CERIUM(III) IMMOBILISED CHITOSAN AS AN EFFICIENT AND RECYCLABLE HETEROGENEOUS CATALYST*

Functionalised piperidines form the core of a large family of natural products particularly alkaloids and in various biologically active compounds.[10] The presence of these motifs in drug molecules has led to huge amount of efforts being directed towards developing ever more efficient methodologies for their syntheses. Spiro-substituted piperidines, due to their important pharmacological profiles like selective and potent σ receptor ligands which can be used in the treatment of cocaine abuse, depressions, epileptic disorders and 5-HT_{2B} receptor antagonists, have received considerable attention during the last few decades.[11-16] This privileged unit also forms the core of a large family of alkaloids and natural products with strong biological profiles and interesting structural properties.[17] Therefore, because of the pharmacological and medicinal importance of these compounds, it is highly desirable to develop an efficient protocol for the synthesis of spiropiperidine derivatives which is highly efficient, environmental friendly, tolerates wide range of substrates and involves the reuse of the catalyst.

4.2. REVIEW OF LITERATURE

Some recent examples of the synthesis of 3,5-dispirosubstituted piperidine derivatives.

* Nayeem Ahmed and Zeba N. Siddiqui, ***ACS Sustainable Chemistry & Engineering***, 3 (2015) 1701.

4.2.1. Three-component synthesis of 3,5-dispirosubstituted piperidines in ethanol.[18]

N. G. Kozlov *et al.* reported the synthesis of 3,5-dispirosubstituted piperidines via three-component condensation of anilines, dimedone and formaldehyde. The highlights of the reaction are mild conditions, operationally simplicity and high yields.

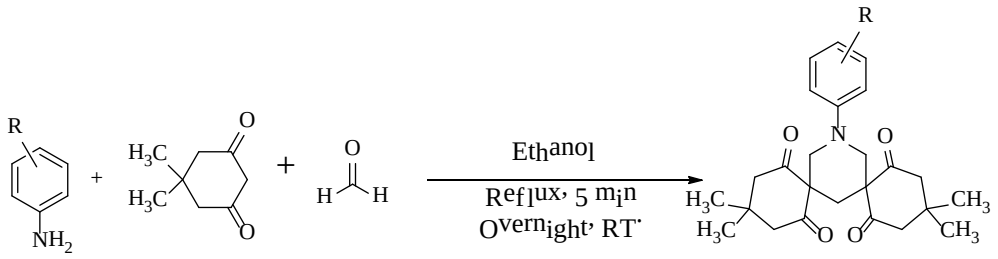

R= H, 4-Br, 4-Me, 4-OMe, 4-NH_2, OEt, NO_2, OPh, COOMe

4.2.2. Silica tungstic acid catalysed synthesis of 3,5-dispirosubstituted piperidines.[19]

A.B. Atar *et al.* reported the synthesis of 3,5-dispirosubstituted piperidines via a three component, one-pot reaction of aromatic amines, formaldehyde and dimedone using silica supported tungstic acid as heterogeneous catalyst. Recyclable catalyst, short reaction time and good yields are the merits of the reported protocol.

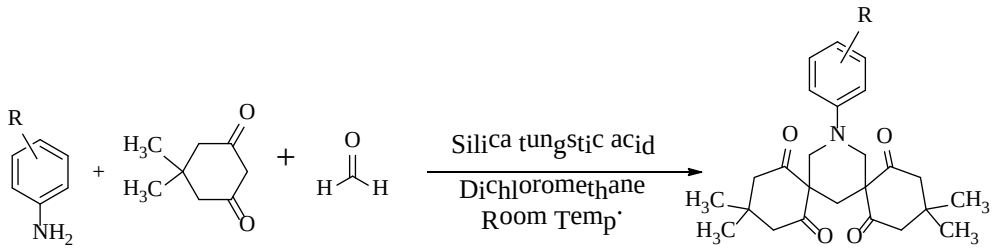

R= H, 4-F, 4-Me, 3-Me, 4-OMe, 4-Cl, 2-OMe, OEt, OPh, Ph

4.2.3. Superparamagnetic iron oxide catalysed synthesis of spiro-piperidines.[20]

F. Janati *et al.* reported the synthesis of spiropiperidines catalysed by superparamagnetic iron oxide nanoparticles. The catalyst was easily recovered by the use of an external magnet, reused several times and showed good efficiency.

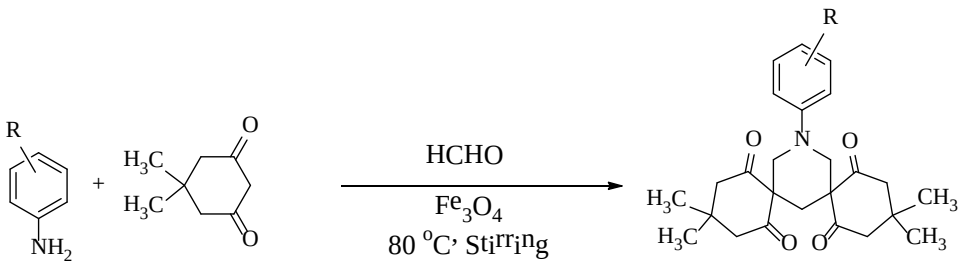

R= 4-Me, 3-Me, 4-OMe, 4-Cl

4.2.4. $FeCl_3$ catalysed synthesis of 3,5-dispirosubstituted piperidines.[21]

C. Mukhopadhyay *et al.* reported the synthesis of 3,5-dispirosubstituted piperidines via multicomponent reaction of 1,3-dicarbonyl compound, amines and formaldehyde catalysed by $FeCl_3$ in dichloromethane at room temperature.

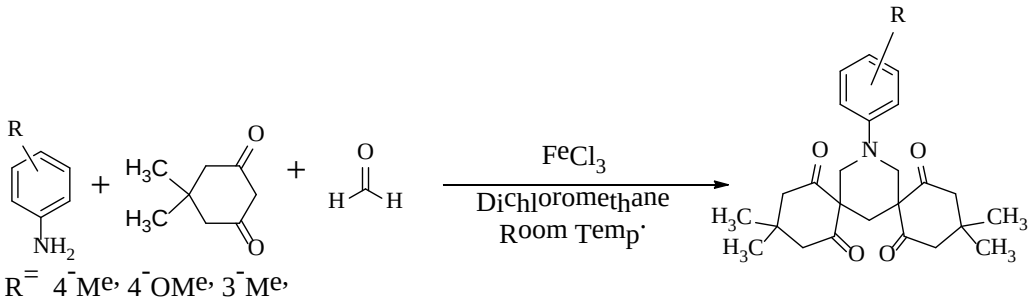

R = 4-Me, 4-OMe, 3-Me,

4.3. PRESENT WORK

Nanoparticles have a characteristic high surface-to-volume ratio, and as a result large fraction of surface atoms are exposed to reactant molecules, making them promising catalysts in chemical synthesis.[22] However, the direct application of the ultra-fine nanoparticles in catalysis is often difficult as their small size increases the tendency towards agglomeration because of van der Waals forces. Thus, for the development of efficient and recyclable catalytic systems, it is very important to employ suitable support materials which will enable fine dispersion and prevent agglomeration of these nanoparticles. Among lanthanides, cerium salts have been extensively used as catalysts in synthetic organic chemistry.[23] The extensive use of Ce salts in reduction, C–C, C–N and C–O bond formation reactions is ascribed to their properties like moderate to low toxicity, water tolerance, easy handling, availability at moderate cost and suitability for use without purification.[24] Nonetheless, from economic and environmental view point their use in stoichiometric amounts is the main limitation. Therefore, the development of heterogenised version of Ce salts by immobilisation on a solid support is a very good means to overcome this limitation. In the present work, taking advantage of the above mentioned interesting properties of chitosan, cerium(III) has been supported on chitosan and used for the highly efficient and sustainable synthesis of spiropiperidine derivatives via multicomponent reaction of substituted anilines, formaldehyde and different active methylene compounds at room temperature.

4.4. RESULTS AND DISCUSSION

The synthesis of the catalyst from chitosan is illustrated in **scheme 9**. The chitosan was suspended in water maintained at pH 9 by using ammonia solution. $CeCl_3.7H_2O$

was added, and the mixture was stirred overnight at room temperature to obtain the catalyst.

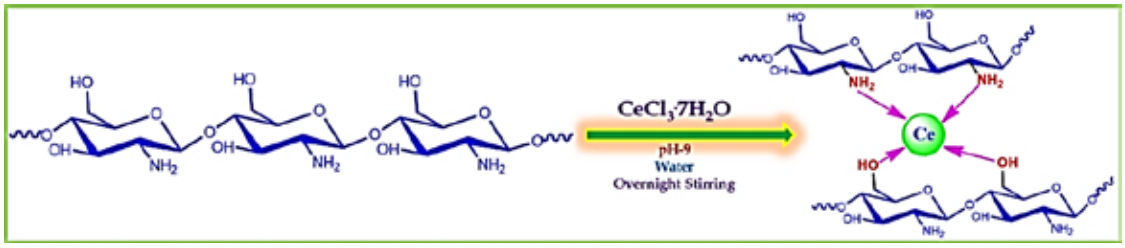

Scheme 9: Schematic representation of the synthesis of the catalyst.

4.4.1. Characterization of the catalyst

4.4.1a. FT-IR spectral analysis

FT-IR spectra of pure chitosan and Ce(III) immobilised chitosan are shown in figure 32. In the spectra of chitosan **(Figure 32a)** a broad band centred at 3419 cm^{-1} is assigned for stretching of OH and NH groups. The presence of the NH_2 groups is confirmed by bending vibrations at 1588 cm^{-1}. The stretching vibrations of C—O and C—N groups were obtained at 1076 and 1379 cm^{-1}, respectively. The band obtained at 2920 cm^{-1} is ascribed to the C—H stretching of methylene groups.[25] In the FT-IR spectra of Ce(III) immobilised chitosan **(Figure 32b)** the bands obtained in the low-frequency region (600–500 cm^{-1}) indicated the formation of Ce–N and Ce–O coordinate bonds .[26,27] Moreover, decrease in the intensity of –NH band at 1596 cm^{-1}, is indicative of the complexation of cerium with $–NH_2$ groups. Similarly, shifting of the OH-bending band at 1071 cm^{-1} is accounted for the interaction of cerium species with the OH groups of chitosan.[28]

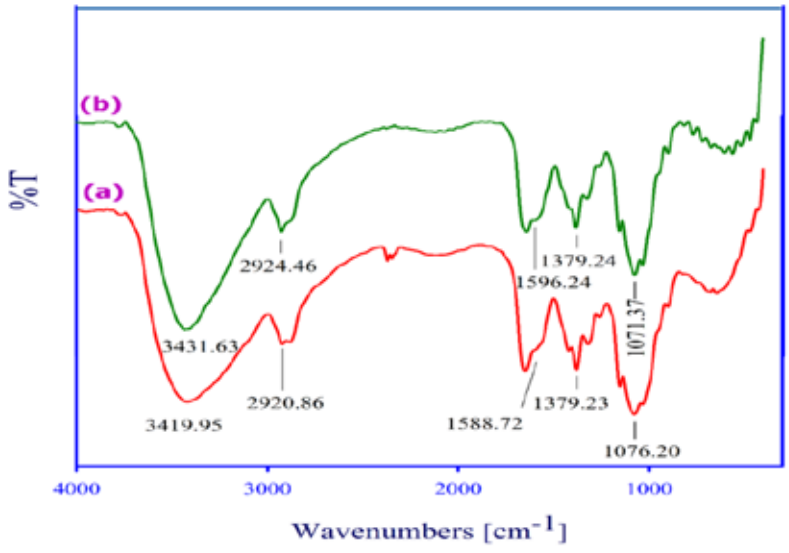

Fig. 32. FT-IR spectral analysis (a) of chitosan, (b) of Ce immobilised chitosan.

4.4.1b. XRD and EDX analyses

The XRD patterns of the catalyst **(Figure 33a)** were similar to that of support **(Figure 33b)**. The absence of peaks pertaining to cerium in the XRD of the catalyst may be due to complexation of cerium with chitosan through coordinate bonds coupled with its low content and small size. However, the presence of Ce in the catalyst was confirmed by EDX analysis **(Figure 33c)** which showed peaks for Ce in addition to C, N and O elements. Moreover, the EDX spectrum does not show presence of Cl, therefore, the active species, immobilised on the support, is Ce(III) in the form of $Ce(OH)_3$.

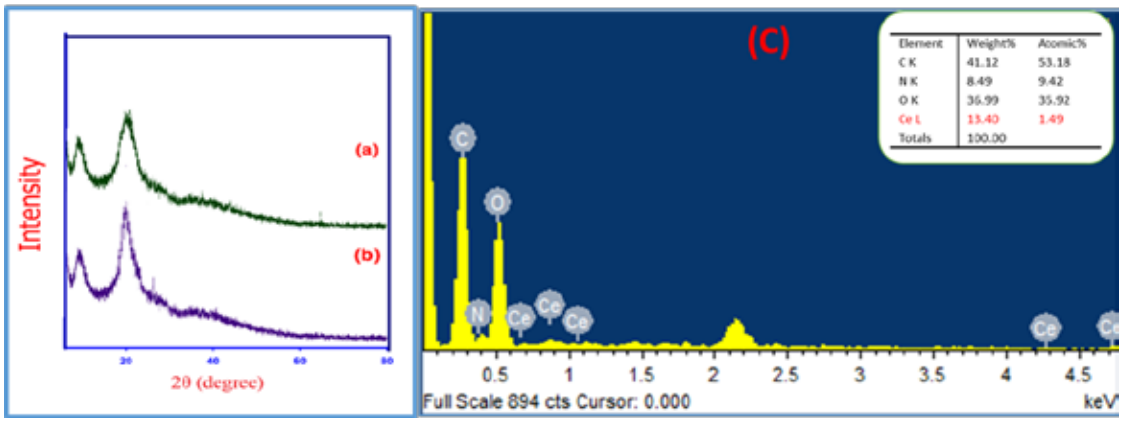

Fig. 33. XRD analysis (a) of Ce immobilised chitosan (b) of chitosan and (c) EDX spectra of Ce immobilised chitosan.

4.4.1c. ICP-AES analysis

ICP-AES analysis was performed in order to obtain the actual amount of Ce in the catalyst. The analysis showed the weight percentage of Cerium to be 7.94%, which corresponded to the loading amount of 0.57 mmol/gram of catalyst.

4.4.1d. TEM analysis

TEM images **(Figure 34a & b)** of the catalyst showed a very well dispersion of Ce nanoparticles (dark spots) in the form of $Ce(OH)_3$, with a particle diameter of 3-8 nm, on the surface of chitosan.

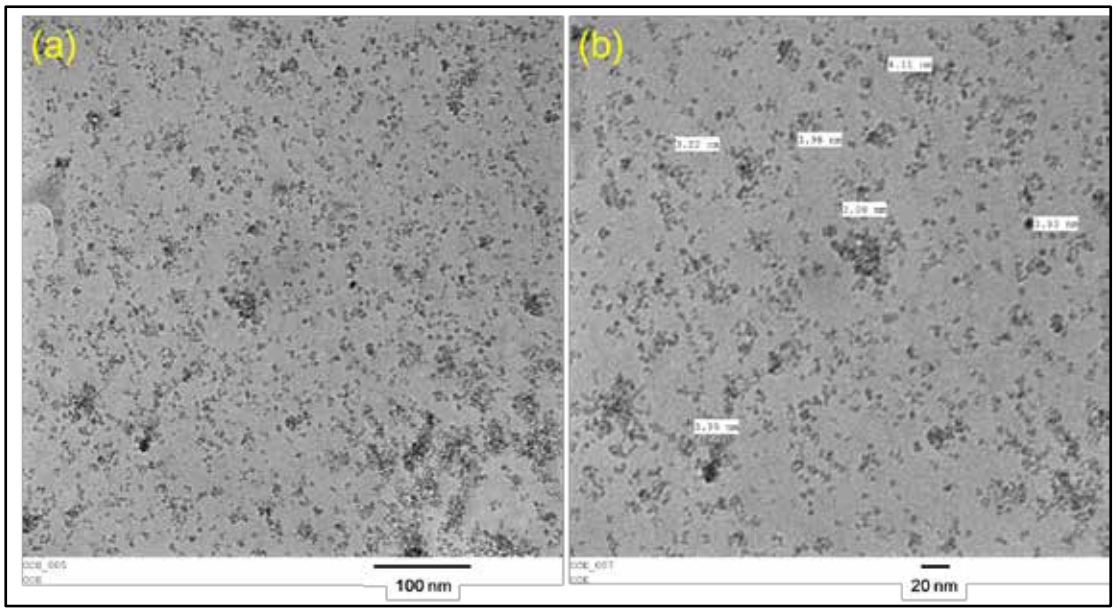

Fig. 34. TEM images (a) and (b) of the synthesised catalyst at different magnifications.

4.4.2. Optimization of reaction conditions

Various control experiments using indane-1,3-dione **(4j)** (2 mmol), formaldehyde (3 mmol) and aniline **(9a)** (1 mmol) as model substrates were carried out at room temperature in PEG-200 in order to make sure that Ce sites bound to chitosan are responsible for the catalytic activity. Reaction in the absence of any catalyst could not lead to any product formation, whereas using chitosan (10 mol%) as a catalyst gave unsatisfactory results. When the reaction was tried using $CeCl_3.7H_2O$ (10 mol%) as a catalyst, the reaction proceeded with good results (product yield of 74% in 2.5h), which clearly demonstrated that the catalytic activity originated from Ce sites. The $CeCl_3.7H_2O$ could not be recovered or recycled because of its homogeneous nature, therefore, we performed the reaction using Ce(III) immobilised on chitosan (200 mg, 0.114 mmol of Ce) as a catalyst and a remarkable increase in its catalytic activity was observed affording the product with high yield (92%) in shorter time period. We then focused our attention towards finding the right solvent and catalyst amount for this reaction. The optimization of reaction conditions involved indane-1,3-dione (2 mmol), formaldehyde (3 mmol) and aniline (1 mmol) as substrates for the model reaction.

4.4.2a. Effect of different solvents

The effect of different solvents on the model reaction was examined at room temperature. Various solvents like water, methanol, ethanol, isopropanol, PEG-200, PEG-400 and PEG-600 were screened to test the efficiency of our catalyst and the

results are summarised in **table 16**. When water was used as a solvent, no transformation of the reactants was observed. Using methanol as a solvent unsatisfactory result was obtained. Using ethanol and isopropanol as solvents average results were obtained. We then used PEG's as solvents and the results obtained were very much satisfactory **(Table 16, entries 5-7)**. PEG-200 was found to be most efficient with excellent product yield in 35 min. The high viscosity of PEG-600 at room temperature may be the reason for its poor performance **(Table 16, entry 7)**. Therefore, PEG-200 was used as a solvent of choice for this reaction.

Table 16: Effect of different solvents on the model reaction[a]

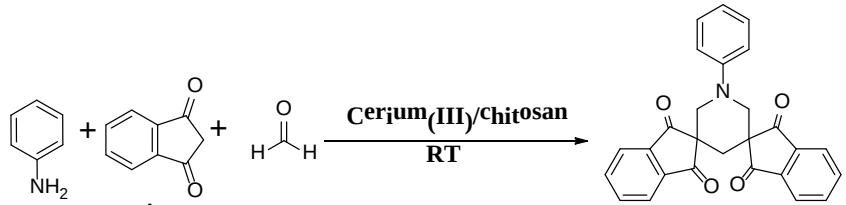

(**9a**) (**4j**) (**10a**)

Entry	Solvent	Time (min)	Yield (%)
1	Water (5mL)	60	No reaction
2	Methanol (5mL)	53	68
3	Ethanol (5mL)	48	78
4	Isopropanol (5mL)	45	81
5	PEG-200 (5mL)	35	92
6	PEG-400 (5mL)	42	85
7	PEG-600 (5mL)	65	45

4.4.2b. Effect of catalyst loading

To investigate effect of catalyst loading, the model reaction was carried out in the presence of varying amounts of the catalyst **(Table 17)**. It was observed that upon increasing the amount of catalyst from 50-200 mg the conversion of spiropiperidine derivative increased linearly. No further increase in product formation was observed when amount of the catalyst increased to 250 mg. Therefore, 200 mg of the catalyst was found to be the optimum amount for the model reaction **(entry 4)**.

Table 17: Effect of different catalyst loading on the model reaction.

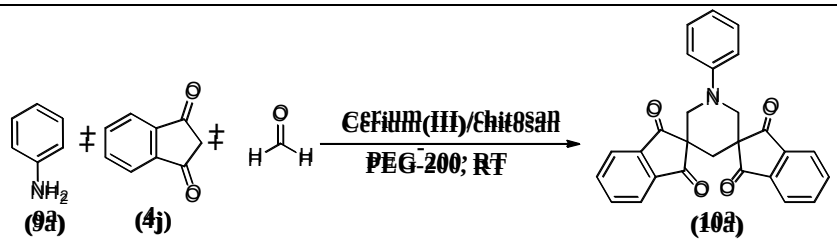

(9a) (4j) (10a)

Entry	Catalyst loading (mg)	Time (min)	Yield (%)
1	50	85	70
2	100	65	81
3	150	45	87
4	200	35	92
5	250	35	92

4.4.3. Catalytic reaction

After optimization of reaction conditions, the substrate scope of Ce(III)/chitosan catalysed synthesis of spiropiperidine derivatives was examined **(Scheme 10)**. It was found that the reaction efficiently tolerated amines with activating and deactivating groups. The reactions with alicyclic amine also gave very good results. Moreover, the reaction with different cyclic active methylene compounds was also investigated and it was found that the reaction efficiently proceeded with indane-1,3-dione as well as with 4-hydroxycoumarin and dimedone also, giving products in excellent yields **(Table 18)**. The results demonstrated the scope and generality of this protocol as a range of cyclic active methylene substrates and amines can be used for the synthesis of spiropiperidine derivatives.

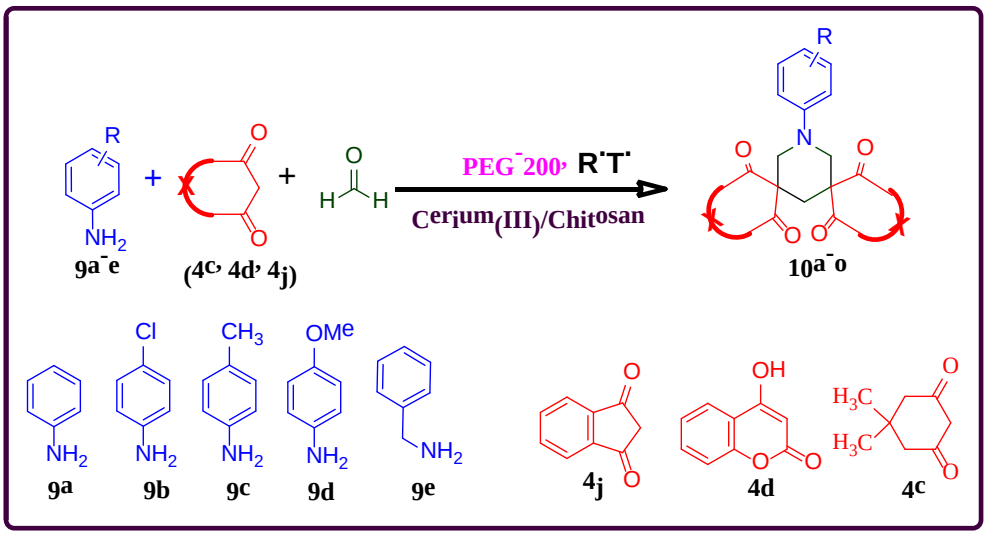

Scheme 10: General scheme for the formation of spiropiperidine derivatives

The structures of the final products were determined from their IR, ^{1}H NMR, ^{13}C NMR and ESI-MS spectra. I.R. spectrum of **10a (Figure 35)** showed carbonyl stretching frequencies of four carbonyl groups at 1704 and 1731 cm^{-1}. The ^{1}H-NMR spectrum **(Figure 36)** showed distinctive singlet at δ 2.77 for two H-4' hydrogens of piperidine ring. Two methylene protons of piperidine were discernible as singlet at δ 3.94. Thirteen aromatic hydrogen atoms were present as multiplet in the range δ 6.94-7.96. ^{13}C-NMR **(Figure 37)** showed a distinctive peak at δ 197.5 ppm for carbonyl groups of indane-1,3-dione moieties and all other peaks were obtained at respective places and are given in the experimental section. Further, structure **10a** was confirmed by ESI-Mass spectrum **(Figure 38)** which showed the molecular ion peak as base peak at m/z 422.1 (M^{+}+1).

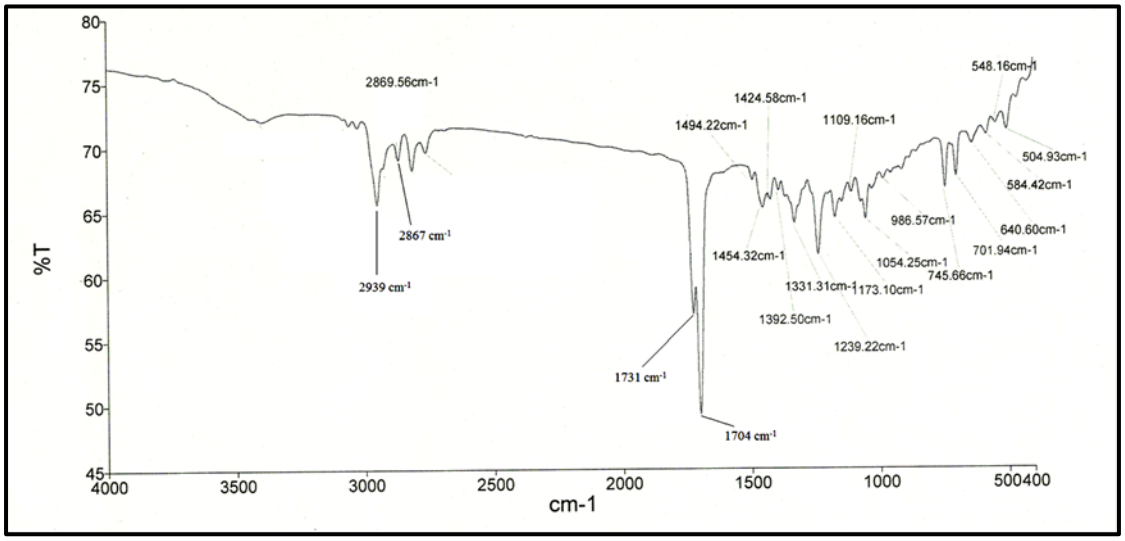

Fig 35. FT-IR spectrum of **10a**

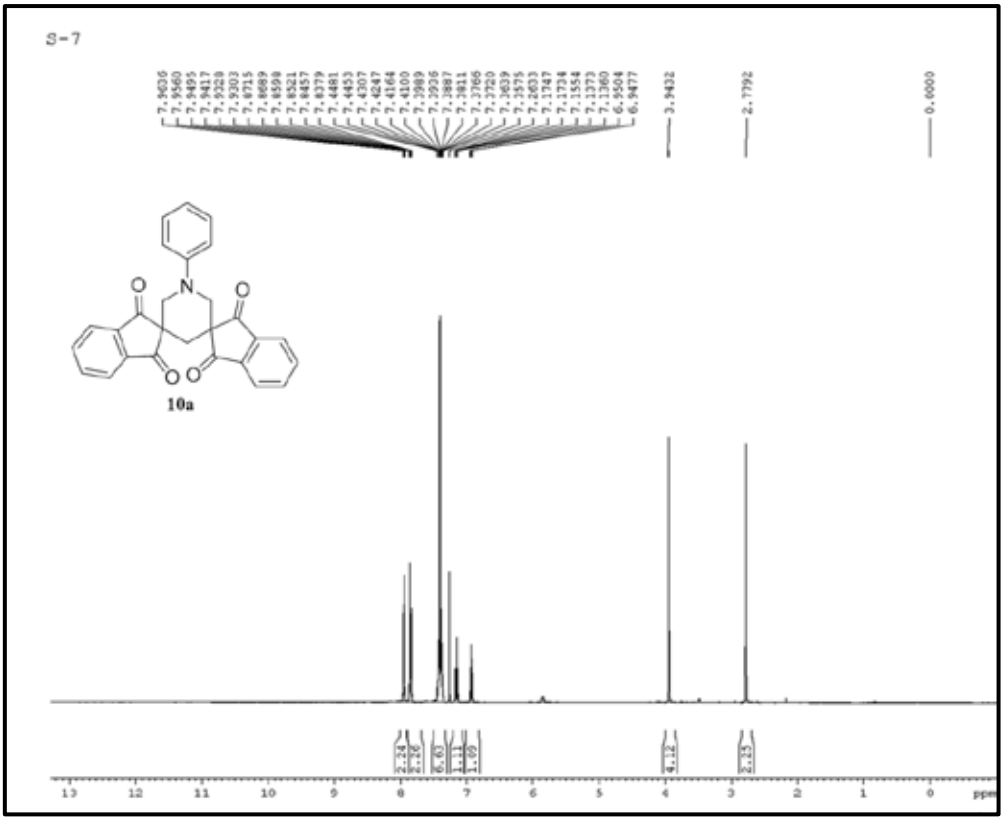

Fig 36. ^{1}H-NMR spectrum of **10a**

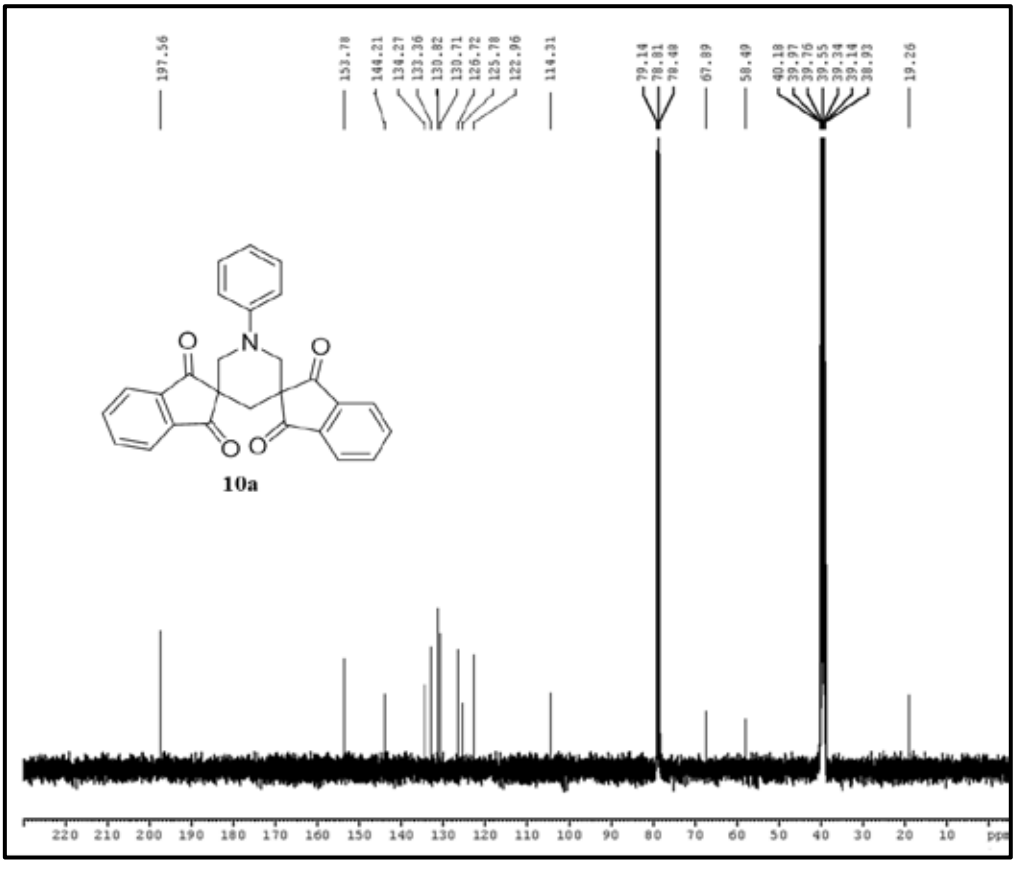

Fig 37. ^{13}C-NMR spectrum of **10a**

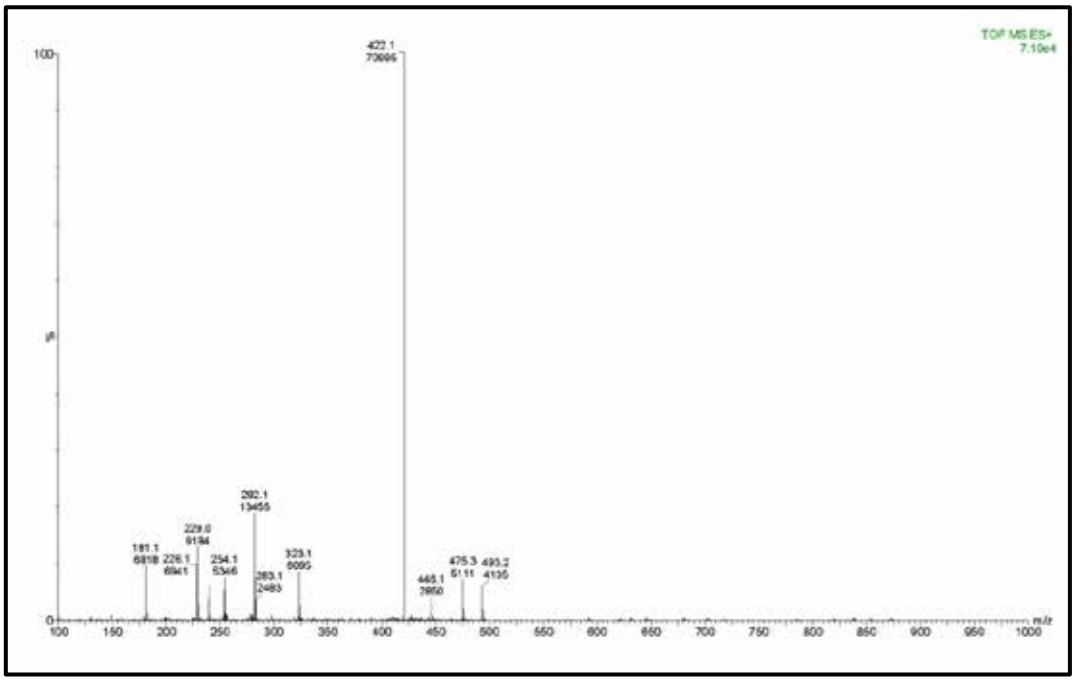

Fig 38. ESI-Mass spectrum of **10a**

In order to further show the efficiency of our protocol, a comparison with available reported protocols in the literature was done **(Table 19)**. The data showed the superiority of our catalytic system for the synthesis of spiropiperidines in terms of efficiency, environment compatibility and practical applicability in comparison to reported procedures.

Table 18: Scope of different active methylene compounds and amines for the synthesis of spiropiperidine derivatives.

Entry	Amines	Active methylenes	Products	Time (min)	Yield (%)
1	 **9a**	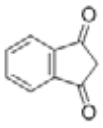 **4j**	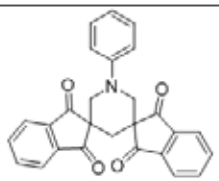 **10a**	35	92
2	 **9b**	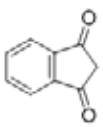 **4j**	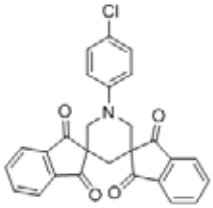 **10b**	41	85

3	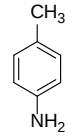 9c	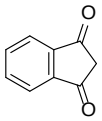 4j	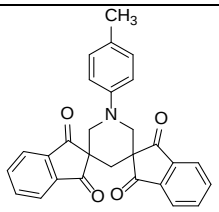 10c	**35**	**89**
4	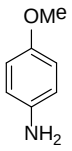 **9d**	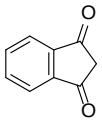 **4j**	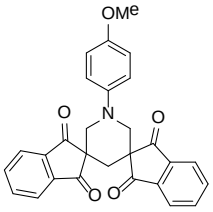 **10d**	38	85
5	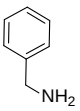 **9e**	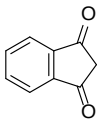 **4j**	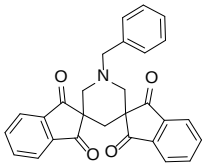 **10e**	33	87
6	 **9a**	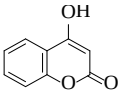 **4d**	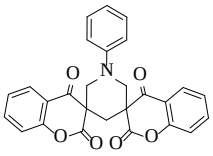 **10f**	45	83
7	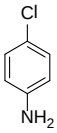 **9b**	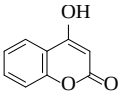 **4d**	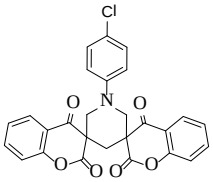 **10g**	48	81
8	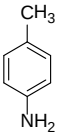 **9c**	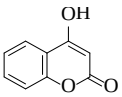 **4d**	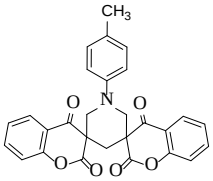 **10h**	42	87
9	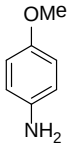 **9d**	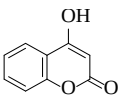 **4d**	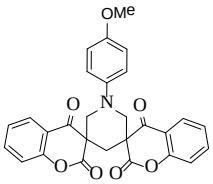 **10i**	47	85
10	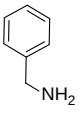 **9e**	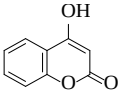 **4d**	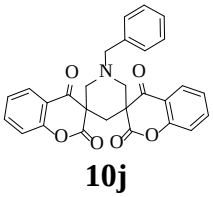 **10j**	40	89

11	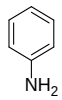 **9a**	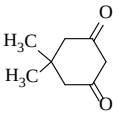 **4c**	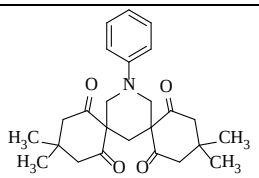 **10k**	38	94
12	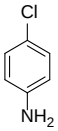 **9b**	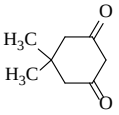 **4c**	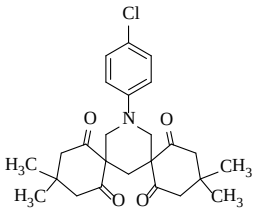 **10l**	41	93
13	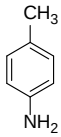 **9c**	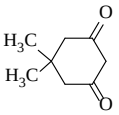 **4c**	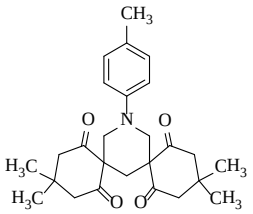 **10m**	35	96
14	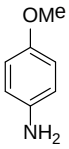 **9d**	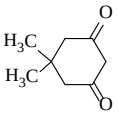 **4c**	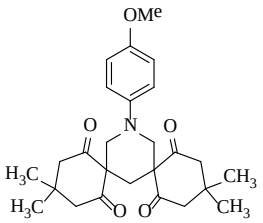 **10n**	40	91
15	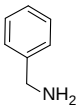 **9e**	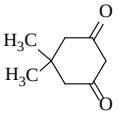 **4c**	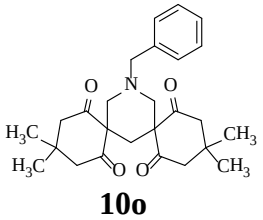 **10o**	32	92

Table 19: Comparison of the efficiency of Ce(III)/chitosan catalyst with reported procedures.

Entry	Catalyst	Condition	Solvent	Yield (%)	Time	Ref.
1	Ce(III)/ chitosan	R. T.	PEG-200	96	35 min	Present work.
2	STA	R. T.	DCM	92	4h	19
3	$FeCl_3$	R. T.	DCM	88	6h	21
4	Fe_3O_4	80 °C	Solvent-free	89	3h	20
5	-	Reflux (5 min)/ overnight/R. T.	Ethanol	84	12h	18

4.4.4. Reaction mechanism

A plausible mechanism for the synthesis of spiropiperidine derivative **(10a)** is proposed in **Scheme 11**.[18-21] In the first step the catalyst activates both indane-1,3-dione **(4j)** and formaldehyde to undergo Knoevenagel condensation to give intermediate **(N)**. The intermediate **(N)** and another activated molecule of indane-1,3-dione **(4j)** then undergo Michael addition to generate **(O)**. The intermediate **O,** formaldehyde and aniline **9a** react via Mannich reaction to generate (**P)** which undergoes another Mannich reaction with formaldehyde to form final product **10a**. The catalyst could be regenerated in the last step and reused for further catalytic cycles.

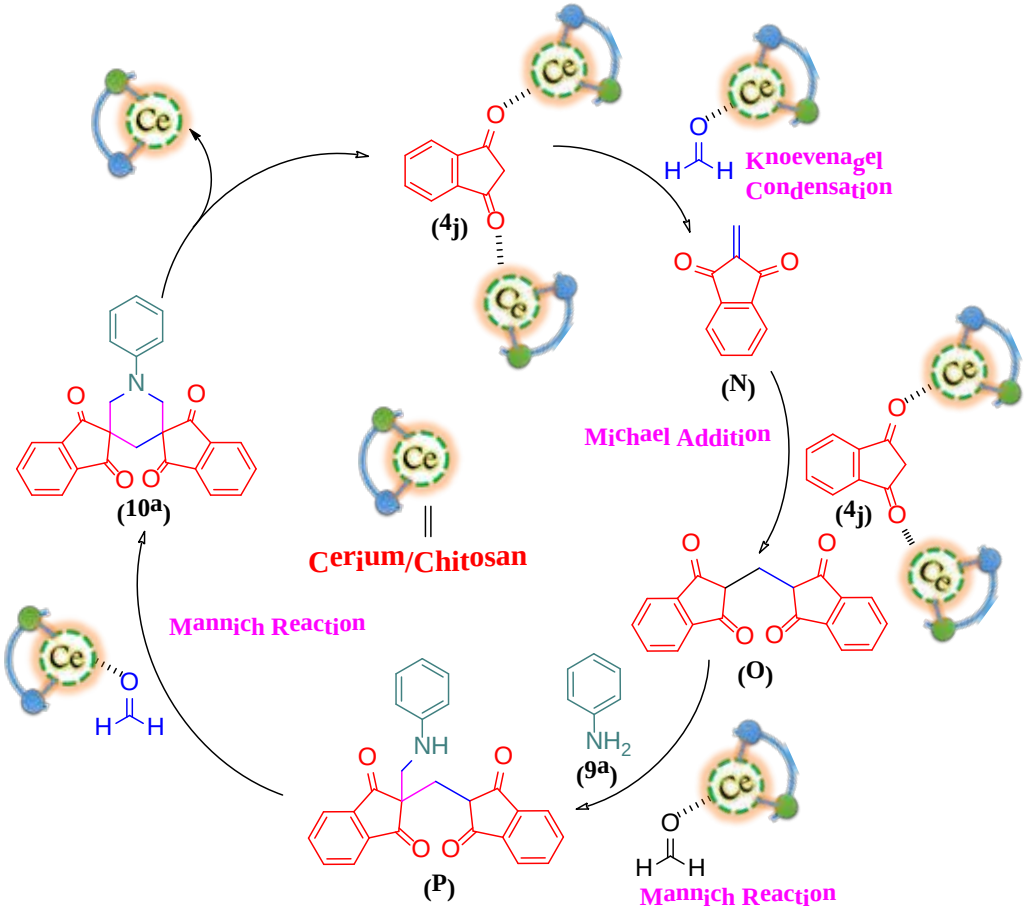

Scheme 11: Proposed reaction mechanism for the formation of **10a**

4.4.5. Leaching study of Ce(III)/chitosan catalyst

ICP-AES analysis of the catalyst before and after five catalytic cycles was performed in order to carry out the leaching study. The Ce concentration before (7.94 Wt. % Ce) and after recycling experiments (7.90 Wt. % Ce) was found to be fairly in agreement (within the experimental error) which denoted that Ce is tightly bound to the support

and no leaching of the catalyst occurs upon its reuse. The TEM image of the catalyst after five cycles **(Figure 39)** did not show any significant change in the morphology of the catalyst, which indicated that the integrity of the catalyst is maintained throughout the recycling studies. The above studies thus, confirm that the structure of the catalyst is stable and cerium is tightly bound to the support.

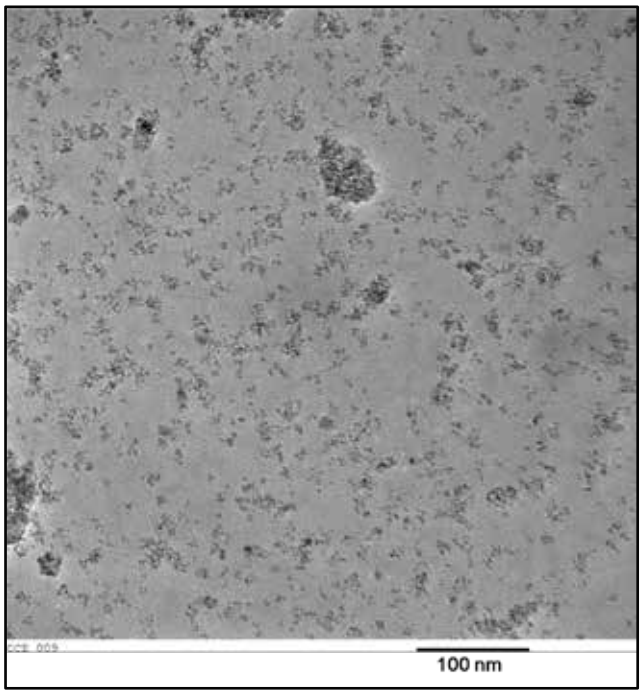

Fig. 39. TEM image of the recycled catalyst after five cycles.

4.4.6. Catalyst Recycling

The catalyst recycling experiment was done using the model reaction of indane-1,3-dione, formaldehyde, aniline and 200 mg of the catalyst in PEG-200 at room temperature. After completion of the reaction water was added to the reaction mixture in order to dissolve PEG-200, a 1:10 mixture of isopropanol and ethyl acetate was then added to extract the product. The remaining catalyst in aqueous layer was filtered, washed with isopropanol/ethyl acetate (1:10) and reused. It was found that the catalyst maintained good activity for a minimum of five cycles **(Figure 40)** displaying a high catalytic performance with over 83% yield of the product after fifth run.

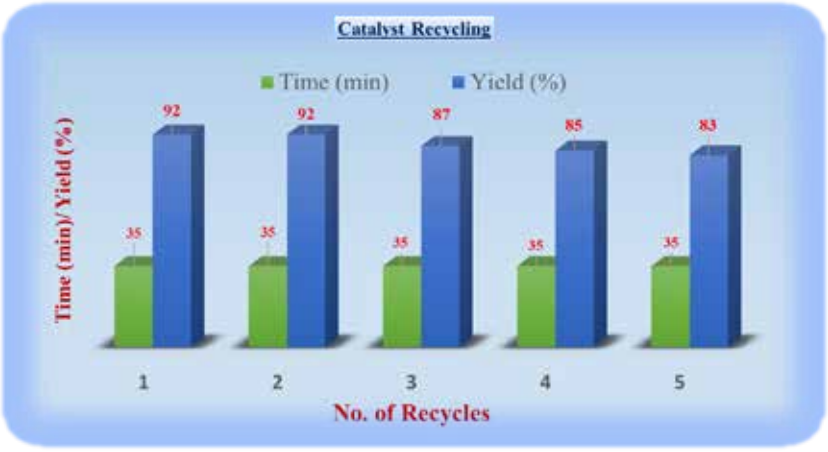

Fig. 40. Recycling data of Ce/Chitosan catalyst

4.5. CONCLUSION

In summary, an efficient and heterogeneous Ce(III)/chitosan catalyst has been synthesised and used for the simple, efficient and environmentally benign synthesis of spiropiperidine derivatives at room temperature using PEG-200 as a green solvent. The substrate scope of the reaction was also demonstrated by the tolerance of aromatic and alicyclic amines in addition to various cyclic active methylene compounds. Low catalyst loading, clean reaction profiles, one pot multi-component procedure, reusability of the catalyst and operational simplicity are the important features of this methodology.

4.6. EXPERIMENTAL

4.6.1. Synthesis of Ce(III)/Chitosan catalyst

1g of $CeCl_3.7H_2O$ was added to the suspension of Chitosan (80% deacetylated) (5g) in 100 mL of water with continuous stirring. The pH of the solution was adjusted at 9 using 25% ammonia solution. The mixture was then continuously stirred overnight at room temperature and the resulting catalyst was separated by filtration and dried under vacuum at 60 °C.

4.6.2. General Procedure for the synthesis of 3,5-dispirosubstituted piperidines (10a-e, 10k-o)

A mixture of amines **(9a-e)** (4 mmol), active methylene compounds **4c, 4j** (8 mmol), formaldehyde (12 mmol, 37–41% aqueous solution) and a catalytic amount of Ce(III)/chitosan (0.8 g, 0.456 mmol of Ce) in PEG-200 (15 mL) was stirred at room temperature for the stipulated period of time **(Table 18)**. The appearance of solid compound denoted the formation of products. After completion of the reaction (monitored by TLC), water (20 mL) was added in order to dissolve the PEG-200 and

a mixture of isopropanol/ethyl acetate (1:10) was then added to extract the products. Solid products were obtained by further evaporation of this organic layer under reduced pressure. The catalyst in the remaining aqueous phase was filtered, washed with isopropanol/ethyl acetate (1:10) mixture, dried and reused. The pure compounds were obtained by further recrystallization.

4.6.3. General procedure for the synthesis of 3,5-dispirosubstituted piperidines (10f-j)

A mixture of amines **(9a-e)** (4 mmol), 4-hydroxycoumarin **4d** (8 mmol), formaldehyde (12 mmol, 37–41% aqueous solution), and a catalytic amount of Ce(III)/chitosan (0.8 g, 0.456 mmol of Ce) in PEG-200 (15 mL) was stirred at room temperature for the stipulated period of time **(Table 18)**. The appearance of solid compound denoted the formation of products. After completion of the reaction (monitored by TLC), water was added and the mixture of catalyst and solid products was filtered. After filtration, DMSO (10 mL) was added to dissolve the products leaving behind the catalyst. The catalyst was filtered, washed with DMSO, isopropanol/ethyl acetate (1:10) mixture, dried and reused. The solvent containing products was left undisturbed in order to obtain pure compounds.

4.6.4. Spectral data of Synthesized compounds

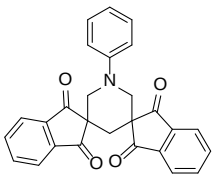 **10a**	*1'-phenyldispiro[indane-1,3-dione-2,3'-piperidine-5',2"-indane-1,3-dione]* Yellow solid, **M.p.** 257-258 °C. **Anal**. **Calcd**. ($C_{27}H_{19}NO_4$) C, 76.95; H, 4.54; N, 3.32. **Anal**. **Found** ($C_{27}H_{19}NO_4$) C, 76.91; H, 4.49; N, 3.36. **IR** (KBr, cm^{-1}): 2939 (C-H), 2867(C-H), 1731 (C=O), 1704 (C=O). **^{1}H NMR** (400 MHz, $CDCl_3$): 2.77 (2H, s), 3.94 (4H, s, CH_2-N-CH_2), 6.94-7.96 (13H, m, Ar-H). **^{13}C NMR** (100 MHz, $CDCl_3$): 19.2, 58.4, 67.8, 114.3, 122.9, 125.7, 126.7, 130.7, 130.8, 133.3, 134.2, 144.2, 153.7, 197.5. **ESI-MS** m/z 422.1 (M^++1).
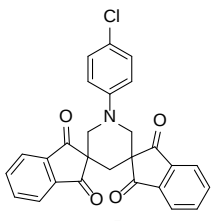 **10b**	*1'-(4-chlorophenyl)dispiro[indane-1,3-dione-2,3'-piperidine-5',2"-indane-1,3-dione]* Yellow solid, **M.p.** 260-261 °C. **Anal**. **Calcd**. ($C_{27}H_{18}ClNO_4$) C, 71.13; H, 3.98; N, 3.07. **Anal**. **Found** ($C_{27}H_{18}ClNO_4$) C, 71.19; H, 3.94; N, 3.11. **IR** (KBr, cm^{-1}): 2940 (C-H), 2871(C-H), 1729 (C=O), 1701 (C=O). **^{1}H NMR** (400 MHz, $CDCl_3$):

	2.71 (2H, s), 3.85 (4H, s, CH_2-N-CH_2), 6.71-7.87 (12H, m, Ar-H). **^{13}C NMR** (100 MHz, DMSO-d_6): 19.5, 59.2, 66.9, 113.4, 126.2, 126.9, 128.5, 131.1, 132.0, 134.8, 135.1, 145.9, 154.7, 197.2. **ESI-MS** m/z 456.1 (M^++1).
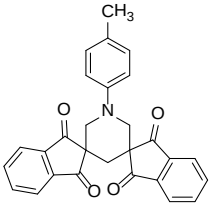 **10c**	*1'-(4-methylphenyl)dispiro[indane-1,3-dione-2,3'-piperidine-5',2"-indane-1,3-dione]* Yellow solid, **M.p.** 265-266 °C. **Anal. Calcd**. ($C_{28}H_{21}NO_4$) C, 77.23; H, 4.86; N, 3.22. **Anal. Found** ($C_{28}H_{21}NO_4$) C, 77.19; H, 4.89; N, 3.27. **IR** (KBr, cm^{-1}): 2932 (C-H), 2854 (C-H), 1741 (C=O), 1704 (C=O). **^{1}H NMR** (400 MHz, $CDCl_3$): 2.40 (3H, s, CH_3), 2.77 (2H, s), 3.90 (4H, s, CH_2-N-CH_2), 6.91-7.96 (12H, m, Ar-H). **^{13}C NMR** (100 MHz, DMSO-d_6): 18.9, 23.8, 59.1, 65.4, 113.1, 125.6, 126.3, 131.8, 133.5, 135.7, 136.0, 143.7, 152.1, 198.9. **ESI-MS** m/z 436.1 (M^++1).
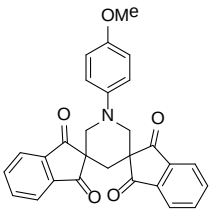 **10d**	*1'-(4-methoxyphenyl)dispiro[indane-1,3-dione-2,3'-piperidine-5',2"-indane-1,3-dione]* Yellow solid, **M.p.** 258-259 °C. **Anal. Calcd**. ($C_{28}H_{21}NO_5$) C, 74.49; H, 4.69; N, 3.10. **Anal. Found** ($C_{28}H_{21}NO_5$) C, 74.44; H, 4.73; N, 3.15. **IR** (KBr, cm^{-1}): 2944 (C-H), 2871 (C-H), 1728 (C=O), 1708 (C=O). **^{1}H NMR** (400 MHz, $CDCl_3$): 2.79 (2H, s), 3.84 (4H, s, CH_2-N-CH_2), 4.02 (3H, s, OCH_3), 6.72-7.95 (12H, m, Ar-H). **^{13}C NMR** (100 MHz, $CDCl_3$): 20.1, 58.5, 60.2, 67.4, 116.5, 119.6, 126.1, 126.9, 127.4, 131.8, 132.1, 134.1, 134.9, 145.1, 152.7, 155.1, 196.1. **ESI-MS** m/z 452.1 (M^++1).
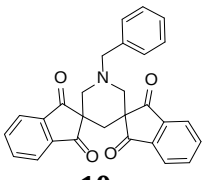 **10e**	*1'-benzyldispiro[indane-1,3-dione-2,3'-piperidine-5',2"-indane-1,3-dione]* Yellow solid, **M.p.** 261-262 °C. **Anal. Calcd**. ($C_{28}H_{21}NO_4$) C, 77.23; H, 4.86; N, 3.22. **Anal. Found** ($C_{28}H_{21}NO_4$) C, 77.28; H, 4.81; N, 3.17. **IR** (KBr, cm^{-1}): 2928 (C-H), 2857 (C-H), 1741 (C=O), 1702 (C=O). **^{1}H NMR** (400 MHz, $CDCl_3$): 2.52 (2H, s), 3.39 (4H, s, CH_2-N-CH_2), 3.68 (2H, s, Ph-CH_2), 7.13-7.93 (13H, m, Ar-H). **^{13}C NMR** (100 MHz, $CDCl_3$): 18.5,

	58.1, 65.7, 69.2, 125.5, 125.9, 127.2, 128.3, 131.2, 132.1, 141.3, 149.7, 196.7. **ESI-MS** m/z 436.2 (M^++1).
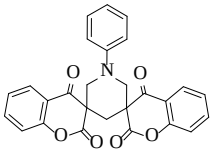 **10f**	*1'-phenyldispiro[chroman-2,4-dione-3,3'-piperidine-5',3"-chroman-2,4-dione]* White solid, **M.p.** 275-276 °C. **Anal. Calcd**. ($C_{27}H_{19}NO_6$) C, 71.52; H, 4.22; N, 3.09. **Anal. Found** ($C_{27}H_{19}NO_6$) C, 71.46; H, 4.27; N, 3.03. **IR** (KBr, cm^{-1}): 2941 (C-H), 2886 (C-H), 1748 (C=O), 1651 (C=O). **^{1}H NMR** (400 MHz, DMSO-d_6): 2.51 (2H, s), 3.51(4H, s, CH_2-N-CH_2), 7.31-8.16 (13H, m, Ar-H). **^{13}C NMR** (100 MHz, DMSO-d_6): 22.4, 59.1, 66.5, 116.8, 119.0, 121.4, 127.2, 128.2, 129.5, 133.5, 137.8, 147.3, 156.8, 176.2, 196.2. **ESI-MS** m/z 454.1 (M^++1).
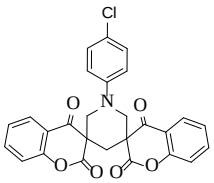 **10g**	*1'-(4-chlorophenyl)dispiro[chroman-2,4-dione-3,3'-piperidine-5',3"- chroman-2,4-dione]* White solid, **M.p.** 279-280 °C. **Anal**. **Calcd**. ($C_{27}H_{18}ClNO_6$) C, 66.47; H, 3.72; N, 2.87. **Anal**. **Found** ($C_{27}H_{18}ClNO_6$) C, 66.51; H, 3.68; N, 2.82. **IR** (KBr, cm^{-1}): 2940 (C-H), 2876 (C-H), 1745 (C=O), 1669 (C=O). **^{1}H NMR** (400 MHz, DMSO-d_6): 2.79 (2H, s), 3.64 (4H, s, CH_2-N-CH_2), 7.14-8.09 (12H, m, Ar-H).**^{13}C NMR** (100 MHz, DMSO-d_6): 21.2, 58.7, 66.1, 115.9, 119.4, 120.1, 127.4, 128.5, 129.5, 130.4, 133.1, 137.9, 151.2, 170.4, 197.2. **ESI-MS** m/z 488.1 (M^++1).
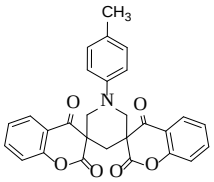 **10h**	*1'-(4-methylphenyl)dispiro[chroman-2,4-dione-3,3'-piperidine-5',3"- chroman-2,4-dione]* White solid, **M.p.** 280-281 °C. **Anal. Calcd**. ($C_{28}H_{21}NO_6$) C, 71.94; H, 4.53; N, 3.00. **Anal. Found** ($C_{28}H_{21}NO_6$) C, 71.99; H, 4.48; N, 2.97. **IR** (KBr, cm^{-1}): 2918 (C-H), 2852 (C-H), 1742 (C=O), 1702 (C=O). **^{1}H NMR** (400 MHz, DMSO-d_6): 2.55 (3H, s, CH_3), 2.75 (2H, s), 3.59 (4H, s, CH_2-N-CH_2), 7.23-8.12 (12H, m, Ar-H). **^{13}C NMR** (100 MHz, DMSO-d_6): 21.3, 26.5, 58.1, 66.2, 118.4, 121.3, 124.7, 125.1, 128.1, 130.5, 131.3, 134.5, 136.2, 149.2, 155.6, 171.2, 197.5. **ESI-MS** m/z 468.1 (M^++1).

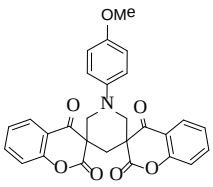 **10i**	*1'-(4-methoxyphenyl)dispiro[chroman-2,4-dione-3,3'-piperidine-5',3"-chroman-2,4-dione]* White solid, **M.p.** 286-287 °C. **Anal. Calcd**. ($C_{28}H_{21}NO_7$) C, 69.56; H, 4.38; N, 2.90. **Anal. Found** ($C_{28}H_{21}NO_7$) C, 69.51; H, 4.43; N, 2.95. **IR** (KBr, cm^{-1}): 2931 (C-H), 2868 (C-H), 1741 (C=O), 1683 (C=O). **^{1}H NMR** (400 MHz, DMSO-d_6): 2.62 (2H, s), 3.89 (4H, s, CH_2-N-CH_2), 4.15 (3H, s, OCH_3), 7.33-8.12 (12H, m, Ar-H). **^{13}C NMR** (100 MHz, DMSO-d_6): 22.5, 54.2, 58.8, 65.4, 117.1, 120.4, 121.2, 123.5, 124.1, 128.3, 129.0, 130.4, 137.2, 148.2, 154.7, 171.6, 196.4. **ESI-MS** m/z 484.1 (M^++1).
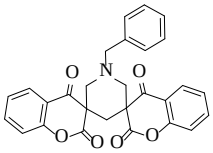 **10j**	*1'-benzyldispiro[chroman-2,4-dione-3,3'-piperidine-5',3"-chroman-2,4-dione]* White solid, **M.p.** 280-281 °C. **Anal. Calcd**. ($C_{28}H_{21}NO_6$) C, 71.94; H, 4.53; N, 3.00. **Anal. Found** ($C_{28}H_{21}NO_6$) C, 71.89; H, 4.48; N, 3.05. **IR** (KBr, cm^{-1}): 2927 (C-H), 2869 (C-H), 1745 (C=O), 1651 (C=O). **^{1}H NMR** (400 MHz, DMSO-d_6): 2.61 (2H, s), 3.73 (4H, s, CH_2-N-CH_2), 3.97 (2H, s, Ph-CH_2), 7.11-8.03 (13H, m, Ar-H). **^{13}C NMR** (100 MHz, DMSO-d_6): 21.5, 57.9, 64.3, 73.6, 118.5, 122.3, 123.1, 127.3, 128.1, 129.3, 131.5, 134.8, 135.3, 139.2, 144.6, 152.1, 172.1, 197.2. **ESI-MS** m/z 468.1 (M^++1).
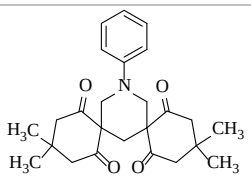 **10k**	**Melting point**: 192 °C **Melting point (literature)**[18-21]**:**191-193 °C
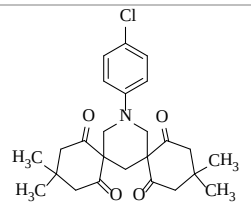 **10l**	**Melting point:** 199 °C **Melting point (literature)**[18-21]**:** 198-200 °C

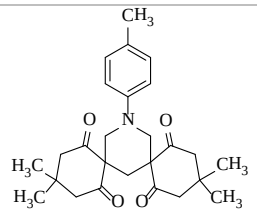 **10m**	**Melting point:** 201 °C **Melting point (literature)**[18-21]**:** 199-201 °C
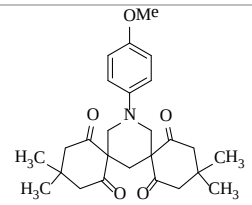 **10n**	**Melting point:** 187 °C **Melting point (literature)**[18-21]**:** 186-188 °C
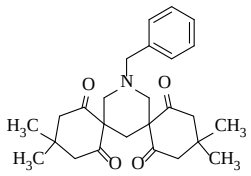 **10o**	*3,3,11,11-Tetramethyl-15-(benzyl)-15 azadispiro [5.1.5.3] hexadecane-1,5,9,13-tetrone* Light yellow crystals, **M.p.** 201-202 °C. **Anal. Calcd**. ($C_{26}H_{33}NO_4$) C, 73.73; H, 7.85; N, 3.31. **Anal**. **Found** ($C_{26}H_{33}NO_4$) C, 73.68; H, 7.79; N, 3.36. **IR** (KBr, cm^{-1}): 2953 (C-H), 2901 (C-H), 1724 (C=O), 1698 (C=O). **^{1}H NMR** (400 MHz, $CDCl_3$): 0.85 (6H, s), 0.94 (6H, s), 2.32 (2H,s), 2.67 (4H, d, *J*=13.6Hz), 2.76 (4H, d, *J*=13.6Hz), 3.52 (4H, s, CH_2-N-CH_2), 3.86 (2H, s, Ph-CH_2), 7.25-7.32 (5H, m, Ar-H). **^{13}C NMR** (100 MHz, $CDCl_3$): 27.2, 31.5, 34.0, 54.7, 67.3, 71.8, 119.7, 123.5, 128.9, 154.7, 198.0. **ESI-MS** m/z 424.1 (M^++1).

REFERENCES:

1. (a) H. B. Kagan, J. L. Namy, Tetrahedron 42 (1986) 6573; (b) G. A. Molander, Chem. Rev. 92 (1992) 29; (c) K. Mikami, M. Terada, H. Matsuzawa, Angew. Chem. Int. Ed. 41 (2002) 3554; (d) S. Kobayashi, Eur. J. Org. Chem. (1999) 15 (e) S. Kobayashi, Top. Organomet. Chem. 2 (1999) 63; (f) R. Anwander, Top. Organomet. Chem. 2 (1999) 1.
2. T. Imamoto, Best Synthetic Methods, Lanthanides in Organic Synthesis, Academic Press, London, (1994); (b) K. Mikami, M. Terada, H. Matsuzawa, Angew. Chem. Int. Ed. 41 (2002) 3554.
3. (a) P. G. Steel, J. Chem. Soc., Perkin Trans. 1 (2001) 2727; (b) S. Kobayashi, Synlett (1994) 689.
4. (a) S. Kobayashi, M. Sugiura, H. Kitagawa, W. W. L. Lam, Chem. Rev. 102 (2002) 2227; (b) S. Kobayashi, Eur. J. Org. Chem. (1999) 15; (c) N. Mine, Y. Fujiwara, H. Taniguchi, Chem. Lett. (1986) 357.
5. (a) V. K. Thakur, M. K. Thakur, ACS Sustainable Chem. Eng. 2 (2014) 2637; (b) L. Gopalakrishnan, L. N. Ramana, S. Sethuraman, U. M. Krishnan, Carbohydr. Polym. 111 (2014) 215.
6. E. Guibal, Prog. Polym. Sci. 30 (2005) 71.
7. (a) J. H. Zhou, Z. P. Dong, H. L. Yang, Z. Q. Shi, X. C. Zhou, R. Li, Appl. Surf. Sci. 279 (2013) 360; (b) Z. D. Wang, L. C. Zheng, C. C. Li, D. Zhang, Y. N. Xiao, G. H. Guan, W.X. Zhu, Carbohydr. Polym. 94 (2013) 505; (c) C. S. Catano, M. Caiado, J. Farinha, I. M. Fonseca, A. M. Ramos, J. Vital, J. E. Castan-heiro, Chem. Eng. J. 230 (2013) 567; (d) A. A. Dabbawala, N. Sudheesh, H. C. Bajaj, Dalton Trans. 41 (2012) 2910; (e) M. N. V. Ravi Kumar, React. Funct. Polym. 46 (2000) 1.
8. (a) D. M. Whitfield, S. Stojkovski, B. Sarkar, Coord. Chem. Rev. 122 (1993) 171; (b) A. Patwardhan, J. A. Cowan, Dalton Trans. 40 (2011) 1795; (c) A. Corma, P. Concepcin, I. Domnguez, V. Fornes, M. J. Sabater, J. Catal. 251 (2007) 39; (d) J. X. Jian, Q. Liu, Z. J. Li, F. Wang, X. B. Li, C. B. Li, B. Liu, Q. Y. Meng, B. Chen, K. Feng, C. H. Tung, L. Z. Wu, Nat. Commun. 4 (2013) 2695; (e) S. E. S. Leonhardt, A. Stolle, B. Ondruschka, G. Cravotto, C. De Leo, K. D. Jandt, T. F. Keller, Appl. Catal. A: Gen. 379 (2010) 30.

9. (a) M. N. V. Ravi Kumar, R. A. A. Muzzarelli, C. Muzzarelli, H. Sashiwa, A. J. Domb, Chem. Rev. 104 (2004) 6017; (b) D. J. Macquarrie, J. J. E. Hardy, Ind. Eng. Chem. Res. 44 (2005) 8499.
10. (a) C. Viegas Jr., V. S. Da Bolzani, M. Furlan, E. J. Barreiro, M. C. M. Young, D. Tomazela, M. N. Eberlin, J. Nat. Prod. 67 (2004) 908; (b) P. M. Dewick, Medicinal Natural Products: A Biosynthetic Approach, 2nd ed.; Wiley: New York, (2002) p 307.
11. H. Bienayme, L. Chene, S. Grisoni, A. Grondin, B. Kaloun, S. Poigny, H. Rahali, E. Tam, Bioorg. Med. Chem. Lett. 16 (2006) 4830.
12. Ch. A. Maier, B. Wunsch, J. Med. Chem. 45 **(**2002) 438.
13. L. Feliu, J. Martinez, M. Amblard, QSAR Comb. Sci. 23 (2004) 56.
14. V. V. Kouznetsov, B. P. Diaz, C. M. M. Sanabria, L. Y. M. Vargas, J. C. Poveda, E. E. Stashenko, A. Bahsas, J. Amaro-Luis, Lett. Org. Chem. 2 (2005) 29.
15. V. V. Kouznetsov, Khim.-Farm. Zh. 25 (1991) 61; (c) P. S. Watson, B. Jiang, B. Scott, Org. Lett. 2 (2000) 3679.
16. W. Quaglia, M. Gianella, A. Piergentili, M. Pigini, L. Brasili, R. D. Torso, L. Rossetti, S. Spompiato, C. Melchiorre, J. Med. Chem. 41 (1998) 1557.
17. (a) J. W. Daly, In Progress in the Chemistry of Organic Natural Products; W. Herz, H. Griesebach, G. W. Kirby, Eds.; Springer: Berlin, (1982) p 205; (b) Daly, J. W. J. Toxicol. Toxin Rev. 1 (1982) 33; (c) J. W. Daly, M. Garraffo, T. F. Spande, M. W. Decker, J. P. Sullivan, M. Williams, Nat. Prod. Rep. 17 (2000) 131; (d) J. W. Daly, C. W. Myers, N. Whittaker, Toxicon 25 (1987) 1023.
18. N. G. Kozlov, A. P. Kadutskii, Tetrahedron Lett. 49 (2008) 4560.
19. A. B. Atar, Y. T. Jeong, Tetrahedron Lett. 54 (2013) 1302.
20. F. Janati, M. M. Heravi, A. Mirshokraie, J. Chem. (2013) doi:10.1155/2013/214617.
21. C. Mukhopadhyay, S. Rana, R. J. Butcher, Tetrahedron Lett. 52 (2011) 4153.
22. V. Polshettiwar, R. S. Varma, Green Chem. 12 (2010) 743.
23. G. Bartoli, E. Marcantoni, M. Marcolini, L. Sambri, Chem. Rev. 110 (2010) 6104.
24. G. Sabitha, J. S. Yadav, *In Encyclopedia of Reagents for Organic Synthesis*; L. A. Paquette, Ed.; Wiley-VCH: Weinheim, (2006).

25. N. Sudheesh, S. K. Sharma, R. S. Shukla, J. Mol. Catal A: Chem. 321 (2010) 77.
26. A. Primo, F. Quignard, Chem. Commun. 46 (2010) 5593.
27. N. V. Kramareva, A. Y. Stakheev, O. P. Tkachenko, K. V. Klementiev, W. Grunert, E. D. Finashina, L. M. Kustov, J. Mol. Catal. A: Chem. 209 (2004) 97.
28. A. J. Varma, S. V. Deshpande, J. F. Kennedy, Carbohydr. Polym. 55 (2004) 77.

SECTION B

DYSPROSIUM(III) ON CHITOSAN: A RECYCLABLE HETEROGENEOUS CATALYST FOR THE SYNTHESIS OF HEXAHYDROPYRIMIDINES IN WATER*

In the field of medicinal chemistry, hexahydropyrimidine derivatives are one of the most important class of compounds with diverse range of biological activities.[1] These scaffolds exhibit interesting biological profiles such as antibacterial,[2] antiviral, analgesic and anti-inflammatory activities.[3] Anti-inflammatory and analgesic activities of some hexahydropyrimidine derivatives were found to be comparable with diclofenac sodium gel and aspirin.[4] A number of alkaloids such as verbamethine and verbametrine[5] also contain this skeleton. Hexetidine, which shows promising anesthetic, deodorant and antiplaque effects,[6] also contains this structural unit. Several hexahydropyrimidine derivatives have also shown promising anti-HIV-1 activity.[7] Some hexahydropyrimidine derivatives were found to be important transport molecules for tumor inhibition and antineoplastic activity.[8] *N*-Substituted hexahydropyrimidines serve as key synthetic intermediates for spermidine-nitroimidazole drugs which are used for the treatment of A549 lung carcinoma.[9] Recently, appropriately substituted hexahydropyrimidines were found to be potent hepatitis C virus inhibitors.[10] Therefore, in view of the very important biological profiles of these derivatives it is highly desirable to develop a method which is efficient, environmentally benign and tolerates a range of substrates.

4.7. REVIEW OF LITERATURE

Some recent examples of the synthesis of hexahydropyrimidines and their spiro analogues.

4.7.1. $FeCl_3$ catalysed synthesis of hexahydropyrimidines and spiro derivatives.[11]

C. Mukhopadhyay *et al.* reported an $FeCl_3$ catalysed synthesis of 1,3-diaryl-hexahydropyrimidines via reaction of 1,3-dicarbonyl compounds, amines and formaldehyde in dichloromethane at room temperature.

* Nayeem Ahmed, Saima Tarannum, Zeba N. Siddiqui, ***RSC Advances***, 5 (2015) 50691.

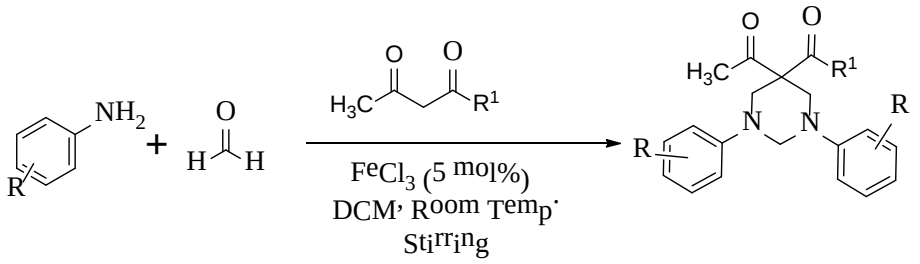

R= H, 4-CH_3, 4-OCH_3, 3-CH_3, 2-CH_3 R^1= OEt, OMe, Ph, *O*-Allyl

4.7.2. *(S)*-Proline catalysed synthesis of 1,3-diaryl-5-spirohexahydropyrimidines.[12]

H. L. Wei *et al.* reported an efficient synthesis of 1,3-diaryl-5-spirohexahydro pyrimidines via one-pot condensation of anilines, formaldehyde, and cyclohexanones catalysed by *(S)*-proline in DMSO.

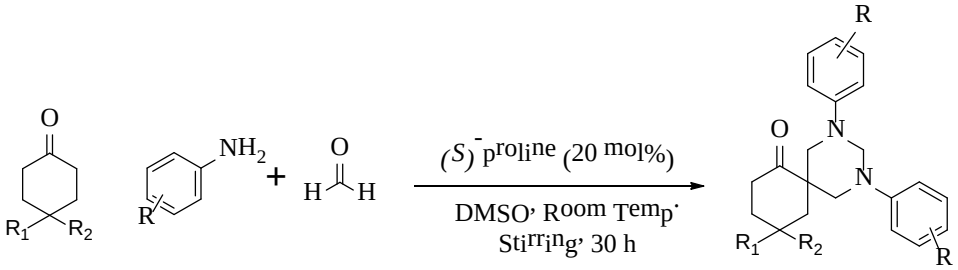

R= H, 4-Br, 4-CH_3, 4-OCH_3, 3-Cl R_1= H, CH_3 R_1,R_2 =  R_2= H

4.7.3. Synthesis of spiropyrimidine derivatives catalysed by magnetically recoverable $CuFe_2O_4$ nanoparticles.[13]

A. Dandia *et al.* reported an efficient protocol for the synthesis of medicinally important fluorinated spiropyrimidine derivatives using a magnetically separable and reusable heterogeneous copper ferrite nano-catalyst under mild reaction conditions

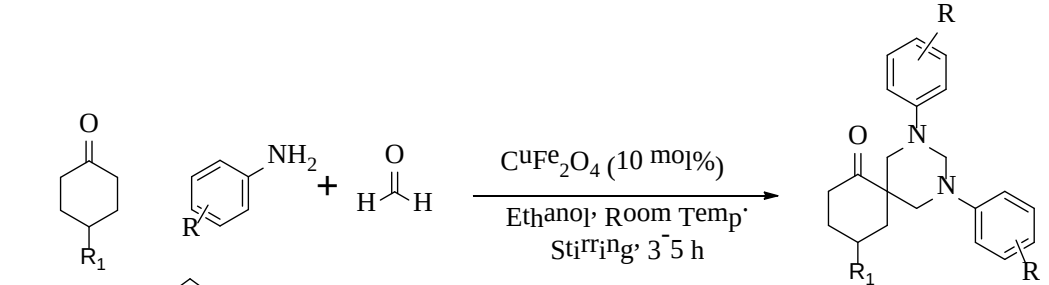

R_1= H, CH_3,  R= 4-F, 4-CF_3, 4-Cl, 4-CH_3

4.7.4. Indium triflate catalysed one-pot synthesis of spiro-hexahydropyrimidines.[14]

A. Dandia *et al.* reported an efficient synthesis of spiro-hexahydropyrimidine derivatives via a three-component, one-pot cyclocondensation reaction of aromatic

amines, formaldehyde, and cyclic ketones using $In(OTf)_3$ as Lewis acid catalyst under mild conditions.

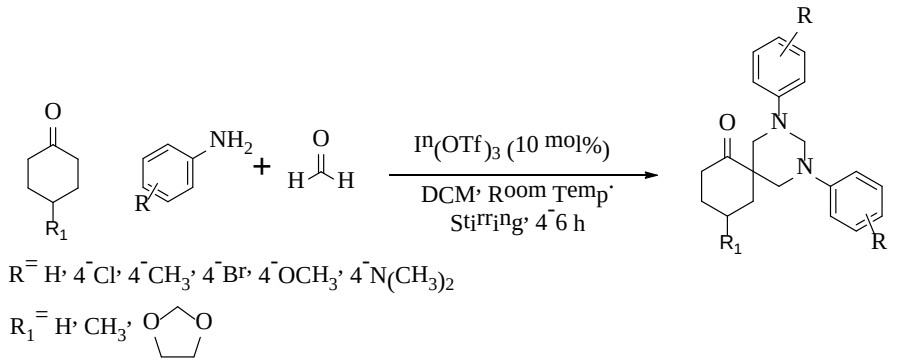

4.7.5. Synthesis of 1,3-diaryl-5-spirohexahydropyrimidines catalysed by supported preyssler nanoparticles.[15]

M. M. Heravi *et al.* reported the preparation of 1,3-diaryl-5-spirohexahydro pyrimidines via a one-pot condensation of anilines, formaldehyde, and cyclohexanone using silica-supported Preyssler nanoparticles $(H_{14}[NaP_5W_{30}O_{110}])/SiO_2$ as a recyclable catalyst.

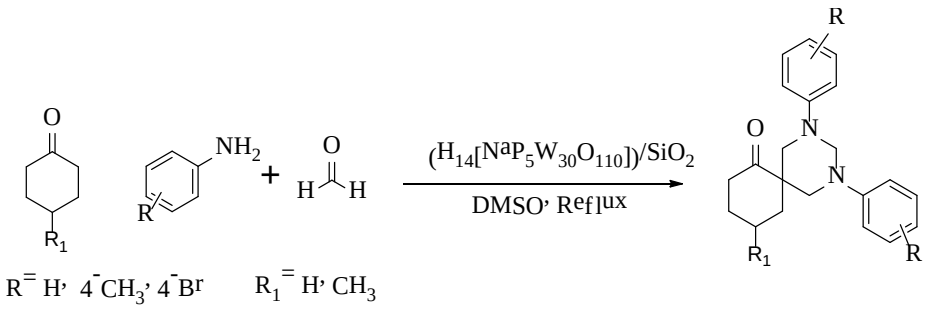

4.8. PRESENT WORK

Based on the principles of green chemistry, the development of practical methods, reaction conditions, and the use of appropriate materials is a very challenging task. During last few decades the use of lanthanides as catalysts in organic synthesis has amplified very rapidly due to their unique physical and chemical properties.[16] Dysprosium, which exhibits similar Lewis acidity, oxophilicity, ease of handling and stability towards air and water as compared to other lanthanides, has not received much attention in the field of synthetic organic chemistry. Analogous to other lanthanides, +III state of dysprosium is the most stable oxidation state, due to which it behaves as an extremely mild and efficient Lewis acid catalyst having the ability to promote various types of carbon-carbon bond forming reactions like Mannich type, Diels-Alder, Povarov, Friedel-Crafts alkylation, electrocyclizations and cycloaddition reactions.[17] It is also used in a variety of transformations with unprotected amines

because of its unique ability to retain its catalytic activity in presence of Lewis basic nitrogen groups.[17]

Organic synthesis in water has received considerable attention due to the environmental impact of using volatile organic solvents (VOCs). Recent research has shown that water as a solvent produces beneficial effects which speed up the reaction and the separation process also becomes easier because of the insolubility of organic compounds in water.[18]

In this section, Dy(III) has been supported on chitosan and used as a catalyst for the eco-friendly synthesis of hexahydropyrimidines and their spiro analogues in water.

4.9. RESULTS AND DISCUSSION

The synthesis of the catalyst is illustrated in **Scheme-12**. To a weighed amount of pre-suspended chitosan in water, was added $Dy(NO_3)_3.6H_2O$ with continuous stirring. The catalyst was then obtained by simple filtration of the mixture after overnight stirring.

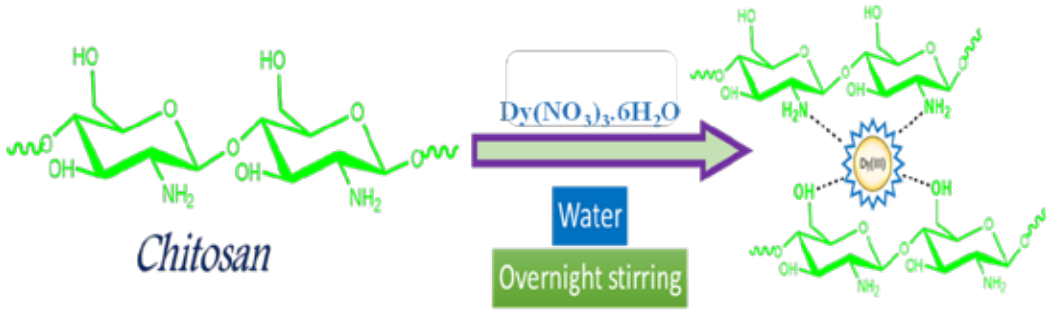

Scheme 12: Schematic representation for the synthesis of Dy(III)/chitosan catalyst.

4.9.1. Characterization of the catalyst

4.9.1a. FT-IR spectral analysis

FT-IR spectrum **(Figure 41a)** of pure chitosan showed a broad OH and NH stretching band at 3419 cm^{-1}. Whereas N–H bending band was present at 1588 cm^{-1}. The absorption bands present at 1076 and 1379 cm^{-1} correspond to the stretching vibrations of C−O and C−N groups, respectively. The band for C−H stretching mode of methylene group was present at 2920 cm^{-1}.[19] In the FT-IR spectrum of Dy(III) supported chitosan **(Figure 41b)**, a different fingerprint region (600-500 cm^{-1}), as compared to that of pure chitosan, was obtained due to the formation of Dy−N and Dy−O coordinate bonds.[20] The decrease in the intensity of N–H bending vibration band of NH_2 group obtained at 1561 cm^{-1} after modification, indicated the coordination of Dy(III) by NH_2 groups. Moreover, increase in the sharpness of the

OH stretching band at 3417 cm^{-1} indicated the coordination of Dy(III) by OH groups of chitosan.[21]

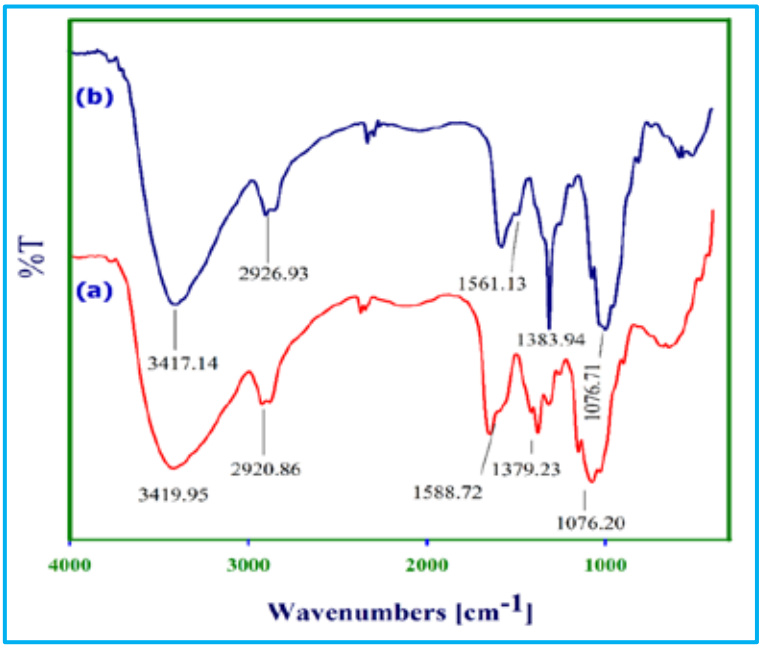

Fig. 41. FT-IR spectra (a) of chitosan and (b) of Dy(III)/chitosan catalyst

4.9.1b. XRD and EDX analyses

The XRD analysis revealed that the diffraction patterns of the support **(Figure 42a)** and the catalyst **(Figure 42b)** were similar. Absence of the peaks pertaining to Dy(III) may be because of its low content and small size of the Dy(III) nanoparticles. However, the presence of Dy in the catalyst was established by EDX analysis which showed peaks for Dy in addition to C, N and O elements **(Figure 43)**.

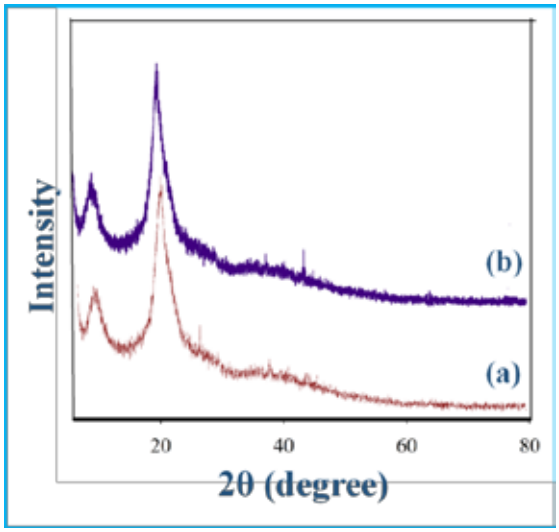

Fig. 42. XRD spectra (a) of chitosan and (b) of Dy(III)/chitosan catalyst.

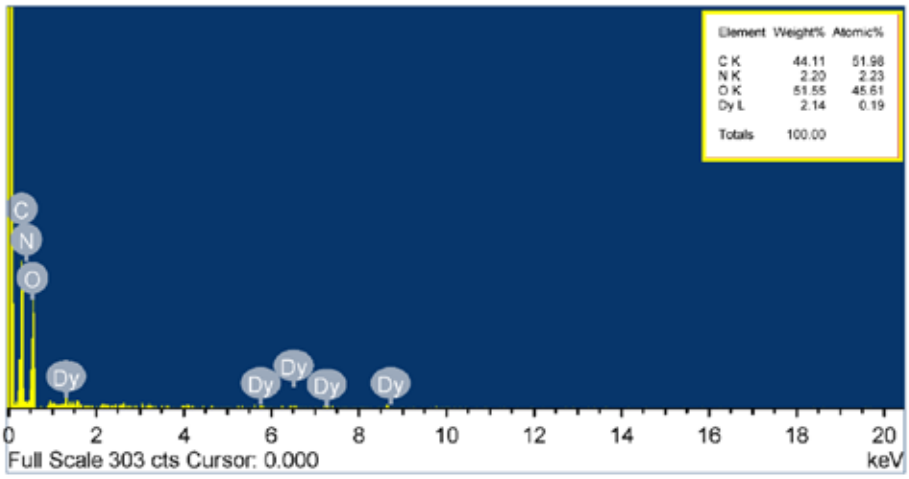

Fig. 43. EDX spectra of Dy(III)/chitosan catalyst.

4.9.1c. ICP-AES, TEM and Elemental Mapping analyses

ICP-AES analysis was performed in order to determine the actual concentration of Dy in the catalyst. The analysis showed the weight percentage of Dysprosium to be 1.38%. The TEM images of the catalyst **(Figure 44)** displayed the spherical shape of the Dy(III) nanoparticles with average diameter in the range of 5-12 nm. The elemental mapping analysis showed that the Dy(III) nanoparticles were uniformly distributed on the surface of chitosan **(Figure 45)**.

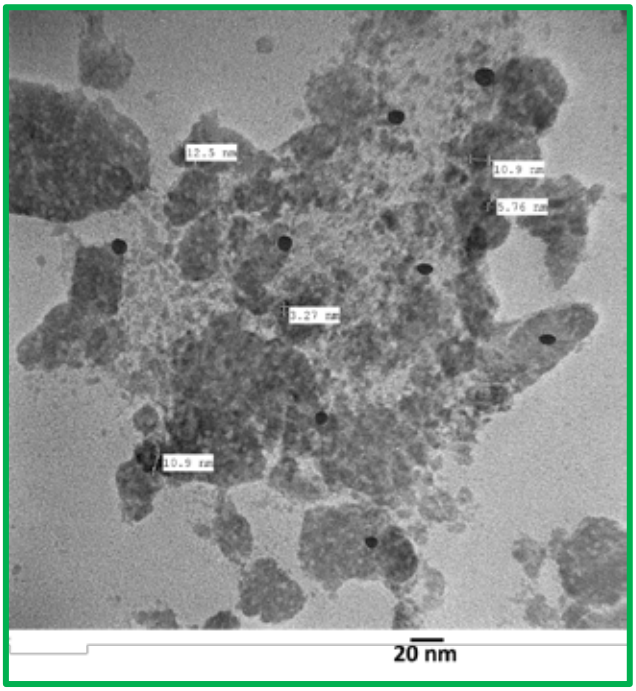

Fig. 44. TEM image of Dy(III)/chitosan catalyst

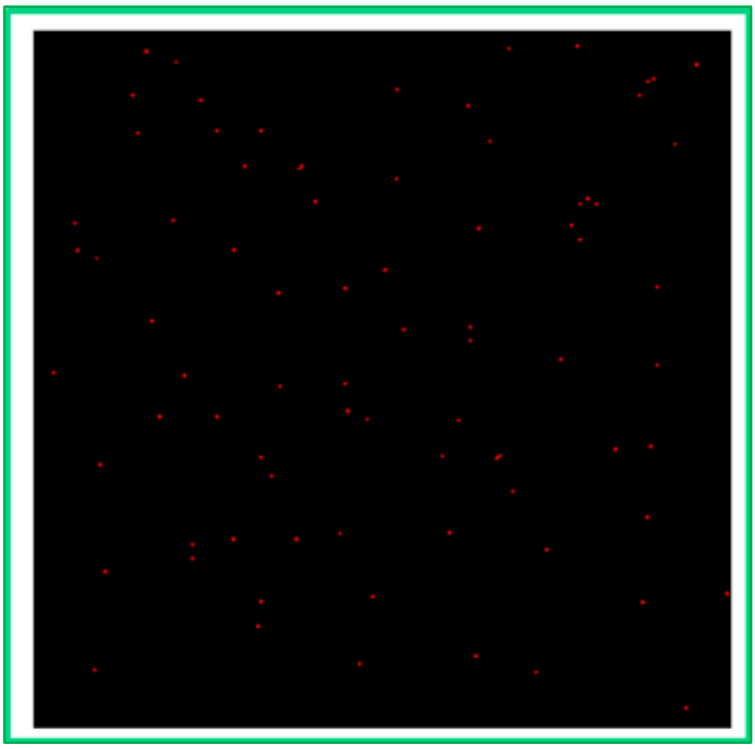

Fig. 45. Elemental mapping analysis of the catalyst showing uniformly distributed Dy

4.9.1d. TG analysis

Thermal behaviour and stability of the catalyst at elevated temperatures was evaluated by TG analysis. In the TG curve of chitosan, a two stage weight loss of 12.7% at 60 °C and 52.2% at 280 °C **(Figure 46a)** was observed. The first weight loss attributed to removal of adsorbed water molecules from polymer matrix and the second weight loss corresponded to the decomposition of the polysaccharide chain. The TG curve of Dy(III)/chitosan catalyst showed a decrease in thermal stability (weight loss of 52.4 % at 260 °C) **(Figure 46b)** with respect to chitosan, which is in agreement with the reported trend. It is reported that chemical modifications as well as metal complexations generally lead to decrease in the thermal stability of chitosan.[22] This observation further supports the formation of Dy(III)/chitosan catalyst.

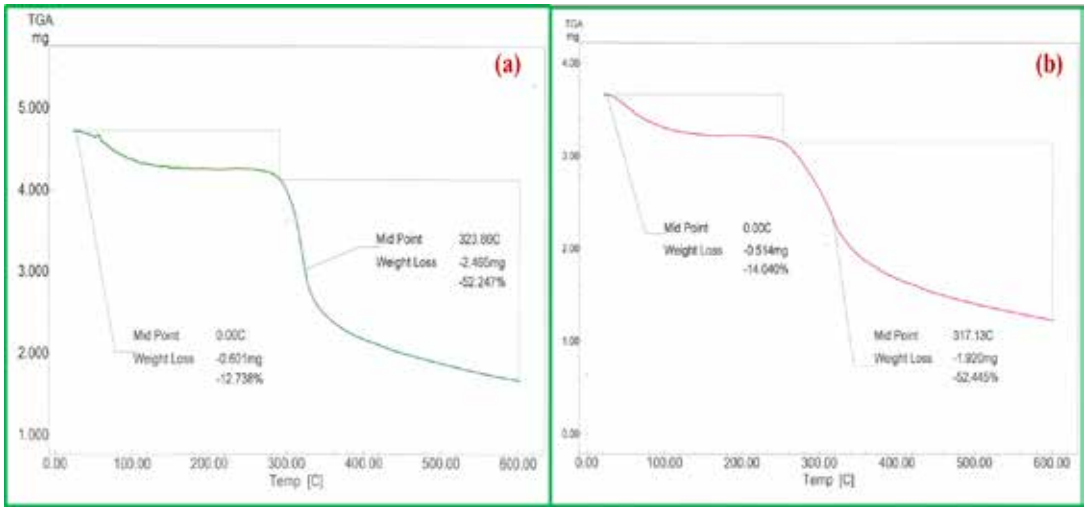

Fig. 46. TG analysis (a) of pure chitosan and (b) of Dy(III)/chitosan catalyst.

4.9.2. Optimization of reaction conditions

4.9.2a. Effect of different catalysts and solvents:

In order to find the optimized conditions for the synthesis of hexahydropyrimidines, various experiments were carried out using aniline **(9a)**, formaldehyde and ethylcyano acetate **(7a)** as model substrates. When the reaction was performed without any catalyst **(Table 20, entry 1)**, no product formation was observed. Using chitosan as a catalyst could not show satisfactory results **(Table 20, entry 7)**. We then used various Lewis acids such as $Dy(NO_3)_3.6H_2O$, $CuCl_2$, $Fe(NO_3)_3$, $Zn(OAc)_2$ and $CeCl_3.7H_2O$ as catalysts in water at room temperature **(Table 20)** and found $Dy(NO_3)_3.6H_2O$ to be most efficient for this reaction. As $Dy(NO_3)_3.6H_2O$ could not be recovered and recycled, we explored the use of chitosan supported Dy(III) as a catalyst and the results obtained were very satisfactory as the product in excellent yield (91%) was obtained in short time period **(Table 20, entry 8)**. After obtaining the right catalyst for this transformation, we then focused our attention towards finding the right solvent for this transformation.

Taking Dy(III)/chitosan as a catalyst for this reaction, the model reaction was conducted in H_2O, as well as other organic solvents like EtOH, MeOH, isopropanol, CH_3CN and ethylene glycol **(Table 20, entries 9-13)**. In comparison to H_2O, other solvents gave low to moderate yields of the product and took long time period (5-6.5 h) for completion of the reaction. H_2O showed significant improvement over other solvents in terms of yield and reaction time **(Table 20, entry 8)**. This rate enhancement of the reaction can be attributed to the unique properties of water like

hydrogen bonding to stabilize the intermediate transition states and hydrophobic effects to decrease the hydrocarbon–water interfacial area.[18]

Table 20: Effect of different reaction media on model reaction.

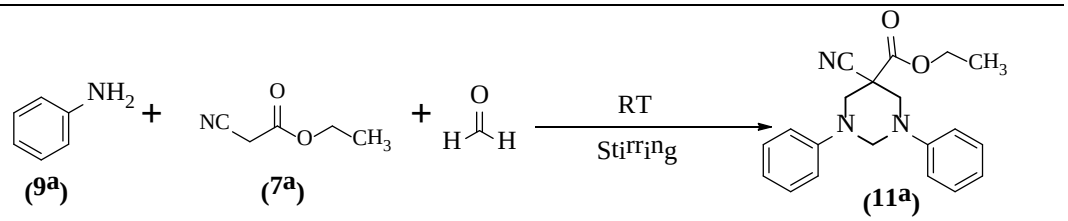

(**9a**) (**7a**) (**11a**)

Entry	Catalyst	Solvent	Time	Yield (%)
1	Nil	H_2O (5mL)	12 h	No reaction
2	$CuCl_2$ (10 mol%)	H_2O (5mL)	3.1 h	58
3	$Fe(NO_3)_3$ (10 mol%)	H_2O (5mL)	2.8 h	62
4	$Zn(OAc)_2$ (10 mol%)	H_2O (5mL)	2.5 h	60
5	$CeCl_3$ (10 mol%)	H_2O (5mL)	2.1 h	69
6	$Dy(NO_3)_3.6H_2O$ (10 mol%)	H_2O (5mL)	1.6 h	78
7	Chitosan (100 mg)	H_2O (5mL)	9.5 h	23
8	Dy(III)/chitosan (100 mg)	H_2O (5mL)	45 min	91
9	Dy(III)/chitosan (100 mg)	EtOH (5mL)	6 h	61
10	Dy(III)/chitosan (100 mg)	MeOH (5mL)	6.1 h	64
11	Dy(III)/chitosan (100 mg)	Isopropanol (5mL)	6.5	62
12	Dy(III)/chitosan (100 mg)	CH_3CN (5mL)	5 h	57
13	Dy(III)/chitosan (100 mg)	Ethylene glycol (5mL)	5.4 h	39

4.9.2b. Effect of catalyst loading

In order to find the effect of the catalyst loading, the model reaction was carried out by varying the amount of the catalyst **(Table 21)**. It was observed that, with the increase in the catalyst amount from 50-100 mg, the formation of hexahydropyrimidine derivative increased linearly. Further increasing the amount of catalyst to 125 mg did not produce any profound effect on the reaction. Therefore, 100 mg of Dy(III)/chitosan was found to be the optimum amount of the catalyst for the synthesis of hexahydropyrimidines.

Table 21: Effect of catalyst loading

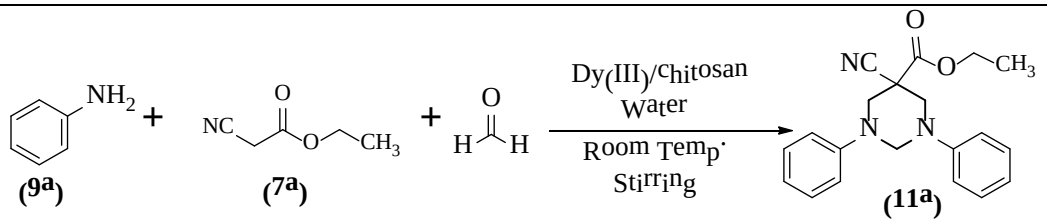

Entry	Catalyst loading (mg)	Time (min)	Yield (%)
1	50	125	69
2	75	65	76
3	100	45	91
4	125	45	91

4.9.3. Catalytic reaction

After optimizing the reaction conditions, the substrate scope and generality of Dy(III)/chitosan catalysed synthesis of hexahydropyrimidine derivatives **(11a-l)** using different amines **(9a-d ,9f)**, formaldehyde and active methylene compounds **(4b,4c,7a)** in water was examined **(Scheme-13)**. It was observed that the designed reaction tolerated both acyclic and cyclic active methylene compounds very efficiently as well as amines with both activating and deactivating groups **(Table 22)**.

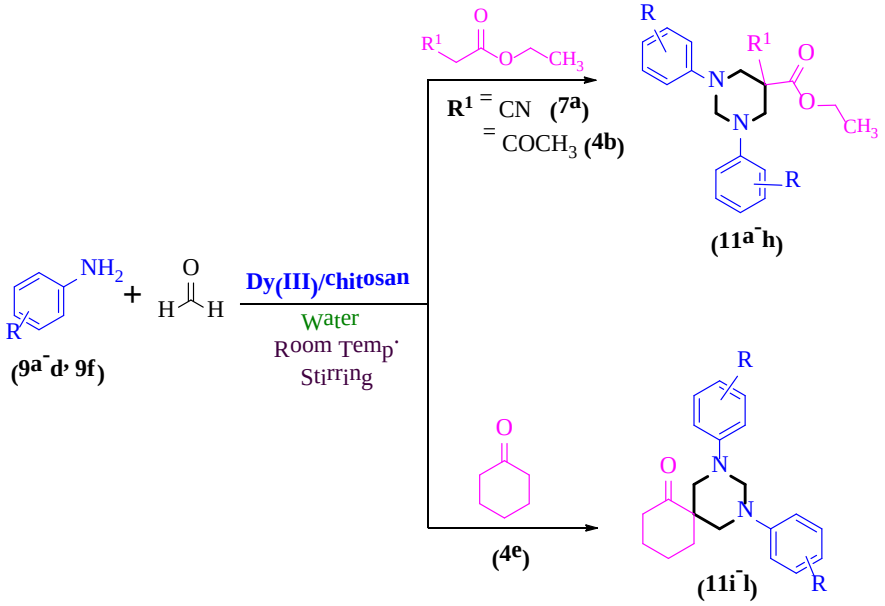

Scheme 13: General scheme for the synthesis of hexahydropyrimidine derivatives

The structures of the final products were elucidated by using spectral (IR, ^{1}H, ^{13}C NMR and ESI-MS) and elemental analysis data. The I.R. spectrum **(Figure 47)** of **11a** showed CN stretching peak at 2251 cm^{-1}. The absorption band at 1738 cm^{-1} was assigned to carbonyl group of ethyl ester. In the ^{1}H-NMR spectrum **(Figure 48)**, four

hydrogens of 2xN–CH_2 moieties exhibited two distinctive doublets at δ 3.63 and δ 3.77, respectively. The two hydrogen atoms of N–CH_2–N moiety exhibited distinctive doublets at δ 4.24 and δ 4.74, respectively. The aromatic protons appeared as multiplet in the range δ 6.91-7.10. ^{13}C-NMR spectrum **(Figure 49)** showed a distinctive peak at δ 164.39 ppm for carbonyl group of ethyl ester. All other peaks were obtained at respective places and are given in the experimental section. Further, structure **11a** was confirmed by ESI-Mass spectrum **(Figure 50)** which showed the molecular ion peak as base peak at m/z 336.1 (M^++1).

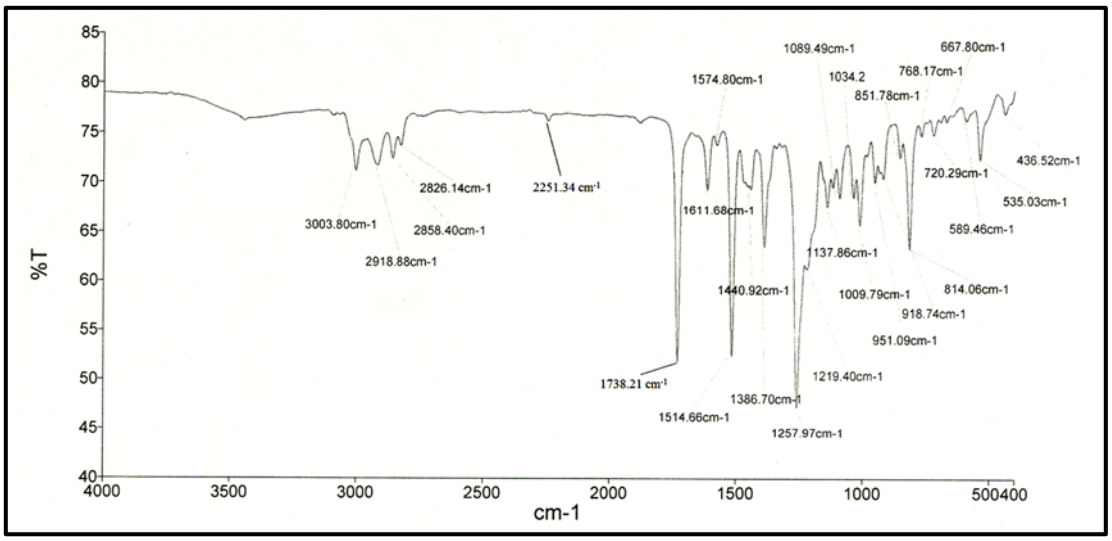

Fig. 47. FT-IR spectrum of **11a**

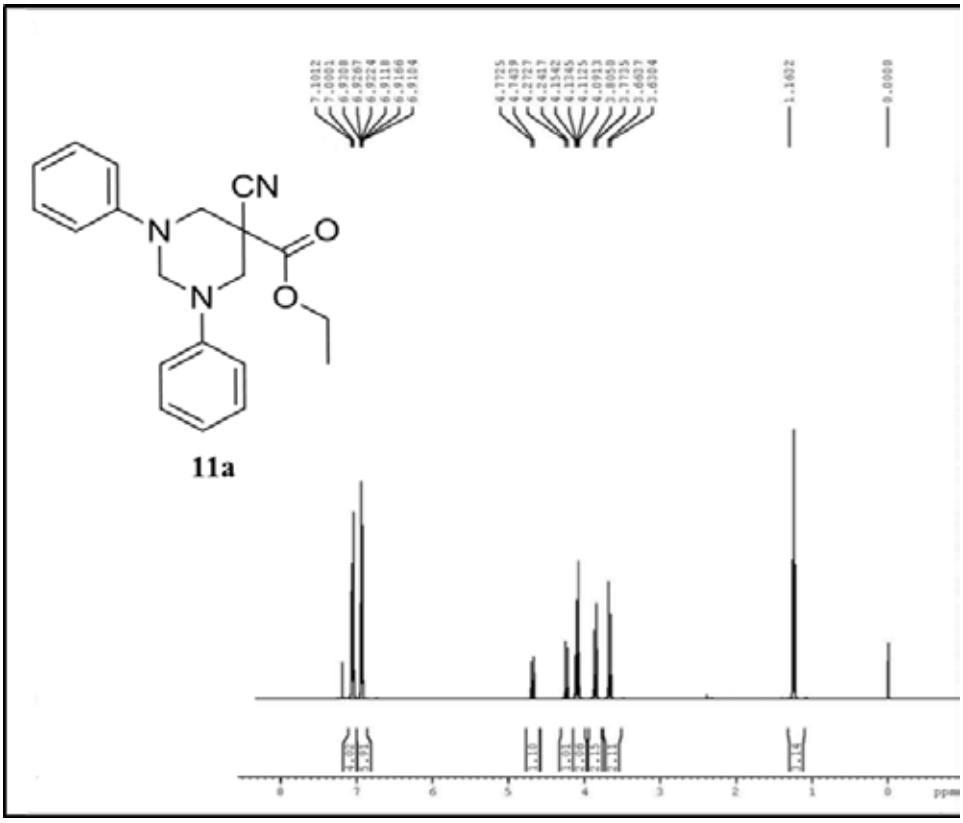

Fig. 48. ^{1}H-NMR spectrum of **11a**

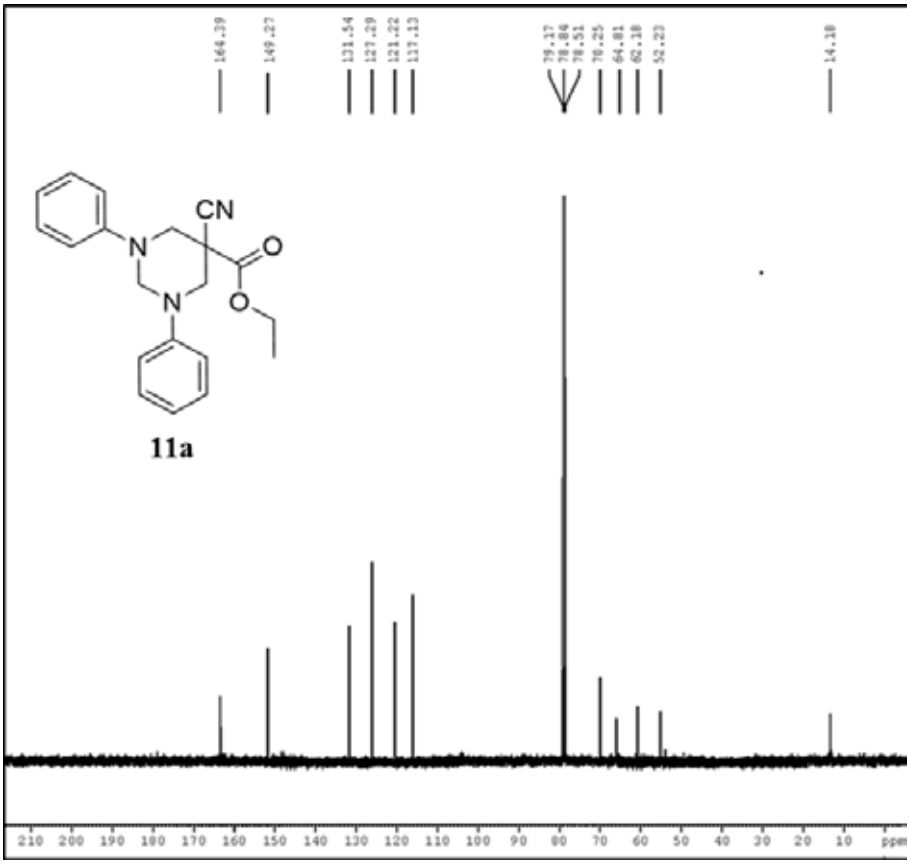

Fig. 49. ^{13}C-NMR spectrum of **11a**

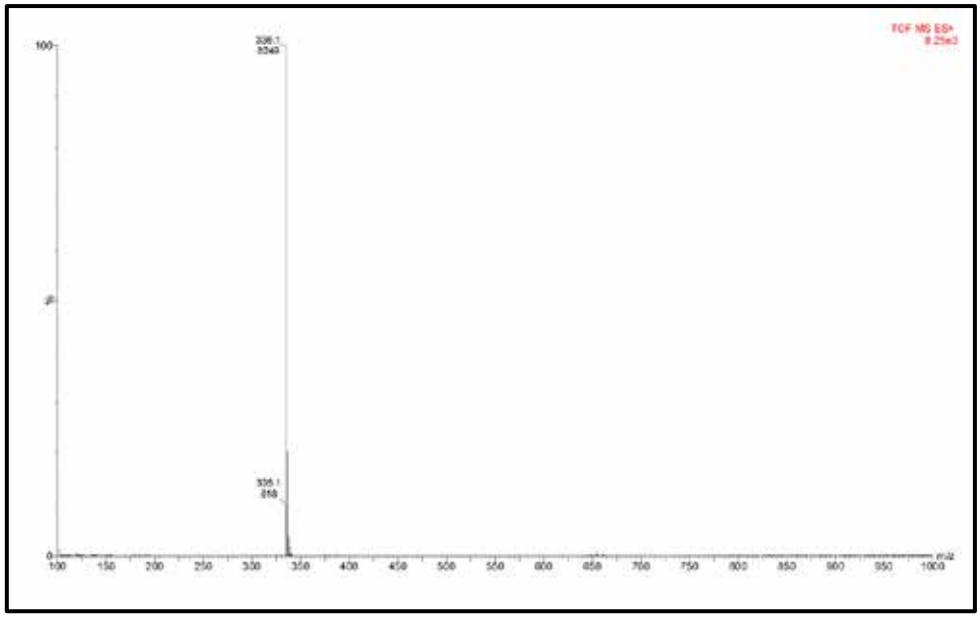

Fig. 50. ESI-Mass spectrum of **11a**

It is pertinent to mention that no product formation was observed when aliphatic amines (ethyl amine) or active methylene compounds like (Meldrum's acid, 4-hydroxycoumarin, 1,3-dimethylbarbituric acid) were used as substrates. In order to further show the superiority of our protocol, a comparison with reported methods revealed our catalytic system to be more efficient in terms of time period (40-58 min) and product yield (85-94%) **(Table 23)**.

Table 22: Synthesis of hexahydropyrimidines and spiro analogues.

Entry	Amines	Active methylenes	Product	Time (min)	Yield (%)
1	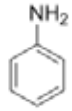 **9a**	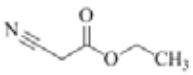 **7a**	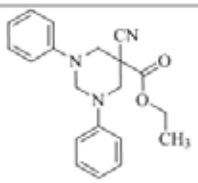 **11a**	45	91
2	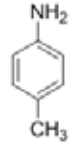 **9c**	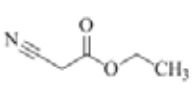 **7a**	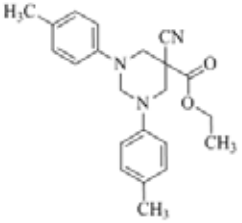 **11b**	40	92

3	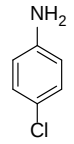 **9b**	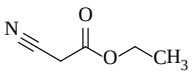 **7a**	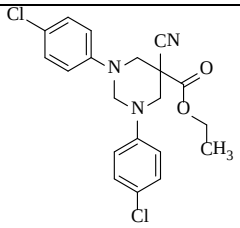 **11c**	45	90
4	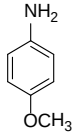 **9d**	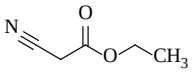 **7a**	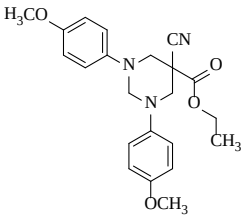 **11d**	43	93
5	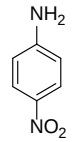 **9f**	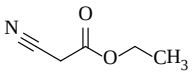 **7a**	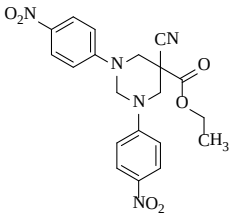 **11e**	48	89
6	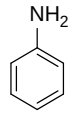 **9a**	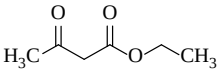 **4b**	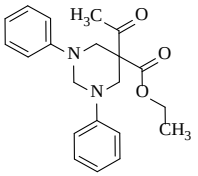 **11f**	58	93
7	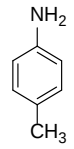 **9c**	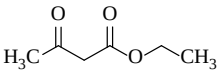 **4b**	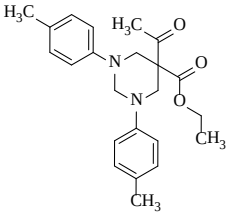 **11g**	55	94
8	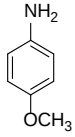 **9d**	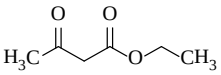 **4b**	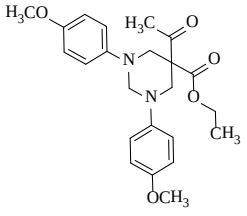 **11h**	54	93
9	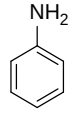 **9a**	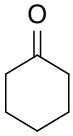 **4e**	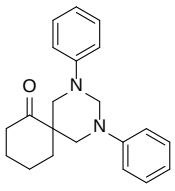 **11i**	50	87

10	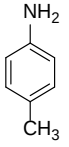 **9c**	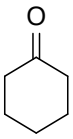 **4e**	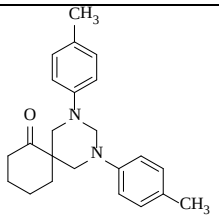 **11j**	45	89
11	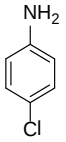 **9b**	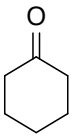 **4e**	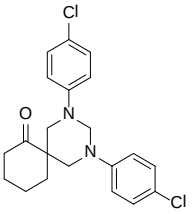 **11k**	51	87
12	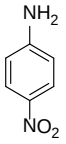 **9f**	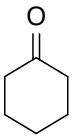 **4e**	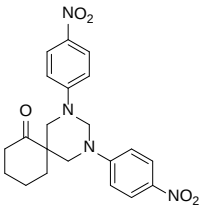 **11l**	53	85

Table 23: Comparison of efficiency of Dy(III)/chitosan catalyst with reported procedures.

Entry	Catalyst	Condition	Solvent	Yield (%)	Time	Ref.
1	Dy(III)/chitosan	RT stirring	Water	91	45 min	Present work.
2	$In(OTf)_3$	RT stirring	DCM	78	4h	14
3	$CuFe_2O_4$	RT stirring	Ethanol	74	4h	13
4	*S*-Proline	RT stirring	DMSO	73	30h	12
5	$(H_{14}[NaP_5W_{30}O_{110}])/SiO_2$	Reflux	DMSO	60	30h	15

4.9.4. Reaction mechanism:

The mechanism of the reaction is outlined in **scheme-14** and was proposed on the basis of reported literature.[11-14] In the first step, activated active methylene compound **(7a)** and imine **Q** undergo Michael addition to form **R**. In the next step, the intermediate **R** is activated by the catalyst which then undergoes Michael addition with second molecule of imine **Q,** to form propane-1,3-diamine intermediate **S.** The final product **(11a)** is obtained via condensation of intermediate **S** with formaldehyde and the catalyst is freed for subsequent recycles.

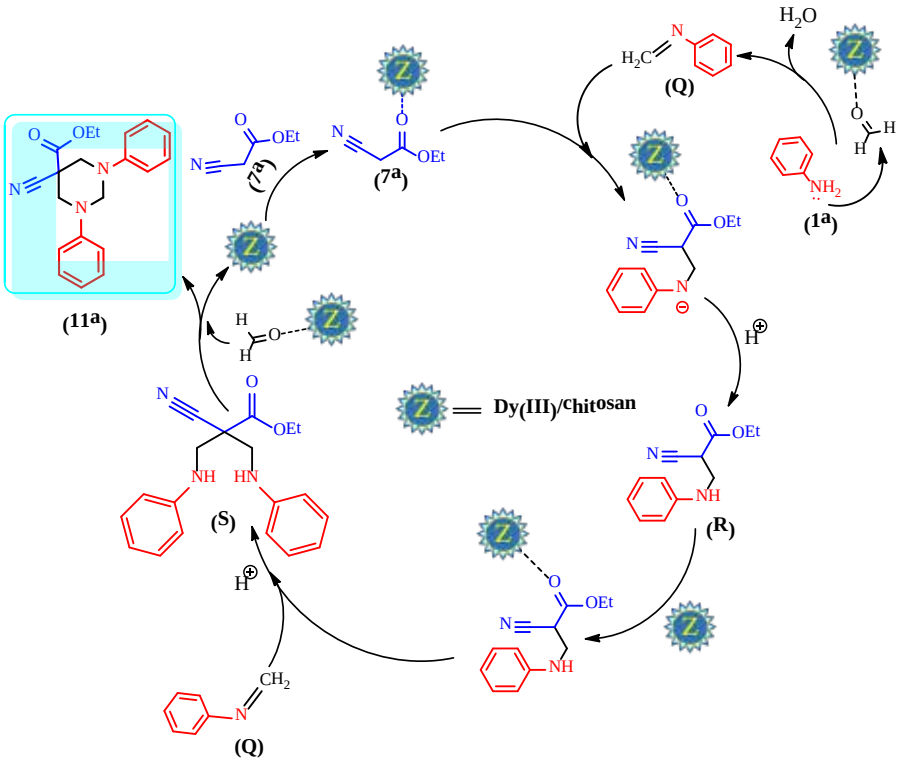

Scheme 14: Plausible reaction mechanism for the formation of hexahydropyrimidine derivative **11a**.

4.9.5. Leaching study of Dy(III)/chitosan catalyst:

The metal leaching of the catalyst before and after six catalytic cycles was evaluated by ICP-AES analyses in order to understand the heterogeneous nature of the catalyst. The analysis revealed that the metal concentration before (1.38Wt.% Dy) and after recycling experiments (1.36Wt.% Dy) remained unchanged with a very marginal reduction (within the experimental error of ICP-AES analysis), indicating that the metal is tightly bound to the support and no leaching of the Dy(III) occurs upon reuse of the catalyst.

4.9.6. Catalyst recycling

In order to explore the extent of recyclability of our catalytic system, the reaction between aniline, formaldehyde (37–41% aqueous solution) and ethyl cyanoacetate in water at room temperature using Dy(III)/chitosan as a catalyst was chosen as model reaction. After completion of the reaction, the catalyst was recovered by extracting the mixture with ethyl acetate followed by filtration. The catalyst was then washed with ethyl acetate, reused, and was found to retain its activity for a minimum of six reaction cycles in water **(Table 24)**. The TEM images of the catalyst after six cycles **(Figure 51)** also did not show any significant change in the morphology of the

catalyst indicating that the structural integrity of the catalyst is maintained throughout the recycling processes.

Table 24: Recycling potential of Dy(III)/chitosan catalyst.

No. of cycles	Fresh	Run 1	Run 2	Run 3	Run 4	Run 5
Yield (%)	91	91	89	86	85	83
Time (min)	45	45	45	45	45	45

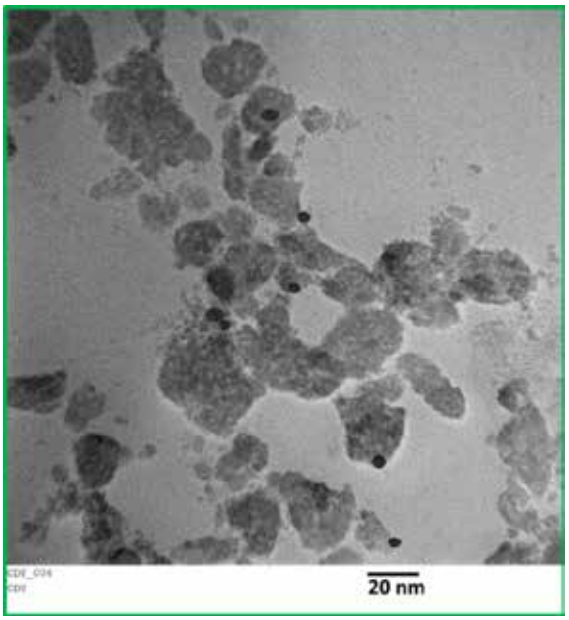

Fig. 51. TEM image of recycled catalyst after six cycles.

4.9.7. CONCLUSION

In summary, Dy(III) supported chitosan was found to be highly efficient catalyst for the green and energy sustainable synthesis of hexahydropyrimidine derivatives in aqueous media. The catalyst was able to maintain good efficiency for six catalytic cycles. The use of a recyclable catalyst, water, substrate tolerance, and ambient conditions are the advantages of this energy sustainable protocol.

4.9.8. EXPERIMENTAL

4.9.8a. Synthesis of Dy(III)/chitosan catalyst

Chitosan (3g) was suspended in 100 mL of distilled water in a round bottomed flask and stirred for 30 min. $Dy(NO_3)_3.6H_2O$ (0.2g) was then added to the suspension with continuous stirring. The mixture was then continuously stirred overnight and the solid catalyst was separated by filtration, washed with water and dried at 80 °C for 6 h.

4.9.8b. General procedure for the synthesis of hexahydropyrimidine derivatives

A mixture of amine (2 mmol), active methylene compound (1 mmol), formaldehyde (3 mmol, 37–41% aqueous solution) and catalyst (100 mg) in 5 mL water was stirred at room temperature for appropriate period of time **(table 22)**. After completion of reaction (monitored by TLC), the reaction mixture was allowed to cool, extracted by ethyl acetate, washed with water (3 × 10 mL), dried over anhydrous Na_2SO_4 and evaporated under reduced pressure to obtain the products. The remaining solid catalyst in aqueous phase was separated by filtration, washed with ethyl acetate (3 x 10 mL) and reused for further catalytic cycles. The crude products were recrystallized to afford the pure products. Compounds **(11f-h)** were separated by column chromatography using (60–120 mesh) column chromatography with 5% ethyl acetate in petroleum ether as eluent.

4.9.8c. Spectral data of synthesised compounds

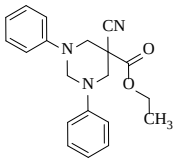 **11a**	*5-cyano-1,3-diphenyl-hexahydro-pyrimidine-5-carboxylic acid ethyl ester* White crystals, **M.p.** 120-125 °C; **Anal. Calcd**. ($C_{20}H_{21}N_3O_2$): C, 71.62; H, 6.31; N, 12.53; **Anal. Found** ($C_{20}H_{21}N_3O_2$): C, 71.66; H, 6.28; N, 12.57. **IR** (KBr, cm^{-1}): 2251 (CN), 1738 (C=O). **^{1}H NMR** (400 MHz, $CDCl_3$): δ 1.16 (s, 3H), 3.63 (d, 2H, N–CH_2), 3.77 (d, 2H, N–CH_2), 4.09 (q, 2H), 4.24 (d, 1H, N–CH–N), 4.74 (d, 1H, N–CH–N), 6.91-7.14 (m, 10H, Ar-H). **^{13}C NMR** (100 MHz, $CDCl_3$):164.39, 149.27, 131.54, 127.29, 121.22, 117.13, 70.25, 64.81, 62.18, 52.23, 14.18. **ESI-MS** m/z 336.1 (M^++1).
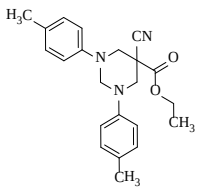 **11b**	*5-cyano-1,3-di-(4-methylphenyl)-hexahydro-pyrimidine-5-carboxylic acid ethyl ester* White crystals, **M.p.** 115-120 °C; **Anal. Calcd**. ($C_{22}H_{25}N_3O_2$): C, 72.70; H, 6.93; N, 11.56; **Anal. Found** ($C_{22}H_{25}N_3O_2$): C, 72.75; H, 6.89; N, 11.52. **IR** (KBr, cm^{-1}): 2244 (CN), 1729 (C=O). **^{1}H NMR** (400 MHz, $CDCl_3$): δ 1.22 (s, 3H), 2.29 (s, 6H), 3.71 (d, 2H, N–CH_2), 3.90 (d, 2H, N–CH_2), 4.12 (q, 2H), 4.27 (d, 1H, N–CH–N), 4.72 (d, 1H, N–CH–N), 6.97-7.12 (m, 8H, Ar-H). **^{13}C NMR** (100 MHz, $CDCl_3$): 166.14, 148.10, 131.27, 127.01, 122.75, 118.52, 69.07, 64.22, 61.59, 51.88, 21.35, 14.86. **ESI-MS** m/z 364.1(M^++1).

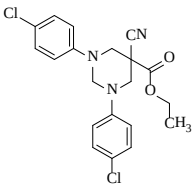 **11c**	*5-cyano-1,3-di-(4-chlorophenyl)-hexahydro-pyrimidine-5-carboxylic acid ethyl ester* White crystals, **M.p.** 110-115 °C; **Anal. Calcd**. ($C_{20}H_{19}Cl_2N_3O_2$): C, 59.42; H, 4.74; N, 10.39; **Anal. Found** ($C_{20}H_{19}Cl_2N_3O_2$): C, 59.46; H, 4.78; N, 10.36. **IR** (KBr, cm^{-1}): 2241 (CN), 1725 (C=O). **^{1}H NMR** (400 MHz, $CDCl_3$): δ 1.24 (s, 3H), 3.72 (d, 2H, N–CH_2), 3.93 (d, 2H, N–CH_2), 4.15 (q, 2H), 4.31 (d, 1H, N–CH–N), 4.68 (d, 1H, N–CH–N), 6.89-7.21 (m, 8H, Ar-H). **^{13}C NMR** (100 MHz, $CDCl_3$): 165.11, 149.19, 132.87, 129.27, 124.81, 117.95, 71.03, 64.44, 61.94, 51.76, 14.43. **ESI-MS** m/z 405.1 (M^++1).
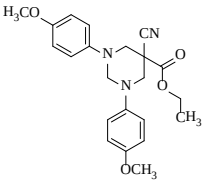 **11d**	*5-cyano-1,3-di-(4-methoxyphenyl)-hexahydro-pyrimidine-5-carboxylic acid ethyl ester* White crystals, **M.p.** 120-125 °C; **Anal. Calcd**. ($C_{22}H_{25}N_3O_4$): C, 66.82; H, 6.37; N, 10.63; **Anal. Found** ($C_{22}H_{25}N_3O_4$): C, 66.78; H, 6.34; N, 10.68. **IR** (KBr, cm^{-1}): 2249 (CN), 1731 (C=O). **^{1}H NMR** (400 MHz, $CDCl_3$): δ 1.25 (s, 3H), 3.69 (d, 2H, N–CH_2), 3.75 (s, 6H, 2xOCH_3), 3.87 (d, 2H, N–CH_2), 4.11 (q, 2H), 4.40 (d, 1H, N–CH–N), 4.74 (d, 1H, N–CH–N), 6.88-7.25 (m, 8H, Ar-H). **^{13}C NMR** (100 MHz, $CDCl_3$): 168.07, 148.23, 134.42, 129.08, 124.27, 119.18, 71.13, 63.18, 62.54, 55.81, 51.88, 15.11. **ESI-MS** m/z 396.1 (M^++1).
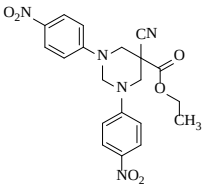 **11e**	*5-cyano-1,3-di-(4-nitrophenyl)-hexahydro-pyrimidine-5-carboxylic acid ethyl ester* White crystals, **M.p.** 125-130 °C; **Anal. Calcd**. ($C_{20}H_{19}N_5O_6$): C, 56.47; H, 4.50; N, 16.46; **Anal. Found** ($C_{20}H_{19}N_5O_6$): C, 56.43; H, 4.53; N, 16.49. **IR** (KBr, cm^{-1}): 2238 (CN), 1724 (C=O). **^{1}H NMR** (400 MHz, $CDCl_3$): δ 1.27 (s, 3H), 3.76 (d, 2H, N–CH_2), 3.92 (d, 2H, N–CH_2), 4.14 (q, 2H), 4.28 (d, 1H, N–CH–N), 4.78 (d, 1H, N–CH–N), 7.14-8.26 (m, 8H, Ar-H). **^{13}C NMR** (100 MHz, $CDCl_3$): 167.12, 149.22, 135.82, 131.21, 125.03, 117.73, 72.02, 64.11, 63.58, 51.97, 15.77. **ESI-MS** m/z 426.1 (M^++1).

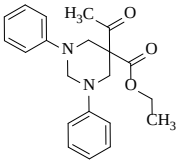 **11f**	*5-acetyl-1,3-diphenyl-hexahydro-pyrimidine-5-carboxylic acid ethyl ester*[11] Viscous liquid, **^{1}H NMR** (400 MHz, $CDCl_3$): δ 1.19 (t, 3H), 2.27 (s, 3H), 3.88 (d, 2H, N–CH_2), 3.97 (d, 2H, N–CH_2), 4.02 (q, 2H), 4.29 (d, 1H, N–CH–N),4.38 (d, 1H, N–CH–N), 6.79-7.31 (m, 10H, Ar-H). **^{13}C NMR** (100 MHz, $CDCl_3$): 195.64, 164.39, 147.38, 129.52, 121.41, 117.13, 67.91, 61.39, 60.23, 50.31, 26.43, 13.24. **ESI-MS** m/z 353.1 (M^++1).
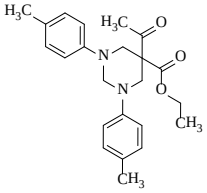 **11g**	*5-acetyl-1,3-di-(4-methylphenyl)-hexahydro-pyrimidine-5-carboxylic acid ethyl ester*[11] Viscous liquid, **^{1}H NMR** (400 MHz, $CDCl_3$): δ 1.13 (t, 3H), 2.25 (s, 3H), 2.64 (s, 6H), 3.79 (d, 2H, N–CH_2), 3.88 (d, 2H, N–CH_2), 4.06 (q, 2H), 4.31 (d, 1H, N–CH–N), 4.51 (d, 1H, N–CH–N), 6.73-7.24 (m, 8H, Ar-H). **^{13}C NMR** (100 MHz, $CDCl_3$): 194.70, 166.23, 148.15, 130.07, 129.17, 117.49, 68.65, 61.23, 59.15, 54.37, 26.18, 20.43, 14.36. **ESI-MS** m/z 381.1 (M^++1).
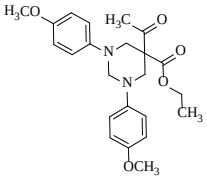 **11h**	*5-acetyl-1,3-di-(4methoxyphenyl)-hexahydro-pyrimidine-5-carboxylic acid ethyl ester*[11] Viscous liquid, **^{1}H NMR** (400 MHz, $CDCl_3$): δ 1.11 (t, 3H), 2.28 (s, 3H), 3.71 (s, 6H), 3.84 (d, 2H, N–CH_2), 3.96 (d, 2H, N–CH_2), 4.13 (q, 2H), 4.33 (d, 1H, N–CH–N), 4.59 (d, 1H, N–CH–N), 7.13-7.92 (m, 8H, Ar-H). **^{13}C NMR** (100 MHz, $CDCl_3$): 195.82, 165.30, 148.00, 130.78, 129.27, 120.22, 68.94, 62.08, 58.23, 55.91, 54.18, 26.68, 20.37, 13.78. **ESI-MS** m/z 413.1 (M^++1).
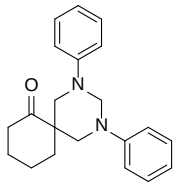 **11i**	*2,4-Bis-phenyl-2,4-diazaspiro[5.5]undecan-7-one*[12,14] Viscous liquid, **^{1}H NMR** (400 MHz, $CDCl_3$): δ 1.58-1.63 (m, 2H), 1.83-1.95 (m, 4H), 2.45 (t, 2H), 3.46 (d, 2H), 3.63 (d, 2H), 4.09 (d, 1H), 4.66 (d, 1H), 6.79-7.23 (m, 10H, Ar-H). **^{13}C NMR** (100 MHz, $CDCl_3$): 198.13, 149.65, 129.33, 120.21, 118.49, 68.21, 55.11, 50.73, 39.78, 34.36, 27.73, 20.33. **ESI-MS** m/z 321.1 (M^++1).

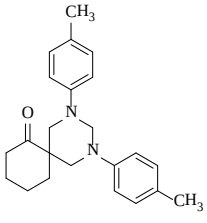 **11j**	*2,4-Bis-(4-methylphenyl)-2,4-diazaspiro[5.5]undecan-7-one*[12,14] White solid, **M.p** 127 ºC; **^{1}H NMR** (400 MHz, $CDCl_3$): δ 1.61-1.67 (m, 2H), 1.81-1.92 (m, 4H), 2.35 (s, 6H), 2.51 (t, 2H), 3.42 (d, 2H), 3.61(d, 2H), 4.12 (d, 1H), 4.74 (d, 1H), 6.67-7.38 (m, 8H, Ar-H). **^{13}C NMR** (100 MHz, $CDCl_3$): 198.68, 148.51, 129.95, 121.52, 118.11, 69.53, 55.11, 50.28, 39.16, 34.98, 27.10, 22.44, 20.13. **ESI-MS** m/z 349.1 (M^++1).
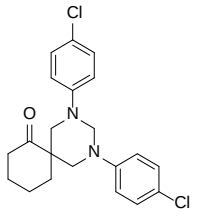 **11k**	*2,4-Bis-(4-chlorophenyl)-2,4-diazaspiro[5.5]undecan-7-one*[12,14] White solid, **M.p** 161 ºC; **^{1}H NMR** (400 MHz, $CDCl_3$): δ 1.64-1.69 (m, 2H), 1.81-1.90 (m, 4H), 2.42 (t, 2H), 3.44 (d, 2H), 3.64 (d, 2H), 4.17 (d, 1H), 4.63 (d, 1H), 6.79-7.13 (m, 8H, Ar-H). **^{13}C NMR** (100 MHz, $CDCl_3$): 199.57, 148.87, 128.38, 125.61, 118.51, 67.30, 56.25, 49.21, 39.37, 34.96, 27.32, 20.08. **ESI-MS** m/z 390.1 (M^++1).
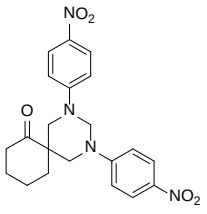 **11l**	*2,4-Bis-(4-nitrophenyl)-2,4-diazaspiro[5.5]undecan-7-one*[12,14] White solid, **M.p** 170-175 ºC; **^{1}H NMR** (400 MHz, $CDCl_3$): δ 1.68-1.72 (m, 2H), 1.88-1.95 (m, 4H), 2.45 (t, 2H), 3.41 (d, 2H), 3.62 (d, 2H), 4.10 (d, 1H), 4.58 (d, 1H), 7.09-8.11(m, 8H, Ar-H). **^{13}C NMR** (100 MHz, $CDCl_3$): 199.52, 147.73, 138.87, 124.34, 117.62, 68.01, 56.44, 49.93, 38.89, 34.54, 27.11, 20.52. **ESI-MS** m/z 411.1 (M^++1).

REFERENCES:

1. K. S. Jain, T. S. Chitre, P. B. Miniyar, M. K. Kathiravan, V. S. Bendre, V. S. Veer, S. R. Shahane, C. J. Shishoo, Curr. Sci. 90 (2006) 793.
2. J. A. Bisceglia, M. B. Garcia, R. Massa, M. L Magri, M. Zani, G. O. Gutkind, L. R. Orelli, J. Heterocycl. Chem. 41 (2004) 85.
3. (a) S. Tu, C. Miao, F. Fang, F. Youjian, T. Li, Q. Zhuang, X. Zhang, S. Zhu, D. Shi, Bioorg. Med. Chem. Lett. 14 (2004) 1533; (b) C. O. Kappe, Tetrahedron 49 (1993) 6937; (c) C. O. Kappe, Eur. J. Med. Chem. 35 (2000) 1043; (d) D. Russowski, R. F. S. Canto, S. A. A. Sanches, M. G. M. D'Oca, A. D. Fatima, J. E. D. Carvalho, Bioorg. Chem. 34 (2006) 173.
4. M. Khan, M. Gupta, Pharmazie 57 (2002) 377.
5. (a) A. Guggisberg, K. Drandarov, M. Hesse, Helv. Chim. Acta 83 (2000) 3035; (b) J. C. Braekman, D. Daloze, R. Flammang, A. Maquestiau, Org. Mass Spectrom. 24 (1989) 837; (c) K. Drandarov, A. Guggisberg and M. Hesse, Helv. Chim. Acta 82 (1999) 229.
6. P. A. S. Smith, R. N. Loeppky, J. Am. Chem. Soc. 89 (1967) 1147.
7. D. Enders, L. Wortmann, Heterocycles 58 (2002) 293.
8. (a) J. Billman, S. Khan, J. Med. Chem. 9 (1966) 347; (b) J. Billman, S. Khan, J. Med. Chem. 8 (1965) 498.
9. A. Q. Siddiqui, L. Merson-Davies, P. M. Cullis, J. Chem. Soc., Perkin Trans., 1 (1999) 3243.
10. J. W. Hwang, H.-W. Kim, S. Jo, E. Park, J. Choi, S. Kong, D.-S. Park, J. M. Heo, J. S. Lee, Y. Ko, I. Choi, J. Cechetto, J. Kim, J. Lee, Z. No, M. P. Windisch, Eur. J. Med. Chem. 70 (2013) 315.
11. C. Mukhopadhyay, S. Rana, R. J. Butcher, Tetrahedron Lett. 52 (2011) 4153.
12. H. L. Wei, Z.-Y. Yan, Y. N. Niu, G. Q. Li, Y. M. Liang, J. Org. Chem. 72 (2007) 8600.
13. A. Dandia, A. K. Jain, S. Sharma, RSC Adv. 3 (2013) 2924.
14. A. Dandia, A. K. Jain, S. Sharma, Tetrahedron Lett. 53 (2012) 5270.
15. M. M. Heravi, S. Sadjadi, S. Sadjadi, H. A. Oskooie, R. H. Shoar, F. F. Bamoharram, J. Chin. Chem. Soc. 56 (2009) 246.
16. (a) H. B. Kagan, J. L. Namy, Tetrahedron 42 (1986) 6573; (b) G. A. Molander, Chem. Rev. 92 (1992) 29; (c) K. Mikami, M. Terada, H.

Matsuzawa, Angew. Chem. Int. Ed. 41 (2002) 3554; (d) S. Kobayashi, Eur. J. Org. Chem. (1999) 15 (e) S. Kobayashi, Top. Organomet. Chem. 2 (1999) 63; (f) R. Anwander, Top. Organomet. Chem. 2 (1999) 1.

17. G. K. Veits, J. R. de Alaniz, Tetrahedron 68 (2012) 2015.
18. J. E. Klijn, J. B. F. N. Engberts, Nature 435 (2005) 746; (b) A. Manna, A. Kumar, J. Phys. Chem. A. 117 (2013) 2446; (c) Y. Jung, R. A. Marcus, J. Am. Chem. Soc. 129 (2007) 5492; (d) C. J. Li, Chem. Rev. 105 (2005) 3095.
19. N. Sudheesh, S. K. Sharma, R. S. Shukla, J. Mol. Catal A: Chem. 321 (2010) 77.
20. (a) A. Primo, F. Quignard, Chem. Commun. 46 (2010) 5593; (b) N. V. Kramareva, A. Y. Stakheev, O. P. Tkachenko, K. V. Klementiev, W. Grunert, E. D. Finashina, L. M. Kustov, J. Mol. Catal. A: Chem. 209 (2004) 97.
21. A. J. Varma, S. V. Deshpande, J. F. Kennedy. Carbohydr. Polym. 55 (2004) 77.
22. K. D. Trimukhea, A. J. Varma, Carbohydr. Polym. 75 (2009) 63.

CHAPTER 5

SILICA MOLYBDIC ACID (SMA) CATALYSED MULTICOMPONENT SYNTHESIS OF TETRAZOLE DERIVATIVES UNDER MICROWAVE IRRADIATION IN AQUEOUS MEDIA

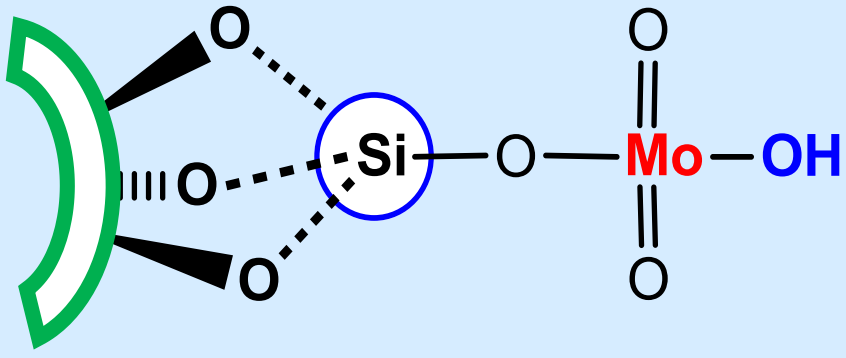

SILICA MOLYBDIC ACID (SMA) CATALYSED MULTICOMPONENT SYNTHESIS OF TETRAZOLE DERIVATIVES UNDER MICROWAVE IRRADIATION IN AQUEOUS MEDIA*

5.1. INTRODUCTION

Tetrazoles and their derivatives represent an important class of *N*-containing heterocycles with wide range of applications. These derivatives are not found in nature and possess a unique property of being resistant to biological degradation. This property makes it possible to use tetrazoles as isosteric substitutes for various functional groups in order to develop them as potential medicinal agents.[1] The tetrazole group has been used as a successful bioisosteric replacement for carboxylic acid groups[2] which has led to the development of drug compounds like Lasortan, Irbesartan, Tomelukast, and PTZ(2) **(Figure 52)**. 5-Substituted tetrazoles are reported to possess important biological profiles like potential drugs against schizophrenia and cerebral ischemia,[3] antidiabetic,[4] antiviral,[5] antibacterial[6] and antihypertensive activities.[7] These compounds are also regarded as important synthetic intermediates in synthetic organic chemistry.[8] They also show good coordination properties and are used as ligands in coordination chemistry. These derivatives also find use in the fields of propellants, explosives and material chemistry.[9-10]

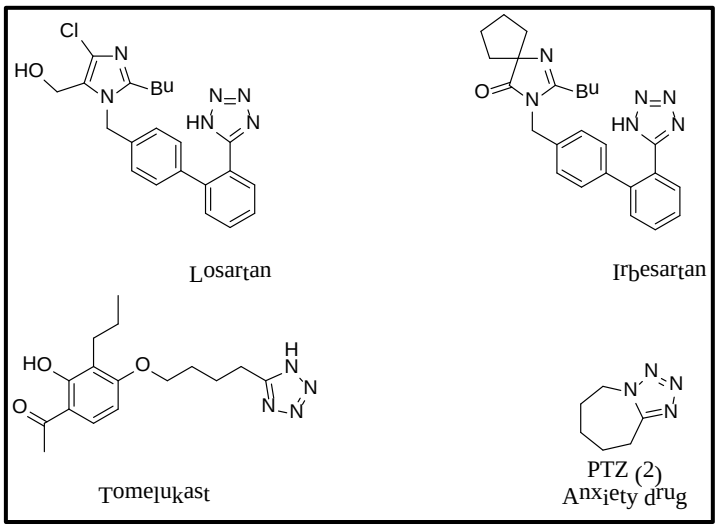

Fig. 52: Representative drugs based on tetrazoles.

Many available methods for the synthesis of tetrazoles include [3 + 2] cycloaddition of azide to nitriles,[11] reaction of primary amines with NaN_3 and triethyl

* Nayeem Ahmed, Zeba N. Siddiqui, ***RSC Advances***, 5 (2015) 16707.

orthoformate,[12] nucleophilic substitution by an azide anion[13] and addition of $NaNO_2$ to aminoguanidine.[14] But [3+2] cycloaddition still remains the most employed method for the synthesis of 5-substituted tetrazoles. Few efforts were devoted to develop multicomponent protocols for the synthesis of 5-substituted tetrazoles, but long reaction times and limited substrate tolerance hampers their practical applicability.

5.2. REVIEW OF LITERATURE

Some recent examples of the synthesis of tetrazole derivatives via three component reaction of aldehydes, malononitrile and sodium azide

5.2.1. Multicomponent diastereoselective synthesis of new 5-substituted 1*H*-tetrazoles.[15]

Z. N. Tisseh *et al.* reported multicomponent synthesis of new 5-substituted-tetrazoles via domino Knoevenagel condensation/1,3 dipolar cycloaddition reaction of carbonyl compounds, malononitrile and sodium azide in water.

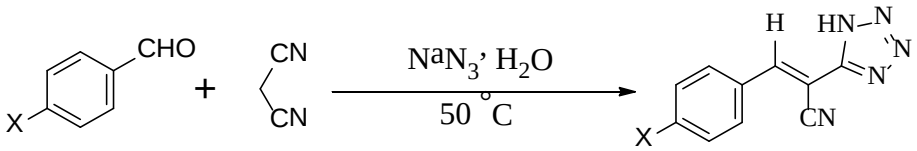

$X^{=}$ H, Br, OH

5.2.2. Synthesis and characterization of new 5-substituted 1*H*-tetrazoles in water.[16]

M. Mahkam *et al.* reported a catalyst-free protocol for the synthesis of tetrazoles. The merits of the presented protocol were catalyst-free conditions, water as a solvent and good yields.

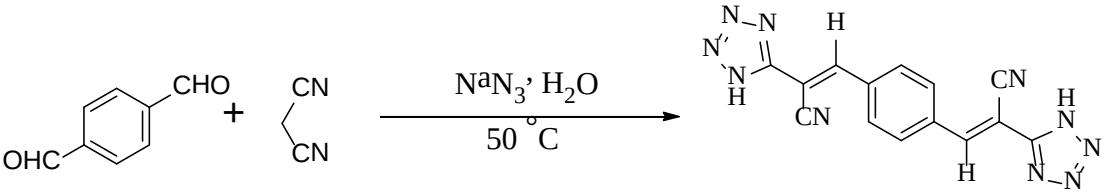

5.2.3. Multicomponent synthesis of 3-(1*H*-tetrazol-5-yl)coumarins.[17]

Z. N. Tisseh *et al.* reported a straightforward synthesis of 3-(1*H*-tetrazol-5-yl) coumarins via domino Knoevenagel condensation, Pinner reaction, and 1,3-dipolar cycloaddition of substituted salicylaldehydes, malononitrile, and sodium azide in water.

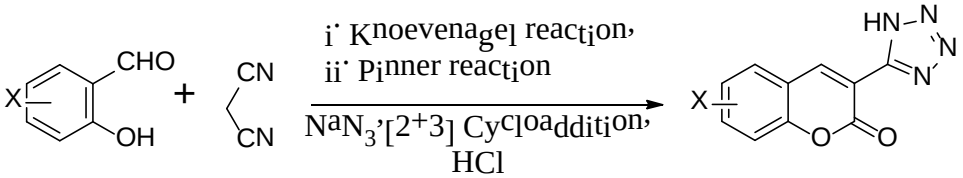

$X^{=}$ H, OMe, Br, OH

5.2.4. Synthesis of *N*-rich heterocycles via multi-component reactions.[18]

Z. N. Tisseh *et al.* reported the synthesis of 1*H*-tetrazoles via multicomponent reaction of α-dicarbonyl compounds, 2,3-diaminomaleonitrile and sodium azide without any catalyst using DMSO as a solvent.

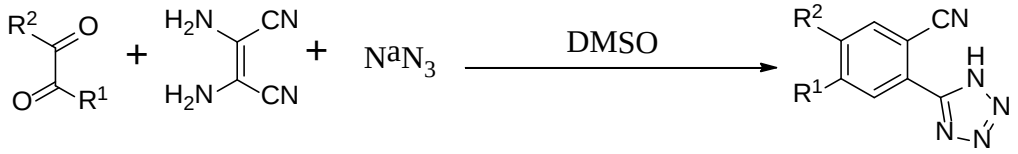

$R^{1=}$ H, CH_3, C_6H_5, $4\text{-}OCH_3C_6H_4$, $4\text{-}FC_6H_4$
$R^{2=}$ H, CH_3, C_6H_5, $4\text{-}OCH_3C_6H_4$, $4\text{-}FC_6H_4$

5.3. PRESENT WORK

Meeting the challenges of sustainability and global energy requirements are currently the major concerns of the scientists throughout the world. Catalysis is an important tool which can assist in meeting those challenges via the development of sustainable pathways for the production of industrially important organic chemicals. With the advent of green chemistry, catalysis has taken the centre stage by leading to efficient and eco-friendly synthetic protocols that avoid the use of volatile organic solvents, toxic reagents, and harsh reaction conditions.[19] Heterogenisation of a successful homogeneous catalyst is a very good way to design a sustainable catalyst. Among many techniques available for heterogenisation, covalent binding is considered to be the best, because the catalyst becomes sufficiently robust to survive the harsh reaction conditions and simultaneously minimizes leaching, which in turn allows the catalyst to be recycled and reused.[20]

The important aspect of reducing the environmental impact of a synthetic process is the optimization of energy consumption and in this context, the use of microwave (MW) irradiations as a heat source represents a good alternative to conventional heating.[21] The use of MW irradiations in conventional solvents has developed very rapidly, and now the main focus has shifted towards the use of greener solvents such as water, for the development of environmentally benign processes. As water is abundantly available in nature and devoid of any toxic properties, it is advantageous

to carry out reactions in aqueous media. Moreover, it is a well-established fact that the combination of heterogeneous catalysts and microwaves has led to the development of effective, rapid and environmentally benign synthetic methods.[22] Keeping in view the environmental concerns, we describe, in this chapter, the synthesis of silica molybdic acid (SMA), its characterization, and its application for the synthesis of functionalized tetrazoles via three component addition of aldehydes, malononitrile and sodium azide in water using microwaves.

5.4. RESULTS AND DISCUSSION

Scheme 15 illustrates the concise route for the preparation of the catalyst. The reaction of silica with $SOCl_2$ gives silica chloride, which further undergoes nucleophilic substitution by sodium molybdate followed by stirring in 0.1N HCl solution to afford silica molybdic acid (SMA). The amount of H^+ is determined by back titration analysis using standard 0.01N NaOH solution and is found to be equal to 0.23 meq/gm of the catalyst.

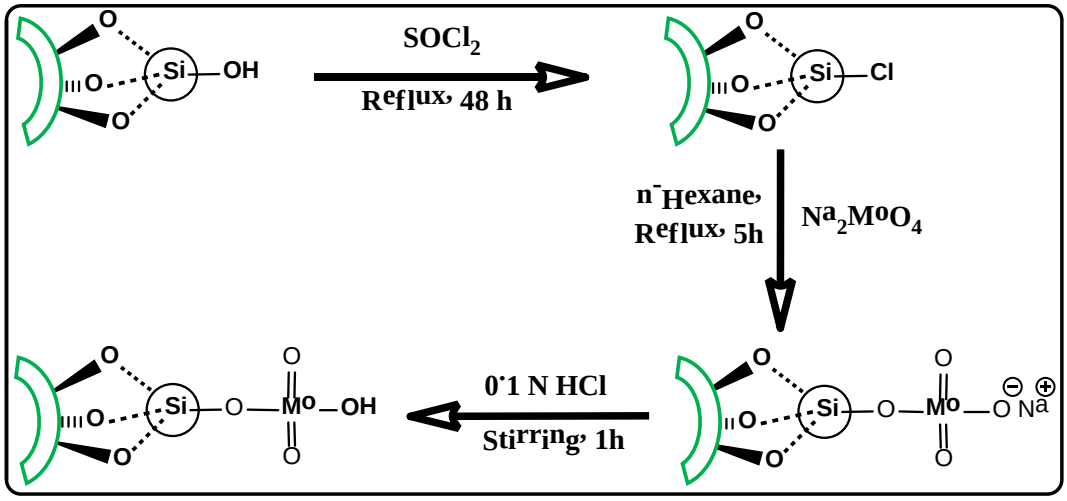

Scheme 15: Schematic representation of the synthesis of silica molybdic acid (SMA)

5.4.1. Characterization of the catalyst

5.4.1a. FT-IR spectral analysis

The FT-IR spectra of sodium molybdate and SMA were studied in order to confirm the presence of molybdate moieties on silica surface. In FT-IR spectrum of sodium molybdate **(Figure 53a)** characteristic Mo−O stretching frequencies were obtained at 865 and 912 cm^{-1}.[23] In the FT-IR spectrum of SMA **(Figure 53b)** characteristic frequencies corresponding to silica and molybdate groups were observed. The Mo−O stretching vibrations in $[MoO_4]^{2-}$ species were obtained at 873 and 975 cm^{-1} and the broad peak in the range 1000-1200 cm^{-1} was attributed to antisymmetric Si−O−Si

stretching. The Si−O−Si symmetric stretching was obtained at 803 cm^{-1}. The FT-IR spectra, thus, shows successful functionalization of molybdate groups on the surface of silica.

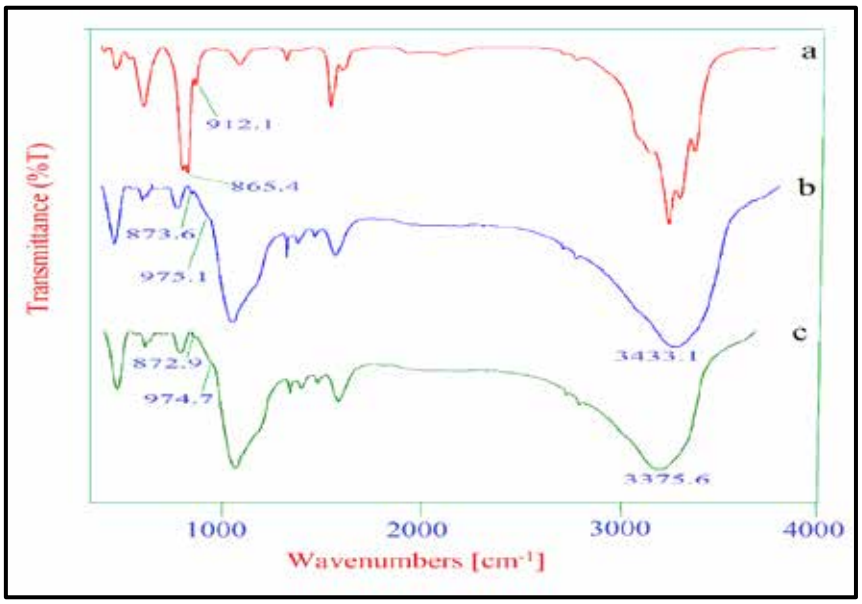

Fig. 53: FT-IR spectrum (a) of sodium molybdate, (b) of silica molybdic acid and (c) of recycled silica molybdic acid.

5.4.1b. XRF analysis

XRF analysis was performed in order to determine the actual composition of the catalyst **(Table 25)**. The analysis confirmed the presence of molybdate groups in the silica matrix. The actual composition of the catalyst was found as 84.60 (%W/W) SiO_2 **(entry 1)** and 1.58 (%W/W) MoO_4 **(entry 2)**.

Table 25: XRF data of Silica Molybdic acid

Entry	Compound	Concentration
1	SiO_2	84.60%
2	MoO_4	1.58%
3	V_2O_5	0.34%
4	Cl	0.04%
5	SO_3	0.04%
6	CaO	0.03%
7	Al_2O_3	0.02%
8	Fe_2O_3	0.02%
9	TiO_2	0.02%
10	Others + LOI*	13.25%
*LOI= Loss on ignition		

5.4.1c. XRD analysis

The XRD analysis showed that the diffraction pattern of the catalyst **(Figure 54a)** was similar to that of support **(Figure 54b)**. The peaks of MoO_4 group obtained in the range of 2θ 20-35° merged with the broad peak of SiO_2, at 2θ 20-30°.[24] The presence of MoO_4 groups was further confirmed by comparing the data with *PDF#852405*. The peaks obtained at 24.086, 25.921, 27.672 and 29.558 confirmed the presence of molybdate groups on the silica surface.

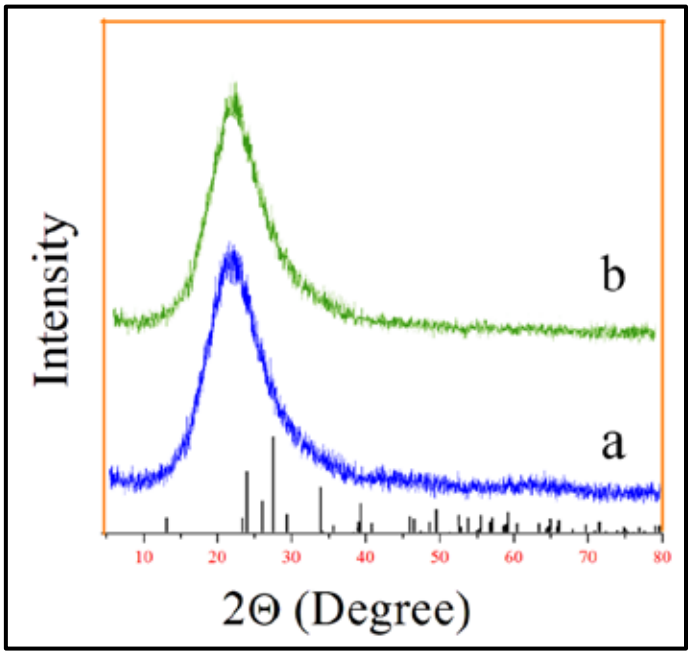

Fig. 54: XRD analysis (a) of fresh SMA and (b) of silica.

5.4.1d. Thermogravimetric (TG) analysis

TG analysis was performed in order to determine the stability and the amount of molybdate groups on the surface of silica **(Figure 55)**. The TG curve showed a first weight loss of 15.09% up to 200 °C which can be attributed to loss of physisorbed water molecules. The second weight loss of 5.12% in the range 301 °C - 579 °C, shown by TG curve, was due to the loss of molybdate groups covalently bound to silica surface. Thus, it can be concluded that the catalyst is stable up to 300 °C.

The amount of molybdate groups bound to silica surface was also calculated by TG analysis. The weight loss of 5.12 % corresponded to 0.051gm of molybdate in 1 gm of catalyst, which, therefore, amounted to loading of 0.21mmol/gm of the catalyst, as also confirmed by back titration analysis.

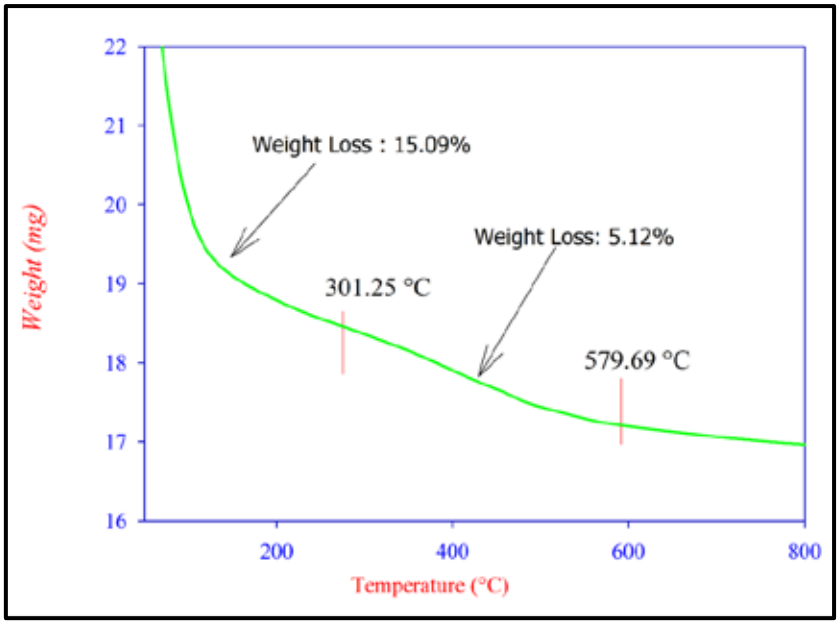

Fig. 55: TG analysis of SMA.

5.4.1e. SEM-EDX and Elemental mapping analyses

The SEM analysis was performed in order to observe the changes in the surface morphology of silica after functionalization. The images showed the change in surface morphology of the silica **(Figure 56a)** after functionalization with molybdate groups **(Figure 56b)**. The EDX analysis confirmed the successful incorporation of molybdate groups on the silica surface **(figure 57)**, by showing the presence of Mo in addition to O and Si elements. The elemental mapping analysis **(Figure 58)** showed a uniform distribution of molybdate groups on the surface of the silica.

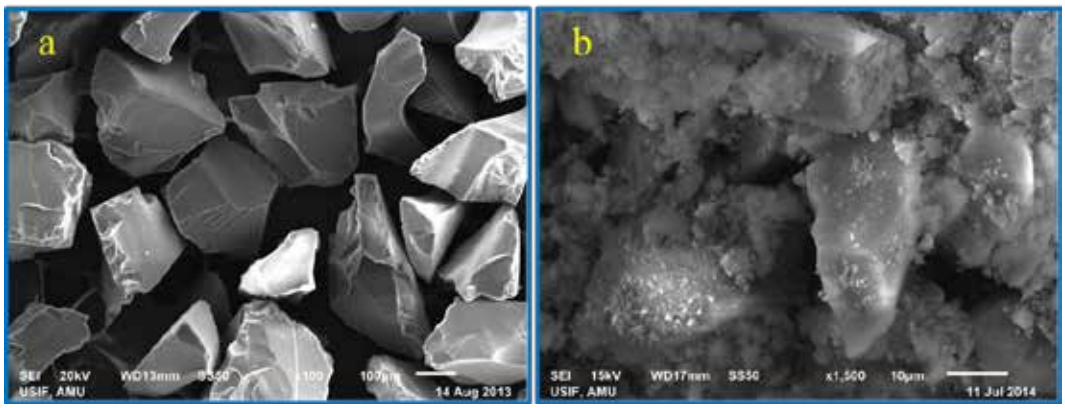

Fig. 56: SEM images (a) of silica and (b) of silica molybdic acid (SMA).

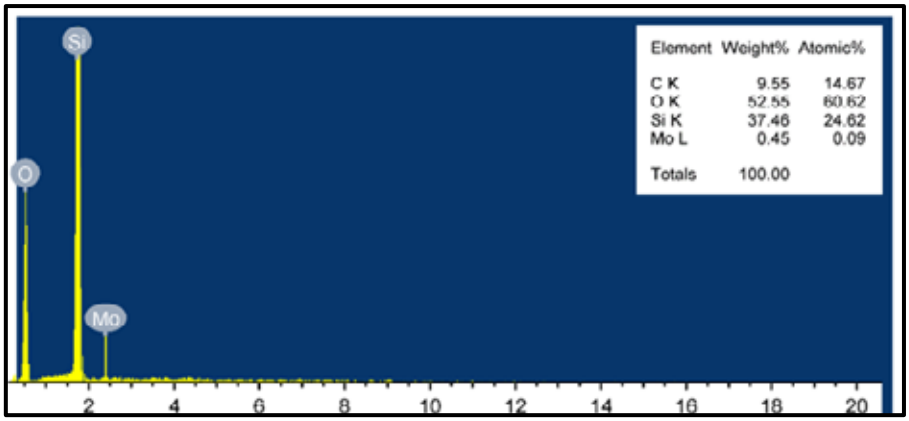

Fig. 57: EDX analysis of SMA showing presence of Mo in addition to Si and O.

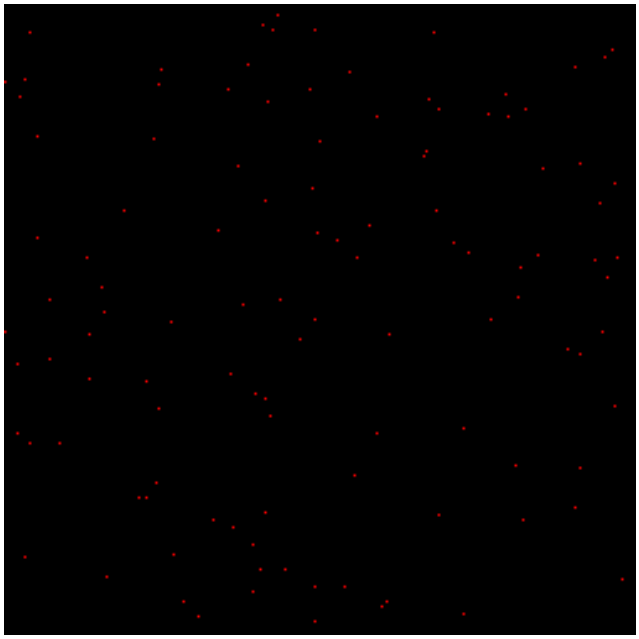

Fig. 58: Elemental mapping showing distribution of Mo on the surface of silica.

5.4.2. Optimization of reaction conditions

5.4.2a. Effect of different catalysts and solvents

The optimization studies were initiated by carrying out model reaction between thiophene-2-carboxaldehyde **(6h)**, malononitrile **(7c)** and sodium azide. The reaction was tested under a variety of reaction conditions, which included screening of different catalysts, solvents and influence of the catalyst amount. The reaction without any catalyst afforded the product with moderate yield in 24h **(Table 26, entry 1)**. Unsatisfactory results were obtained by using silica gel and silica chloride as catalysts **(Table 26, entries 2&3)**. Moderate yield of the product was obtained in longer reaction time period when $FeCl_3$ and $AlCl_3$ were used as catalysts **(entries 4&5)**. AcOH as a catalyst also couldn't show promising result **(entry 6)**. Reaction catalysed

by H_2MoO_4 gave good yield of the product in 6.1h **(entry 7)**. However, best result, (product yield of 85% in 4.5h) was obtained when SMA was used as a catalyst **(entry 8)**. After obtaining the right catalyst for this reaction, the reaction conditions were further optimized by the screening of different solvents. Solvents like ethanol, methanol, toluene, benzene, ethylene glycol, PEG-200 and water were screened to test the efficiency of the catalyst and the results are summarized in Table 26 **(entries 8-14)**. The results clearly indicated the superiority of water over the other solvents **(entry 8)**. The increased reactivity in water can be attributed to the development of hydrogen bonding between water and azide ion, which stabilizes the intermediate structures during the formation of products. The hydrophobic effects generated by water also help in increasing the rate of reaction by decreasing the hydrocarbon–water interfacial area. In order to further improve the protocol to make it energy sustainable, the reaction mixture was irradiated with microwaves. As visualized a remarkable improvement in the yield of the product was observed in very short time period **(Table 26, entry 15)**. The rate enhancement of reaction is due to the efficient interaction of molecules in reaction mixture with microwaves. Further water being a polar solvent has a good potential to absorb microwaves and convert them into heat energy, consequently accelerating the rate of reactions in aqueous medium as compared to results obtained using conventional heating **(Table 26, entries 8 & 15)**.

Table 26: Effect of different catalysts and solvents on model reaction

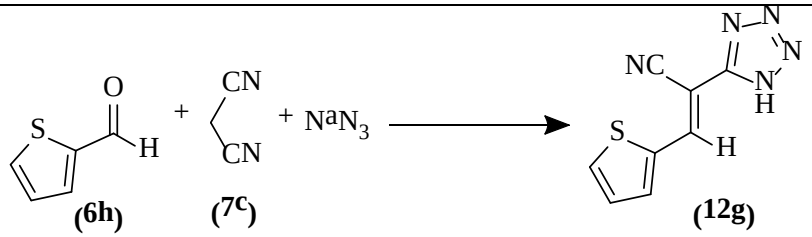

(6h) **(7^c)** **(12g)**

Entry	Solvent	Reaction condition	Time	Yield (%)
1	Water (5mL)	50 °C, Heat, without catalyst	24 h	76
2	Water (5mL)	50 °C, Heat, Silica gel (100 mg)	19h	72
3	Water (5mL)	50 °C, Heat, Silica Chloride (100 mg)	22h	69
4	Water (5mL)	50 °C, Heat, $FeCl_3$ (10 mol%)	6.4h	77

5	Water (5mL)	50 °C, Heat, $AlCl_3$ (10 mol%)	6.2h	73
6	Water (5mL)	50 °C, Heat, AcOH (10 mol%)	7.6h	69
7	Water (5mL)	50 °C, Heat, H_2MoO_4 (100 mg)	6.1h	77
8	Water (5mL)	50 °C, Heat, SMA (100 mg)	4.5 h	85
9	Ethanol (5mL)	50 °C, Heat , SMA (100 mg)	6 h	65
10	Methanol (5mL)	50 °C, Heat, SMA (100 mg)	6.5 h	61
11	Toluene (5mL)	50 °C, Heat, SMA (100 mg)	9 h	25
12	Benzene (5mL)	50 °C, Heat, SMA (100 mg)	9 h	23
13	Ethylene glycol (5mL)	50 °C, Heat, SMA (100 mg)	10 h	33
14	PEG-200 (5mL)	50 °C, Heat, SMA (100 mg)	8.5 h	35
15	Water (5mL)	50 °C, Microwaves, SMA (100 mg)	15 min	93

5.4.2b. Effect of catalyst loading

The effect of the catalyst loading on the model reaction **(Table 27)** revealed that 0.1 g of the catalyst was sufficient to get the maximum yield of the product **(Table 27, entry 3)**. Decreasing the amount of catalyst to 0.03 g decreased the yields with increase in time period for completion of the reaction **(entries 1,2)**. Increasing the catalyst amount did not have any effect on the reaction **(entries 4,5)**. Therefore, 0.1 g SMA was found to be the optimum amount of catalyst.

Table 27: Effect of catalyst loading

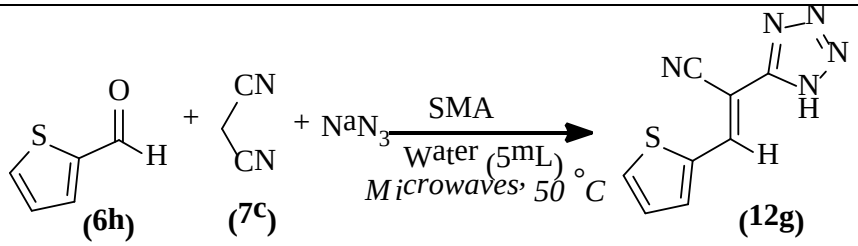

(6h) **(7c)** **(12g)**

Entry	Catalyst loading (g)	Time(min)	Yield (%)
1	0.03	35	71
2	0.05	20	87

3	0.10	15	93
4	0.15	15	93
5	0.20	15	91

5.4.2c. Effect of temperature

The effect of temperature on the model reaction was studied and it was found that reaction was influenced by the change in temperature **(Table 28)**. At room temperature the reaction completed in 75 min with poor yield of the product **(Table 28, entry 1)**. When the temperature was increased to 40 °C, improved product yield was obtained in 35 min **(entry 2)**. When the temperature was increased to 50 °C, best result of 93 % product yield in 15 min was obtained **(entry 3)**. Further increase in temperature to 70 °C resulted in decrease in the product yield **(entry 4)**.

Table 28: Effect of reaction temperature

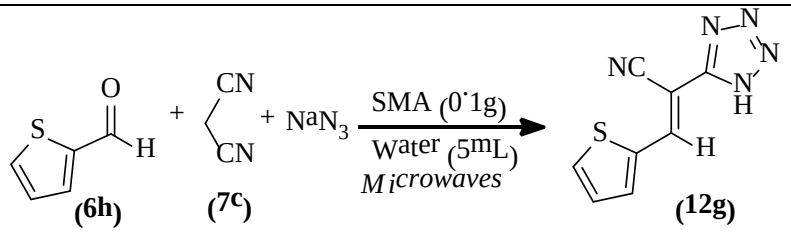

(6h) **(7c)** **(12g)**

Entry	Temperature (°C)	Time (min)	Yield (%)
1	Room Temp.	75	25
2	40	35	66
3	50	15	93
4	70	15	90

5.4.2d. Effect of the amount of NaN_3

The effect of the amount of the NaN_3 on the product formation **(Table 29)** was also evaluated and it was observed that under the optimum thermal reaction conditions, without any catalyst, 2 mmols of NaN_3 were required for the satisfactory product formation **(Table 29, entry 2)**. With the use of 0.1g of SMA as a catalyst, 1.5 mmol NaN_3 was required to obtain good yield of the product **(entry 4)**. By irradiating the reaction mixture under the optimized reaction conditions, it was observed that 1 mmol of NaN_3 was enough to give maximum product yield **(entry 5)**. Thus, the use of microwaves further added to greenness of the procedure by making the reaction atom economical.

Table 29: Effect of the amount of NaN_3

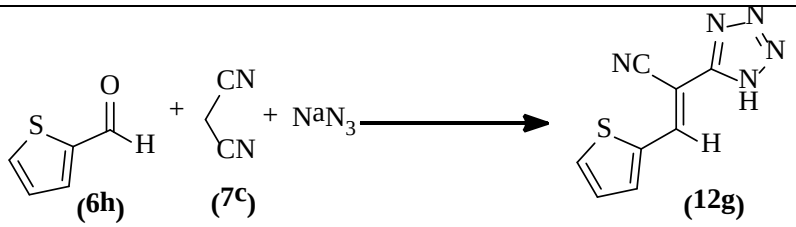

(6h) (7c) (12g)

Entry	Condition	NaN_3 (mmol)	Yield (%)
1	50 °C, Stirring	1	57
2	50 °C, Stirring	2	79
3	50 °C, Stirring, SMA (0.1g)	1	73
4	50 °C, Stirring, SMA (0.1g)	1.5	85
5	50 °C, Microwaves, SMA (0.1g)	1	93

5.4.2e. Catalytic reaction

With the optimal conditions in hand, the substrate scope of SMA catalysed synthesis of tetrazole derivatives was examined under both conventional and microwave heating **(scheme 16)**. The results indicated that aldehydes containing both activating and deactivating groups reacted efficiently with malononitrile and sodium azide to afford the corresponding tetrazoles in excellent yields **(Table 30)**. The heterocyclic aldehydes bearing substituents like chromone, quinoline and thiophene also reacted effortlessly giving the expected products in good to excellent yields. Under conventional heating, the catalyst showed good efficiency giving the products in 3.5-5.5 h, whereas excellent efficiency of 89-95% product yield in 15 min was observed under microwave irradiation. The results thus, demonstrated SMA to be an efficient catalyst for the preparation of large spectrum of substituted tetrazoles in very high yields under aqueous conditions.

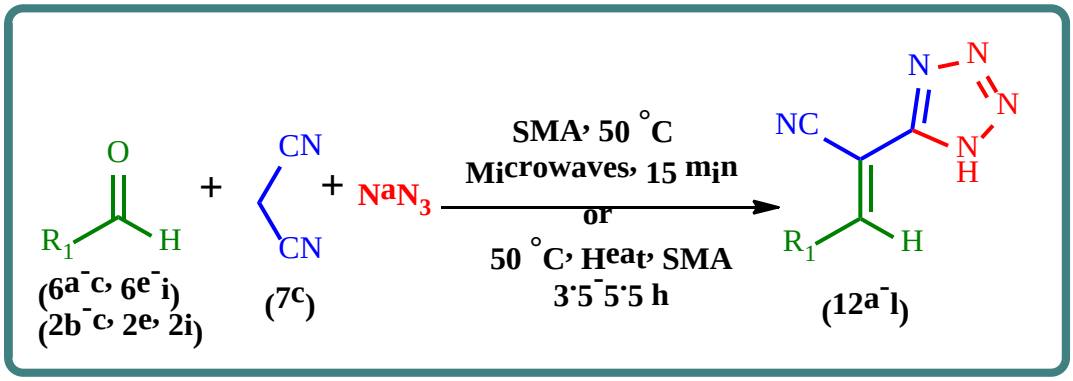

(6a-c, 6e-i)
(2b-c, 2e, 2i)
(7c)
(12a-l)

Scheme 16: General scheme for the synthesis of tetrazole deriatives.

The structural assignment of all the compounds was done by elemental and spectroscopic data (IR, NMR and mass). The IR spectrum of **12h (Figure 59)** showed NH strtetching frequency at 3439 cm^{-1} and CN stretching band at 2220 cm^{-1}. The C=C stretchig frequency was obtained at 1575 cm^{-1}. The ^{1}H-NMR spectrum **(Figure 60)** showed a singlet for olefinic proton at δ 8.45. The two hydrogen atoms of thiophene ring gave characteristic doublets at δ 7.75 and 7.04, respectively. The NH proton was discernible at δ 3.33. The ^{13}C-NMR spectrum **(Figure 61)** showed peaks for all the carbon atoms and are provided in spectral data section. Further structural confirmation was provided by ESI-Mass spectrum **(Figure 62)** which showed the molecular ion peak as the base peak at m/z 218.1 (M^{+}+1).

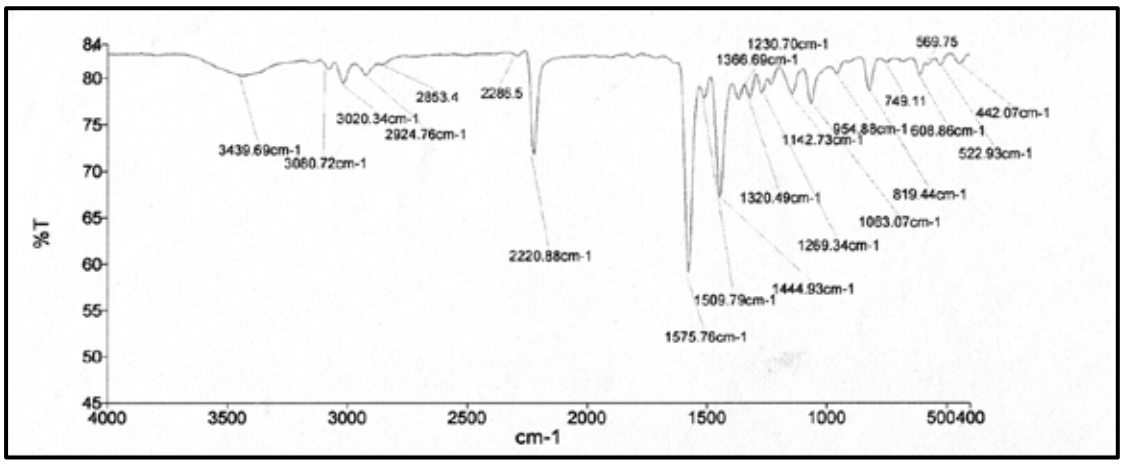

Fig. 59: FT-IR spectrum of **12h**

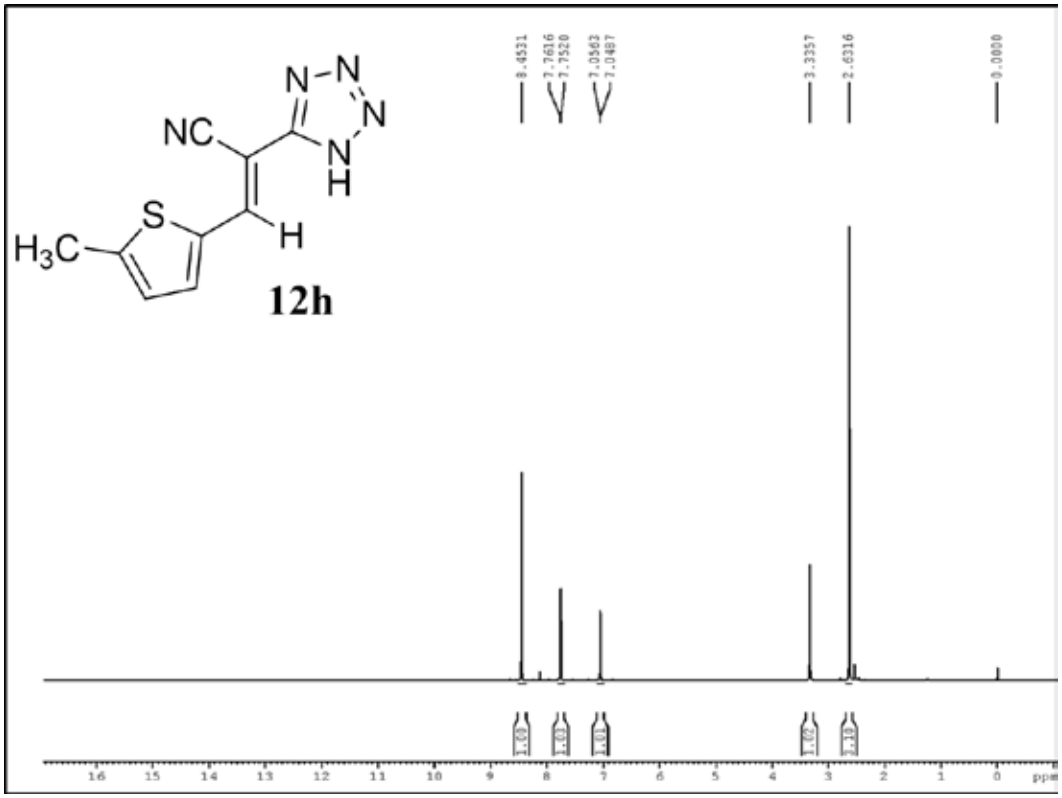

Fig. 60: ^{1}H-NMR spectrum of **12h**

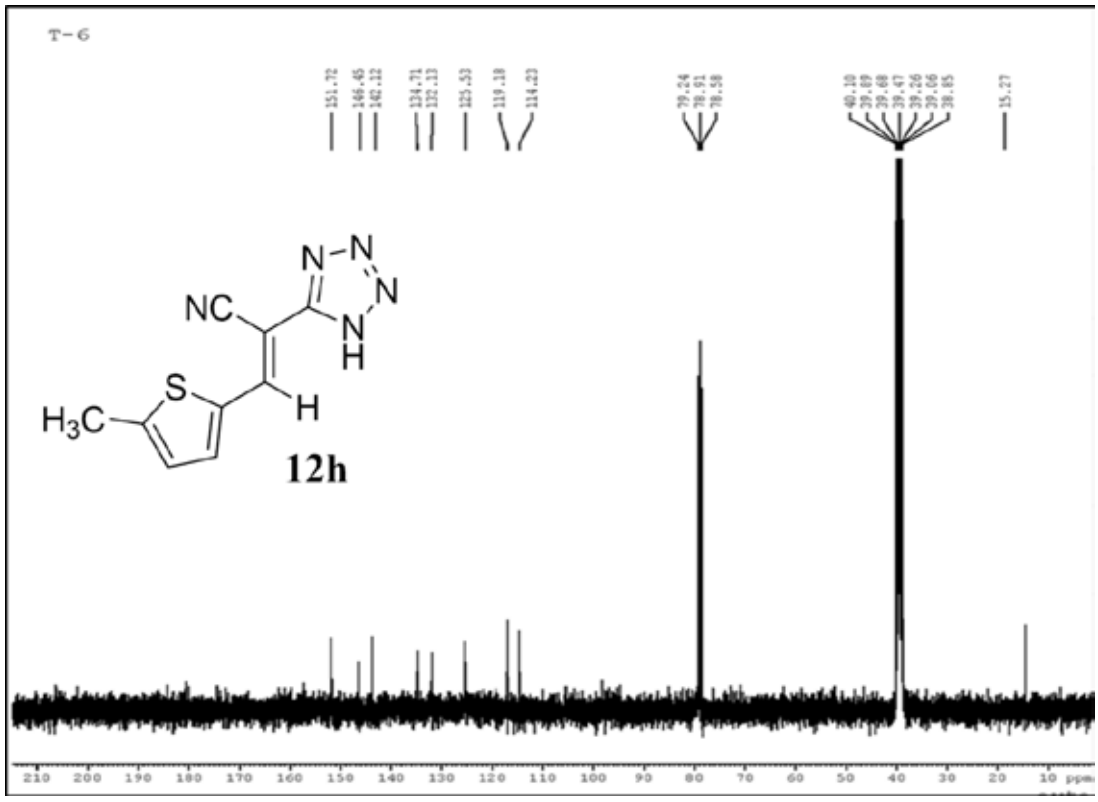

Fig. 61: ^{13}C-NMR spectrum of **12h**

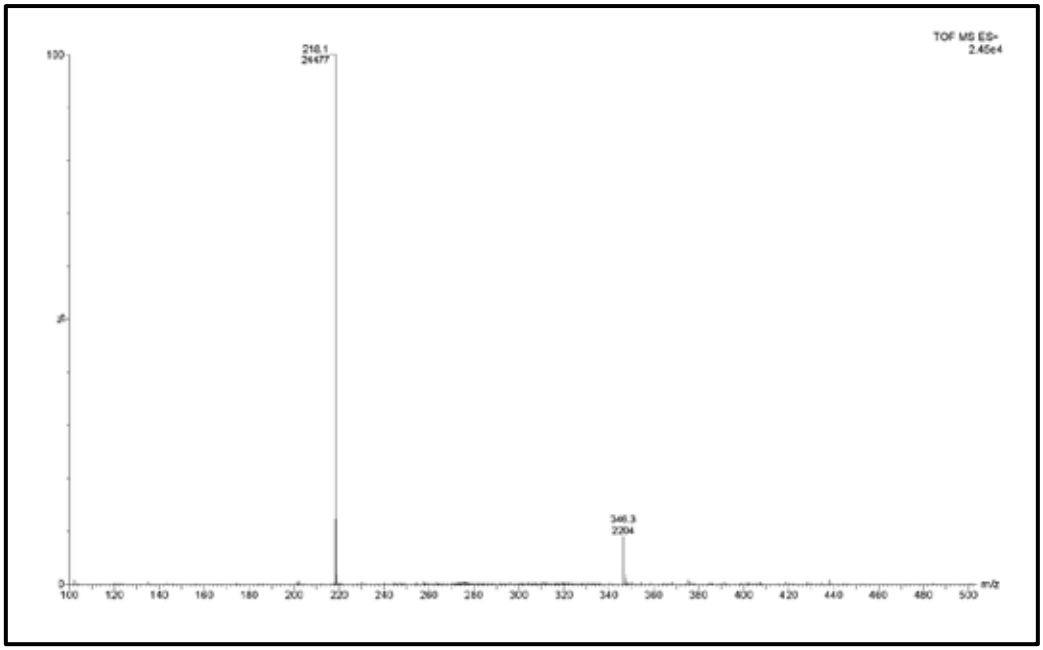

Fig. 62: ESI-Mass spectrum of **12h**

Table 30: Synthesis of tetrazole derivatives

Entry	Aldehyde	Product	Conventional method		Microwave Irradiation	
			Time (h)	Yield (%)	Time (min)	Yield (%)
1	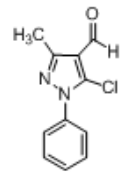 **6g**	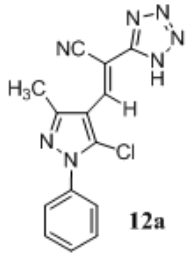 **12a**	4.5	81	15	92
2	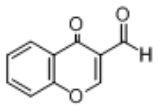 **6a**	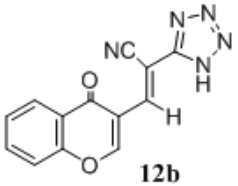 **12b**	4	78	15	89
3	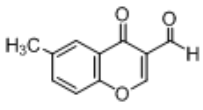 **6b**	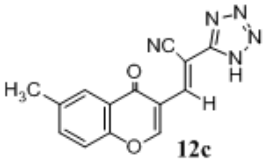 **12c**	4	80	15	91
4	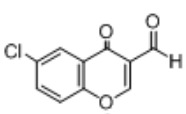 **6c**	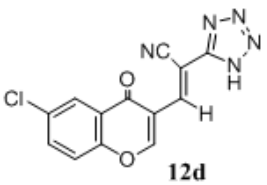 **12d**	4	81	15	90

5	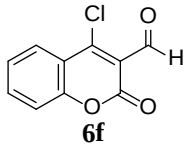 **6f**	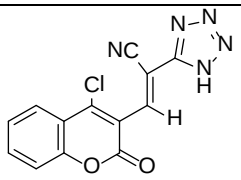 **12e**	3.5	77	15	91
6	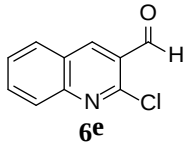 **6e**	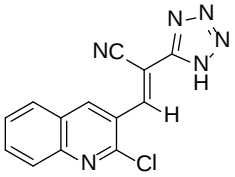 **12f**	3.5	79	15	90
7	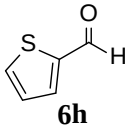 **6h**	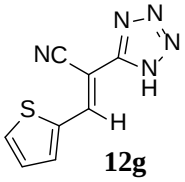 **12g**	4.5	85	15	93
8	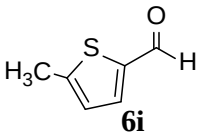 **6i**	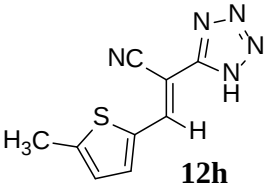 **12h**	4.5	85	15	94
9	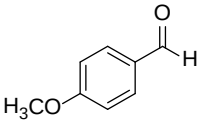 **2c**	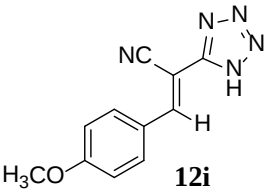 **12i**	5	88	15	95
10	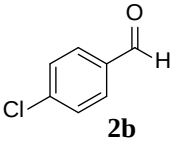 **2b**	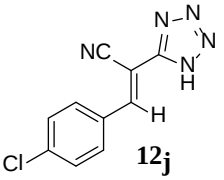 **12j**	5	87	15	93
11	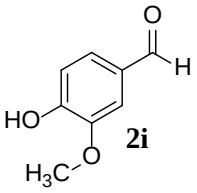 **2i**	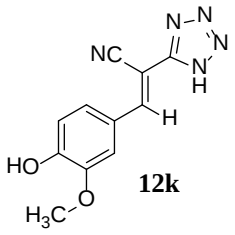 **12k**	5.5	83	15	91
12	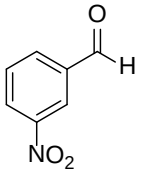 **2e**	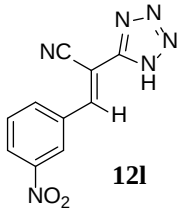 **12l**	5.5	86	15	92

5.4.3. Reaction mechanism

The plausible reaction mechanism is presented in **Scheme 17**. Protonation of aldehyde **6** by the catalyst initiates the reaction by generating the active species **T**, which undergoes knoevenagel condensation reaction to form aryl/heteroarylidenemalononitrile **U**. The activation of the nitrile group of the intermediate **U** by protonation stimulates the attack of the azide ion, which leads to the formation of an open imidoyl azide intermediate **V**. This intermediate **V** subsequently cyclises to intermediate **W** via [3+2] cycloaddition reaction and upon further addition of HCl, finally generates the product **12**.[25]

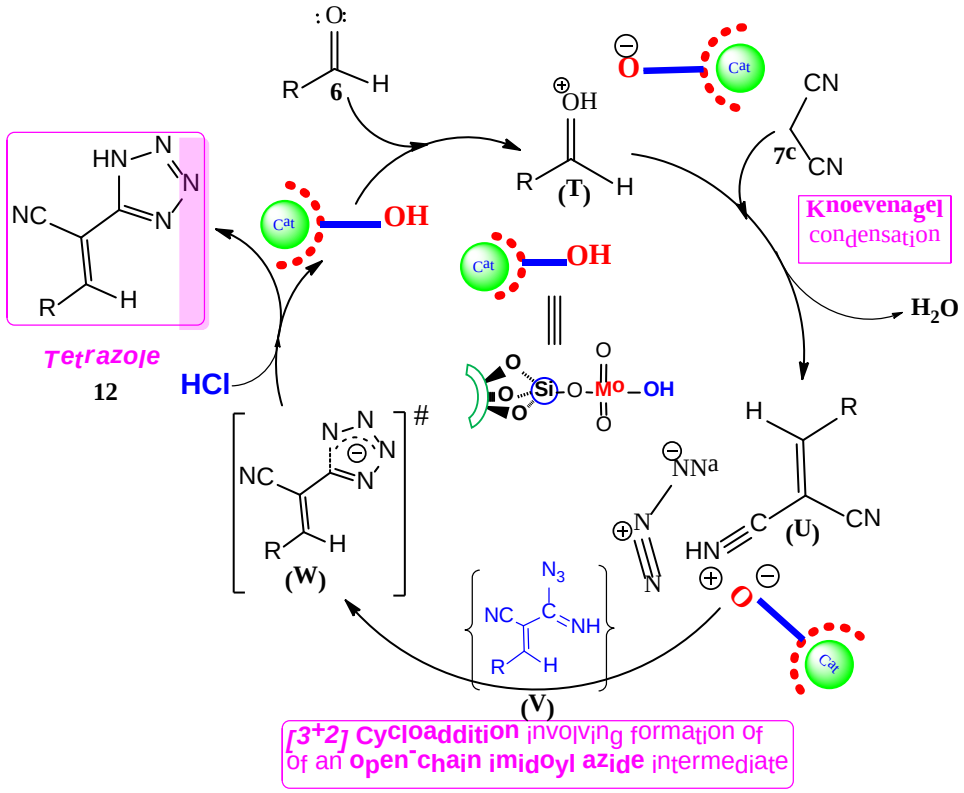

Scheme 17: Plausible reaction mechanism for the formation of tetrazoles.

5.4.4. Recyclability of the catalyst

The potential of recyclability of SMA was evaluated using model reaction. After completion of the reaction, the reaction mixture was extracted with ethyl acetate followed by filtration of the catalyst. The catalyst was then reused for subsequent cycles and was found to maintain good activity for a minimum of seven reaction cycles in water with over 83 % product yield **(Figure 63)**. The FT-IR spectra of the catalyst after seven runs **(Figure 53c)** displayed the same vibrational fingerprint of the freshly prepared catalyst indicating the stability of the catalyst throughout the recycling study.

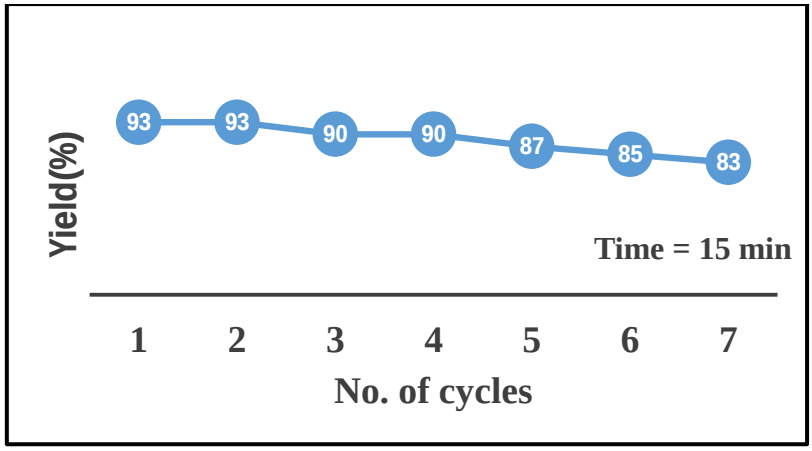

Fig. 63: Recycling data of SMA

5.5. CONCLUSION

In conclusion we successfully synthesised silica molybdic acid and used it for the synthesis of tetrazole derivatives in water under both conventional and microwave irradiation. The protocol tolerated aldehydes with diverse structural motifs giving corresponding tetrazoles in excellent yields. Use of water as a green solvent coupled with microwaves, low reaction times, recyclable catalyst and excellent yields of the products are advantages of the presented protocol.

5.6. EXPERIMENTAL

5.6.1. Synthesis of silica chloride [26]

A mixture of silica–gel (10 g) and thionyl chloride (40 mL) was refluxed for 48 h in a round bottomed flask (250 mL) equipped with a condenser and a drying tube ($CaCl_2$ as a drying agent). The resulting white-greyish powder was filtered and stored in a tightly capped bottle.

5.6.2. Synthesis of silica molybdic acid (SMA)

A mixture of silica chloride and sodium molybdate in n-hexane (10 mL) was stirred under refluxing conditions for 5 h. The reaction mixture was then filtered, washed with distilled water and dried at 120 °C in an oven for 6h. The resulting mixture was then further stirred in 0.1N HCl solution (40 mL) for 1 h, filtered, washed with distilled water and dried in an oven at 120 °C for 6h to finally obtain the catalyst.

5.6.3. General procedure for the synthesis of tetrazoles under thermal condition

A mixture of aldehyde (2 mmol), malononitrile (2 mmol), sodium azide (3 mmol) and catalyst (SMA, 200 mg) in 10 mL water was stirred at 50 °C for appropriate period of time **(Table 30)**. After completion of reaction (monitored by TLC), the reaction mixture was allowed to cool and added 10 mL of 2N HCl solution with vigorous

stirring. The precipitate obtained was extracted by ethyl acetate, washed with water (3 × 10 mL), dried over anhydrous Na_2SO_4 and evaporated under reduced pressure to obtain the product. The remaining solid catalyst was separated by filtration, washed with ethyl acetate (3 x 10 mL) and reused for further catalytic cycles. The crude product was recrystallized from ethanol to afford the pure product.

5.6.4. General procedure for the synthesis of tetrazoles under microwave irradiation

A mixture of aldehyde (2 mmol), malononitrile (2 mmol), sodium azide (2 mmol) and catalyst (SMA, 200 mg) in 10 mL water was taken in a G30 vial and irradiated with microwaves with continuous stirring at 50 °C for 15 min **(Table 30)**. After completion of reaction (monitored by TLC), the reaction mixture was allowed to cool and added 10 mL of 2N HCl solution with vigorous stirring. The precipitate as obtained was extracted by ethyl acetate, washed with water (3 × 10 mL), dried over anhydrous Na_2SO_4 and evaporated under reduced pressure to obtain the product. The remaining insoluble solid catalyst in aqueous phase was separated by filtration, washed with ethyl acetate (3 x 10 mL) and reused for further catalytic cycles. The crude product was recrystallized from ethanol to afford the pure product.

5.6.5. Spectral data of synthesised compounds

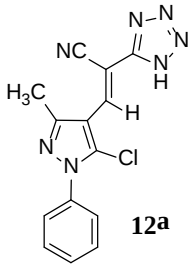 **12a**	3-*(5-chloro-3-methyl-1-phenylpyrazol-4-yl)-2-(1H-tetrazol-5-yl) acrylonitrile* Cream coloured solid, **M.p.** 125-130 °C. **Anal. Calcd**. ($C_{14}H_{10}ClN_7$) C, 53.94; H, 3.23; N, 31.45. **Anal. Found** ($C_{14}H_{10}ClN_7$) C, 53.88; H, 3.28; N, 31.51. **IR** (KBr, cm^{-1}): 3435 (NH), 2227 (CN), 1676 (C=C). **^{1}H NMR** (400 MHz, $CDCl_3$) δ 8.30 (s, 1H), 7.51-7.59 (m, Ar-H, 5H), 3.34 (s, 1H, NH), 2.52 (s, 3H, CH_3). **^{13}C NMR** (100 MHz, $CDCl_3$):159.71, 155.48, 149.29, 137.53, 134.32, 129.17, 127.62, 123.98, 118.13, 116.49, 114.21, 15.14. **ESI-MS** m/z 312.1 (M^++1).
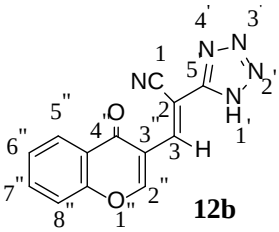 **12b**	*3-(4-oxo-4H-[1]benzopyran-3-yl)-2-(1H-tetrazol-5-yl) acrylonitrile* Cream coloured solid, **M.p.** 255-260 °C. **Anal. Calcd**. ($C_{13}H_7N_5O_2$) C, 58.87; H, 2.66; N, 26.41. **Anal. Found**. ($C_{13}H_7N_5O_2$) C, 58.81; H, 2.70; N, 26.45. **IR** (KBr, cm^{-1}): 3462 (NH), 2228 (CN), 1653 (C=O), 1605 (C=C). **^{1}H NMR** (400 MHz, DMSO-d_6) δ 8.27 (s, 1H), 7.18-8.11 (m, Ar-H, 4H), 6.79

	(s,1H, H2"), 4.08 (s, NH, overlap with solvent). **^{13}C NMR** (100 MHz, DMSO-d_6): 185.64, 164.39, 150.38, 147.12, 146.49, 135.77, 129.52, 128.51, 127.28, 119.02, 117.13, 114.57, 112.28. **ESI-MS** m/z 266.2 (M^++1).
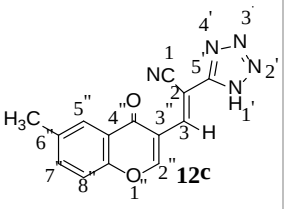 **12c**	*3-(6-Methyl-4-oxo-4H-[1]benzopyran-3-yl)-2-(1H-tetrazol-5-yl) acrylonitrile* Cream coloured solid, **M.p.** 260-265 °C. **Anal. Calcd**. ($C_{14}H_9N_5O_2$) C, 60.21; H, 3.25; N, 25.08. **Anal. Found** ($C_{14}H_9N_5O_2$) C, 60.25; H, 3.31; N, 25.03. **IR** (KBr, cm^{-1}): 3414 (NH), 2229 (CN), 1659 (C=O), 1598 (C=C). **^{1}H NMR** (400 MHz, DMSO-d_6) δ 8.23 (s, 1H), 7.26-8.15 (m, Ar-H, 3H), 6.88 (s, 1H, H2"), 4.10 (s, NH, overlap with solvent), 2.27 (s, 3H, CH_3). **^{13}C NMR** (100 MHz, DMSO-d_6): 188.21, 162.54, 151.22, 147.36, 145.91, 137.44, 135.18, 129.11, 128.34, 121.09, 118.22, 113.63, 111.79, 25.38. **ESI-MS** m/z 280.1 (M^++1).
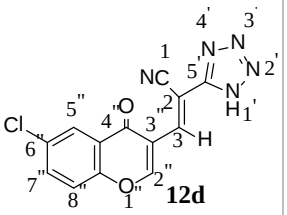 **12d**	*3-(6-chloro-4-oxo-4H-[1]benzopyran-3-yl)-2-(1H-tetrazol-5-yl) acrylonitrile* Cream coloured solid, **M.p.** 263-268 °C. **Anal. Calcd**. ($C_{13}H_6ClN_5O_2$) C, 52.10; H, 2.02; N, 23.37. **Anal. Found** ($C_{13}H_6ClN_5O_2$) C, 52.16; H, 1.95; N, 23.42. **IR** (KBr, cm^{-1}): 3423 (NH), 2225 (CN), 1665 (C=O), 1585 (C=C). **^{1}H NMR** (400 MHz, DMSO-d_6) δ 8.31 (s, 1H), 7.25-8.23 (m, Ar-H, 3H), 6.73 (s, 1H, H2"), 3.90 (s, NH, overlap with solvent). **^{13}C NMR** (100 MHz, DMSO-d_6): 183.51, 163.22, 150.57, 146.88, 144.91, 136.22, 131.27, 130.17, 126.22, 120.55, 119.86, 114.18, 112.54. **ESI-MS** m/z 300.1 (M^++1).
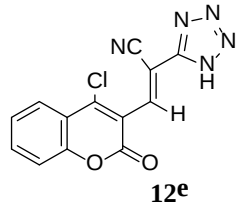 **12e**	*3-(4-chloro-2-oxo-2H-[1]benzopyran-3-yl)-2-(1H-tetrazol-5-yl) acrylonitrile* Light yellow solid, **M.p.** 230-235 °C. **Anal. Calcd**. ($C_{13}H_6ClN_5O_2$) C, 52.10; H, 2.02; N, 23.37. **Anal. Found** ($C_{13}H_6ClN_5O_2$) C, 52.07; H, 2.07; N, 23.41. **IR** (KBr, cm^{-1}): 3441 (NH), 2219 (CN), 1642 (C=O), 1591 (C=C). **^{1}H NMR** (400 MHz, DMSO-d_6) δ 8.72 (s, 1H), 7.38-7.77 (m, Ar-H, 4H), 3.28 (s, NH, overlap with solvent). **^{13}C NMR** (100 MHz, DMSO-d_6): 167.23, 158.56, 151.18, 148.54, 142.71, 138.44, 131.52, 129.76,

	127.94, 126.33, 121.41, 119.92, 110.55. **ESI-MS** m/z 300.1 (M^++1).
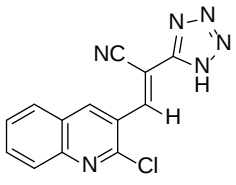 **12f**	*3-(2-chloro-4quinolinyl)-2-(1H-tetrazol-5-yl) acrylonitrile* Light yellow solid, **M.p.** 240-245 °C. **Anal. Calcd**. ($C_{13}H_7ClN_6$) C, 55.23; H, 2.50; N, 29.73. **Anal. Found** ($C_{13}H_7ClN_6$) C, 55.19; H, 2.55; N, 29.77. **IR** (KBr, cm^{-1}): 3432 (NH), 2220(CN), 1588(C=C). **^{1}H NMR** (400 MHz, DMSO-d_6) δ 8.74 (s, 1H), 7.24-7.80 (m, Ar-H, 5H), 3.30 (s, NH, overlap with solvent). **^{13}C NMR** (100 MHz, DMSO-d_6): 157.56, 154.05, 149.33, 146.68, 136.88, 130.07, 129.17, 128.62, 127.58, 126.96, 117.49, 115.29. **ESI-MS** m/z 283.1 (M^++1).
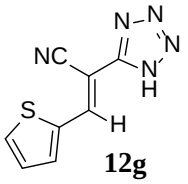 **12g**	*3-(thiophen-2-yl)-2-(1H-tetrazol-5-yl) acrylonitrile* White solid, **M.p.** 132-137 °C. **Anal. Calcd**. ($C_8H_5N_5S$) C, 47.28; H, 2.48; N, 34.46. **Anal. Found** ($C_8H_5N_5S$) C, 47.33; H, 2.43; N, 34.50. **IR** (KBr, cm^{-1}): 3456 (NH), 2223(CN), 1571(C=C). **^{1}H NMR** (400 MHz, $CDCl_3$) δ 8.41 (s, 1H), 7.72 (d, 1H, CH, *J*=3.74), 6.97 (d, 1H, CH, *J*=3.11), 3.34 (s, 1H, NH). **^{13}C NMR** (100 MHz, $CDCl_3$): 151.22, 145.67, 142.51, 133.76, 132.41, 127.87, 118.58, 112.09. **ESI-MS** m/z 204.1 (M^++1).
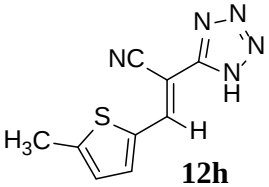 **12h**	*3-(5-methyl-thiophen-2-yl)-2-(1H-tetrazol-5-yl) acrylonitrile* White solid, **M.p.** 135-140 °C. **Anal. Calcd**. ($C_9H_7N_5S$) C, 49.76; H, 3.25; N, 32.24. **Anal. Found** ($C_9H_7N_5S$) C, 49.82; H, 3.21; N, 32.27. **IR** (KBr, cm^{-1}): 3439 (NH), 2220 (CN), 1575 (C=C). **^{1}H NMR** (400 MHz, $CDCl_3$) δ 8.45 (s, 1H), 7.75 (d, 1H, CH, *J*=3.84), 7.04 (d, 1H, CH, *J*=3.04), 3.33 (s, 1H, NH), 2.63 (s, 3H, CH_3). **^{13}C NMR** (100 MHz, $CDCl_3$): 151.72, 146.45, 142.12, 134.71, 132.13, 125.53, 119.18, 114.23, 15.27. **ESI-MS** m/z 218.1 (M^++1).
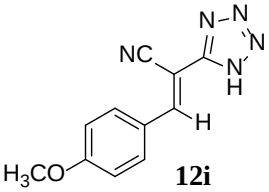 **12i**	*3-(4-methoxyphenyl)-2-(1H-tetrazol-5-yl) acrylonitrile* White solid, **M.p.** 156-160 °C. **Anal. Calcd**. ($C_{11}H_9N_5O$) C, 58.14; H, 3.99; N, 30.82. **Anal. Found** ($C_{11}H_9N_5O$) C, 58.19; H, 3.94; N, 30.87. **IR** (KBr, cm^{-1}): 3433 (NH), 2219 (CN), 1566 (C=C). **^{1}H NMR** (400 MHz, $CDCl_3$) δ 8.28 (s, 1H), 7.10-8.00 (m, Ar-H, 4H), 3.90 (s, 3H, OCH_3), 3.33 (s, 1H, NH). **^{13}C NMR** (100 MHz, $CDCl_3$): 163.04, 151.52, 141.97, 132.25, 126.18,

	120.11, 119.44, 100.37**.** 59.88**. ESI-MS** m/z 228.1 (M^++1).
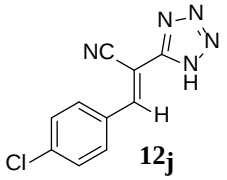 **12j**	3-*(4-chlorophenyl)-2-(1H-tetrazol-5-yl) acrylonitrile* White solid, **M.p.** 165-168 °C. **Anal. Calcd**. ($C_{10}H_6ClN_5$) C, 51.85; H, 2.61; N, 30.23. **Anal. Found** ($C_{10}H_6ClN_5$) C, 51.79; H, 2.66; N, 30.27. **IR** (KBr, cm^{-1}): 3434 (NH), 2224 (CN), 1580 (C=C). **^{1}H NMR** (400 MHz, $CDCl_3$) δ8.32(s, 1H), 7.15-8.21 (m, Ar-H, 4H), 3.35 (s, 1H, NH). **^{13}C NMR** (100 MHz, $CDCl_3$): 165.18, 152.26, 143.71, 134.21, 125.07, 121.81, 119.13, 101.56. **ESI-MS** m/z 232.1 (M^++1).
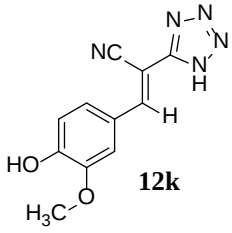 **12k**	*3-(4-hydroxy-3-methoxyphenyl)-2-(1H-tetrazol-5-yl) acrylonitrile* White solid, **M.p.** 164-169 °C. **Anal. Calcd**. ($C_{11}H_9N_5O_2$) C, 54.32; H, 3.73; N, 28.79. **Anal. Found** ($C_{11}H_9N_5O_2$) C, 54.36; H, 3.68; N, 28.81. **IR** (KBr, cm^{-1}): 3441 (NH), 3122(OH), 2220 (CN), 1588 (C=C). **^{1}H NMR** (400 MHz, $CDCl_3$) δ 8.18 (s, 1H), 6.79-7.52 (m, Ar-H, 3H), 10.21 (s, 1H, OH), 3.98 (s, 3H, OCH_3), 3.31 (s, 1H, NH). **^{13}C NMR** (100 MHz, $CDCl_3$): 168.05, 154.22, 140.54, 131.31, 130.89, 130.17, 129.58, 127.19, 119.55, 102.28, 54.25. **ESI-MS** m/z 244.1 (M^++1).
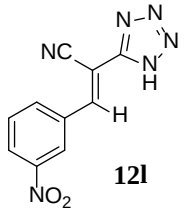 **12l**	*3-(3-nitrophenyl)-2-(1H-tetrazol-5-yl) acrylonitrile* White solid, **M.p.** 159-163 °C. **Anal. Calcd**. ($C_{10}H_6N_6O_2$) C, 49.59; H, 2.50; N, 34.70. **Anal. Found**. ($C_{10}H_6N_6O_2$) C, 49.63; H, 2.56; N, 34.67. **IR** (KBr, cm^{-1}): 3430 (NH), 2219 (CN), 1575 (C=C). **^{1}H NMR** (400 MHz, $CDCl_3$) δ 8.25 (s, 1H), 7.86-8.18 (m, Ar-H, 4H), 3.34 (s, 1H, NH). **^{13}C NMR** (100 MHz, $CDCl_3$): 157.23, 149.17, 146.38, 140.27, 136.71, 130.88, 127.27, 125.35, 119.88, 102.72. **ESI-MS** m/z 243.1 (M^++1).

REFERENCES:

1. G. A. Patani, E. J. LaVoie, Chem. Rev. 96 (1996) 3147.
2. L. V. Myznikov, A. Hrabalek, G. I. Koldobskii, Chem. Heterocycl. Compd. 43 (2007) 1.
3. P. L. Ornstein, M. B. Arnold, N. K. Allen, T. Bleisch, P. S. Borromeo, C. W. Lugar, J. D. Leander, D. Lodge, D. D. Schoepp, J. Med. Chem. 39 (1996) 2219.
4. K. L. Kees, R. S. Cheeseman, D. H. Prozialeck, K. E. Steiner, J. Med. Chem. 32 (1989) 11.
5. (a) J. K. Witkowski, R. K. Robins, R.W. Sidwell, L. N. Simon, J. Med. Chem. 15 (1972) 1150; (b) V. C. Bary, M. C. Conalty, J. P. O'Sllivan, D. Twomey, Chemother. 8 (1977) 103.
6. T. Okabayashi, H. Kano, Y. Makisumi, Chem. Pharm. Bull. 8 (1960) 157.
7. S. K. Figdor, M. S. Von Wittenau, J. Med. Chem. 10 (1967) 1158.
8. T. Jin, S. Kamijo, Y. Yamamoto, Tetrahedron Lett. 45 (2004) 9435.
9. K. Koguro, O. Toshikazu, M. Sunao, O. Ryozo, Synthesis (1998) 910.
10. J. Sauer, R. Huisgen, H. J. Strum, Tetrahedron 11 (1960) 241.
11. (a) B. Das, C. R. Reddy, D. N. Kumar, M. Krishnaiah, R. Narender, Synlett (2010) 391; (b) B. Gutmann, J. P. Roduit, D. Roberge, C. O. Kappe, Angew. Chem., Int. Ed. 49 (2010) 7101; (c) J. Bonnamour, C. Bolm, Chem. Eur. J. 15 (2009) 4543; (d) M. Habibi, Y. Bayat, D. Habibi, S. Moshaee, Tetrahedron Lett. 50 (2009) 4435; (e) B. Schmidt, D. Meid, D. Kieser, Tetrahedron 63 (2007) 492.
12. (a) P. N. Gaponik, V. P. Karavai, Y. V. Grigor'ev, Chem. Heterocycl. Compd. 21 (1985) 1255; (b) W. K. Su, Z. Hong, W. G. Shan, X. X. Zhang, Eur. J. Org. Chem. (2006) 2723.
13. (a) W. Ried, H. E. Erle, Liebigs Ann. Chem. 1982, 201; (b) Y. Yu, J. M. Ostresh, R. A. Houghten, Tetrahedron Lett. 45 (2004) 7787.
14. (a) W. G. Finnegan, R. A. Henry, E. Lieber, J. Org. Chem. 18 (1953) 779; (b) K. A. Jensen, A. Holm, S. Rachlin, Acta Chem. Scand. 20 (1966) 2795; (c) D. F. Percival, R. M. Herbst, J. Org. Chem. 22 (1957) 925.
15. Z. N. Tisseh, M. Dabiri, M. Nobahar, H. R. Khavasi, A. Bazgir, Tetrahedron 68 (2012) 1769.

16. M. Mahkam, Z. Namazifar, M. Nabati, J. Aboudi, Iran. J. Org. Chem. 6 (2014) 1217.
17. Z. N. Tisseh, M. Dabiri, A. Bazgir, Helv. Chim Acta 95 (2012) 1600.
18. Z. N. Tisseh, M. Dabiri, M. Nobahar, A. A. Soorki, A. Bazgir, Tetrahedron 68 (2012) 3351.
19. (a) M. L. Kantam, M. Roy, S. Roy, B. Sreedhara, R. L. De, Catal. Commun. 9 (2008) 226; (b) A. D. Murkute, J. E. Jackson, D. J. Miller, J. Catal. 278 (2011) 189.
20. J. C. Hicks, B. A. Mullis, C. W. Jones, J. Am. Chem. Soc., 129 (2007) 8426.
21. (a) C. Gabriel, S. Gabriel, E. H. Grant, B. S. J. Halstead, D. M. P. Mingos, Chem. Soc. Rev. 27 (1998) 213; (b) P. Lidstrom, J. Tierney, B. Wathey, J. Westman, Tetrahedron 57 (2001) 9225; (c) M. Larhed, C. Moberg, A. Hallberg, Acc. Chem. Res. 35 (2002) 717; (d) A. Loupy, ed., Microwaves in Organic Synthesis, 2nd ed.; Wiley-VCH: Weinheim, (2006).
22. A. Dastan, A. Kulkarni, B. Torok, Green Chem. 14 (2012) 17.
23. V. Palermo, G. P. Romanelli, P. G. Vazquez, J. Mol. Catal. A: Chem. 373 (2013) 142.
24. E. McCarron III, J. Calabrese, J. Sol. State Chem. 91 (1991) 121.
25. (a) D. Cantillo, B. Gutmann, C. O. Kappe, J. Org. Chem. 77 (2012) 10882; (b) F. Himo, Z. P. Demko, L. Noodleman, K. B. Sharpless, J. Am. Chem. Soc. 124 (2002) 12210.
26. A. Cornelis, P. Laszlo, Synthesis (1985) 909.

Tetrahedron Letters 54 (2013) 3599–3604

Contents lists available at SciVerse ScienceDirect

Tetrahedron Letters

journal homepage: www.elsevier.com/locate/tetlet

Highly efficient solvent-free synthesis of novel pyranyl pyridine derivatives via β-enaminones using ZnO nanoparticles

Zeba N. Siddiqui *, Nayeem Ahmed, Farheen Farooq, Kulsum Khan

Department of Chemistry, Aligarh Muslim University, Aligarh 202002, India

ARTICLE INFO

Article history:
Received 13 February 2013
Revised 16 April 2013
Accepted 18 April 2013
Available online 7 May 2013

Keywords:
ZnO nanoparticles
Heterogeneous catalyst
Pyridine derivatives
Solvent-free

ABSTRACT

Highly efficient ZnO nanoparticle catalyzed one-pot solvent-free synthesis of novel pyridine derivatives by three-component reaction of β-enaminones, different active methylene compounds, and ammonium acetate via Michael addition, cyclodehydration, and elimination sequence is reported. The catalyst was recyclable up to six catalytic cycles without a significant loss in the catalytic activity. This new protocol has the advantages of environmental friendliness, higher yields, solvent-free, low loading of catalyst, shorter reaction times, and convenient operation procedure. ZnO nanoparticles were characterized by XRD, SEM, and TEM analyses.

The greenest solvent, in terms of reducing waste, is no solvent. Due to the toxic, flammable, and expensive nature of organic solvents,[1] special emphasis has been placed toward solvent-free reactions. Overall the advantages of solvent-free organic synthesis are shorter reaction times, cleaner reaction products, and environmentally more benign conditions compared with the classical reactions.[2] The use of nano-sized inorganic solid oxides as heterogeneous catalysts has received much attention because of their high level of chemoselectivity, environmental compatibility, simplicity of operation, and their availability at low cost.[3] Catalytic efficiency depends on the surface area of the catalyst. As nanoparticles provide a very large surface area because of their high surface to volume ratio and low-coordinated sites, their use as catalysts is quite encouraging.[4]

Among the nitrogen-containing heterocycles, pyridine derivatives constitute one of the most important classes of compounds as they widely occur as key structural subunits in numerous natural products that exhibit many interesting biological activities.[5–7] These derivatives possess a large spectrum of biological activities like anti-prion,[8] anti-hepatitis B virus,[9] anti-bacterial,[10] and anti-cancer.[11] Recently, some of these compounds have been recognized as potential targets for the development of new drugs for the treatment of Parkinson's disease, hypoxia, asthma, kidney disease, epilepsy, cancer, and Creutzfeldt–Jakob disease.[12–14]

β-Enaminones turned out to be simple synthetic intermediates for the subject of the present synthesis due to the presence of ambident nucleophilic character of enamine moiety and the ambident electrophilic character of enone moiety. Taking advantage of their electronic properties we used heteroaryl β-enaminones for the synthesis of these substituted pyridines. Synthesis of these substituted pyridines is reported by the reaction of β-enaminones with β-dicarbonyls in the presence of ammonium acetate in refluxing acetic acid,[15] using Montmorillonite K10 in 2-propanol,[16] $K_5CoW_{12}O_{40}{\cdot}3H_2O$,[17] and $CeCl_3$/NaI.[18] However, these methods exhibit limited substrate tolerance and reactivity, suffer from low yields, and use of toxic solvents. Owing to numerous advantages due to its eco-friendly nature, ZnO NPs have been explored as a powerful catalyst for several organic transformations.[19–21] On the basis of our progressive endeavors in exploring novel one-pot reactions[22,23] we, herein, report an efficient ZnO nanoparticle catalyzed, solvent-free, regioselective synthesis of novel substituted pyridines through Michael addition, cyclodehydration, and elimination sequence.[24]

To recognize the optimization of the reaction conditions, the reaction was studied by employing a series of catalysts in solvents and solvent-free conditions with the expectation to maximize the product yield in short reaction time (Table 1). Initially, β-enaminone **1a**, ethyl acetoacetate **3b**, and ammonium acetate were refluxed in AcOH as the solvent without any catalyst. The reaction took a longer time period of 24 h to complete and afforded product in less yield (Table 1, entry 1), demonstrating the need of a catalyst. The reaction was then studied in the presence of catalysts such as sulfamic acid, P_2O_5, P_2O_5–silica, $NaHSO_4$–SiO_2, ZnO, MgO, and ZnO NPs under solvents EtOH and AcOH, and solvent-free reaction conditions (Table 1). Among all the catalysts and solvents, ZnO NPs under solvent-free condition proved to be most efficient in terms of reaction time and product yield.

* Corresponding author. Tel.: +91 9412653054.
E-mail address: siddiqui_zeba@yahoo.co.in (Z.N. Siddiqui).

0040-4039/$ - see front matter © 2013 Elsevier Ltd. All rights reserved.
http://dx.doi.org/10.1016/j.tetlet.2013.04.072

Journal of Molecular Catalysis A: Chemical 394 (2014) 232–243

Contents lists available at ScienceDirect

Journal of Molecular Catalysis A: Chemical

journal homepage: www.elsevier.com/locate/molcata

Mesoporous alumina sulphuric acid: A novel and efficient catalyst for on-water synthesis of functionalized 1,4-dihydropyridine derivatives via β-enaminones

Nayeem Ahmed, Zeba N. Siddiqui*

Department of Chemistry, Aligarh Muslim University, Aligarh 202 002, India

ARTICLE INFO

Article history:
Received 10 June 2014
Received in revised form 9 July 2014
Accepted 10 July 2014
Available online 19 July 2014

Keywords:
On-water
Dihydropyridines
Mesoporous alumina sulphuric acid
Heterogeneous catalyst

ABSTRACT

A simple, efficient and environmentally benign on-water protocol for the synthesis of novel 1,4-dihydropyridine derivatives via pseudo four component addition and cyclization sequence using mesoporous alumina sulphuric acid as a recyclable and heterogeneous catalyst, has been described. The catalyst showed excellent catalytic activity giving products in high yields and could be reused for seven successive catalytic cycles. The catalyst was characterized by FT-IR, XRD, FE-SEM, EDX and TG analyses. The mesoporosity of alumina was determined by BET and TEM analyses.

1. Introduction

In the light of green chemistry water is uniquely advantageous as a solvent. It is environmentally benign, non-flammable, possesses a high heat capacity, and tolerates a wide range of temperature, making it inherently safe. It also possesses the remarkable ability to catalyze chemical transformations between some insoluble organic reactants and this phenomenon, termed as "on-water" catalysis by Sharpless and co-workers, was first observed in the late 1930s but is only now being widely adopted [1–8]. Subsequent mechanistic studies have established that this behaviour results from enforced hydrophobic interactions [9] and stabilization of the activated complex by hydrogen-bond formation [10]. Sharpless's group has shown that several uni- and bimolecular reactions are greatly accelerated when carried out in vigorously stirred aqueous suspensions. These reactions include the important classes such as cycloadditions, ene reactions, Claisen rearrangements and nucleophilic substitutions [1].

Multicomponent reactions (MCRs) have become powerful tools of synthetic organic chemistry in recent years owing to exceptional synthetic efficiency, intrinsic atom economy, high selectivity, and procedural simplicity [11]. These reactions enable straightforward access to large libraries of structurally related, drug-like compounds and thereby facilitating lead generation and lead optimization in drug discovery [12]. In a true sense, these represent environmentally friendly processes by reducing the number of steps, energy consumption and waste production [13].

Nitrogen containing heterocycles are subunits found in numerous natural products and many biologically active pharmaceuticals. Among these 1,4-dihydropyridine substructures are among the most prevalent, the most famous ones certainly being the calcium agonists Felodipine, Nicardipine, Nimodipine, Nifedipine (Fig. 1) and NADPH. In addition, these compounds show other versatile biological profiles such as anticonvulsant activity, selective adenosine-A3 receptor antagonism, radioprotective activity, sirtuin activation and inhibition, antitumor, antidiabetic, or photosensitizing activities [14–16]. Conventionally, 1,4-DHPs can be synthesized via the Hantzsch reaction, reduction of pyridines, addition to pyridines or cycloadditions, etc. but the Hantzsch reaction still remains a frequently employed tactic for the synthesis of these compounds [17]. New efforts to develop structurally diverse 1,4-DHPs led to the utilization of enaminones as substrates and few reports available in literature employing L-proline/MeOH, TMSCl, TsOH/DCE, $NaAuCl_4$ and AcOH [17,18] as catalytic systems. However, these methods exhibit limited substrate tolerance and reactivity, suffer from low yields, and use of toxic solvents. Hence it is highly desirable to develop a new protocol for the synthesis of 1,4-DHPs using enaminones, which is highly efficient, environmentally benign and tolerates wide range of substrates.

* Corresponding author. Tel.: +91 9412653054.
E-mail addresses: siddiqui_zeba@yahoo.co.in, zns.siddiqui@gmail.com (Z.N. Siddiqui).

http://dx.doi.org/10.1016/j.molcata.2014.07.015
1381-1169/

Journal of Molecular Catalysis A: Chemical 387 (2014) 45–56

Contents lists available at ScienceDirect

Journal of Molecular Catalysis A: Chemical

journal homepage: www.elsevier.com/locate/molcata

Sulphated silica tungstic acid as a highly efficient and recyclable solid acid catalyst for the synthesis of tetrahydropyrimidines and dihydropyrimidines

Nayeem Ahmed, Zeba N. Siddiqui *

Department of Chemistry, Aligarh Muslim University, Aligarh 202 002, India

ARTICLE INFO

Article history:
Received 9 December 2013
Received in revised form 16 February 2014
Accepted 18 February 2014
Available online 4 March 2014

Keywords:
SSTA
Tetrahydropyrimidines
Heterogeneous
Solvent-free
Recyclability

ABSTRACT

For the first time sulphated silica tungstic acid (SSTA) has been synthesized and used as an acidic catalyst in organic synthesis. The catalyst was prepared by a simple method based on the reaction of silica with $SOCl_2$ followed by addition of sodium tungstate and then functionalization with chlorosulfonic acid. The three-component Biginelli-like condensation of different heteroaldehydes, urea and ethyl cyanoacetate or phenyl acetic acid catalyzed by SSTA under solvent-free conditions afforded novel tetrahydropyrimidines in high yields. The catalyst tolerated different heteroaldehydes and also catalyzed the synthesis of Biginelli compounds efficiently giving excellent yield of products. The catalyst was characterized by FT-IR, XRD and SEM-EDX analyses. The stability of the catalyst was evaluated by DSC and TG analyses. The major advantages of the present method are high yields, short reaction times, and solvent-free reaction conditions. The activity and simple recyclability without losing catalytic activity make this catalyst a good replacement to literature methods.

1. Introduction

The catalysts which make the organic reactions environmentally benign and economically feasible are extremely demanded by the chemical industries. In recent years, preparation of new heterogeneous catalysts with improved efficiency has been the subject of immense interest [1]. The ideal method for combining the advantages of homogeneous catalysts (high activity and selectivity, etc.) with the advantages of heterogeneous catalysts (available active sites, easy catalyst separation, long catalytic life, thermal stability, low hygroscopic properties, easy handling and reusability) is by immobilization of catalysts on solid support, which leads to clean chemical synthesis from both environmental and commercial point of view [2–5]. In modern material science, silica is the ubiquitous inorganic platform used in systems designed for catalysis, separation, filtration, sensing, optoelectronics and environmental technology. Due to the favourable chemical and physical properties of silica surfaces, it is possible to impart nearly any reactive functional group that one requires on a silica surface (e.g., sulfonic, amine, carboxyl, thiol, epoxy, and so forth) through well-known silane chemistry [6–8]. As a result, numerous variations can be made for specific applications with the use of a combination of inorganic materials and functional groups which often result in synergetic effects that lead to increased physical stability and enhanced chemical functionality [9,10].

The Biginelli multicomponent reaction is a very elegant methodology to obtain 3,4-dihydropyrimidin-2(1H)-one (DHPMs) derivatives in a one-step procedure [11]. DHPMs usually display various biological activities such as calcium channel modulators, adrenergic receptor antagonists, mitotic kinesin inhibitors, antivirals, antibacterials [12] and compounds such as enastron, monastrol, piperastrol and other derivatives [13] are well known biologically active compounds which have already been developed into drugs.

Moreover tetrahydropyrimidine ring is found in both natural as well as synthetic organic compounds. Many tetrahydropyrimidines containing an amino acid show interesting and diverse pharmacological activities like HIV protease inhibiting activity [14], antineoplastic activity [15], antiproliferative [16], herbicidal activity [17], muscarinic agonist activity [18], anti-inflammatory [19] and antiviral properties [20]. The presently known MCR protocols for the synthesis of THPMs are via Biginelli-like transformation [21] or alternatively, using the two-step operation of Knoevenagel condensation and urea annulation [22]. To the best of our knowledge, not a single multicomponent protocol for the synthesis of THPMs tolerating heteroaldehydes under heterogeneous

* Corresponding author. Tel.: +91 9412653054.
E-mail address: zns.siddiqui@gmail.com (Z.N. Siddiqui).

http://dx.doi.org/10.1016/j.molcata.2014.02.019
1381-1169/

ACS Sustainable Chemistry & Engineering

Research Article

pubs.acs.org/journal/ascecg

Cerium Supported Chitosan as an Efficient and Recyclable Heterogeneous Catalyst for Sustainable Synthesis of Spiropiperidine Derivatives

Nayeem Ahmed and Zeba N. Siddiqui*

Department of Chemistry, Aligarh Muslim University, Aligarh 202 002, India

Supporting Information

ABSTRACT: A new Ce/chitosan catalyst has been prepared and used for the highly efficient synthesis of diverse range of spiropiperidine derivatives via multicomponent reaction of substituted anilines, formaldehyde and different cyclic active methylene compounds at room temperature in PEG-200. The catalyst could be reused for five consecutive cycles without appreciable loss in catalytic activity. The structure of the catalyst was determined by IR, XRD, EDX, TEM and ICP-AES techniques. The present green protocol has advantages such as novel products, energy sustainability, short reaction times, high yield of products, economic viability and recyclability of the catalyst.

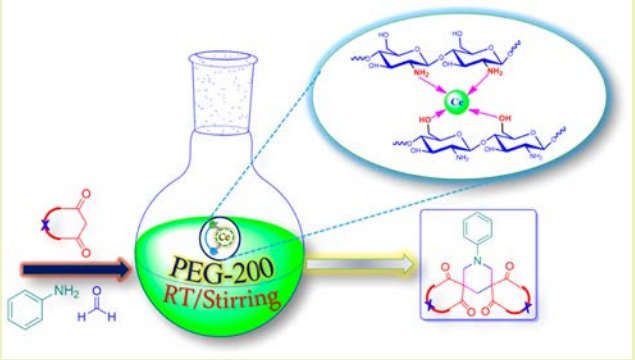

KEYWORDS: *Heterogeneous, Multicomponent, Spiropiperidine, PEG-200, Green*

INTRODUCTION

In the last decades, the use of lanthanides as Lewis acids in organic synthesis has increased enormously[1,2] and among them Ce salts, being the most abundant, have been extensively used in reduction, C−C, C−N and C−O bond formation reactions.[3] This extensive use of Ce salts is attributed to moderate to low toxicity, water tolerance, easy to handle, availability at moderate cost and suitability for use without purification. However, the main limitation from economic and environmental point of views is their use in stoichiometric amounts. Therefore, the development of heterogenized version of Ce salts remains a major objective of modern organic chemistry, and the simplest strategy to perform this task is by immobilization on a solid support. In recent years, biopolymers have gained lot of attention for their use as supporting materials.[4] Chitosan is a natural, abundant and low-cost polymer that exhibits interesting properties like nontoxicity, easy chemical modification due to presence of both amino and hydroxyl groups, inertness toward air and moisture, biocompatibility and biodegradability, and thus, make it a versatile supporting material.[5−8]

The piperidine ring unit forms the core of a large family of alkaloids and natural products with strong medicinal and interesting structural properties. The presence of piperidine motifs in drug molecules has generated a lot of interest in development of efficient protocols for the synthesis of these compounds.[9−14] Recently, spiro-substituted piperidines have received considerable attention due to their important pharmacological profiles like selective and potent σ receptor ligands that can be used in the treatment of cocaine abuse, depression and epileptic disorders and 5-HT_{2B} receptor antagonists.[15−20] Owing to the importance of these compounds in the field of medicine, unexpectedly, there are only few protocols available in the literature documenting the synthesis of these spiro compounds.[21−24] However, many shortcomings associated with these protocols include the use of homogeneous catalysts, toxic solvents, long reaction times and very limited substrate tolerance. Therefore, it is highly desirable to develop an efficient protocol for the synthesis of spiropiperidine adducts that is highly efficient, environmental friendly, tolerates a wide range of substrates and involves the reuse of the catalyst.

In the present work, taking advantage of the above-mentioned properties of chitosan, we have synthesized a new, effective, inexpensive and recyclable chitosan supported cerium catalyst and used it for the synthesis of novel spiropiperidine derivatives via multicomponent reaction of substituted anilines, formaldehyde and different active methylene compounds at room temperature using PEG-200 as a green solvent. It is worthy to mention that polyethylene glycols (PEGs) are inexpensive, nontoxic, nonvolatile and thermally stable compounds that serve as suitable media for environmentally sustainable organic transformations.[25] Their solubility in water leads to easy separation and recovery of products from the reaction medium.

Received: March 18, 2015
Revised: May 28, 2015
Published: June 22, 2015

DOI: 10.1021/acssuschemeng.5b00223
ACS Sustainable Chem. Eng. 2015, 3, 1701−1707

RSC Advances

PAPER

Cite this: *RSC Adv.*, 2015, **5**, 50691

Dy/chitosan: a highly efficient and recyclable heterogeneous nano catalyst for the synthesis of hexahydropyrimidines in aqueous media†

Nayeem Ahmed, Saima Tarannum and Zeba N. Siddiqui*

Received 3rd May 2015
Accepted 29th May 2015

DOI: 10.1039/c5ra08160b

www.rsc.org/advances

A chitosan supported Dy(III) nanocatalyst was synthesised by a simple procedure. It was used as a catalyst for one pot, three component synthesis of hexahydropyrimidine derivatives. All the reactions were completed in a short time period at room temperature and the products were obtained in high to excellent yields. The catalyst was characterized by FT-IR, XRD, SEM-EDX, TEM and ICP-AES analyses. The stability of the catalyst was evaluated by TG analysis. Use of water, ambient conditions, recyclability and high TOF of the catalyst make this protocol a sustainable alternative to existing protocols.

Introduction

Hexahydropyrimidines are an important class of compounds with a diverse range of biological activities.[1] These scaffolds are one of the most commonly encountered heterocycles in medicinal chemistry with various profiles such as antibacterial,[2] antiviral, antitumor and anti-inflammatory activities.[3] This skeleton is also found in a number of alkaloids such as verbamethine[4] and verbametrine.[5] Hexetidine, which is a hexahydropyrimidine based drug molecule, has promising anesthetic, deodorant and antiplaque effects.[6] N-substituted hexahydropyrimidines serve as key synthetic intermediates for spermidine–nitroimidazole drugs which are used for the treatment of A549 lung carcinoma.[7] New trypanothione reductase inhibiting ligands used for the regulation of oxidative stress in parasite cells also contain this structural unit.[8] Recently, appropriately substituted hexahydropyrimidines were found to be potent hepatitis C virus inhibitors.[9]

Recently, lanthanides have found widespread use in the development of green chemistry as mild and efficient Lewis acids.[10] A prominent feature of lanthanides is their stability and activity in protic media, making them ideal for use as stable Lewis acids in water. Dysprosium(III) is an extremely mild and efficient Lewis acid catalyst having the ability to promote various types of carbon–carbon bond-forming reactions, electrocyclizations and cycloaddition reactions.[11] Compared to other lanthanides, dysprosium has not received much attention from the synthetic community even though it exhibits similar stability towards air and water, ease of handling, Lewis acidity and oxophilicity. It also has the unique ability to retain its catalytic activity in presence of Lewis basic nitrogen groups, which allows its use in a variety of transformations with unprotected amines.[11]

Chitosan is a naturally occurring and versatile hydrophilic polysaccharide derived from chitin. The high density of amino and hydroxyl groups of chitosan enables an effective functionalization and avoids the aggregation of metallic nanoparticles.[12–16] Therefore, its use as a biodegradable supporting material for various catalysts is quite promising.

With the emphasis on the use of cleaner processes and concerns over the environmental impact of using volatile organic solvents (VOCs), increasing attention has been focused towards the use of water as reaction medium in organic syntheses. Recent research has shown that the speed of heterogeneous mixture of reactants and water is dramatically faster than for aqueous solutions. Under these heterogeneous conditions the water plays the role of a medium and not of solvent, and hence are termed as on-water reactions.[17]

Therefore, in continuation of our interest in developing water compatible processes,[18] we herein, report the synthesis of novel Dy(III)/chitosan and its application as catalyst for the synthesis of hexahydropyrimidines and their spiro analogues in water.

Results and discussion

Scheme 1 illustrates the synthesis of the catalyst. Weighed amount of chitosan was first suspended in water and stirred for 30 min. $Dy(NO_3)_3 \cdot 6H_2O$ was then added to the suspension with continuous stirring. The mixture was then continuously stirred overnight and the catalyst was obtained by simple filtration.

Catalyst characterization

FT-IR spectra (Fig. 1a) of chitosan showed broad stretching band for OH and NH groups at 3419 cm^{-1}. The band at

Department of Chemistry, Aligarh Muslim University, Aligarh, 202 002, India. E-mail: siddiqui_zeba@yahoo.co.in; Tel: +91 9412653054

† Electronic supplementary information (ESI) available. See DOI: 10.1039/c5ra08160b

RSC Advances

PAPER

Cite this: *RSC Adv.*, 2015, **5**, 16707

Silica molybdic acid catalysed eco-friendly three component synthesis of functionalised tetrazole derivatives under microwave irradiation in water

Nayeem Ahmed and Zeba N. Siddiqui*

Received 19th January 2015
Accepted 27th January 2015

DOI: 10.1039/c5ra01073j

www.rsc.org/advances

The catalytic multicomponent reaction between different aldehydes, malononitrile and sodium azide, for the synthesis of functionalised tetrazoles in pure water was performed using silica molybdic acid as an acidic catalyst under microwave irradiation at ambient temperature. The catalyst showed remarkable activity by decreasing the time period of the reaction from 24 h (without catalyst) to 15 min under microwave irradiation. The catalyst successfully tolerated different aromatic and heterocyclic aldehydes furnishing the desired products in excellent yields. The major advantages of this protocol are recyclable catalyst, water as a green solvent, excellent yields, very short reaction times, use of microwaves and high TOF of the catalyst.

Introduction

Application of clean technologies in chemical synthesis has currently been the major area of focus in green chemistry. The eco-friendly and reusable heterogeneous catalysts have till now been the leaders in providing such clean technologies. The promising applications shown by such catalysts have in turn been exploited by industry and presently there are more than 100 industrial transformations being catalysed by over 103 solid acid catalysts.[1–4] Due to rapid advances in medicinal chemistry, ever increasing attention has been paid towards the development of novel clean processes employing nontoxic reagents, catalysts and solvents as a majority of drug-like compounds and natural products contain a heterocyclic nucleus at their core.[5–9]

Among various heterocycles tetrazoles and their derivatives represent an important class of N-containing heterocycles. The close similarity between the acidity of tetrazole group and carboxylic group has led to their development as potential medicinal agents[10] and compounds like lasortan, irbesartan, tomelukast, and PTZ (2) (Fig. 1), which have been developed into drugs, have proven to be successful bioisosteric replacements for carboxylic acid groups. Moreover, 5-substituted tetrazoles are reported to possess biological profiles like potential drugs against schizophrenia and cerebral ischemia,[11] antidiabetic,[12] antiviral,[13] antibacterial[14] and antihypertensive activities.[15] Also, the role of tetrazoles as important synthons in synthetic organic chemistry,[16] as ligands in coordination chemistry and applications in material chemistry[17,18] has led to the development of various efficient protocols for their synthesis.

Many available methods for the synthesis of tetrazoles include [3 + 2] cycloaddition of azide to nitriles,[19] reaction of primary amines with NaN_3 and triethyl orthoformate,[20] nucleophilic substitution by an azide anion[21] and addition of $NaNO_2$ to aminoguanidine.[22] But [3 + 2] cycloaddition still remains the most employed method for the synthesis of 5-substituted tetrazoles. New efforts to develop multicomponent protocols for the synthesis of 5-substituted tetrazoles have led to the utilization of 2-benzylidenemalononitrile and sodium azide.[23] Water is the most abundant and environmentally benign solvent in nature, but due to low solubility of organic compounds in water, its application in organic synthesis is currently limited.[24] Recently a great deal of

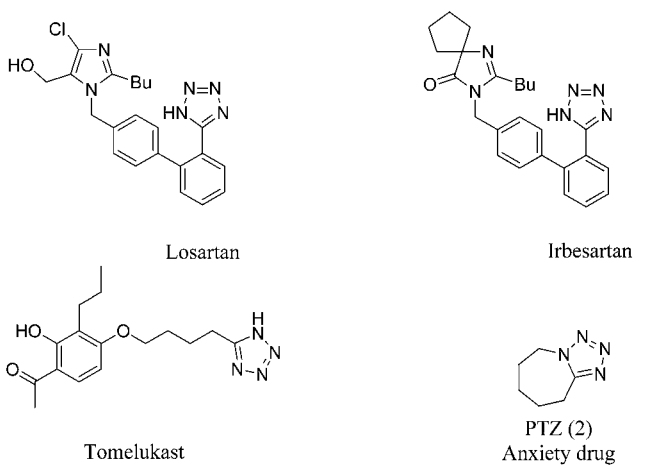

Fig. 1 Representative drugs based on tetrazoles.

Department of Chemistry, Aligarh Muslim University, Aligarh, 202 002, India. E-mail: siddiqui_zeba@yahoo.co.in; Tel: +91 9412653054